THE DEVELOPMENT OF SHAFT FRICTION IN SEMI-FULLSCALE PILES PASSING THROUGH GRANULAR SOILS

by

W.F. KAY BSc.

Thesis presented in fulfilment of the requirement for the Degree of Doctor of Philosophy, Council for National Academic Awards, London, 1980.

Sponsoring Establishment

Department of Civil Engineering and Building, The Polytechnic of Wales, Wales, United Kingdom.

Collaborating Establishments

Building Research Station, Watford, U.K., and Construction Industry Research and Information Association, London, U.K.

November 1980

Certification of Research

This is to certify that, except when specific reference to other investigations is made, the work described in this Dissertation is the result of the investigation of the candidate.

W. F. Kay
(Candidate)

14th April 1981
(Date)

Dr. R. Delpak
(Director of Studies)

14th April 1981
(Date)

Mr. G. O. Rowlands
(Supervisor)

14th April 1981
(Date)

DECLARATION

This is to certify that neither this thesis, nor any part of it, has been presented, or is being currently submitted, in candidature for any degree at any other University.

.....
(Candidate)

ACKNOWLEDGEMENTS

The candidate wishes to express his gratitude to Dr.R.Delpak, his Director of Studies, and Mr.G.O.Rowlands, his Supervisor, at The Polytechnic of Wales for their valuable suggestions and criticisms.

He wishes to thank Mr.R.W.Cooke of the Building Research Establishment and Mr.A.Weltman formerly of the Construction Industry Research Information Association for their helpful advice and discussions.

The help and advice of Mr.H.Davies and the technical staff in the Department of Civil Engineering and Building at The Polytechnic of Wales in the design and manufacture of the testing apparatus is acknowledged.

Credit is also due to Messrs.G.T.Jones and R.Thornton and the technical staff at the Computer Centre of The Polytechnic of Wales for their assistance with the computer programs and graph plotting routines of the processed data.

He would also like to thank Mrs.A.Davies for typing the thesis, Mr.B.Dimery for his drafting work and Miss D.L.Thaler for checking the manuscript.

He would finally like to acknowledge the help of Northeastern University (U.S.A.) and The Polytechnic of Wales (U.K.) for arranging the student exchange programme and to the Polytechnic for providing the research assistantship which enabled the candidate to carry out this work.

CONTENTS

SUMMARY

The present study examines the load transfer mechanism and subsequent soil displacements around a 0.114m diameter pile passing through a sand stratum.

The available literature on deep foundations is reviewed. It was found that the amount of literature pertaining to pile behaviour in layered soils, was limited.

A model pilot study showed that the most efficient means of eliminating end bearing, while simulating an underlying clay stratum, was by driving the base of the pile into a frictionless cylinder.

The composite test pile incorporated load cells for the measurement of the load distribution. The sensitivity of the initial 'Shell' type cell was found to be insufficient at the smaller loads which were developed near the pile base. Subsequently, the more sensitive 'Core' type cell was designed and proved satisfactory.

The test pile was loaded in a 3m diameter by 3m deep concrete testing tank equipped with sand placement machinery and a dust extraction unit. Small plates, linked to transducers, were used to measure the sand displacements around the pile.

A small dynamic probe was used to monitor the uniformity of placement and degree of compaction of each sand layer.

A series of loading tests was carried out in loosely placed and compacted sand layers.

The test data was recorded on punched tape. Processing and plotting of the test results was accomplished using the facilities of the DECsystem-20 computer. The results showed :

1. the stress transfer curves were similar to those proposed by Vesic, in sand, and those obtained by Meyerhof and Sastry in layered soils. No skin friction was developed at the top or the bottom of the sand,

2. the vertical sand displacement decreased with increasing depth, radial distance, and sand density,

3. the CRP, MLT, and pull-out tests showed that the skin friction was dependent on the direction and sequence of testing,

4. an expression for the coefficient of earth pressure Ks along the pile shaft was determined, based on the experimental data. The values of Ks were found to increase with increasing density and to decrease with embedded length.

NOTATION

Ab	=	Pile base area
As	=	Pile shaft area
B	=	Pile breadth (or diameter)
Ca	=	Adhesion between pile shaft and adjacent soil
Cu	=	Cohesion of soil
D	=	Depth of foundation below ground level
d	=	Pile spacing
Ef	=	Pile group efficiency
Ep	=	Young's Modulus of pile
Es	=	Young's Modulus of soil
fs	=	Skin friction
G	=	Shear Modulus
I	=	Influence factors developed by Poulos
K	=	Pile stiffness factor
Ka	=	Active earth pressure coefficient
Ko	=	Earth pressure coefficient at rest
Kp	=	Passive earth pressure coefficient
Ku	=	Coefficient of lateral earth pressure to uplift
L	=	Length of Pile
l	=	Width of pile group
N	=	SPT value
$N_{c,q,\gamma}$	=	Bearing capacity factors
Pu	=	Applied load
qc	=	Static cone resistance
Qp	=	Total pile point resistance
qp	=	Unit pile point resistance
Qs	=	Total pile shaft resistance
qs	=	Unit pile shaft resistance
Qu	=	Ultimate bearing capacity
qu	=	Unit ultimate bearing capacity
Qul	=	Ultimate uplift capacity
R	=	Pile radius
$R_{k,h,b}$	=	Settlement correction factors developed by Poulos
S	=	Settlement
s	=	Ratio of pile spacing to pile diameter
sq	=	Settlement of a pile group

μ = Coefficient of friction between pile shaft and adjacent soil

γ = Soil unit weight

ν = Poisson's ratio

σ = Overburden pressure

σ'_{vo} = Effective overburden pressure

σ_{hf} = Horizontal pressure on a pile shaft at failure

ϕ = Angle of internal friction

δ = Angle of friction between soil and pile

ζ = Shape factors

τ = Shearing stress

τ_f = Shear strength

LIST OF FIGURES

CHAPTER 1

CHAPTER 2

CHAPTER 6

CHAPTER 7

LIST OF PLATES

CHAPTER 1

CHAPTER 3

CHAPTER 4

CHAPTER 5

CHAPTER 6

Chapter 1

Relation to Previous Work and Objectives of the Present Research

CHAPTER 1

RELATION TO PREVIOUS WORK AND OBJECTIVES OF THE PRESENT RESEARCH

1.1 Introduction and Relation to Previous Work

The current research forms an integral part of an ongoing investigation into pile behaviour at The Polytechnic of Wales.

The work carried out on the behaviour of piles in glacial tills by Perren (1978) showed that when piles are placed in granular materials, contractors are reluctant to terminate the pile in the said strata and prefer to found them deeper in underlying clays or soft rock formations. The main reasons for this are :

1. difficulties in obtaining a dry hole,
2. the granular material is loosened beneath the pile tip, and
3. the difficulties of ensuring the installation of good quality concrete.

There is little information on the behaviour of piles in this type of layered soil strata.

Meyerhof and Valsangkar (1977) extended current bearing capacity theory and semi-empirical methods of estimating ultimate pile loads in uniform soils to that of layered soils. This was subsequently compared with the results of model and field tests of piles in

non-uniform soils of two and three layers. The model study of Meyerhof and Valsangkar (1977) investigated the behaviour of 76mm diameter model piles penetrating through a weak stratum into dense sand. Additional tests were made on piles resting in a sand layer of various thicknesses underlain by a weak deposit, to study the resistance to punching of the piles into the underlying soil.

Meyerhof and Sastry (1978) investigated the behaviour of jacked and driven piles in multiple layers of clay and sand. The first part of their study dealt with the case of clay overlying sand and the second part with sand overlying clay.

The second part of Meyerhof and Sastry's (1978) investigation was found to be the closest pertaining to the ground conditions discussed by Perren (1978), i.e. granular material overlying clay. They have presented graphs showing the variation of total load, unit point resistance and radial stress with depth for a dense sand layer embedded in soft clay.

The main objective of the model pile study by Meyerhof and Sastry (1978), as with that of Meyerhof and Valsangkar (1977), was to investigate the failure mechanism when the pile fails by punching into the underlying soil as the pile approaches the sand-clay interface.

The amount of data available in the literature on piles in layered soils is limited particularly when dealing with bored piles.

As mentioned previously, Perren (1978) stated that contractors were reluctant to terminate bored piles in the gravel layer and preferred to found them in the underlying clay or soft rock formations. The bearing capacity of a pile of this type would

comprise the skin friction developed along the shaft of the pile in the granular material and the end bearing in the clay or soft rock.

The purpose of the study presented in this Thesis is to investigate the load transfer mechanism along the shaft of a bored pile and the subsequent soil displacements in the granular stratum when the pile is end bearing in a clay layer.

The skin friction developed in the granular material would only be affected by the end bearing of the pile in the clay, if the effect of the end bearing was to cause movement of the interface between the clay and the granular soil. This movement could be either in the downward direction, caused by dragdown of the granular material into the clay layer, or in the upward direction caused by heaving in the clay or both.

Tomlinson (1977) has suggested that a sand skin could be dragged into an underlying clay layer to a depth of three pile diameters as shown in Figure 1.1.

Heave of the soil surface is caused by a rupture of the underlying soil due to foundation loading. The base of the pile can be located either at the surface or at some depth in the clay.

It is proposed to examine firstly the case where the foundation is located at the soil surface as follows. Prandtl (1920,1921) studied the process of penetration of hard bodies, such as metal punches into another softer, homogeneous, isotropic, material from the viewpoint of plastic equilibrium. This classical work known as Prandtl's theory has also been applied for estimating the bearing capacity of soils. The procedure is based on an analysis of the

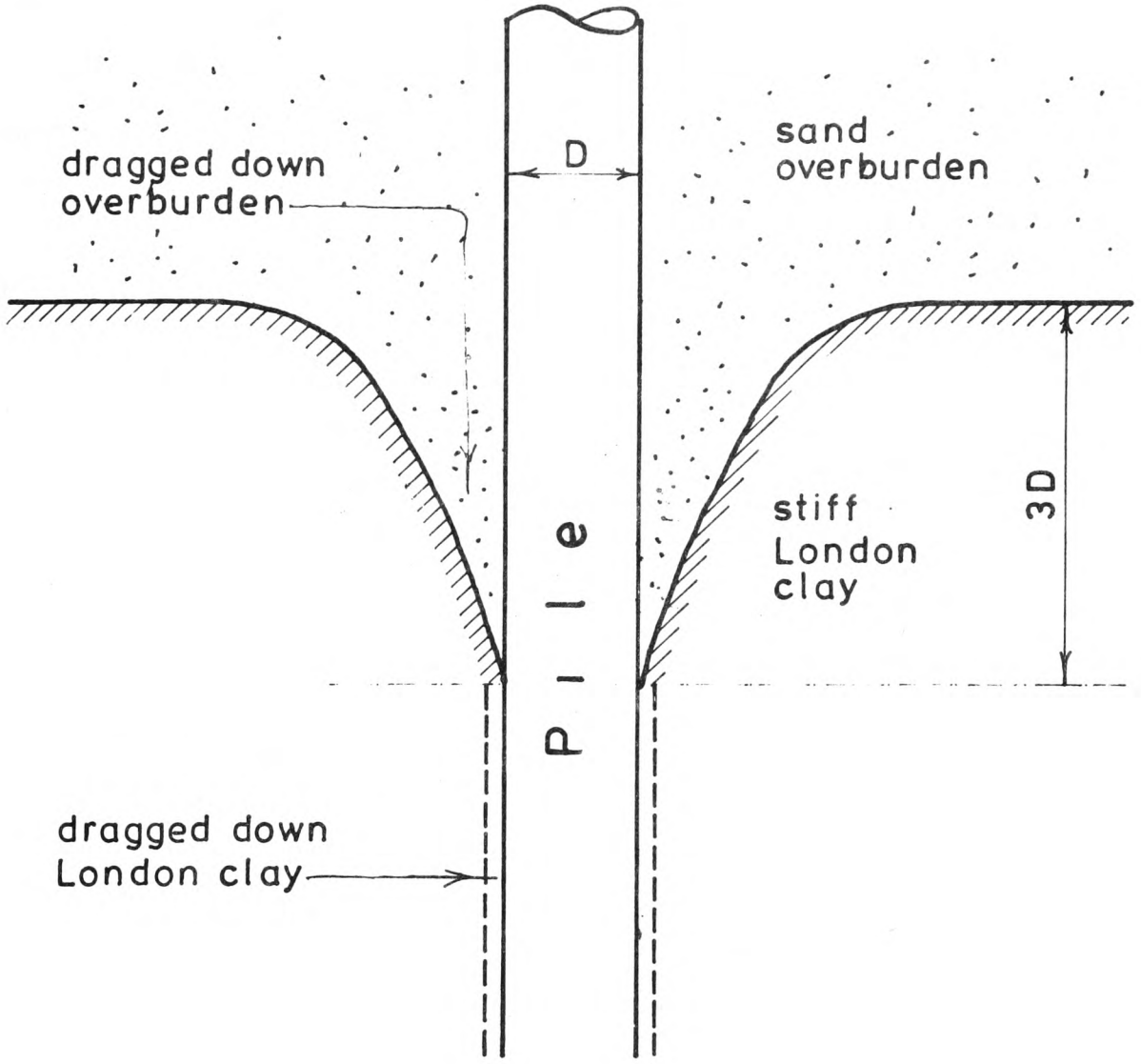

FIGURE 1.1

DRAGDOWN OF OVERBURDEN SOIL ON PILE SHAFT IN CLAY

(from TOMLINSON 1977)

stress conditions for the ultimate failure of the soil. The punch represents the foundation while the softer material represents the soil. When the shear strength of the soil is reached due to loading of the foundation, a two-sided expulsion of soil from underneath the base of the footing may take place according to the mode given in Prandtl's system shown in Figure 1.2, this implies a certain degree of symmetry.

According to Prandtl's theory the triangular wedge (or a cone in the case of a pile) of soil beneath the base of the foundation behaves as a rigid body, and under loading would move downwards with no deformation. This would cause the logarithmically spiralled wedges to deform plastically, exerting a force on the boundary between the zones of plastic flow and the passive state. The volume change in the plastic region of the body is assumed to be zero so that the remaining deformations can be construed as plane sliding along the rupture surface. This in turn would cause heaving of the soil surface. If the soil surface was the interface between a clay layer and overlying sand stratum this heaving of the interface would cause a compaction of the sand in the area above the heaved clay thus influencing the development of skin friction in this region.

Terzaghi (1943) modified Prandtl's theory for shallow foundations. He took into account the cohesion, weight and friction of the soil and assumed a perfectly rough foundation base. Meyerhof (1951) has subsequently modified the theory to allow for shallow and deep foundations. This is based on the plastic theory, the plastic zones near a deep foundation in a cohesive soil are as shown in Figure 1.3. The distance above the pile base where the failure surface

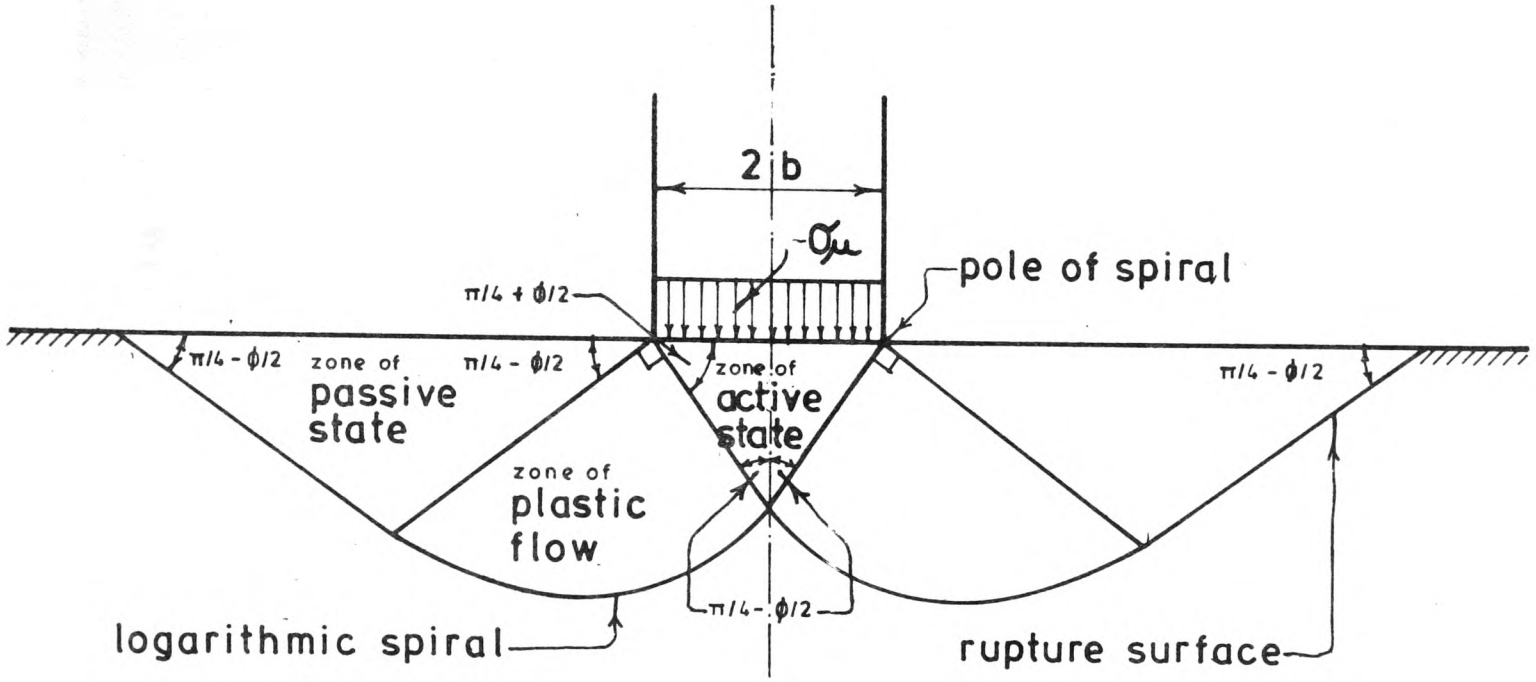

FIGURE 1.2

PRANDTL'S SYSTEM FOR A (ϕ-C) SOIL

(from JUMIKIS 1969)

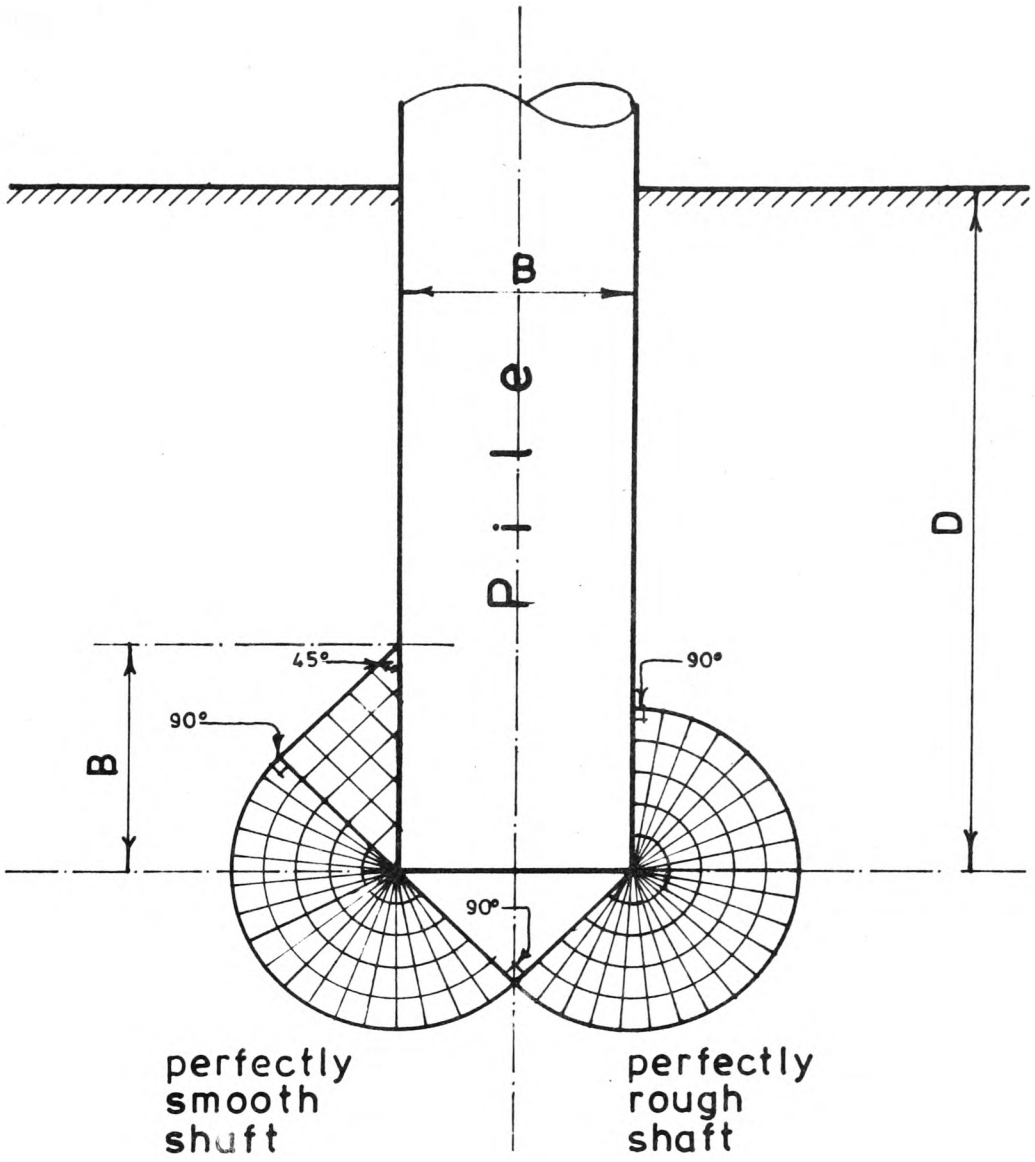

FIGURE 1.3

PLASTIC ZONES NEAR A FOUNDATION WITH A ROUGH BASE IN A PURELY COHESIVE MATERIAL

(from MEYERHOF 1951)

intersects the pile shaft, for the extreme case (i.e. for a perfectly smooth shaft) is equal to the pile diameter, see Figure 1.3.

Meyerhof (1951) stated that the movement of the material in the plastic zones is parallel to the failure surface. As the depth of the foundation increases the direction of the soil movement changes from a general downward and outward direction to an upward one, which for a deep foundation is practically vertical; a movement towards the shaft is, however, unlikely in practice (see Figure 1.3). In the vicinity of a smooth shaft the soil particles are moving upwards while along a rough foundation the particles are being dragged down at the pile soil interface.

According to Tsytovich, et al. (1974) the settlement of a foundation in a C-ϕ soil (i.e soil possessing both cohesion and internal friction) is attributed to two factors :

1. the settlement of a linearly deformable area lying below the foundation base, area A in Figure 1.4, and

2. the deformation of the trapezoidal area B, expanding in the horizontal direction owing to the movement of the top part of the shear areas C. The extent of this movement is dependent upon the consolidation of the areas D.

For the case where a pile is founded in a non-uniform soil mass and the pile base is located at the interface between the two soil layers Prandtl's theory can again be employed with the modification of a surcharge (representing the overburden soil) acting on the horizontal plane passing through the pile base. This is illustrated

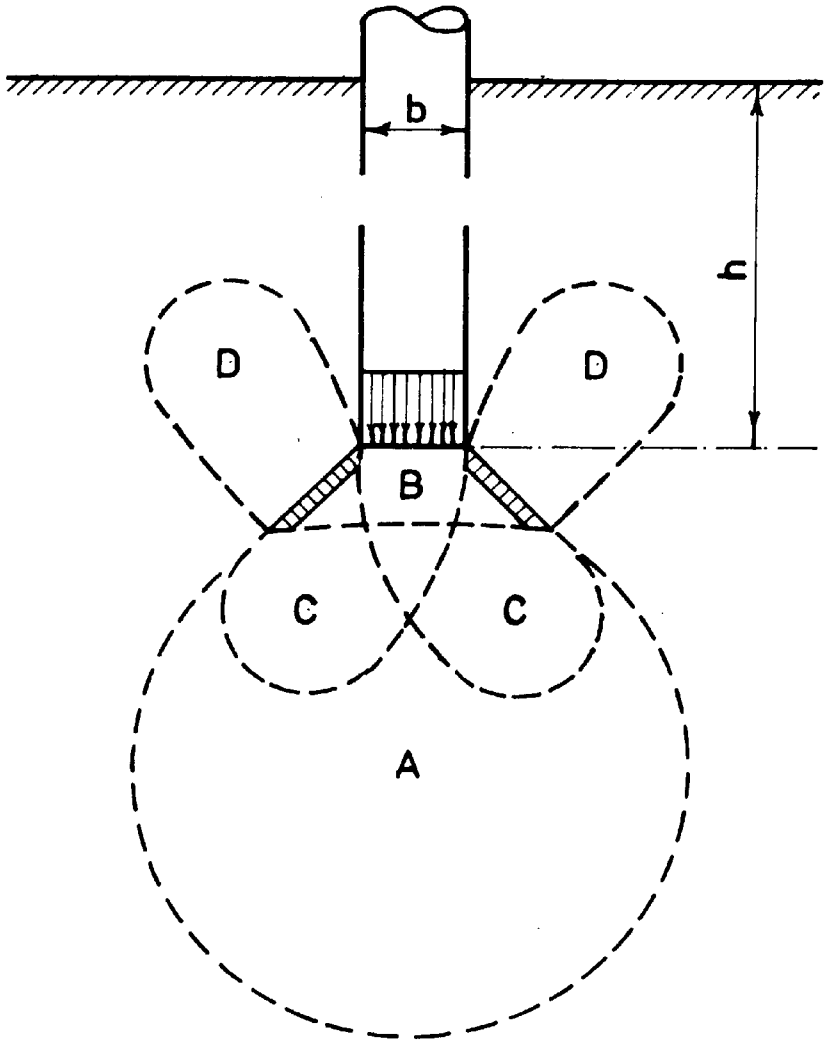

FIGURE 1.4

DIAGRAM FOR AN APPROXIMATE DETERMINATION OF DEEP FOUNDATION SETTLEMENT (from TSYTOVICH, BEREZANTSEV, DALMATOV and ABELEV 1974)

in Figure 1.5.

The upward movement of the passive wedges, due to sliding along the rupture surface (Figure 1.2), of a pile driven into clay, will cause a bulging of the ground surface, since consolidation around the pile is insignificant due to the slow disipation of pore pressures. The protrusion of the ground surface takes some time to occur and often lasts for several days after sinking of the pile. However, Tomlinson (1977) has stated that heaving and the development of high pore pressures do not occur when bored and cast-in-situ piles are installed. This is due to the small volume of soil which is displaced due to pile settlement under loading in comparison to the large displacement volumes for driven (displacement) piles.

For the research study described in this Thesis, for each pile loading test the 114mm diameter steel pile was driven to a penetration of 12mm. This accounts for a displacement volume of $4.9 \times 10^{-4} m^3$. Assuming the heave at the top of the clay layer to be 100% of the displacement volume and the cross-section of the heave to be in the form of a parabola extending to about 6 pile diameters from the pile centre line (as found by Cooke and Price 1973 and others), the average height of the heave would be approximately 0.3mm with a maximum height of 0.6mm, see Figure 1.6.

As the depth of the base of the pile in the clay stratum increases the likelihood of any heave occurring at the clay-sand interface decreases due to a larger amount of clay available for consolidation in area D of Figure 1.4. In general contractors prefer to terminate bored-and-cast-in-situ piles in the underlying clay stratum to ensure a better quality concrete, as discussed on page 1.1.

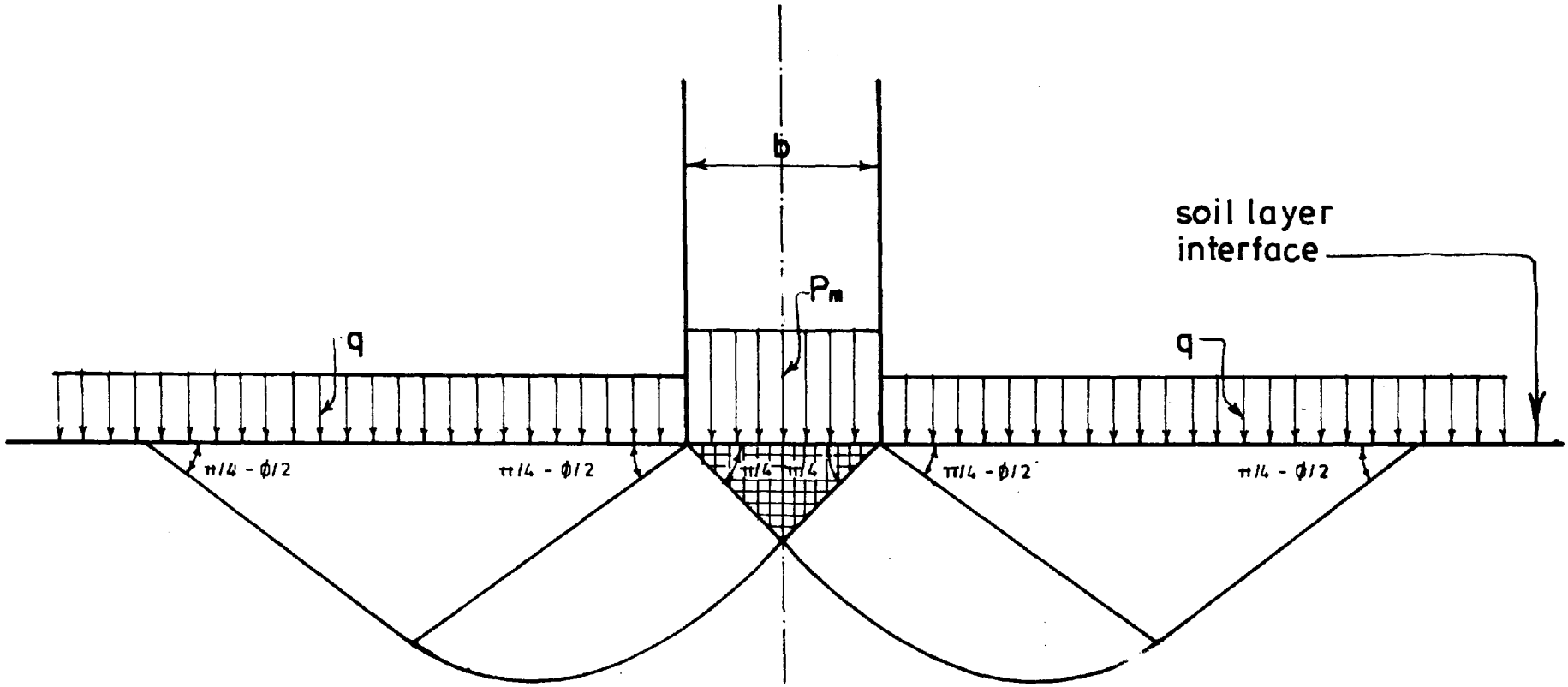

FIGURE 1.5

ADAPTION OF PRANDTL'S SYSTEM FOR A PILE IN LAYERED SOIL WITH ITS BASE LOCATED AT THE SOIL INTERFACE (from TSYTOVICH, BEREZANTSEV, DALMATOV and ABELEV 1974)

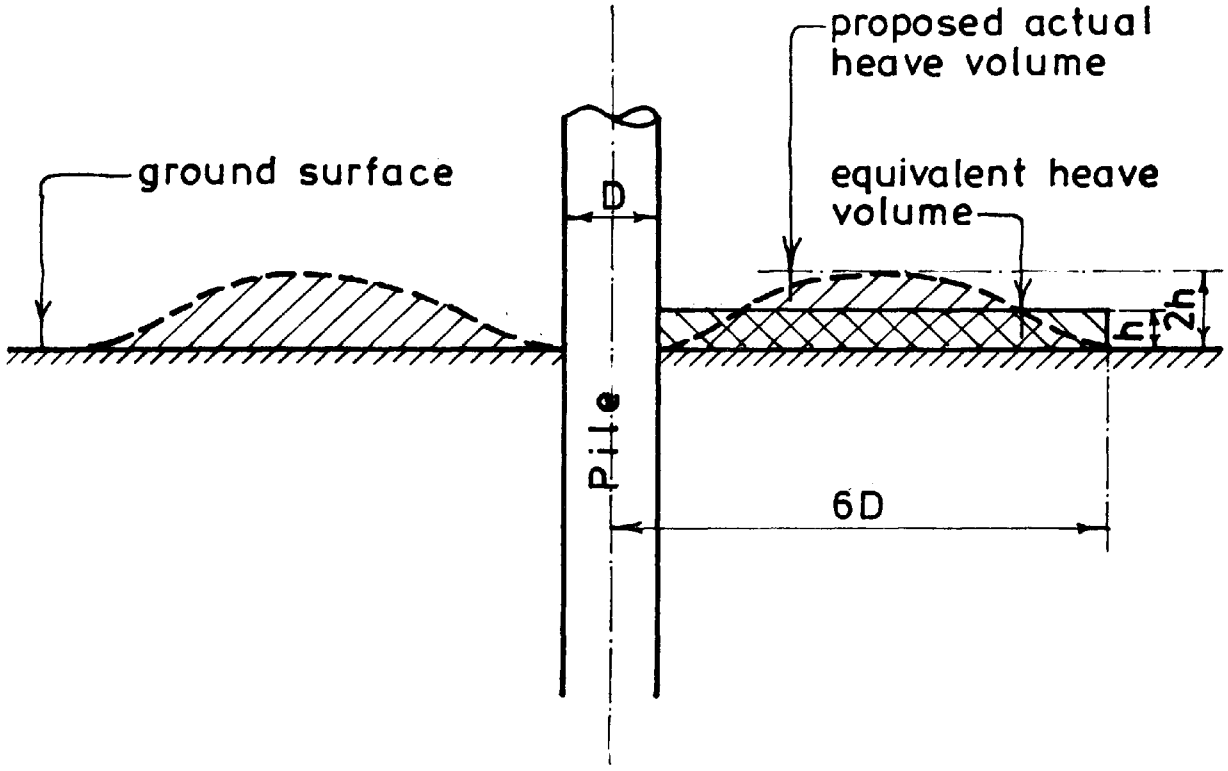

FIGURE 1.6

POSSIBLE CROSS-SECTION OF HEAVED CLAY SURFACE
DUE TO PILE DRIVING

For the present study the assumption has been made that this possible small amount of heaving or bulging of the clay surface, will not take place due to local consolidation of the clay and the weight of the sand overburden.

Assuming, therefore, that the heave of the clay due to the penetration of the pile is negligible it was decided to eliminate the end bearing resistance as well as any possible dragdown of the overlying sand.

During the course of a pilot study, different methods of eliminating end bearing were explored in a series of experiments. These are described in the next section.

To simulate the conditions of a bored pile, the soil was placed around the pile rather than the pile being driven into the soil.

1.2 Pilot Study

The main objectives of the pilot study were :

1. to gather background information for the larger scale experiments to follow,

2. to determine the most efficient means of eliminating end bearing so that the development of skin friction in a granular soil could be investigated independently.

The pilot study also provided for the testing of the equipment and instrumentation to be used in the semi-fullscale tests to follow.

The pilot experiments were carried out in the 0.60 m deep by 0.45 m diameter perspex tank shown in Figure 1.7. Three solid steel model piles (or rods) with diameters of 9.5mm, 12.7mm and 15.9mm were driven into dry Leighton Buzzard sand by a 100 kN triaxial machine at a speed of 0.6mm/min.

Three different methods of end bearing elimination were considered before a satisfactory solution was achieved.

Initially an attempt was made to simulate the situation using a polystyrene block instead of a clay base. The end bearing resistance of the polystyrene was found to be independent of the overburden pressure and, hence, its value could be determined in a separate test. The skin friction could then be determined at any stage by subtracting the end bearing resistance from the applied load. However, a number of problems were encountered. When the test was carried out the sand was found to run into the voids in the sides of the hole in the polystyrene formed by the driving of the pile. This gave rise to an additional frictional resistance on the pile. This movement of the sand also reduced the support from the sand surrounding the pile.

It was next decided to use a gelatine base. However, it was found that the load/penetration curve for a pile driven into a gelatine base was very irregular. The gelatine was found to initially adhere to the pile, then it suddenly yielded producing a bulb of slip line cracks. Being hygroscopic, the gelatine was also found to be unstable. Its strength and volume depended upon humidity and temperature.

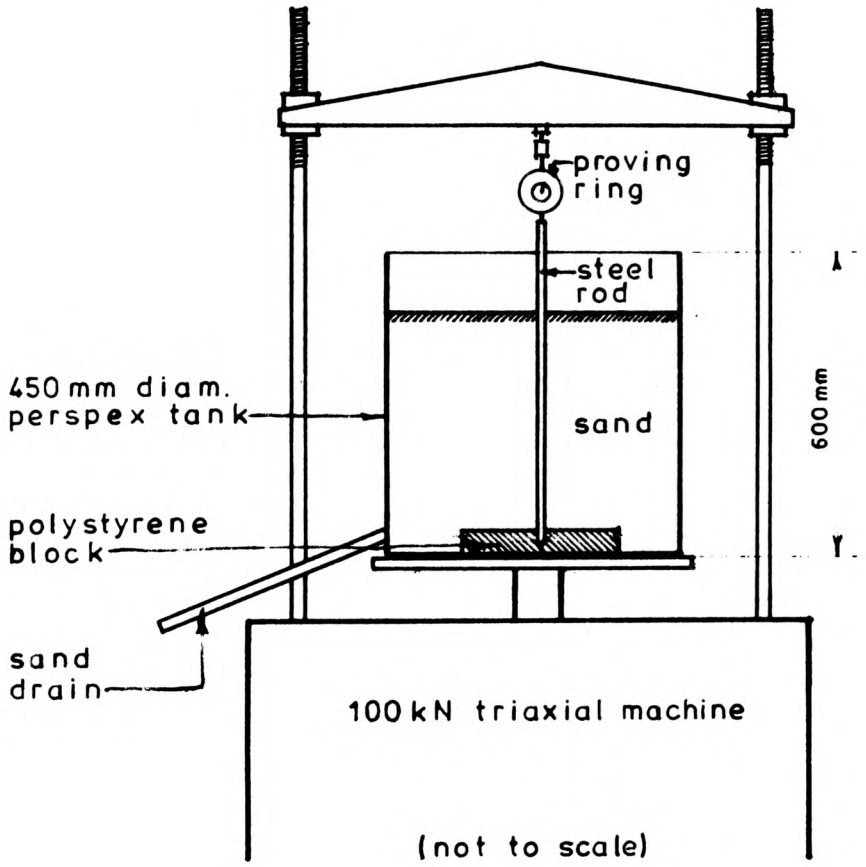

FIGURE 1.7

PILOT STUDY APPARATUS

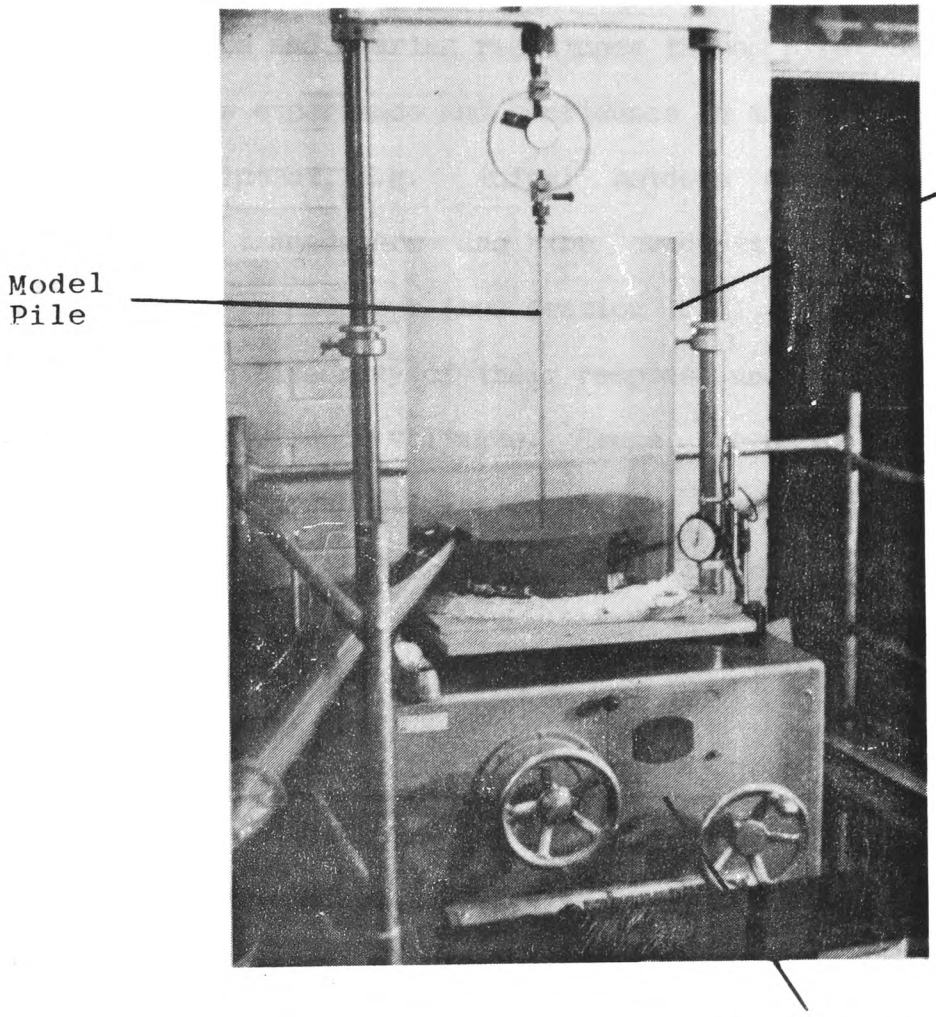

PLATE 1.1

PILOT STUDY APPARATUS

Having encountered these problems with the different materials tested it was concluded that the best method of investigating the skin friction was to eliminate the end bearing resistance by passing the pile into a cylinder provided with a frictionless oil seal for keeping the sand out. No end bearing resistance was measured in this way and the sand surrounding the pile was not disturbed. In addition to eliminating the end bearing resistance these pilot experiments gave the candidate experience and confidence in the use of transducers and recording equipment, e.g. tufnel holders were developed for the displacement transducers and the conductive plastic linear motion potentiometer transducers (see section 6.5) were selected for use because of the linearity of their response and their adaptability to a varying range of input voltages. Hence, the need for an additional conditioning unit was eliminated and the transducers could be operated in the same voltage range as the strain gauges and other electrical recording equipment.

1.3 Objectives and Outline of the Present Research

The semi-fullscale study investigated by the candidate was the development of the measurement of the skin friction resistance along a pile shaft and its effects on the surrounding soil. This involved the design and manufacture of a composite pile comprising eight individual load cells. These load cells allow for the measurement of the load along the length of the pile. The pile was fabricated from 114mm diameter, 4.5mm thick steel pipe.

The pile was assembled in a 3m diameter by 3m deep concrete tank with the lower end of the pile located in a frictionless cylinder. After placing each layer of sand, the pile was further driven through the sand into the above mentioned cylinder located in the bottom of the tank. This cylinder then eliminated end bearing, and the resulting development of skin friction was recorded. The displacement of the sand medium as well as the dissipation of the load along the pile was measured at two ranges of sand density.

In this way it was possible to measure the load transfer mechanism from the point of application on the top of the pile to its dissipation in the sand medium, and to monitor the effects of the movement of the pile and loads applied to the soil on the soil properties and structure.

Chapter 2

Literature Review

CHAPTER 2

LITERATURE REVIEW

2.1 Introduction to Literature Review

At the present time, the amount of available literature on deep foundations is vast. The academic and technological progress in this field in the past century is immense. In the light of this, the scope of this review of literature has been restricted to; a summary of past and present day formulae, and the general concepts which are relevant to the topics of this present research work.

2.2 Early Formulae

The development of "static" formulae over the past century to calculate the ultimate bearing capacity of pile foundations, has primarily been accomplished by using the principles of soil mechanics.

The factors influencing the load carrying capacity of a pile are :

1. As a pile is loaded, the applied load is transferred through the pile shaft to the pile base, causing a downward displacement of the base. This downward movement is opposed by the shearing resistance of the soil.

2. As the pile moves downward, tangential forces act on the pile shaft to oppose the above movement. These forces are caused by skin friction and adhesion between the pile shaft and the soil.

3. The volume of soil displaced by a pile of length D (embedded length) is supported by the soil at the level of the pile base prior to pile installation. This volume of soil produces a pressure on the horizontal plane at depth D equal to $\bar{\gamma}D$; where $\bar{\gamma}$ is the average density of the soil from the surface to depth D. Prior to installation of the pile, the soil is in a state of equilibrium at depth D, supporting the pressure $\bar{\gamma}D$. This will cause a vertical pressure to act on the base of the pile (see Figure 2.1).

Taking these three factors into account, the ultimate bearing capacity of a pile is generally assumed to be reached when

$$Pu + W = q_s As + q_p Ab + \bar{\gamma}DAb \quad (2.1)$$

where Pu = Applied load

W = Weight of the pile

q_s = Ultimate value of tangential force per unit area of the shaft due to adhesion and skin friction.

q_p = Ultimate value of resistance per unit area of base due to the shearing of the soil.

As = Shaft area

Ab = Base area

The terms W and $\bar{\gamma}$DAb in equation (2.1) are generally assumed to be equal and are disregarded.

Therefore, equation (2.1) becomes

$$Pu = q_s\ As + q_p\ Ab \quad (2.2)$$

In order to find a solution for the ultimate bearing capacity of a pile (equation (2.2)), engineers at the turn of the century assumed the soil to be an ideal material. The assumption was made that the soil was a uniform, dry, granular material. The facts that the soil properties changed due to the installation of the pile, the soil compacted or could dilate, and was often saturated, were generally ignored. The time dependency of the soil properties, clay in particular, were also not taken into consideration.

Idealizing the soil as stated above, Paton (1895) applied Rankine's theory of conjugate stresses to obtain a solution for the bearing capacity of a pile.

According to Rankine, when a state of plastic equilibrium is reached in a soil then

$$\frac{\sigma_1}{\sigma_3} = \frac{1 + \sin\phi}{1 - \sin\phi} \quad (2.3)$$

Where σ_1 , σ_3 = conjugate major and minor principal stresses respectively.

ϕ = angle of internal friction of the soil

Paton proposed that the normal pressure on the pile shaft at depth D is between

$$\gamma D \cdot \frac{(1+\sin\phi)}{(1-\sin\phi)} \text{ and } \gamma D \frac{(1-\sin\phi)}{(1+\sin\phi)}$$

depending on whether γD is the minor or major principal stress. If the lower value is taken for safety, then the total force on the pile of length D is

$$\frac{\gamma D(1-\sin\phi)}{2(1+\sin\phi)} \cdot As$$

and the total skin friction on the pile is

$$\frac{\mu\gamma D(1-\sin\phi)}{2(1+\sin\phi)} \cdot As \qquad (2.4)$$

where μ is the coefficient of friction between the pile shaft and the soil.

To obtain the ultimate bearing capacity at the pile base consider the equilibrium conditions under the base (see Figure 2.1).

$$\frac{q_p}{p} = \frac{1+\sin\phi}{1-\sin\phi} \qquad (2.5)$$

where q_p = major principal stress

p = minor principal stress

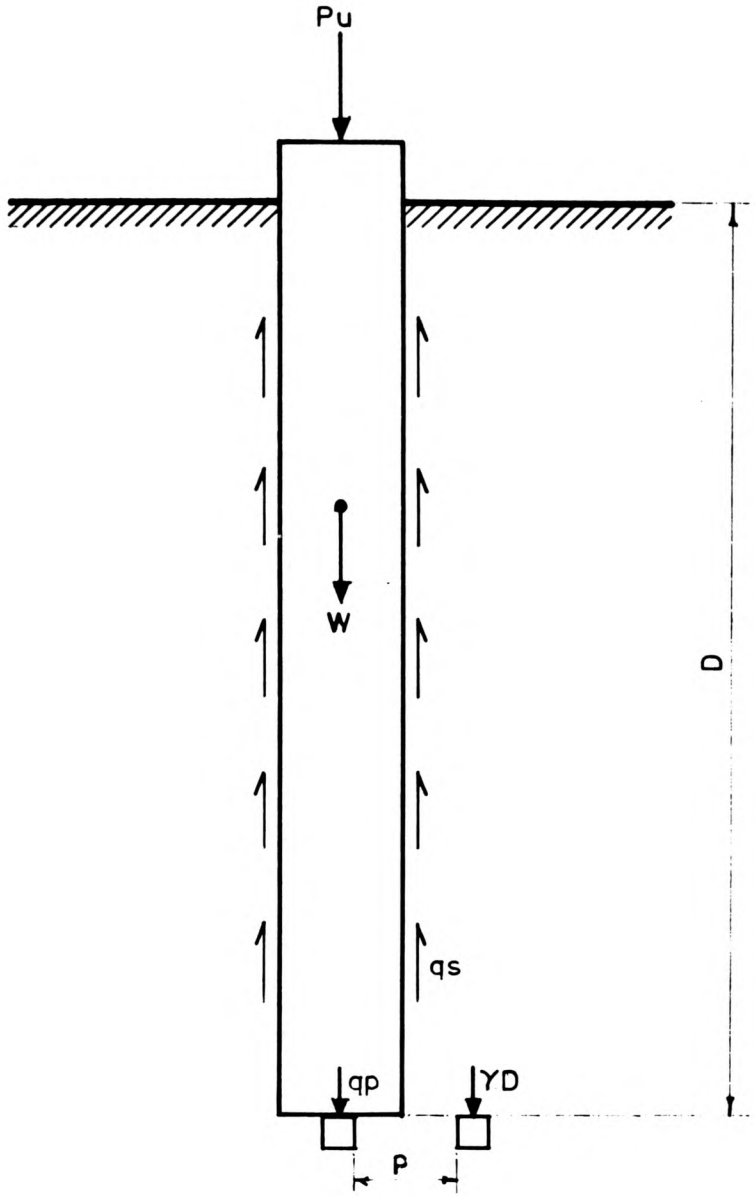

FIGURE 2.1

THE STRESS ON ELEMENTAL CUBES OF SOIL AT THE BASE OF A PILE

considering the equilibrium conditions to one side of the pile base

$$\frac{\sigma_1}{\sigma_3} = \frac{p}{\gamma D} = \frac{(1+\sin\phi)}{(1-\sin\phi)} .$$

Therefore, substituting into equation (2.5)

$$q_p = \gamma D \frac{(1+\sin\phi)^2}{(1-\sin\phi)^2} , \qquad (2.6)$$

the total load Pu can now be determined by substituting equations (2.4) and (2.6) into equation (2.2) :

$$P_u = \mu\gamma D \frac{(1-\sin\phi)}{2(1+\sin\phi)} \cdot As + \gamma D \frac{(1+\sin\phi)^2}{(1-\sin\phi)^2} \cdot Ab. \qquad (2.7)$$

The main source of error with the above equation (2.7) was in the determination of the angle of internal friction ϕ . At that time most engineers considered Rankine's ϕ to be the same as the observed 'angle of repose' of the soil whether it be a sand or a clay (Whitaker 1970).

2.3 Recent Theories

The amount of work done on determining the ultimate bearing capacity of piles in the past century reflects the various conditions a pile can be subjected to in the field. A number of factors accounting for the bearing capacity of a pile are :

1. pile size, shape, and surface roughness,

2. method of installation,

3. soil grain size distribution, shape, and

4. relative density of the soil.

Engineers in the past 100 years have proposed a number of formulae for calculating the ultimate bearing capacity of piles. Each formula is dependent on how the engineer has treated the factors mentioned above and their variations with time.

The problem of calculating the bearing capacity of the base of a pile Qp has been attempted in the past primarily by an approach based on the work by Prandtl (1920), (1921) and Reissner (1924). They presented a solution, to the problem of the penetration of a rigid stamp into an incompressible (rigid plastic) solid. This solution, first applied to the problem of bearing capacity of soils by Caquot (1934) and Buisman (1935) is usually written in the form (Vesic 1963) :

$$qp = CuN_c\zeta_c + qN_q\zeta_q + \tfrac{1}{2}BN\gamma\zeta\gamma \qquad (2.8)$$

where Cu = cohesion of soil

q = overburden pressure

γ = soil unit weight

B = foundation width

$\zeta_c, \zeta_q, \zeta_\gamma$ = shape factors

N_c, N_q, N_γ = bearing capacity factors

Both ζ and N factors are dimensionless functions dependent on the angle of shearing resistance of the soil (see Figure 2.2).

Terzaghi (1943) proposed an equation for the bearing capacity of a cylindrical foundation near the surface :

$$Qu = \pi R^2 (1.3CuN_c + \gamma_1 D_f N_q + 0.6\gamma R N_\gamma) + 2\pi R q_s D_f \quad (2.9)$$

where R = pile radius

γ = unit weight of soil

qs = unit skin friction

Cu = soil cohesion

D_f = embedded depth of pile

N_c, N_q, N_γ = bearing capacity factors dependent on ϕ

$\gamma_1 = \gamma + 2\frac{q_s + n\tau}{(n^2-1)R}$ = adjusted unit weight of the annular area of soil surrounding the pile, of thickness nR. This change in unit weight is caused by the skin friction between the soil and pile shaft and shearing stresses τ on the outer boundary of the annular mass of soil being dragged down. The value of τ is very uncertain and depends on the volume compressibility of the soil.

Terzaghi and Peck (1967) modified the point bearing component of Terzaghi's (1943) equation by changing the shape factor for the cohesive term to 1.2. Therefore, the point bearing capacity of a pile passing through a compressible soil, end bearing in a dense or stiff soil is, for a circular pile of radius R,

$$qp = 1.2CuN_c + \gamma D_f N_q + 0.6\gamma R N_\gamma \quad (2.10)$$

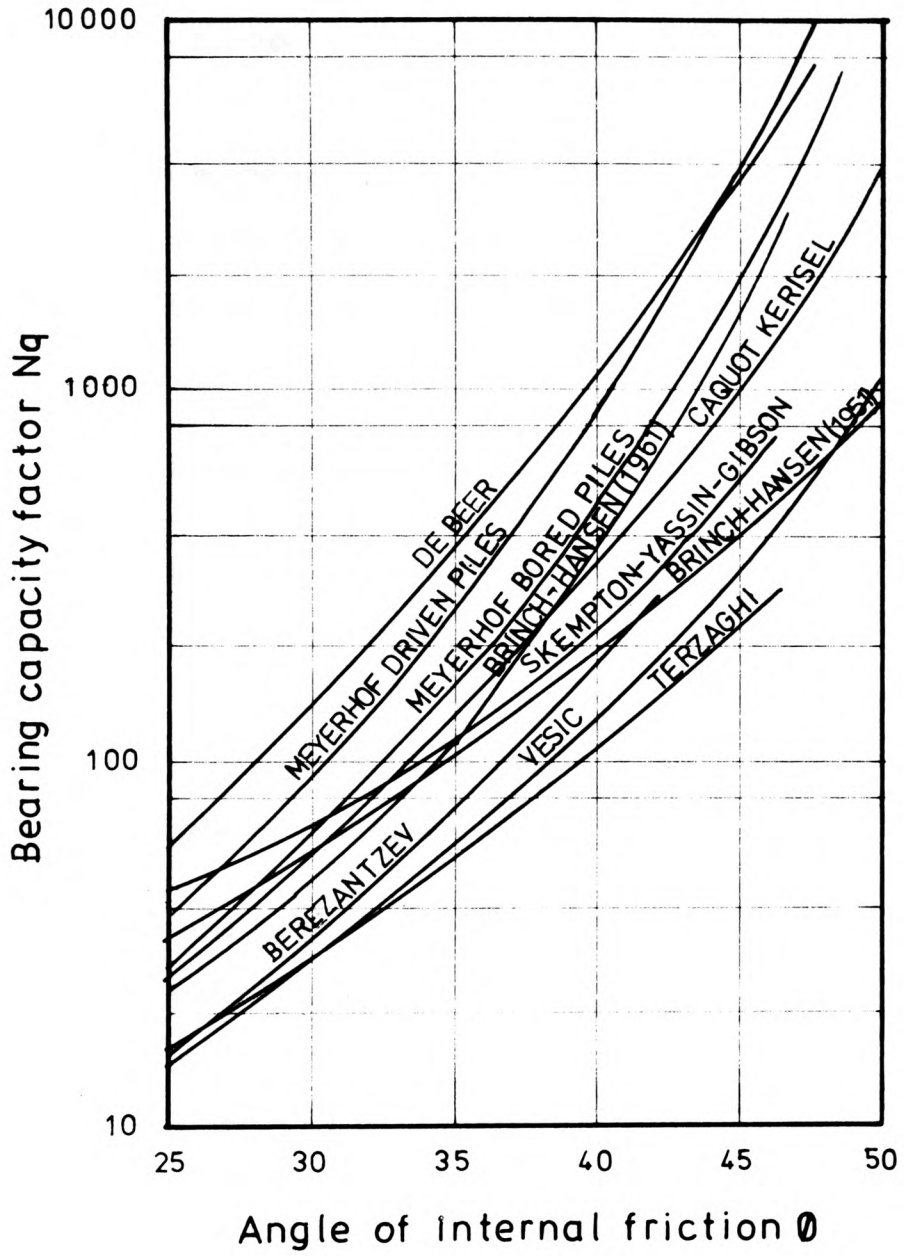

FIGURE 2.2

BEARING CAPACITY FACTORS FOR DEEP CIRCULAR FOUNDATIONS

(FROM VESIC 1965)

and for a square pile, BxB,

$$qp = 1.2CuN_c + \gamma D_f N_q + 0.4\gamma B N_\gamma \qquad (2.11)$$

If the soil is homogeneous the shearing stresses set up in the soil above the base level, as a consequence of the displacements, have two significant effects :

1. They may alter the shear patterns so that the previously determined bearing capacity factors are no longer applicable, or

2. they may alter the intensity of the vertical pressure in the soil near the base of the pile.

The latter effect appears to be the more important and the term $\gamma D_f N_q$ should be changed to $\gamma_1 D_f N_q$ as described for equation (2.9).

Terzaghi and Peck (1967) define the value of the skin friction (qs) in equation (2.9) as;

$$qs = Ca + \bar{\sigma}_{hf} \tan\delta \qquad (2.12)$$

where Ca = adhesion per unit area

$\bar{\sigma}_{hf}$= average horizontal pressure on vertical surface at failure

δ = angle of friction between soil and pile.

Meyerhof (1951) proposed the expression for the base resistance per unit area of a deep foundation with a rough surface as,

$$qp = CuN_c + Ks\gamma DN_q + \tfrac{B}{2}\gamma N_\gamma \qquad (2.13)$$

where Cu = soil cohesion

Ks = coefficient of earth pressure on the shaft within the failure zone, varying between 0.5 for a loose soil and 1.0 for a dense soil

γ = soil unit weight

D = depth of foundation

B = breadth of foundation

N_c, N_q, N_γ = bearing capacity factors dependent on ϕ and D/B ratio.

In 1953 Meyerhof expressed the tangential force on the shaft of a pile due to both adhesion and skin friction as

$$qs = Ca + Ks\gamma D\tan\delta \qquad (2.14)$$

For a pile embedded in clay where the friction angle $\delta = 0$ the value of $qs = Ca$. Whereas, a pile in a noncohesive soil of $Ca=0$, the value of $qs = Ks\gamma D\tan\delta$.

The actual values of qs, Ca, Ks, γ, and δ vary along the pile shaft but for practical purposes Whitaker (1970) suggested that the average values could be used.

Therefore, the value of the ultimate bearing capacity for a soil possessing both cohesion and friction, according to Meyerhof, is;

$$Qu = As(Ca + Ks\gamma D\tan\delta) + Ab(CuN_c + Ks\gamma DN_q + (B/2)N_\gamma). \qquad (2.15)$$

In the case of deep foundations of normal proportions, D/B approximately 30 or more, B is small in relation to the other terms and can be ignored.

Meyerhof (1963) proposed the ultimate bearing capacity for an axially loaded single pile to be approximately,

$$Qu = (CuN_c' + Ks\gamma DN_q')Ab + qsAs. \qquad (2.16)$$

Values of N_c' and N_q' were plotted on a graph versus ϕ for the case where the base was embedded in a load-bearing stratum at a depth of at least $D = 4\sqrt{N_\phi}B$.[1] In other cases, the value of the bearing capacity factors can be interpolated for different ratios of D/B in the usual manner.

If the soil properties vary around the base of the pile Meyerhof (1963) suggests that the average values for the bearing capacity factors between four times the pile diameter above and one times the diameter below the pile base should be used in cohesionless soils, while a somewhat smaller range is sufficient in clays, as indicated by the corresponding failure zone.

Berezantzev et.al. (1961) proposed the expression for the ultimate point resistance of a single axially loaded pile in dense sand to be,

$$qp = Ak\gamma B + Bk\alpha_T\gamma_D D \qquad (2.17)$$

where Ak and Bk are dependent on and are given plotted against ϕ (see Figure 2.3)

γ = unit weight of soil at the pile footing

γ_D = unit weight of overburden soil

α_T is dependent on D/B and ϕ_D, and is given in tabular form (see Figure 2.3).

---

1. $N_\phi = \tan^2(\frac{1}{4}\pi + \frac{1}{2}\phi)$

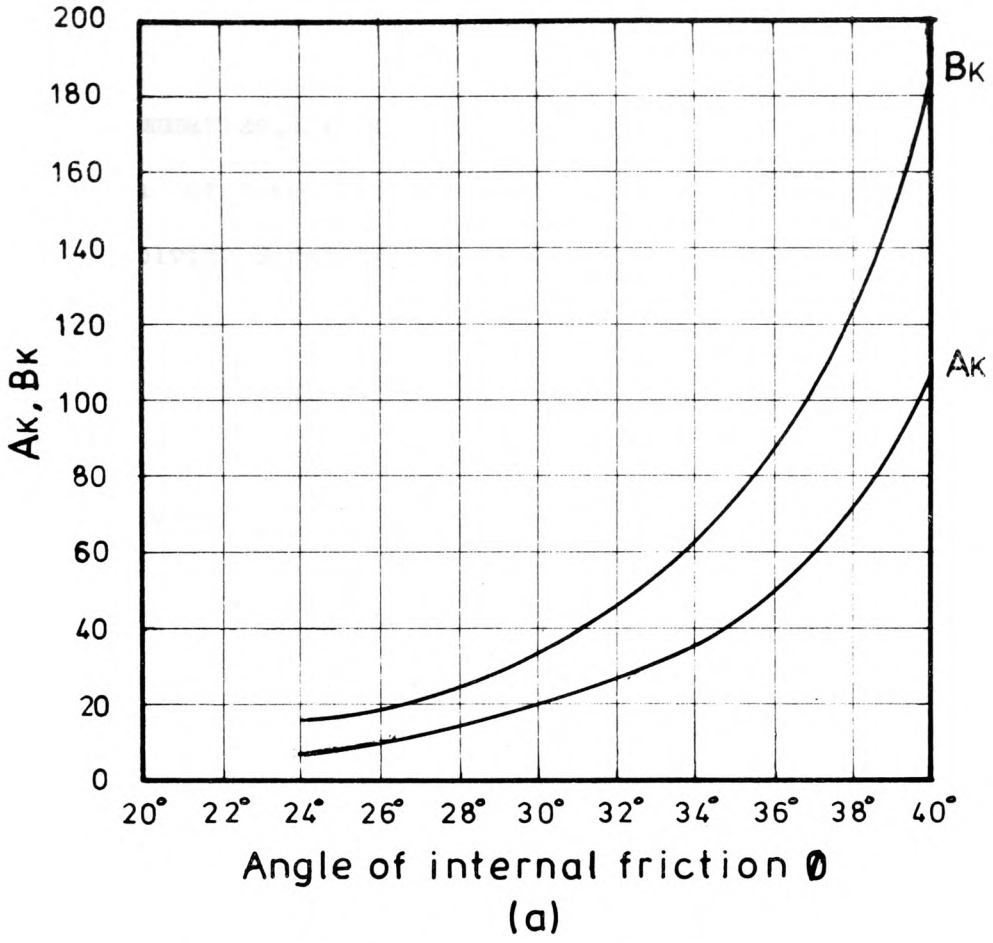

(a)

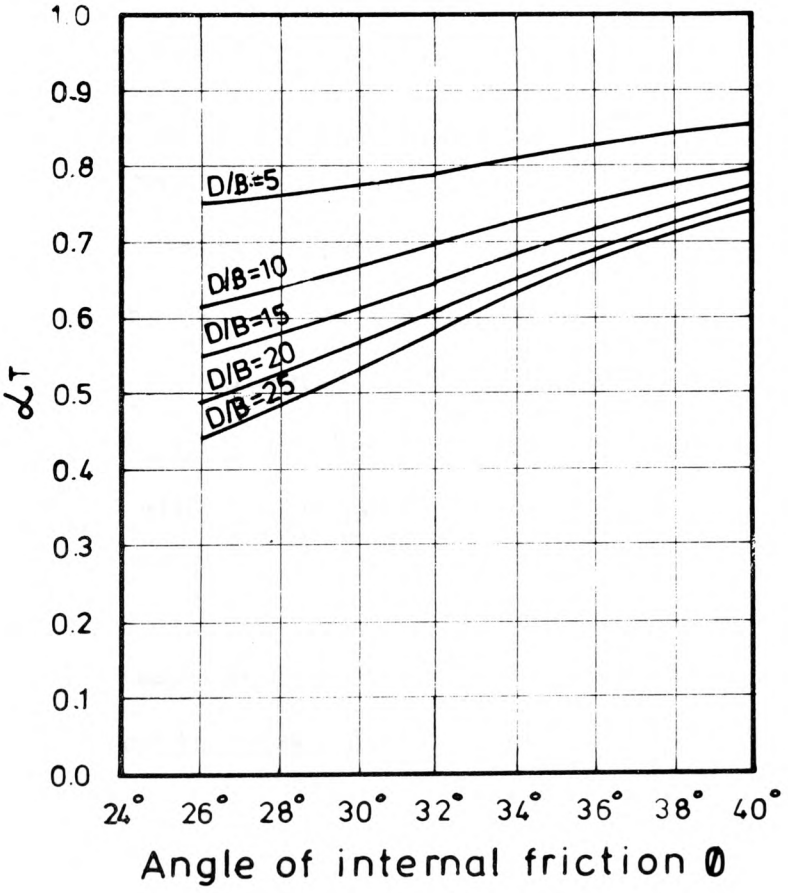

(b)

FIGURE 2.3

CURVES OF COEFFICIENTS FOR BEREZANTZEV et al (1961) BEARING CAPACITY EQUATION

To summarize, the equations for the ultimate bearing capacity per unit area of base, for piles of normal proportions D/B $\geq$ 30 (so that terms involving B can be ignored) are as follows:

Terzaghi	$qp = 1.3CuN_c + \gamma DN_q$	(2.18)
Meyerhof	$qp = CuN_c + Ks\gamma DN_q$	(2.19)
Berezantzev et al.	$qp = Bk\alpha_T\gamma_D D$	(2.20)

Equations (2.18) and (2.19) apply to soils having both cohesion and internal friction, while equation (2.20) is applicable only to a frictional soil.

2.4 Piles End Bearing in Cohesionless Soils

The proportion of the pile load carried by the tip of piles end bearing in a cohesionless stratum depends on a number of factors (see Section 2.3). Among these, the pile type, shape, surface roughness, and method of installation as well as the compressibility of the soil above and below the bearing statum are important. To account for these factors engineers have proposed empirical and theoretical constants and factors to be used in conjunction with the basic equations for the point bearing capacity of piles in cohesionless soils.

The most common equations for calculating the unit point bearing capacity of piles in cohesionless soils are;

Terzaghi	$qp = \gamma DN_q$	(2.21)
Meyerhof	$qp = Ks\gamma DN_q$	(2.22)

Berezantzev et.al. $q_p = Bk\alpha_T \gamma_D D$ (2.20)

The values in the equations (2.20) through (2.22) are as defined in section 2.3.

Ismael and Klym (1979) found the base resistance of a 1.1m diameter x 6.4m deep concrete pier to be only one half of the theoretically predicted value based on Terzaghi's bearing capacity formula. They suggested a possible reason for this could be due to the method of installation. The pier was placed by first augering through sand and using a bentonite slurry to stabilize the hole. Some loosening of the soil at the base occurs resulting in a reduction of the bearing capacity of the base. Ismael and Klym did, however, find good agreement between the measured value of base resistance and that predicted using Meyerhof's (1976) empirical correlation between standard penetration test values and ultimate bearing capacity (see Section 2.11).

Some investigators have found that the ultimate bearing capacity of the base of deep foundations in sand is not directly proportional to the depth of the base.

Vesic (1963) found a practically linear increase in the bearing capacity of the base with depth only at shallow depths, not exceeding approximately D/B = 4 for circular foundations, and D/B = 6 for rectangular foundations. As the foundation depth increases further, the rate of increase of the point resistance with depth decreases. At a relative depth of about D/B = 15 the point bearing capacity reaches asymptotically final values which appear to be functions of sand density only.

Franke and Garbrecht (1977) found no significant difference in the end bearing resistance of full scale piles (with and without enlarged bases) in medium strength sand, for 6m and 13m embedded lengths, when skin friction was eliminated by creating an annular space of a bentonite slurry around the pile shaft.

2.5 Piles End Bearing in Cohesive Soil

The contribution to the ultimate bearing capacity by the base resistance of a pile of normal proportions embedded in clay is generally small compared to that contributed by skin friction. With large diameter bored piles, and those with enlarged bases, however the amount of load carried by the base can far exceed that carried by the pile shaft, and calculation of the base resistance becomes important.

For the case suggested by Meyerhof (1951) when $\phi = 0$, then $N_q = 1$, $N_\gamma = 0$, and $Ks = 1$; and if the factor of 1.3 in Terzaghi's formula (equation (2.18)) is taken into the value of N_c, then both Meyerhof's and Terzaghi's equations (equations (2.18) and (2.19)) for the ultimate base resistance of a pile in cohesive soil may be reduced to the form

$$qp = CbN_c + \gamma D \qquad (2.23)$$

where Cb = soil cohesion at the base.

The main problem in calculating the base resistance from equation (2.23) is determining a value for the bearing capacity factor N_c. Skempton (1951), taking account of the various theoretical values, and those found by experiments on models, concluded that a semi-empirical

value of $N_c = 9$ was probably sufficiently accurate for practical purposes. Cooke and Price (1973) found the bearing capacity factor N_c in London Clay to vary with depth as follows:

depth of penetration	0.35m	1.7m	2.7m	3.9m
Nc values	6.5	9.5	13.1	16.4

The ultimate value of the base resistance calculated will depend to a great degree on the value chosen for N_c, while the percentage of applied load carried by the base will depend on the dimensions of the pile and its method of installation.

2.6 Skin Friction of Piles in Cohesionless Soils

The skin friction resistance of a pile whose shaft is in contact with a granular soil depends on a number of factors:

1. size, shape, and surface roughness of the pile, (Broms and Silberman 1964),
2. method of pile installation (Hunter and Davisson 1969),
3. relative density, gradation, effective grain size, composition, and moisture content of the soil (Tejchmen 1969, Vesic 1963, Coyle and Sulaiman 1967, Potyondy 1961 and Broms and Silberman 1964),
4. intensity of normal load. (Coyle and Sulaiman 1967 and Potyondy 1961), and
5. embedded pile length (Vesic 1963).

The basic expression for the tangential force per unit area acting on the pile shaft is :

$$qs = Ca + Ks\gamma D\tan\delta \qquad (2.14)$$

where Ca = adhesion per unit area.

δ = angle of friction between the soil and pile shaft.

Ks = coefficient of earth pressure.

In cohesive soil, $\delta = 0$ so that $qs = Ca$

In non-cohesive soil, $Ca = 0$ so that $qs = Ks\gamma D\tan\delta$.

Researchers have developed a number of equations and methods for calculating the skin friction on a pile shaft. The various factors used in conjunction with equation (2.14) are due to the method of determining values of qs, Ca, Ks, γ , and δ; and their variations along the pile shaft. Meyerhof (1953) suggested that for practical purposes the average values along the pile shaft are adequate.

Dörr (1922) assumed that the frictional resistance qs, which develops at the surface of a pile in cohesionless soil, is proportional to the lateral effective pressure σ'_h ,

$$\text{therefore } qs = \sigma'_h \tan\delta \ .$$

Since, the lateral effective pressure can be expressed in terms of the vertical effective pressure σ'_v and the coefficient of lateral earth pressure (K) as $\sigma'_h = K\sigma'_v$; and σ'_v at depth D can be expressed as $\sigma'_v = \gamma' D$ where γ' is the effective unit weight of the soil, then

$$qs = K\acute{\gamma}D\tan\delta. \qquad (2.24)$$

Brinch Hansen (1968) derived the following equations for the skin friction on the shaft of a pile in compression,

$$\tau_D = \gamma' D N^c_{m\gamma} + pN^c_{mp} + CuN^c_{mc} + CaN^c_{ma} \qquad (2.25)$$

and in tension,

$$-\tau_D = \gamma' D N^t_{m\gamma} + pN^t_{mp} + CuN^t_{mc} + CaN^t_{ma} \qquad (2.26)$$

where τ_D = skin friction at depth D

γ' = effective unit weight of soil

p = uniformly distributed surcharge on soil surface

Cu = cohesion of soil

Ca = adhesion between pile and soil

ϕ = plane angle of friction for soil

δ = angle of friction between pile and soil

$\mu = \tan\delta$ = coefficient of friction between pile and soil

K's are earth pressure coefficients dependent on method of installation and initial stresses in the soil

$Ko = 1-\sin\phi$ = coefficient of earth pressure at rest

$N^c_{m\gamma} = \mu Km\gamma/(1-\mu Ko)$

$N^c_{mp} = \mu Kmp/(1-\mu Ko)$

$N^c_{mc} = \mu Kmc/(1-\mu Ko)$

$N^c_{ma} = 1/(1-\mu Ko)$

$N^t_{m\gamma} = \mu Km\gamma/(1+\mu Ko)$

$N^t_{mp} = \mu Kmp/(1+\mu Ko)$

$N^t_{mc} = \mu Kmc/(1+\mu Ko)$

$N^t_{ma} = 1/(1+\mu Ko)$

Values for the coefficients K and N can be determined through back analysis of model pile tests. Tejchman (1969) explains a method of determining a relationship between Nm and ϕ (or the void ratio e) from a number of model tests in sand. For the particular soil used, density range, and method of pile installation, Tejchman (1969) found $N_m^c = 0.181e^{-2.84}$ and $N_m^t = 0.278e^{-1.59}$.

Ismael and Klym (1979) expressed the ultimate skin friction resistance of piles in sand as

$$qs = \tfrac{1}{2}\gamma' DKc\tan\phi. \qquad (2.27)$$

They calculated a value of Kc in compression of 2.1 from back analysis of field tests and a value in uplift of 1.6 in the same manner. Ismael and Klym did suggest however, that Kc increased with increasing penetration and increasing density.

Potyondy's (1961) equation for the skin friction on the shaft of a pile embedded in a soil containing both skin friction and cohesion (c-ϕ soil) is expressed as

$$qs = fcCu + \sigma_h \tan(f_\phi \phi) \qquad (2.28)$$

where fc and f_ϕ are coefficients derived by Potyondy (1961)

σ_h = normal stress.

For sand $C_u = 0$, and $qs = \sigma_h \tan(f_\phi \phi)$. The values of fc and f_ϕ are dependent on the roughness of the pile, and the type and density of the soil.

The value of the ultimate frictional resistance acting on a pile does not only depend on the magnitude of the relative displacement between the pile and the surrounding soil, but also on the direction of this displacement. Brinch Hansen (1968) derived separate equations for the skin friction acting on the pile shaft for pushing and pulling of the pile (see quation 2.25 and 2.26).

Broms and Silberman (1964) found at low relative densities ($D_r<0.35$) the skin friction in compression to be three times the value measured in tension, and thirty times the value measured in torsion. While, for higher relative densities ($D_r>0.70$) they found the skin friction in compression to be twice that in tension and four times the value measured in torsion.

Müller (1939) found the skin friction of steel piles with a smooth surface to be eight times as high in compression as in tension, and for concrete piles with a rough surface he found the compression value to be five times the tension value. Tejchman (1968) stated that the skin friction in compression was about twice the value found in tension. Hunter and Davisson (1969) found the skin friction observed during compression to be approximately 30% higher than that observed in tension for 300mm to 500mm diameter steel piles in sand.

This difference in skin friction found in compression and tension tests is due to the fact that when a pile is pushed into the ground, the shear forces transmitted from the pile to the soil must increase the vertical load on the lower layers. This increase in effective overburden pressure causes an increase in the lateral pressure acting normal to the pile at the lower levels. In the case of a pulling test, as the skin friction develops it relieves part of the overburden

pressure which acts close to the loaded pile, (Brinch Hansen 1968, Broms and Silberman 1964, and Terzaghi and Peck 1967).

Tejchman (1969) has shown that the sequence of loading must be taken into consideration when a pile is to be subjected to a number of loading modes. Although the loading history of a pile tested in tension is not essential, its effects on piles tested in compression are significant. Tejchman further suggests that the effects of negative skin friction on a pile are similar to that of a primary tension test and unfavourably alter the development of the frictional resistance of the pile. The amount of reduction caused by negative skin friction depends on the amount of displacement between the pile and soil (while negative skin friction occurred) and the soil density. Tejchman (1969) found the average value of skin friction for a compression test caused by first conducting a primary tension test to be about 67% of the value when a tension test had not been performed.

A number of investigators have found that, as the pile is pushed into the soil the skin friction increases to a maximum value and then remains constant for any further penetration. Vesic (1963) found the skin friction measured along the pile shaft appeared to intially increase linearly to a limiting depth of about 4 pile diameters. Beyond this depth the skin resistance turns sharply into a practically final value varying with sand density only. Vesic found the amount of displacement needed to reach the ultimate skin resistance to be independent of the foundation width, depth, and sand density. He found these displacements to be in the order of about 7.5 to 10mm for circular foundations, and about half that for rectangular foundations, to achieve ultimate skin resistance.

Coyle and Sulaiman (1967) found the value of skin friction to reach a peak value for pile displacements of about 5mm after which for further displacements the skin friction dropped off and remained relatively constant for large movements.

Mansur and Kaufman (1956) found the unit skin friction along piles with widths ranging from 0.36m to 0.51m, bearing in a sand stratum, to be less in the area of the base. This decrease in friction, in the vicinity of the base, may reflect the pattern of shearing failure beneath a pile tip as suggested by Terzaghi (1948). The compressive forces at the pile tip result in a zone of radial shear beneath the base, which causes radial movement of the soil. This tends to reduce the lateral earth pressure and skin friction of the sand on the surface of the pile immediately above the tip. From the load distribution curves of Mansur and Kaufman the skin friction appears to be reduced significantly for a distance of from 2m to 4m (3.5 to 10 pile diameters) above the pile tip.

The value of the skin friction calculated from any of the previous equations quoted will depend on the value chosen for K, which depends on the method of installation and the loading conditions. Broms and Silberman (1964) have stated that, for a driven non-displacement pile, K approaches the coefficient of lateral earth pressure at rest and may be taken as 0.5. Whereas for driven displacement piles K can be taken conservatively as 1.5. They suggest the value of K can be greater than one, due to the tendency of dense sand to expand when subjected to high shear stresses.

Depending on the passive conditions and the arching in the sand adjacent to the pile, K may be greater than one and should vary with depth (Robinsky and Morrison 1964 and Coyle and Sulaiman 1967). Hunter and Davisson (1969) found the lateral earth pressure to be approximately 1.1 for piles driven into sand and a value of 0.75 for jetted piles.

Broms and Silberman (1964) suggested that the relative density of the sand surrounding the test site was the major factor affecting the skin friction resistance of piles placed or driven into cohesionless soils.

Potyondy (1961) indicated that the unit skin friction of a saturated sand is less than that of a dry sand. He proposed that this decrease in skin friction was due to the water acting as a lubricant between the soil particles and the pile material.

The afore mentioned factors determine the proportion of the applied load which will be carried in skin friction and that which will be carried in end bearing for piles in cohesionless soils. Skempton, Yassin, and Gibson (1953) found that the amount of load carried by model piles in skin friction did not exceed 10% to 20% of the total bearing capacity. Meyerhof (1960) suggests that skin friction is small compared to base resistance in non-cohesive soils. While Terzaghi and Peck (1948) stated that the skin friction contribution to bearing capacity for cylindrical or prismatic piles driven into homogeneous layers of sand could be larger than one-half of the total ultimate bearing capacity.

2.7 Skin Friction of Piles in Cohesive Soils

It is common practice in the use of static formulae to assume that the load transferred in soft to medium clay is approximately equal to the shear strength of the clay, as determined by the unconfined compression test.

For a soil imposing both adhesion and friction, on the shaft of the pile, Meyerhof (1953) expressed the tangential force per unit area as

$$qs = Ca + KsYDtan\delta \qquad (2.14)$$

For a clay $\delta = 0$, so that the unit skin friction is equal to the cohesion of the soil around the pile shaft.

The problem of determining the value of Ca (taken as the undrained shear strength or one-half the unconfined compression strength) in the field is relatively easy since satisfactory methods of obtaining undisturbed samples are available for clay. However, the difficulty lies in estimating the effects of driving on this soil property.

It is apparent from the analysis of soil behaviour by Coyle and Reese (1966), that the properties of undisturbed soil may be quite different from the properties of the soil adjacent to the pile wall. The ratios of (load transferred to the soil) /(soil shear strength) greater than 1.0, obtained from field tests on instrumented piles, are the result of comparing measured values of load transferred at the pile wall with the undisturbed soil shear strength values.

The test results of Seed and Reese (1957) showed the shear strength of the soil near the pile to be approximately 1.5 times the shear strength of undisturbed samples, for the soft clay used in their experiments.

A number of investigators have found the ultimate unit skin friction on piles in soft clays to be equal to, and in stiff clays to be less than, the shear strength of the soil (Peck 1958, Meyerhof 1963, Tomlinson 1957, and Terzaghi and Peck 1967).

This reduction in strength in stiff clays is attributed to a small opening between the pile and the soil, resulting from vibration of the pile during driving. This space may not close near the top of the pile, where the lateral pressure is small, because of a low overburden pressure. It can be postulated that the lateral earth pressure acting on a driven pile, is a function of the soil shear strength, overburden pressure, and the construction procedures (Coyle and Reese 1966).

When piles are driven into extremely sensitive clays a shell of undisturbed material 25 to 50mm thick may behave as a liquid during driving and flow upwards along the pile to the surface where it accumulates. The soil outside this shell may remain virtually undisturbed. Within the shell the liquified material regains strength by consolidation and thixotropy, but the final strength may not necessarily equal that of the undisturbed soil (Terzaghi and Peck 1967, Coyle and Reese 1966). Casagrande (1932) found the soil to be remoulded in an area of about twice the pile diameter and the soil to be affected within a zone of four times the pile diameter around the pile.

Coyle and Reese (1966) proposed adjustment factors for the undisturbed shear strength from field data for use in computing load-settlement curves as follows :

1. for soft clays, undisturbed shear strength less than $24kN/m^2$ a factor of 1.5 should be used,

2. for medium clays, undisturbed shear strength between 24 and $48kN/m^2$ a factor of 1.0 should be used,

3. for stiff clays, undisturbed shear strength greater than $48kN/m^2$ a reduction factor from the graph (Figure 19, Coyle and Reese 1966) should be used.

Burland (1973) and Chandler (1968), in contrast to others, outlined an approach to calculate the shaft resistance of piles in clay using simple effective stress principles. Whereas, using undrained shear strength for calculating the end bearing of a pile appears justified, Burland (1973) saw little justification for relating shaft adhesion to undrained shear strength for the following reasons :

1. major shear distortions are confined to a relatively thin zone around the pile shaft and drainage to and from this narrow zone will therefore take place rapidly during loading,

2. the installation of the pile must disturb and remould the ground adjacent to the pile shaft, and

3. apart from the disturbances caused by the pile there is no simple relationship between undrained strength and drained strength of the ground.

The basic assumptions of Burland's (1973) approach are :

1. excess pore pressure dissipates rapidly,

2. loading takes place under drained conditions, and

3. because of remoulding during pile installation the soil has no effective cohesion. Hence, the shaft friction $qs = \sigma'_h \tan\delta$, where σ'_h = effective horizontal stress.

The effective horizontal stress is proportional to the effective overburden pressure σ'_{vo} i.e. $\sigma'_h = K\sigma'_{vo}$

$$\text{therefore } qs = K\sigma'_{vo} \tan\delta$$

$K\tan\delta$ may be denoted by β so that

$$\beta = K\tan\delta = q_s/\sigma'_{vo}$$

K depends on the soil type, stress history of the soil, method of installation of the pile. and δ depends on the soil type and the properties of the pile surface. For a driven pile K would be expected to be greater than Ko (coefficient of earth pressure before driving) so that setting K = Ko would give a lower limit for the shaft friction.

Assuming failure takes place in the remoulded soil close to the pile shaft, $\delta = \phi_d$ where ϕ_d is equal to the remoulded drained angle of friction of the soil.

For a normally consolidated soft clay $K_o = 1-\sin\phi_d$

Therefore $\beta = (1-\sin\phi_d)\tan\phi_d$ (2.29)

can be used as a lower limit for driven piles in normally consolidated clays.

ϕ_d usually lies between 20^o and 30^o and over this range β varies from 0.24 to 0.29.

Since K is slightly higher than Ko a reasonable value of β to use in design (in soft N.C.clays) would be about 0.3. Burland (1973) found this to agree with a number of reported field results.

For stiff clays the situation is more complex and the main difficulty lies in estimating the value of the coefficient of earth pressure at rest Ko at various depths.

Terzaghi and Peck (1967) state that the skin friction in pulling is commonly, but not always, nearly equal to that in pushing. While Parry and Swain (1977) suggests that the value of skin friction in compression could well be some 10% higher than for tensile loading.

Terzaghi and Peck (1967) suggest that the point resistance of a friction pile embedded in soft clay is negligible compared to the skin friction. This skin friction is independent of the depth of penetration and method of installation, and depends almost entirely on the properties of the clay.

Coyle and Reese (1966) stated that at large lateral pressures the soil apparently adhered to a smooth pile and failure occurred in the soil.

2.8 Relationship Between Skin Friction and End Bearing

Over the years, investigators have devised methods of separating skin friction and end bearing, both in the field and in the laboratory, to form a better understanding of their interdependence.

Tejchman (1969) performed tests on two types of model piles to test the influence of skin friction on point resistance. In the first model pile the skin friction and end bearing of the pile were applied simultaneously. In the second type an internal shaft allowed the base of the pile to be loaded independently of the shaft.

Tejchman found the point resistance to increase an average amount of approximately 10% as a result of the skin friction reaction. This increase was found to be proportional to the pile diameters when a number of different size piles were tested.

Caquot and Kerisel (1948) experimenting with piles in a homogeneous medium showed that as the skin resistance decreased, the end bearing increased, and the total pile capacity remained unchanged.

Coyle and Sulaiman (1967) have suggested that skin friction and end bearing are interdependent.

Tejchman (1969) discusses how the additional stress due to the skin friction on a pile increases the bearing capacity, and how to calculate these additional stresses using Mindlins equations.

Geddes (1969) presented a method of estimating the additional stress imposed upon underlying soil layers produced by a point load and two types of skin friction distribution (uniform and a linear variation). Geddes employed Boussinesq solutions to derive dimensionless coefficients to enable the evaluation of these stresses in practice.

In sands the extent of the 'arching ring,' (Terzaghi 1943) as described in the previous section, caused by the base resistance, tends to decrease the skin friction in the vicinity of the pile.

Not all static formulae for the pile bearing capacity take the influence of the skin friction on the point resistance into consideration (for example Terzaghi's formulae for calculating unit ultimate point resistance disregards this influence).

2.9 Types of Failure in Sand

Vesic (1963) observed that the analysis of the shear patterns indicate that, depending on relative density of the sand, all three types of failure occur at shallow depths: general shear failure, local shear failure, and punching shear failure (see Figure 2.4). However, at greater depths only punching shear failure occurs irrespective of relative density. The three types of failure are characterised by :

1. General Shear Failure

(i) relative density Dr>0.7 (relatively dense sand)

(ii) sudden failure

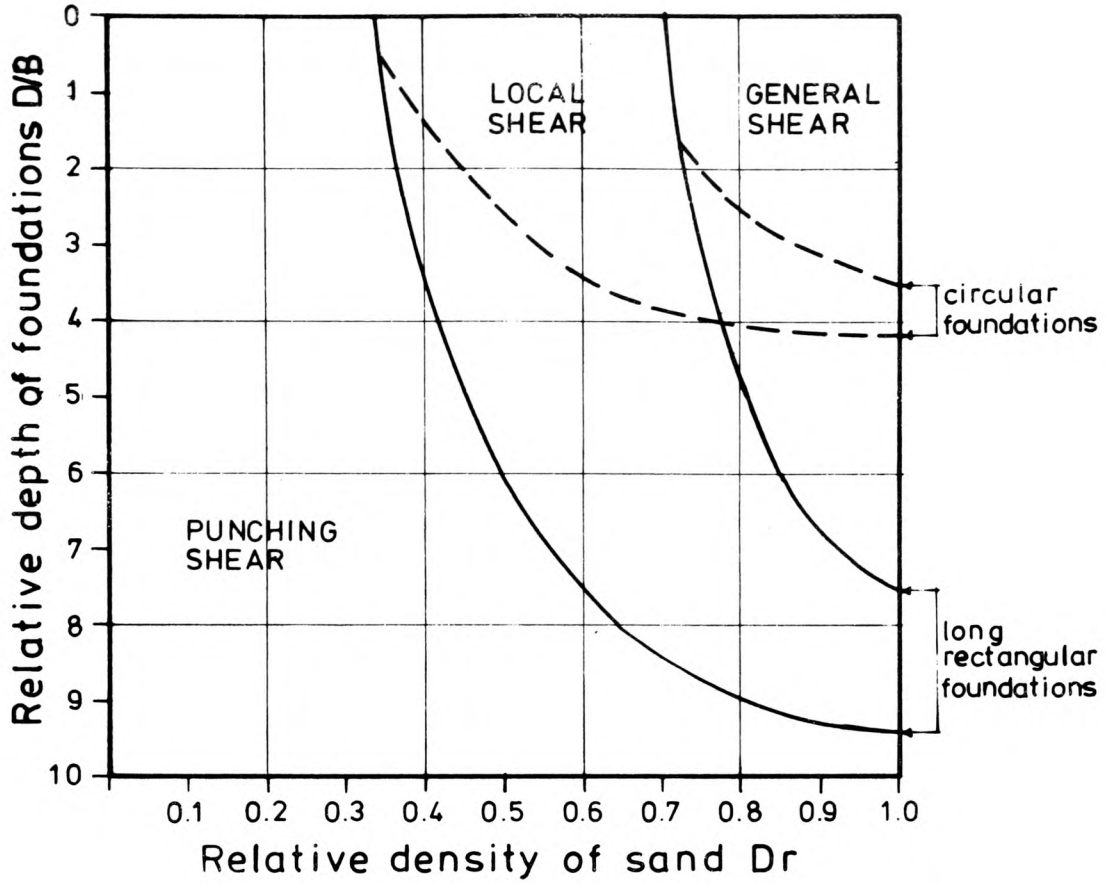

FIGURE 2.4

TYPES OF FAILURE AT DIFFERENT RELATIVE DEPTH D/B OF FOUNDATIONS IN SAND (FROM VESIC 1963)

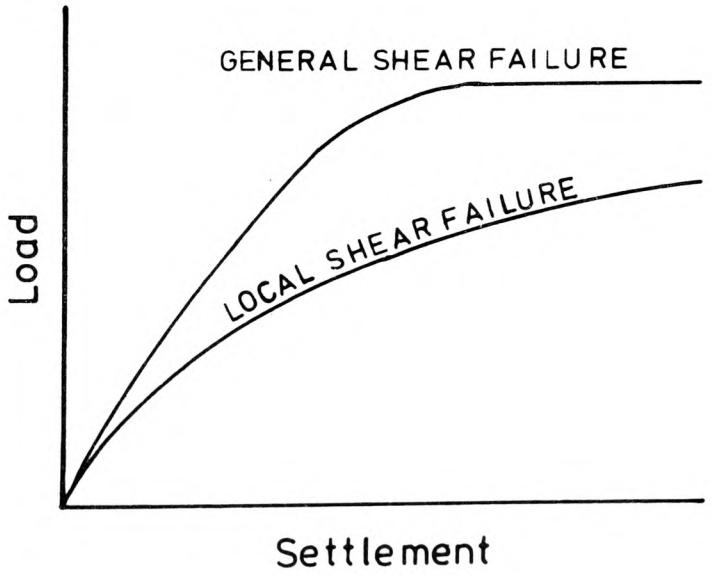

FIGURE 2.5

LOAD-SETTLEMENT CURVES (FROM TERZAGHI 1943)

(iii) very pronounced peaks of base resistance at settlements of about 7% foundation width (B)

(iv) failure accompanied by appearance of failure surfaces at ground level

(v) considerable bulging of sheared mass of sand

(vi) corresponds exactly to that described by Terzaghi (1943)

2. Local Shear Failure

(i) $0.35<Dr<0.70$ (medium dense sand)

(ii) no sudden failure

(iii) at settlements greater than 8% B small sudden shears within the sand mass apparent from observations of load and settlement gauges, simultaneously, bulging of the sand surface starts

(iv) at settlements of about 15% B a visible boundary of shear zone at the sand surface appears

(v) peak of base resistance may never be reached

(vi) described by Terzaghi (1943).

3. Punching Shear Failure

(i) $Dr<0.35$ (relatively loose sand)

(ii) no bulging of the sand surface

(iii) rate of settlement increases until reaching a maximum at a settlement of about 15 to 20% B

(iv) sudden shears observed as settlement reaches about 6 to 8% B

(v) failure surface vertical or slightly inclined and follows perimeter of base but never reaches sand surface.

Under some conditions there is no peak value of load for the load settlement curve and a criterion of failure or ultimate load must be decided upon. Vesic (1963) outlines the following criterion of failure for the base resistance of piles in sand :

1. General Shear Failure - peak of base resistance always reached corresponding to appearance of failure surfaces at sand surface and abrupt change of rate of settlement from positive to negative.

2. Local Shear Failure - not always peak of base resistance, however, rate of settlement reaches a maximum at the same load at which failure becomes visible at the surface.

3. Punching Shear Failure - no peak of base resistance nor any appearance of failure surface. Peak of the settlement rate can be noted.

An analogous criterion can be adopted for skin loading tests.

Vesic found the ultimate loads to be reached at settlements of about 20 to 30% of the foundation depth.

Mansur and Kaufman (1956) suggested five different criteria for selecting the failure loads, and suggested the average value be taken. The criteria are :

1. load that produces plastic or net settlement of 6mm,

2. load indicated by intersection of the tangents drawn through the initial, flatter section, and the steeper part of the gross settlement curve,

3. load beyond which there is an increase in gross settlement disproportionate to the increase in load,

4. load at which the slope of the plastic or net settlement curve is four times the slope of the elastic deformation curve,

5. load beyond which there is an increase in plastic or net settlement disproportionate to the increase in load.

2.10 Stress Distribution and Load Transfer

In 1936 Professor Karl Terzaghi in addressing the Boston Society of Civil Engineers stated that "One of the most striking contradictions between customary earth-pressure theories and experience in actual construction work lies in the distribution of pressure on lateral supports". It is thought that what Professor Terzaghi was referring to, was the fact that the pressure distribution acting on the sides of an excavation, whether it was a trench or a bored shaft, does not increase as hydrostatic pressures do in direct proportion to depth.

According to Rankine's earth-pressure theory, the ratio between the lateral and vertical pressure is equal to Kr, the coefficient of earth pressure. Rankine assumed Kr for an undisturbed deposit to be equal to

$$Kr = \tan^2(45^\circ - \phi/2) \qquad (2.30)$$

In sands, the mechanisms of boring, driving, and testing piles tends to cause lateral expansion of the soil in the vicinity of the pile base. This lateral expansion is accompanied by a vertical shortening, and the sand located above the expanding zone has a tendancy to move downwards. Since both the lateral expansion and the vertical shrinkage are limited to a cylindrical zone surrounding the shaft, shearing stresses develop along the outer boundary of this zone. These shearing stresses transfer part of the weight of the sand adjoining the shaft onto the unaltered material outside the zone of expansion. This transfer is called the 'bin effect' because it closely resembles the transfer of part of the weight of the contents of a storage bin to the wall of the bin. This transfer of weight and loosening of the downward annular zone of soil adjacent to the pile wall, decreases the lateral pressure on the pile shaft, thus decreasing the skin friction value in the vicinity of the pile base.

The resultant stress distribution along the pile shaft, for a number of applied loads, would be similar to that shown in Figure 2.6. Vesic (1963), Coyle and Reese (1966), Meyerhof and Valsangkar (1977), Chan and Hanna (1979), and others have found the load distribution of piles in sand and clay to be similar to Figure 2.6, where the amount of load transferred in skin friction in the vicinity of the pile base is greatly reduced.

As pointed out by Mansur and Kaufman (1956), the slope of the load distribution curve at any depth, is a measure of the rate at which the load is transferred from the pile to the soil at that depth. The slope is also a measure of the frictional resistance mobilised at that point.

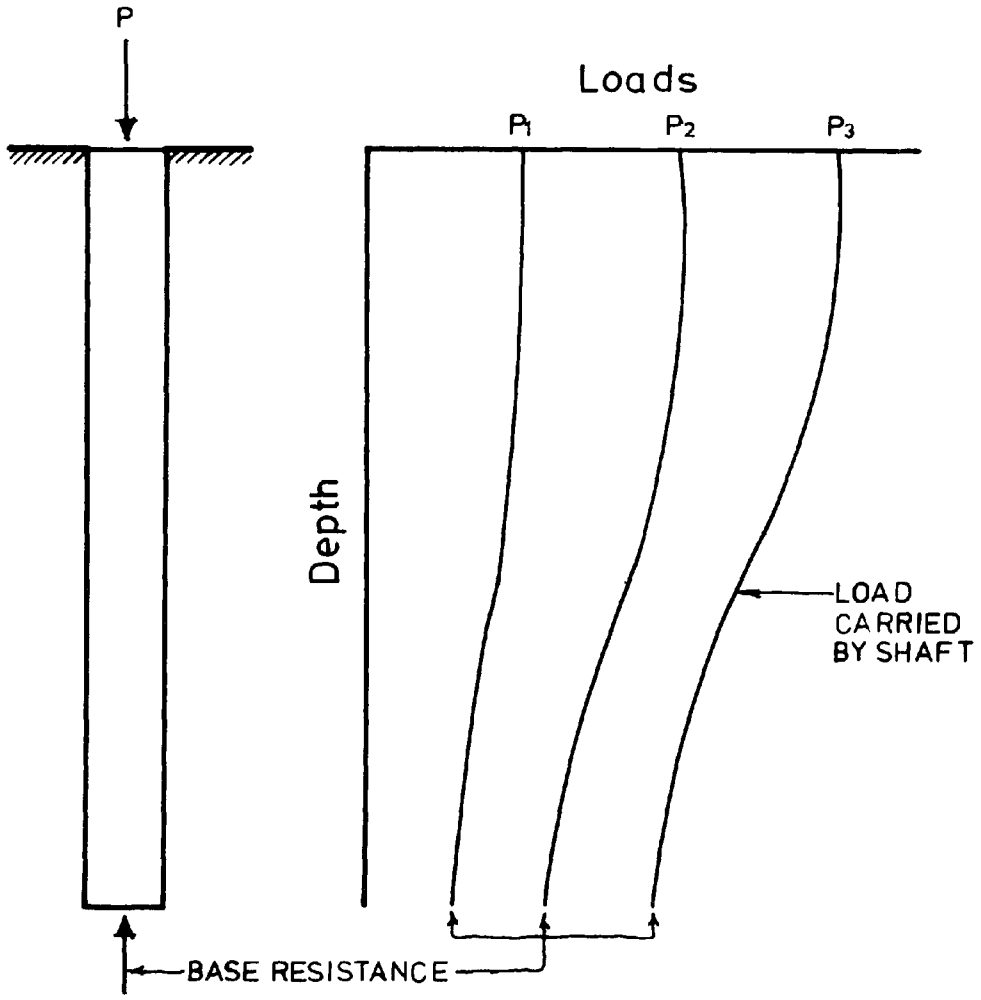

FIGURE 2.6

TYPICAL LOAD DISTRIBUTION CURVES
FOR DIFFERENT APPLIED LOADS

Tejchman (1969) showed that the tangential stresses acting along a pile shaft in sand are not proportional to depth or the effective overburden pressure, and they are not the same in pulling as in compression. Coyle and Reese (1966) found the load transferred to a clay to be a function of depth and the pile movement. According to Coyle and Reese at large lateral pressures, the clay apparently adheres to even a smooth pile, and failure occurs in the soil. Therefore, the stress distribution would be directly related to the shear strength of the clay.

Tomlinson (1977) suggests that the stress distribution along a pile depends on the soil density and method of installation of the pile.

Poulos and Mattes (1969) state that a triangular distribution of the limiting adhesion is likely to be relevant to the case of piles in sand or in a relatively thick layer of soft clay, while a uniform adhesion distribution will be relevant to overconsolidated clays and to relatively thin layers of normally consolidated clays. They also suggest that the load transfer in skin friction is markedly affected by the stiffness of the pile relative to the surrounding soil, where a stiffer pile will transfer less load. Poulos and Mattes also suggest that the amount of load transferred is increased as the Poissons ratio of the soil decreases for relatively compressible piles. Therefore, providing the effects of negative skin friction are absent, the decrease in Poissons ratio and increase in Youngs modulus of the soil surrounding the pile, with time, will lead to an increase in the proportion of load being transferred to the soil.

Cooke and Price (1973) found a way of detecting, with reasonable accuracy, the strains and displacements in the soil as a friction pile is installed and loaded, without noticeably affecting the pile behaviour and the load transfer mechanism.

Cooke, Price and Tarr (1979) describe a method of determining the shear modulus for the remoulded clay close to the pile shaft, from the shear stress along the pile, and the shear strains in the soil the the load distribution and soil displacement versus depth curves.

2.11 Empirical Methods of Calculating Pile Loads

The ultimate bearing capacity in cohesive soils can generally be estimated from bearing capacity theory and the shear strength of undisturbed samples. For soils with little or no cohesion, however, the difficulty and expense of obtaining undisturbed samples makes estimates of the bearing capacity from penetration tests on the site, frequently the most economical procedure. For this purpose dynamic or static penetration tests may be utilised.

The two most common penetration tests in use today are the standard penetration test (SPT) and the Dutch cone penetrometer test.

The standard penetration test is a dynamic test, where the penetrometer is driven into the soil at the bottom of a cased borehole, by the blows of a standard weight hammer. The number of blows from the hammer required to cause a penetration of a specific distance is termed the standard penetration value N. When the test is made in very fine silt or sand below the water table a reduced value of N is determined, for values of N greater than 15, where the

equivalent N = $15+\frac{1}{2}(N'-15)$; where, N' = value obtained from test .

The Dutch cone penetration test is a static test. For this test a cone is pushed into the soil at a constant rate of penetration and the force required to cause the penetration (qc) is measured.

A description of each of the above mentioned penetrometer test can be found in Whitaker (1970).

While static penetration methods are to be preferred, they suffer from the disadvantage that in dense soils a substantial reaction to jacking has to be provided and the load capacity of customary equipment may be reached. Dynamic methods are cheap, simpler to carry out, and are fairly reliable in cohesionless soils.

A number of investigators have derived expressions for relating the results of penetrometer tests to the ultimate bearing capacity of piles.

Meyerhof (1956) plotted graphs of standard versus static penetration test values which showed a reasonably good linear correlation between resistances. Generally Meyerhof found qc=4N (N in blows/ft).

For calculating the ultimate bearing capacities for driven displacement piles in cohesionless soil using penetration tests Meyerhof (1956) suggests

$$qp = 4N \text{ (tons/ft}^2\text{)} \qquad (2.31)$$

$$qs = \bar{q}c/200 \text{(tons/ft}^2\text{) or} \qquad (2.32)$$

$$qs = \bar{N}/50 \text{ (tons/ft}^2\text{)} \qquad (2.33)$$

where qp = unit point resistance (tons/ft^2)

q_s = unit skin resistance (tons/ft^2)

$\bar{q}_c$ = average cone resistance (tons/ft^2)

$\bar{N}$ = average standard (or equivalent) pen. resist. (blows/ft)

An upper limit of the unit skin friction of 1ton/ft^2 has been suggested by Meyerhof.

Ismael and Klym (1979) used Meyerhof's empirical correlation of SPT results and calculated $q_s = N/100$ and $q_p = 1.2N$(ton/ft^2) for piles in sand.

The cone penetrometer has a tube with an external diameter equal to that of the cone base. After the cone has been pushed into the soil, independent of the tube, the tube itself is advanced to join the cone. The force required to do this is recorded and the unit skin friction is obtained.

Field loading tests on driven displacement piles have shown the observed skin friction q_s of the piles to vary from about 1½ to 3 times the static skin friction on the shaft of a penetrometer f_s, and on the average $q_s = 2f_s$ (Meyerhof 1956). The greater skin friction of piles compared with that observed from a penetrometer test may be explained by the greater lateral compression of the soil during installation of full sized piles compared with that of the smaller penetrometer.

Dutch engineers have suggested a method of adjusting the unit cone penetration resistance to qc where

$$q_c = \tfrac{1}{2}[\tfrac{1}{2}(q_u' + q_u'') + q_u'''] \qquad (2.34)$$

where q_u' = average unit cone resistance over the range from 0.7B to 4B

below the pile,

qu'' = minimum over the range of qu'

qu''' = average of the envelope of minimum cone resistance above the pile toe to a height which varies from 6 to 8B.

For a detailed explanation see Tomlinson (1977).

For large displacement piles Dutch engineers also use the expression,

$$qs = qc/2.5 \ (kN/m^2).$$

It must be pointed out that the empirical correlations found by different investigators, between penetration resistance and bearing capacity in one soil, is not necessarily applicable to other cohesionless soils (Tomlinson 1977).

2.12 Pile Driving Formulae

Other methods of calculating the bearing capacity of piles (which have had much development in the past 100 years) are by the use of driving formulae.

Driving formulae relate the energy applied to the top of the pile (by the fall of a hammer) during driving and the subsequent pile penetration, to its ultimate bearing capacity. If the resistance of the soil to penetration is equal to Qdy, the hammer weighs W_H, and falls through a distance H, driving the pile a distance S into the ground; then according to Sander's pile formula published around 1850,

$$W_H \cdot H = QdyS. \qquad (2.35)$$

Therefore $Q_{dy} = W_H H/S$

However, the values obtained by using this formula are too great due to a portion of the energy of the falling hammer being converted into heat and elastic deformation.

Since 1850 engineers have dealt with the energy losses during driving in a number of different ways. The variation in the determination of the energy losses accounts for the large number of driving formulae in use today.

It has been suggested that when using driving formulae for determining driving resistances that a number of formulae be used which are applicable to the given conditions and the average value taken.

Pile driving formulae do not take into consideration the time affects of soil behaviour and fail to recognise the fallacy of the basic assumption of Newtonian impact. Isaacs (1931) first pointed out that the energy transferred from the hammer to the pile tip was not instantaneous at impact; but rather a wave action occured in the pile after impact so that the best way of analysing the hammer-pile-soil system was by the theory of wave propagation. Development of computers in the 1950's made numerical solutions of the wave equation possible within an acceptable amount of time and effort.

The dynamic wave equation provides a means of evaluating the pile capacity that is mathematically well founded and probably provides the most realistic mathematical model available for depicting actual behaviour of the hammer-pile-soil system (Ramey and Hudgins 1977).

Development of the wave equation resulted from a consideration of the internal forces and motion of a segment of a freely suspended prismatic bar, that was subjected to an impact at one end, and modified to consider external resistance to the segment motion offered by the soil.

Tavenas and Audibert (1977) have shown that the wave equation predictions are no better than any of the predictions made by the pile driving formulae. However, this does not mean the wave equation is not reliable but, simply that the energy input is so variable that it destroys any value of the method.

In order for the wave equation method to be used to its full potential in production piling, it appears necessary to resort to direct measurement of the driving energies. In the absence of such direct measurements, Tavenas et al. (1977) suggest that the wave equation method appears, from a practical point of view, to be no more than a complicated and expensive pile driving formula, at least as far as the reliability of production pile capacity predictions is concerned.

2.13 Analytical Methods of Calculating Settlements

The settlement of a pile top under load involves :

1. elastic compression of the pile,

2. elastic compression of the subgrade, and

3. plastic settlement of the subgrade.

Some of the factors affecting the settlement of a pile in sand are :

1. relative density of the soil,

2. grain shape,

3. mineralogy,

4. grain size distribution,

5. overburden pressure,

6. water content,

7. precompression or in-situ stress state, and

8. cohesive admixtures.

A number of theoretical methods for the analysis of the settlement of a pile have been developed. These approaches can be classified into three broad categories :

1. methods based on the theory of elasticity, which employ Mindlin's (1936) equations for subsurface loading within a semi-infinite mass,

2. step-integration methods, which use measured relationships between pile resistance and pile movement at various locations along the pile,

3. numerical methods, in particular the finite element method.

Many investigators have used Mindlin's equations to calculate the settlement of piles, among them : D'Appolonia and Romualdi (1963), Thurman and D'Appolonia (1965), Salas and Belzunce (1965), Poulos and Davis (1968), Mattes and Poulos (1969), and Poulos and Mattes (1969).

The basic approach is to :

1. divide the pile into a number of uniformly-loaded elements,

2. obtain the displacement of the pile by considering the compressibility of the pile under axial loading, and

3. obtain soil displacements by using Mindlin's equations for determining the displacement within a soil mass due to loading within the mass.

Mindlin's equations assume the soil to be a linear elastic material, although the analysis can be expanded to account for more realistic soil behaviour. It is a rapid method of carrying out studies of the effects of pile and soil characteristics. This method can be used for preparing a series of solutions, which may be used for design, and do not call for the use of a computer. It can also be applied to the analysis of pile groups.

Poulos (1974) employed elastic theory to determine the settlement(s) at the top of a pile expressed in terms of a basic influence factor for a rigid pile in a deep layer. This was accomplished by using correction factors for the effects of pile

compressibility, finite soil layer depth, and the Young's modulus of the bearing stratum at the base of the pile.

For a floating or friction pile in a uniform soil,

$$S = (PI_1/E_s d)\ R_k R_h \qquad (2.36)$$

For a pile bearing on a stiffer stratum

$$S = (PI_1/E_s d)\ R_k R_b \qquad (2.37)$$

where P = load applied to pile head

d = pile diameter

E_s = Youngs Modulus of soil adjacent to shaft

I_1 = Settlement Influence factor

R_k, R_h and R_b = settlement correction factors for the effects of pile compressibility, finite layer depth, and bearing stratum rigidity respectively.

Poulos (1974) gives graphs for I_1, R_k, R_h and R_b. The influence factor I_1 is the ratio of the actual displacement of a pile top to its elastic compression if the pile acted as a simple column.

Poulos and Mattes (1969) have obtained, using elastic theory, numerical solutions for load transfer, top displacement, and tip displacement of an end-bearing pile. They found that the behaviour of end-bearing piles is influenced by :

1. the length to diameter ratio of the pile,

2. E_b/E_s, the ratio of Youngs moduli of the bearing stratum to that of the soil adjacent the pile shaft, and

3. the stiffness of the pile relative to the soil as expressed by the pile stiffness factor K.

The more slender a pile, the greater the load transferred to the soil in skin friction and the greater is the increase in the top movement as compared with the movement of the pile acting as a simple column.

As the ratio E_b/E_s increases, the amount of load transferred decreases, and the top and tip displacements also decrease, the tip displacement in particular decreases rapidly. However, Poulos et al. (1969) also found that the more compressible a pile is in relation to its surrounding soil, the less influence the bearing stratum has on the behaviour of the pile.

The occurrence of slip between the soil and the pile shaft, also affects the behaviour of the pile, and leads to a decrease in the relative amount of load transferred to the soil in skin friction and an increase in the displacement of the pile.

The departure from elastic analysis depends primarily on the distribution of the maximum adhesion with depth and on the compressibility of the pile. For a highly compressible pile, a significant increase in the displacement of the pile top over that predicted by elastic analysis may occur. For most piles however, local yield should not seriously influence the behaviour at working

loads.

Poulos and Mattes (1969) found close agreement between published measurements of pile behaviour and those predicted from elastic analysis. They found an overall average ratio of calculated to observed settlement to be 1.11.

When a single pile is loaded (in an ideal elastic soil mass) the major part (approximately 90%) of the settlement occurs immediately (Poulos and Davis 1968).

The step-integration method was proposed by Coyle and Reese (1966). This method utilises soil data from field tests on instrumented piles and laboratory tests on model piles. The procedure for this method is :

1. divide the pile into elements,

2. assume a tip movement,

3. from the load transfer curves obtained from the instrumented piles, determine the load and movement of successive elements up the pile until a value of load and displacement for the top of the pile are obtained, and

4. repeat the procedure for different assumed tip movements and a load-settlement curve may thus be computed.

The step-integration method has a theoretical limitation in that it assumes that the movement of the pile at any point is related only to the shear stress at that point and is independent of the stresses

elsewhere along the pile. No account is taken for continuity of the soil mass. Consequently, this method can not be used for analysing pile groups.

The advantage of using numerical methods, such as finite element methods (Girijavallabhan and Reese 1968, Cooke and Price 1973), is that soil behaviour such as nonhomogeneity, anisotropy, nonlinearity, and the time dependent stress-strain relationship can be readily taken into account.

The finite element method is the most powerful method, but it requires a complete solution for each new problem considered, and pile groups present difficulties. Unlike a single pile which is readily analysed as a radially-symmetrical problem; with groups the loss of axial symmetry requires that a three dimensional analysis be carried out.

The difficulty with using numerical methods for predicting pile movements and load transfer is in the accuracy of determining the lateral earth pressure, modulus of elasticity of the soil, and the elastic-plastic tip movement.

Driving and boring disturbs the soil in zones of unknown size around the pile and modifies the soil properties in these zones. Thus, soil properties may vary with radial distance and depth. The extent of this variation probably depends on the type, care, and time of installation of the pile. Since, neither laboratory tests of soil samples, nor in-situ soil tests can account for these factors, pile loading tests are likely to remain the best method of estimating settlement of a single pile in the forseeable future (Cooke 1975).

Parry (1971) suggested an equation for the settlement of a foundation in sand from standard penetration test results which is

$$S = 300\sigma_{vo}B/Nm(mm) \qquad (2.38)$$

where σ_{vo} = overburden pressure in MN/m^2

B = foundation width

Nm = SPT value N at a depth of $\frac{3}{4}B$ below foundation level.

Terzaghi has used the static cone resistance for calculating the consolidation settlement of a given soil layer

$$S_f=(H/C)\log_e(\bar{\sigma}_{vo}+\sigma_z)/\bar{\sigma}_{vo} \qquad (2.39)$$

where H = soil layer thickness

$\bar{\sigma}_{vo}$ = mean initial effective overburden pressure, i.e. effective overburden pressure before applying the foundation load

σ_z = vertical stress induced at the centre of a layer by the net foundation pressure

$C = \frac{3}{2}(q_c/\bar{\sigma}_{vo})$ = constant of compressibility

qc = static cone resistance.

Parry (1978) suggested a method of estimating foundation settlements in sand from plate loading tests and standard penetration tests. Unlike the empirical expression of Terzaghi and Peck (1967) for the settlement ratio, Parry's expression takes account of changes in ground conditions, particularly in-situ stresses due to ground water movement and site excavation or filling.

According to Parry, the settlement S_B of a foundation of width B , may be obtained from the plate settlement S_1, by the expression

$$S_B = S_1 \; B/B_1 \; (N_{m1}/N_{mB}) \qquad (2.40)$$

where B_1 = plate width

Nm_1= Nm for plate

Nm_B= Nm for foundation

$Nm = \frac{1}{6}(3N_1+2N_2+ N_3)$

N_1 = SPT value from foundation level to a depth of $\frac{2}{3}B$ below foundation level,

N_2 = SPT value from $\frac{2}{3}B$ to $\frac{4}{3}B$

N_3 = SPT value from $\frac{4}{3}B$ to 2B.

Terzaghi and Peck's (1967) correlation between test plate settlement S_1 and the standard penetration test value N is

$$S_1 = 3q_a/N \qquad (2.41)$$

where q_a = bearing pressure at that level and the settlement of a full size foundation is then found using

$$S_B/S_1 = [2B/(B+0.3)]^2 \qquad (2.42)$$

where S_1 = settlement of standard 0.3m square plate

S_B = settlement of foundation for same bearing capacity

B = foundation width (m)

Parry (1978) pointed out that the fundamental flaw with Terzaghi and Peck's equation was that the N value was measured before excavation, while the plate loading test was done after the excavation, and the N values had not been adjusted. Meyerhof (1956) suggested that Terzaghi and Peck's equation over estimated the settlement and suggested the constant be reduced from 3 to 2.

Jorden (1977) has tabulated eleven methods of calculating settlement in sand and reviews the factors affecting the magnitude of this settlement. The methods vary in their treatment of measured N values, overburden pressure, depth of ground water, and depth of embeddment.

From the analysis of these methods Jorden suggests that :

1. penetration testing is the most practical means of assessing the settlement in sands (SPT. or static Dutch cone tests),

2. correction for the overburden pressure is most important,

3. engineering judgment should be used in deriving final settlements for each method, keeping in mind the factors affecting settlement and published comparisons between predicted and observed settlements for various methods,

4. a reasonable prediction of the settlement can be obtained by averaging results from the methods by Schmertmann (1970), Meyerhof (1974), Peck and Bazaraa (1969), Alpan (1964), and Parry (1971) where this is possible. The range of values, as well as the average should be reported.

The differential, or relative settlement between one part of a structure and another, is of greater significance to the stability of the superstructure than the magnitude of the total settlement. Total settlement is usually only significant in relation to neighbouring works.

Some causes of differential settlement are :

1. Variations in soil strata
2. variation in foundation loading, and
3. differences in the time of construction of adjacent parts of a structure.

Tomlinson (1969) has suggested some methods of preventing excessive differential settlements :

1. formation of a rigid raft foundation with thick slabs or deep beams in two or three directions,
2. excavation of deep basements to reduce the net bearing capacity,
3. transfer of foundation loading to deeper, less compressible, soil by means of basements, piers, or piles,
4. provision of jacking pockets or brackets in columns to relevel the superstructure, and
5. additional loading on lightly loaded areas in the form of kentledge or embankments.

Poulos (1972) has suggested a method of constructing the load-settlement curve to failure for a pile or pier as follows. First, the shaft load versus settlement relationship up to the ultimate resistance Psu of the shaft is

$$S = (I/E_s d)P_s/(1-\beta) \qquad (2.43)$$

where Ps = shaft load

I = $I_1 R_k R_h$ for a floating pile or $I_1 R_k R_b$ for an end-bearing pile

β = proportion of the load transferred to the base = $\beta_1 C_k C_b$

β_1 = value of β for a pile in a uniform deep soil layer, dependent on length to diameter ratio and the ratio of base width to shaft width

C_k, C_b = correction factors for the effects of pile compressibility and bearing stratum rigidity.

E_s = Young's modulus of the soil

The base load versus settlement relationship up to the ultimate resistance P_{bu} of the base is

$$S = (I/E_s d)(P_b/\beta)+[P_b-P_{su}\ \beta/(1-\beta)]\ L/A_p E_p \qquad (2.44)$$

where P_b = base load

A_p = area of pile section

E_p = Youngs modulus of pile

L = pile length

The second term in the above equation represents the additional compression of the shaft after full shaft slip has occurred, and is only operative if the shaft has fully slipped. Ultimate base and shaft loads P_{bu} and P_{su} may be estimated from ultimate bearing

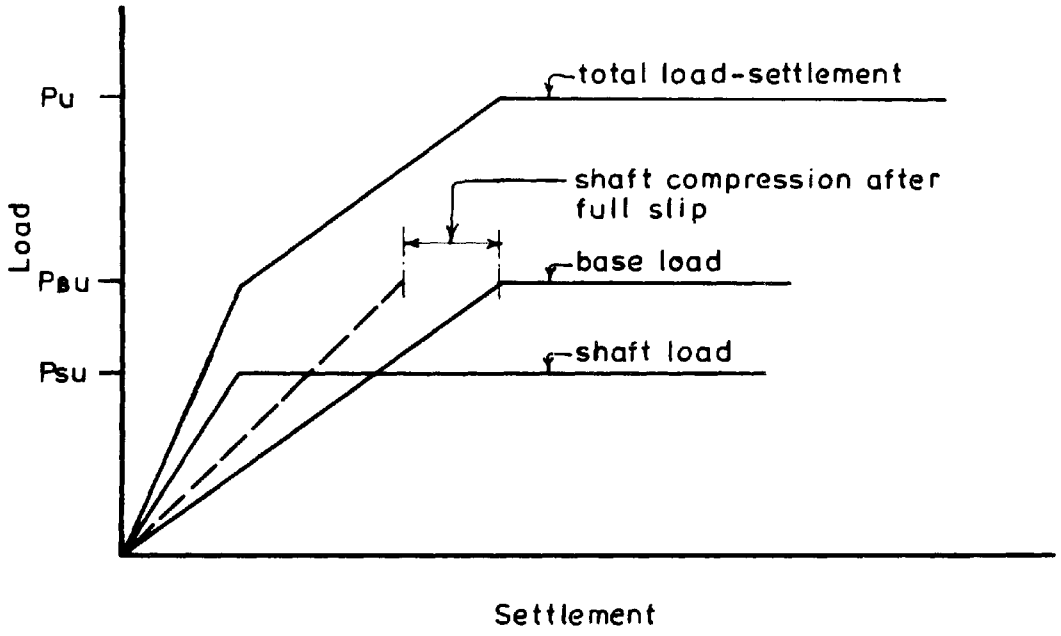

FIGURE 2.7

CONSTRUCTION OF LOAD-SETTLEMENT CURVE (POULOS FROM LEE 1974)

capacity theory (see Figure 2.7).

2.14 Negative Skin Friction

When a mass of soil is settling, because of incomplete consolidation under its own weight or under the weight of a fill or surcharge, the insertion of piles into the mass interferes with the settlement. As the soil moves downward it exerts a downward drag known as negative skin friction on the piles. This is the most common cause of negative skin friction but, it can also be caused by a lowering of the ground water table.

Brinch Hansen (1968) suggested that lowering the ground water table by p meters in a clay will have the same effect (below the original water table) as a surface load of p tons/m^2. He also stated that the negative skin friction could not exceed the pulling capacity of a pile.

According to Tomlinson (1969) the negative skin friction on a pile will never be higher than the skin friction that can be carried on the pile shaft; which is equal to the surface area of the shaft times the adhesion between the soil and the pile.

Burland (1973) analysed a number of field tests in soft clay, and suggested that by using a value of $\beta = 0.25$ ($\beta = K\tan\delta$) for calculating the negative skin friction, where $NF = p\beta$ (p=vertical effective overburden pressure), a reasonable upper limit for negative skin friction in soft clay will be obtained.

Tejchman (1969) recommended a method of testing the influence of negative skin friction on piles in the field :

1. load test the pile to its ultimate bearing capacity in compression (Q_t^c),
2. load test the pile to its ultimate bearing capacity in tension (Q_t^{tc}), then
3. load test the pile again to its ultimate bearing capacity in compression (secondary compression Q_t^{ct}).

The difference between the primary and secondary compression tests ($Q_t^c - Q_t^{ct}$) will indicate the maximum influence that negative skin friction can have on the pile.

Denman, Nicholls and Symons (1977) found the negative skin friction acting on model pile groups to be time dependent and to reach a maximum value prior to the cessation of consolidation of the compressible stratum. They also found no evidence of group action in terms of either total negative friction action on, or settlement of the individual piles. This implies that negative friction, although caused by consolidation of the entire compressible stratum, is a localised interaction at the pile-soil interface. Analysis of this by means of direct friction or adhesion methods which are based on knowledge of the shearing resistance of the soil and the surface texture of the piles was suggested as the best method.

Denman et al. (1977) recommend that for calculating the negative skin friction on a pile group the measured or predicted single equivalent pile negative friction can be used, since the piles act independent of one another. However, thev suggest using an efficiency ratio of less than unity, because the probability of arching occuring in the fill, which supplies the surcharge, is more in the group than for a single pile. Denman et al. (1977) found an efficiency ratio of 0.84 for the pile groups used in their experiments.

Gregersen and DiBiagio (1973) found considerable axial forces due to negative friction remained in 280mm diameter piles after being driven into loose sand.

Tomlinson (1969) recommends 3 methods of limiting the "drag down" forces on a pile by :

1. installing a sleeve around the pile through the compressible layer,

2. surrounding the pile by a plastic membrane with a low frictional value, or

3. coating the pile with a layer of asphalt.

Negative skin friction must be allowed for when considering safety factors on the ultimate carrying capacity of a pile.

2.15 Residual Stresses

Most methods of analysing the load-settlement behaviour of piles assume the pile to be stress free after installation and before loading. As has been shown many times in both cohesive and cohesionless soils, this is not the case (Hunter and Davisson 1969, Hanna and Tan 1971, Gregersen and DiBiagio 1973, Chan and Hanna 1979). The processes of installation of the pile and the redistribution of stresses in the soil after the pile has been placed create, sometimes large, residual stresses in the pile. Cooke, Price and Tarr (1979) found residual loads at the base of piles with large penetrations in London Clay approximately 75% of the resistance to penetration at this level.

Hunter and Davisson (1969) suggested that the residual loads caused by installation of a pile by vibratory drivers should not exceed the weight of the driver. Hunter et al. (1969) further stated that if the load transfer measurements were made assuming zero residual loads, then there was a possibility of serious error with respect to the division of load between friction and end bearing. The total load, however, would not be affected.

Many investigators have found that the stress history of a pile has a significant effect on residual loads. Chan and Hanna (1979), Mansur and Kaufman (1956), Gregersen and DiBiagio (1973), and others have found the residual loads in a pile to be considerably reduced after loading as compared to those present after driving and before testing.

Mansur et al. (1956) found residual compressive stresses in a pile after compression loading tests appeared to be less for those piles that failed by plunging, than those that were not tested to failure.

Chan and Hanna (1979) found large residual bending moments, locked into bent piles, after failure and removal of the load. These moments were two or three times the moments present in the pile just prior to the ultimate load being applied.

Piles which are to be used to resist uplift forces are usually load tested in the field, first in compression and then in tension. Hanna and Tan (1971) have suggested that a compression test reduces the ultimate capacities obtained in subsequent tensile tests. Therefore, design loads based on these tensile tests are unduly conservative. To best evaluate the results of loading tests on instrumented piles in the field, a complete stress history of the pile starting before the pile is driven should be obtained.

2.16 Effects of Pile Driving on Soil Properties

In most published theoretical studies it is presumed that the soil is created around the piles. Soil displacements and forces which may be locked into the pile-soil system by the installation process prior to the start of structural loading can not therefore be taken into account.

As a pile is driven (or bored) and loaded in the ground, the stresses induced and subsequent movements of the soil in the vicinity of the pile alter the soil properties. If the changes of these soil

properties are not accounted for in calculating loads and settlements of the pile, serious errors could occur. Methods of accounting for these changes have been to either : find methods of estimating the new soil properties, or by introducing factors into the equations to account for the different methods of installation of the foundation.

A number of investigators have measured the extent of the envelope of soil disturbance around a pile in different soils.

Meyerhof (1959) found a zone of failure around the base and a further zone of volume change surrounding the entire pile, using model piles driven into cohesionless material (Figure 2.8). Meyerhof gave values of the widths of the failure zone and compaction zone in loose sand, as four and eight times the shaft diameter respectively. Kishida (1963) observed widths of 4B for the failure zone and 7B for the compaction zone.

In loose sand, Robinsky and Morrison (1964) observed the visible displacement envelope extended 3 to 4 pile diameters to the side and $2\frac{1}{2}$ to $3\frac{1}{2}$ diameters below the pile point. The same authors found the envelope to extend to $4\frac{1}{2}$ to $5\frac{1}{2}$ diameters to the side and 3 to $4\frac{1}{2}$ diameters below the pile point, in medium dense sand.

Using a cone penetrometer Meyerhof and Sastry (1978) found the zone of compaction around 76mm diameter piles driven into sand was limited to about 8 pile diameters from the pile.

In clay, Cooke and Price (1973) found considerable disturbance, and a significant reduction in shear modulus in a zone of approximately one pile diameter around the pile shaft.

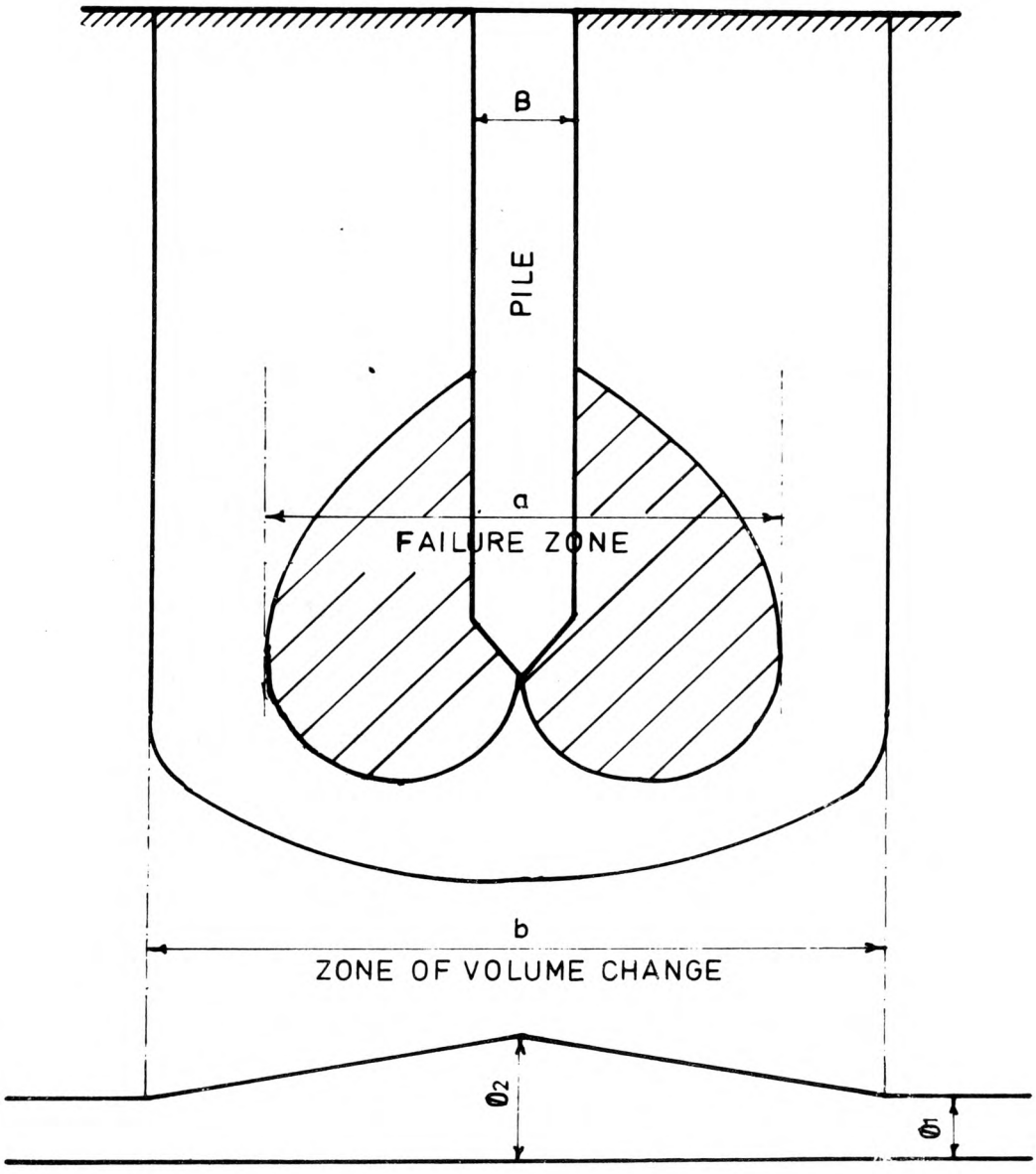

FIGURE 2.8

ZONES OF FAILURE AND VOLUME CHANGE, AND CHANGES IN THE ANGLE OF INTERNAL FRICTION NEAR A SINGLE PILE (FROM KISHIDA 1967)

Orrje and Broms (1967) found the shear strength measured immediately after driving 100 to 250mm diameter concrete piles 15.5m into normally consolidated clay, to be reduced from 0% to 40% in a zone 1.5 diameters around the piles.

Measuring the heave of soil caused by driving 168mm diameter steel piles into London Clay, Cooke, Price and Tarr (1979) showed a considerable disturbance in the soil, in a zone of approximately 4 diameters around the pile, over most of its length. They measured this heave to be approximately 75% of the embedded volume of the pile. Cooke et al. (1979) calculated the value of the shear modulus (G) within the zone of disturbance to be considerably less than values outside it. Near the surface, the value of G for the clay adjacent to the pile shaft was found to be approximately one third the value outside the disturbed zone, at the same level.

The changes in the angle of internal friction in the vicinity of the base of a pile, driven into sand, can be determined by using a method described by Meyerhof (1959). The procedure is as follows :

1. calculate the major principal stresses in the plastic and elastic zones.

   (i) In the plastic zone the major principal stresses σ_1 follow the path of the bisector of the angle between the radial and tangential slip lines and are calculated from plastic theory :

   $$\sigma_1 = \lambda K \gamma D e^{2\theta} \tan\phi \cdot \tan^2(45+\phi/2) \qquad (2.45)$$

   where θ = angle between the vertical and the direction of stress

   λ = shape factor

ϕ = reduced angle of friction allowing for compressibility of the soil

K = coefficient of earth pressure

D = depth of base

γ = soil unit weight

(ii) in the elastic zone the major principal stresses are determined from Bousinesq-Mindlin equations (see Terzaghi 1943)

$$\phi_1 = 3qpB^2/16r^2.\cos\theta \qquad (2.46)$$

where B = base width

r = distance from centre of base

qp = base pressure

2. Next, calculate the relative densities (Dr) from the principal stresses σ_1 from

$$Dr = D_2 - (D_2 - D_1)/[1+2.3(\sigma_1/p_c)c] \qquad (2.47)$$

where D_1 = initial Dr

D_2 = Dr at final void ratio for large pressures

p_c = pressure constant

c = compaction index determined from void ratio-pressure curves similar to the compression index.

3. ϕ values can now be obtained from Dr values either,

(i) from laboratory drained shear test on representative samples obtained from the site, or

(ii) approximated from results of standard or static penetration tests. Meyerhof (1959) found $\phi = 28^\circ + 15^\circ$ Dr in sands.

4. Using the new values of ϕ recalculate the major principal stresses which give a new set of relative densities and revised values of ϕ. This process is repeated until final stresses p_1 correspond to final values of the angles ϕ.

Adjusted values of the bearing capacity factors can be determined from the new ϕ values (Meyerhof 1959).

The theoretical limits of the zone of soil compaction are at the points where the major principal stress ratio is equal to the coefficient of passive earth pressure.

In the compacted zone Kishida (1967) made the assumption that the angle of internal friction changed linearly with the distance from the pile (where $\phi = \phi_2$) to a radius of approximately 3.5 times the pile diameter (where $\phi = \phi_1$) (see Figure 2.8). The relationship between ϕ_2 and ϕ_1 in sand has been expressed by Kishida and Meyerhof (1965) as

$$\phi_2 = (\phi_1 + 40^\circ)/2 \qquad (2.48)$$

where ϕ_1 = original value of ϕ

ϕ_2 = final value of ϕ due to pile driving, directly under the pile tip.

Kishida (1967) found the relative density of loose cohesionless soil to increase due to pile driving. Stresses developed in a sand when a pile is driven into it are of two kinds (Kishida 1963, 1967) :

1. Stresses developed due directly to the applied load which disappear when the load is removed (load stresses).

2. Displacement stresses developed by displacement of the sands. These remain after removal of the load.

The compaction of loose sand results from the development of the displacement stresses. The stress distribution of the load stresses may be calculated by the theory of elasticity when the equivalent depth is to be considered, and it can be superimposed when the pile spacing is more than twice the pile diameter (Kishida 1963).

The process of sand displacement and compaction below a pile point is followed by sand movement adjacent to the pile walls that tend to decrease the sand density in the immediate vicinity of the pile wall. This creates a "bin effect" (as described in section 2.10) when the thin sleeve of soil moving down with the pile transfers some of its weight to the adjacent soil mass. At the same time this induces lateral earth pressures to be carried around the pile by "arching" (Terzaghi 1936, 1943). Robinsky and Morrison (1964) showed the extent of this "arching ring" around piles driven into sand using radiographic techniques. Robinsky and Morrison (1964) showed that for tapered piles, the above process appeared to take place, but was compensated in part, by the wedging action of the pile taper, which recompacted adjacent surrounding sand. This permitted the development

of high friction stresses, thus most of the load was transferred through skin friction. Tapered piles created a greater envelope of visible displacement, carried 40% more load than straight sided piles, and transfered this load at higher levels.

Studying the results of three sets of piled foundations in deep clay deposits, Orrje and Broms (1967) found high pore pressures to develop within pile groups during driving which may exceed the total overburden pressure. Massarsch and Broms (1977) suggested that while driving piles into normally consolidated clays, cracks could develop in the clay. These cracks temporarily increase the permeability of the clay in the plastic zone around the pile and cause a rapid dissipation of excess pore water pressures.

As discussed earlier, piles driven into clay deposits will cause the soil within a pile group to heave. This heave can cause substantial reduction in the end bearing capacity of piles founded on rock or a layer of dense sand since the heaving action will lift pre-driven piles off their supports. Redriving of these piles will be necessary.

When driving piles into dense granular soils, jetting of the piles can reduce driving resistances. Jetting however, may also reduce the ultimate carrying capacity of a pile, since the process loosens the soil material at the base of the pile. Hunter and Davisson (1969) found the load carried by a double-jetted pile to be only 66% that of a non-jetted pile. This was believed to be an extreme condition.

2.17 Layered and Nonhomogeneous Soil

When piles are placed in layered soils an extensive site investigation is needed to determine the best location for the pile toe. Since the skin friction resistance on piles in cohesive soils is high, as well as the end bearing resistance on piles in cohesionless soil, the location of the pile toe is important to limit the pile settlement during loading.

If piles penetrate into a sand stratum overlying clay, failure may occur by punching (see Chapter 1) into the underlying clay as the pile tip approaches the sand-clay interface. The level up to which piles can safely be driven when a soft soil layer underlies the bearing stratum depends on the ratio q_{1w}/q_{1s}, where q_{1w} and q_{1s} are the limiting point resistances in the weaker and stronger layers respectively. Meyerhof and Sastry (1978) found the critical distance between the pile tip and the soil interface, in order to avoid punching failure, to increase with increasing strength difference of the two soil layers, from about 1.5B for $q_{1w}/q_{1s} = 0.67$ to about 6B when $q_{1w}/q_{1s} = 0.02$.

The maximum point resistance on a pile end bearing in a strong layer, overlying a softer more compressible deposit, is equal to q_{1s} (for a relatively thick bearing stratum with a strength ratio near unity, end bearing near the top of the strong layer). Meyerhof and Sastry (1978) proposed the following equation for the maximum point resistance (q_p) in a strong layer overlying a weaker one :

$$q_p = q_i + 4SpKps\sigma'_{vo}\, h' \tan\phi_s/B \leq q_{1s} \quad (2.49)$$

where q_i = unit point resistance at the soil interface

$= CuN_{co} + \gamma(D+h')N_{qo} \leq q_{lw}$

Cu = unit soil cohesion

Sp = shape factor for punching

Kps = average punching coefficient

h' = maximum punching height

σ'_{vo} = effective overburden pressure at centre of h'

ϕ_s = angle of internal friction of the strong soil

B = pile diameter

γ = unit weight of soil

D = depth of pile point

N_{co} and N_{qo} = surface bearing capacity factors for circular footings on weak soil.

Values of Sp, Kps, N_{co} and N_{qo} can be obtained from the literature. Meyerhof and Sastry (1978) also cited cases where, for a small punching thickness (h) below the pile tip, no punching failure took place because the sand layer bends. This occurs when h/B is less than approximately 2.

Considerable amounts of settlement can occur in pile groups driven to sufficient set in a dense stiff stratum overlying a weaker more compressible layer. This is caused by the deeper heavily stressed zone of the pile group reaching down into the weaker layer (Tomlinson 1977).

When piles are driven into clay, a thin skin can adhere to the pile shaft and be dragged down with it. In the case of layered soils a weaker skin from a weak overlying layer can be dragged down into a

firmer layer with the effect of lowering the piles ultimate bearing capacity. Tomlinson (1977) measured this dragging down of weaker soil into the stronger lower layers to be approximately three pile diameters.

Terzaghi and Peck (1967) suggest, that for piles passing through compressible material into cohesionless soils the safe load should not exceed two-thirds of the point resistance, ignoring skin friction entirely.

Poulos (1979) considered various methods of adapting Mindlin-based analysis, for a pile in a uniform soil, to nonhomogeneous soils. He found that by using an average weighted soil modulus, the solutions best agreed with finite element results :

$$E_{eq} = \sum_{k=1}^{m} E_k \delta_k / D \qquad (2.50)$$

where E_{eq} = the equivalent modulus over depth D

E_k = Modulus of layer

δ_k = thickness of layer

m = number of layers in depth D

Poulos further suggsts that in calculating the base resistance, an average modulus be taken within a depth of five base diameters below the base.

2.18 Effects of Base Shape on Pile Bearing Capacity

The extent of the influence of the base shape on the carrying capacity of a pile, is dependent on : the soil type and properties, and the surface roughness and method of installation of the pile.

As a pile is driven into the soil a compacted cone of soil is driven in front of the pile, acting as a conical base. The central angle of the actual cone of a pile base could influence this compacted zone of soil beneath the pile tip. Meyerhof (1953) has presented graphs for the value of the bearing capacity factors for conical and wedge shaped tips of differing central angles. In this paper Meyerhof stated that as the cone angle of the tip increased, the point resistance of piles with smooth tips decreased, while those with rough tips increases, for both cohesive and noncohesive soils.

Eastwood and Anagnostov (1962) performed small model tests on flat, hemispherical, and 45° and 90° conical bases in dense sand. They found that the slope of the load-deflection graph was found to be proportional to the base diameter and not to the base area. They postulated that the base shape was not important. The authors, did however suggest, that in the case of a full-scale pile with a 45° conical base, the angle of the base could cause an increase in the skin frictional resistance due to pile driving. This would result in an increase in the slope of the load-deflection curve.

Franke and Garbrecht (1977) found the load-settlement behaviour to deteriorate due to the formation of enlarged bases, for piles in medium strength sands. They found the point resistance at failure to be reduced by approximately 30% for piles with enlarged bases, as

compared to those with constant cross-sections of the same size. This was caused by a loosening of the soil immediately below the pile tip during cutting of the enlarged bases.

2.19 Pulling of Piles

The simplest method of restraining piles against uplift forces, is to employ a pile shaft that is sufficiently long enough to take the whole uplift load in skin friction. However, the tangential force acting on a pile shaft in tension, will not necessarily equal that in compression. This must be accounted for in the design. Published test results have shown uplift skin friction can be as much as 50% less than the skin friction in compression (see section 2.6 and Tomlinson 1977).

Tomlinson (1977) suggests a factor of safety of three be used when applying equations derived for compression to calculate the ultimate uplift resistance.

An explanation for the differences in skin friction in tension and compression has been given earlier (section 2.6). It was suggested that the reduction in skin friction in pulling was due to a relief of some of the overburden pressure on lower levels.

Ismael and Klym (1979) have proposed the following equation for the uplift resistance of short piers in sand :

$$Q_{ul} = \tfrac{1}{2}\gamma' D^2 \pi B K_u \phi' + W \qquad (2.51)$$

where Q_{ul} = ultimate uplift resistance

γ' = effective unit weight of soil

D = depth of footing

B = pier diameter

Ku = coefficient of lateral earth pressure to uplift

ϕ = effective angle of shearing resistance

W = effective weight of the concrete pier

Substituting fullscale field results into this equation, Ismael et al. (1979) calculated a value of 1.6 for Ku.

Brinch Hansen (1968) derived an equation for the tensile skin frictional resistance which is given in section 2.6 (equ.2.26).

The sequence of loading may also effect the ultimate uplift resistance (section 2.15, Hanna and Tan.1971). However, Tejchman (1969) has stated that the bearing capacity of a pile to pulling does not depend very much on the sequence of loading.

Berezantzev et al. (1961) found that the resistance to pulling a pile from sand could be increased by a factor of 1.5 if the uplift force formed an angle of about 18° with the axis of the pile.

2.20 Eccentric, Inclined and Lateral Loading

The bearing capacity of piles subject to a combination .of axial force and bending can be greater than that of piles subject only to axial forces (Berezantzev et al. 1961).

Chin and Chan (1977) reported the following from the results of eccentric loading testson piles at both model and field scales :

1. eccentric loading had a greater effect on a pile as a structural member, than on the capacity of the soil to carry the load transferred from the pile.

2. If the pile head was restrained against lateral movement a small increase in the carrying capacity of the pile resulted.

3. Eccentric loading had very little effect on the load-settlement relationship at the pile top.

4. For the instrumented 25mm diameter by 2m long steel piles used in sand, the effect of eccentric loading was to increase bending movements, shear, and lateral movement of the top half of the pile.

5. Due to pile bending the skin friction in the top half of the pile decreased with increasing eccentricity.

6. Eccentric loading at the top of the pile had little effect on the response of the pile toe.

Meyerhof (1953) found the bearing capacity of model footings on both clay and sand, to decrease rapidly with increasing eccentricity and inclination of load.

Comparison of the findings of Meyerhof (1953), and Chin and Chan (1977) shows the influence of confinement on the pile shaft. In the case of Chin and Chan's results the confining pressure acting on the pile shaft tends to eliminate the effect of eccentric loading of the pile top on the lower portion of the pile. The experiments performed by Meyerhof on footings, showed that in the absence of a confining

pressure, an eccentric load applied to a footing reduces its bearing capacity.

Meyerhof (1953) extended his bearing capacity theory of foundations under central vertical loads to account for eccentric and inclined loads. This was accomplished by incorporating a value of the effective base contact width and the effective shaft contact area into the expressions for skin friction and end bearing resistances. He presented curves for the bearing capacity factors for various inclinations of load; for piles in cohesive and cohesionless material.

The resistance of piles to lateral loads has been found to be improved by either, increasing the pile spacing, or battering the piles (Kim, Sing, and Brungraber 1979).

Kim et al. (1979) found the presence of pile cap-soil contact to have a significant effect on the resistance to lateral loads for groups containing no battered piles. However, for groups with more than one-half of the piles battered the presence or absence of the pilecap-soil contact, had little effect on the lateral resistance of the group.

Full-scale lateral load tests by Kim et al. (1979) showed, that the removal of a 100mm layer of soil beneath the pile cap increased the lateral deflections and bending moments of the pile cap to almost twice the values obtained when there was pile cap-soil contact, for groups with no battered piles.

Kim et al. (1979) also found that as the lateral load on a group of piles reached the yield load, of at least some of the piles, the lateral group efficiency approached unity, and thus, each pile in the group was no more effective than a single pile.

2.21 Pile Testing

A pile loading test is an empirical means of checking the capacity of a pile in the field, when it is felt that theoretical methods will not suffice. The inability of theoretical methods to give a true understanding of a piles' behaviour under load, and determination of the failure loads, could be due to deformities in the pile or unaccounted for anisotropy of the soil.

When a pile that is being driven, comes into contact with a large boulder, further driving could cause the pile to break or buckle. Any indication that this has happened may not be noticed during installation of the pile. For steel piles a duct of steel channel, angle or tubular section, can be welded along the length of the pile for insertion of an inclinometer, to check that the pile has not bent or broken during driving. A tube can be cast inside a precast concrete pile for the same purpose. For any type of pile formed by pouring concrete into a borehole or shell, the quantity of concrete used should be monitored to ensure that the full volume of the bore is accounted for, and that necking or waisting has not occurred.

The presence of loose lenses in the soil, beneath or around piles, may not be detected by the site investigation. This could happen if not enough sample boring or penetration tests are performed

in the vicinity of the piles.

Pile loading tests still remain the most accurate method of determining the load-settlement behaviour of a pile in the field.

Three reasons for conducting a pile loading test, according to Whitaker (1970) are :

1. to determine the load-settlement relationship,

2. to ensure failure does not occur before a load is reached, which is a selected multiple of the working load (multiple = safety factor),

3. to determine the real ultimate bearing capacity, as a check on the calculated value, or

4. to obtain information to be used for design by empirical methods.

A loading test performed on an instrumented pile can be used to measure the portion of load carried by skin friction and point bearing, and to measure the distribution of stress along the length of the pile shaft (Gregersen and DiBiagio 1973).

The ultimate bearing capacity of all piles except those driven to bedrock is not reached until a certain time has elapsed. Therefore, the results of loading tests are not conclusive unless they are made after the pile has reached its ultimate capacity. Terzaghi and Peck (1967) suggest that for piles in permeable ground this period is usually two to three days, and for piles in silt or clay it may be about one month.

Some common types of pile loading systems are :

1. a dead load platform with a kentledge,

2. a bridge over the pile with a heavy kentledge placed on it and a jack between the bridge and pile,

3. the bootstrap method, using anchor piles at least 3 pile diameters from the test pile, and

4. cantilever load tests.

Descriptions, advantages, and disadvantages of each method can be found in most books on piling (Chellis 1961, Little 1961, Whitaker 1970, Tomlinson 1977).

The two load tests most commonly used in practice today are, the maintained load test (MLT) and the constant rate of penetration test (CRP). The procedure for the maintained load test is to apply the load in stages, the load at each stage being maintained constant until the resulting settlement of the pile ceases, before increasing the load to the next higher stage. The load applied to the pile is plotted against its resulting settlement for that stage and thus the load-settlement graph is plotted.

The constant rate of penetration test was developed by Whitaker (1957) for model piles and has proved equally useful for full-scale testing. For this test the pile is pushed into the soil (or pulled out of) at a constant speed from the position, as installed; while the load applied to the top of the pile to maintain the rate of penetration is continuously recorded. From this the load-settlement

curve is drawn and the ultimate loads are determined.

2.22 Scale Effects in Sand

One of the problems of using the results of a small model test, for deriving the factors to be used in calculating the behaviour of full size piles under load, is the influence of the differences in scale.

Hanna (1963) suggested that the compaction and sand strength properties were the chief cause of scale differences between model and field tests. He suggested that the curves obtained from his model tests could be taken as a guide for field analysis and were likely to be modified in detail only.

Steenfelt (1977) found that if the ratio between the mean grain size dk, of the soil, and the footing width B exceeded a value of $dk/B = 0.01$, then the effect of grain size on the bearing capacity of a shallow footing becomes significant. The scale effect could be expressed as a factor of correction to the bearing capacity factor $N\gamma$ and a graph of $N\gamma$ against dk/B has been given by the above author.

De Beer (1963) has given a practical method of using the cone penetration diagram for pile design which allows for scale effects.

2.23 Pile Groups

Very rarely is a pile used singly. Usually a group of piles are installed beneath a foundation, with a cap cast on to the heads of the piles to distribute the load.

Settlement of a group of piles with a given average load may be very different to the settlement of a similar pile under the same load. Similarly, the ultimate load that a group of piles can carry is not necessarily the same ultimate load of a single comparable pile times the number of piles in the group. This behaviour and the mechanism of interference between piles which cause it, is referred to as group action. The importance of group action varies with type of pile and soil conditions. It is important for friction piles in clay, but not as important for end-bearing piles in dense cohesionless soils. For piles driven to a bearing on underlying rock, group action does not affect the capacities and settlements of the piles to any extent.

In sand, the settlement of pile groups is more than that of an individual pile under a load equal to the average load per pile of the group. However, the ultimate carrying capacity of such a group can be more than the sum of the ultimate loads of the same number of individual piles (Berezantzev 1961, Whitaker 1970).

The principal problems with pile groups are :

1. ground heave,

2. interference of closely spaced piles which have deviated from line during driving, and

3. the possibilities of damage to adjacent structures and services.

The efficiency of a pile group correlates the carrying capacity of a single equivalent pile to that of the pile group. Hanna (1963) and Tomlinson (1969) define group efficiency as the ratio of the ultimate group load to the ultimate load of an isolated pile under the same conditions, times the number of piles in the group. Some American building codes give formulae for determining the efficiency of a pile group. The Converse-Labarre formula is one of these. It gives the efficiency E_f of a rectangular group of mxn piles as :

$$E_f = 1 - \theta/90\left[(n-1)m + (m-1)n\right]/mn \qquad (2.52)$$

The value of θ differs slightly for different building codes and is dependent on pile diameter and spacing.

For pile groups in cohesionless soils, Vesic suggests efficiencies of unity, while Kezdi has found efficiencies to be as high as 2. In cohesive soils Tomlinson (1969) suggests for spacings of 2 to 3 diameters an E_f value of 0.2, while at larger spacings (greater than 8 diameters) he suggests a value of $E_f = 1$.

Hanna (1963) states that the performance of a single pile which forms a unit in a group, bears no direct connection either to the performance of a similar isolated pile or to that of the complete group.

The settlement ratio of a pile group is best defined as the settlement of the group divided by the settlement of a single pile, when both carry the same portion of their ultimate load. Model test results have shown settlement ratios, for large groups, can be as great as 20. Therefore, the settlement of a single pile should be

used with caution when predicting the settlement of a group.

Model experiments conducted by the Building Research Establishment in clay (Cooke 1974), show that the efficiency increases with increasing pile spacing, and for a given number of piles, the settlement ratio decreases with increased pile spacing from a maximum value at about 2.5 pile diameters. At spacings closer than 2.5B block failure almost invariably occurs. The efficiency of some large groups of closely spaced piles were found to be as low as 30%.

When calculating the bearing capacity of pile groups, at small spacings, the group can be considered as a pier foundation with its base at the depth of the pile points. The total bearing capacity is therefore practically independent of the pile spacing. For centrally loaded foundations of this type, with vertical piles at customary spacings up to 4 or 5 diameters; the total bearing capacity is the sum of the base resistance of an equivalent pier, and the shearing strength of the soil along the perimeter of the group, less the weight of the enclosed soil (Terzaghi and Peck 1967).

Meyerhof (1963) suggests taking the smaller value of either the bearing capacity of an equivalent pier or the sum of thebearing capacities of individual piles, for free standing pile groups (pile cap not in contact with soil).

At small spacings, less than 2 or 3 diameters, the individual failure zones in the soil around the piles interact. This produces 'arching' between the piles, and leads to pier action of the group. For pile spacings larger than this, the individual piles govern, although deformation and any volume changes of the soil near the piles

have to be considered in estimating the total bearing capacity.

When a group of closely spaced piles is loaded, the soil within the group moves downward with the piles, and at failure piles and soil move together to produce what is known as 'block failure'.

Blocking action, according to Hanna (1963) appears to depend on soil density, pile spacing, pile roughness, and to a lesser degree on pile length and method of intallation.

The stability of a group of driven or bored piles against block failure is equal to the sum of the shearing resistance and the end bearing resistance of the block of soil contained by the piles. Both Terzaghi and Peck (1967) and Tomlinson (1969) have proposed equations for the ultimate carrying capacity of a pile group experiencing block failure as

$$Qu=q_d BL+2D_f(B+L)\bar{\tau} \qquad (2.53)$$

where q_d = ultimate bearing capacity, per unit area, of a rectangular loaded area with dimensions BXL at depth Df, Tomlinson suggests $q_d = 1.3CuN_c$,

$\bar{\tau}$ = average shearing resistance of soil per unit area, between surface and depth D_f, and.

Cu = cohesion of clay beneath group.

Terzaghi and Peck (1967) suggest that a group can be considered safe against such failure if, the total design load (the number of piles times the 'safe design load' per pile) does not exceed Qu/3.

Meyerhof (1956) has proposed semi-empirical equations, incorporating the results of standard penetration and Dutch cone tests, to calculate the allowable load (Qa) on a pile group in cohesionless soil. For a pile in a square pattern

$$Qa = \frac{q_c d^2 (1 + {}^1/_l)^2}{50} = \frac{Nd^2}{12}(1 + {}^1/_l)^2 \quad \text{(tons)} \qquad (2.54)$$

and for a triangular pattern use 0.8 Qa

where d = average pile spacing

l = width of pile group

q_c and N = average penetration resistance between depths of 2D/3 and (2D/3)+B from static and dynamic penetration tests respectively.

For a uniform spacing of driven piles or displacement caissons of 2 to 6 times the base diameter in cohesionless soil, Meyerhof (1959) has proposed equations based on the behaviour of an equivalent pile under the same conditions, for allowable load (Q_q) and settlement (S_q) per pile. In a square group

$$Q_q = \frac{(1+{}^1/r)^2}{s(5-s/3)} \cdot x\ Q_1 \qquad (2.55)$$

and $$S_q = \frac{(1+1/sB)^2 s(5-s/3)}{(2+1/sB)^2} \times S_1 \qquad (2.56)$$

where r = number of rows of piles

s = ratio of spacing to pile diameter

l = width of pile group

Q_1 = allowable load on a single pile

S_1 = settlement of a single pile under the same load as a pile in the group.

To facilitate the calculation of settlement of a pile group engineers have suggested the use of an equivalent pier as discussed earlier. For friction piles the location of the equivalent pier is usually taken at a depth of two-thirds the pile length. However, the dimensions of the pier are not assumed to be the same in all cases. Tomlinson (1969) suggests a pier of width larger than that of the pile group, while Whitaker (1970) suggests a pier of the same dimensions as the group, for friction piles in clay, see Figure 2.9.

For piles driven into sands and gravels, the sequence of driving can affect the stress distribution in the soil, even if the pile spacing remains the same. Tomlinson (1969) has suggested that to avoid 'tightening-up' of the ground, driving should start at the centre of the pile group and work outwards in all directions.

When the piles are constrained by a rigid cap or raft to settle equally under load, the central piles carry less load than those around the periphery (Whitaker 1970, Cooke 1975).

Cooke (1975) has suggested a method of computing individual pile loads for piles in a group constrained by a rigid cap or raft. The method consists of superimposing the computed settlement of each pile and solving a number of simultaneous equations. Each equation

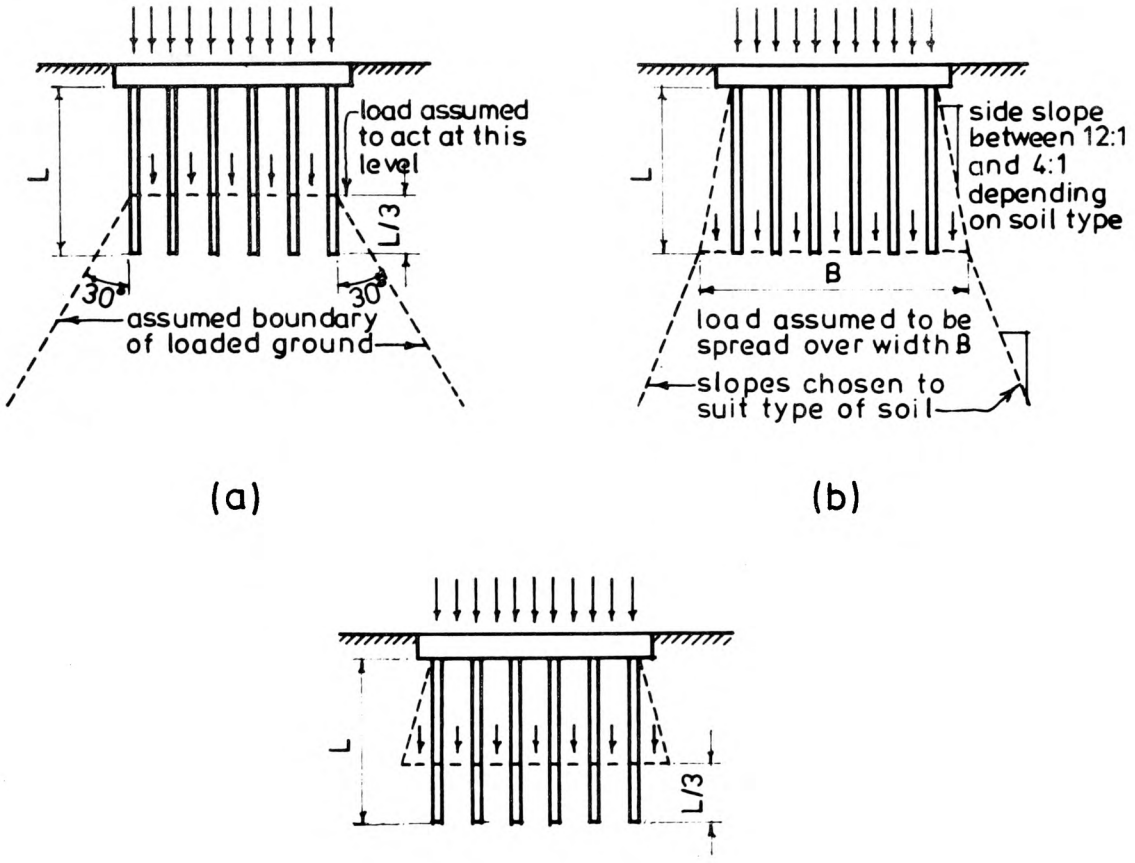

FIGURE 2.9

ASSUMED PATTERNS OF LOAD-SPREADING FROM FRICTION PILE FOUNDATIONS FOR CONSOLIDATION SETTLEMENT CALCULATIONS (a) WHITAKER (1970), (b) DUNHAM (1950), (c) TOMLINSON (1969)

relating to total settlement of each pile in terms of its own settlement and the settlements due to all other loaded piles in the vicinity. Each settlement component is proportional to the unknown pile load causing it. Since, all total settlements are equal, the set of equations can be solved simultaneously and the individual pile loads calculated. Good agreement has been found between this method of predicting loads and those observed for 168mm diameter, 5m long steel piles jacked into London Clay.

The effect of forming a rigid cap directly on the ground surface is to increase the load a given number of piles can carry, when spaced more than 2.5 diameters apart, but only at the expense of greater settlements.

Model pile tests on pile groups in clay (Cooke 1974), fitted with a rigid cap, show the inner piles carry less load than the outer ones. Therefore, it has been suggested that if model tests are representative of full-scale behaviour, then a major saving can be achieved by reducing the number of piles in some foundations in clay soils, as long as the possible accompanying increases in settlement is account for.

The stability of pile groups depends on the ability of the soil around and below the group to carry the load. Methods of installation have little effect, since the zone of soil affected by installation is very small, compared to the very large mass of soil affected by vertical pressures transmitted to it by the piles in the group (Tomlinson 1969).

2.24 Critical Appraisal of the Literature Reviewed

As seen in the preceeding literature review most investigators have considered piles either in sand or in clay. There is only a small amount of work available on the load transfer mechanism of piles passing through granular material, and end bearing in underlying soft rock or clay formations. However, the way in which this particular stratification affects the behaviour of the piles under load is not fully understood.

The many factors affecting the bearing capacity and settlement of piles have been summarized on pages 2.6 and 2.14. The effect of these factors is to cause a vertical and radial variation of the soil properties and consequently influence the parameters used for predicting the load/settlement behaviour of a pile or a pile group. Both Meyerhof's and Terzaghi's equations for the ultimate base resistance in a clay soil are of the form

$$qp = Cb\ Nc + \gamma D. \qquad (2.23)$$

The cohesion of the clay can be determined in the laboratory and from field tests. However, the main problem in determining qp lies in the determination of a value for the bearing capacity factor Nc. Early investigators considered Nc to be a constant. Skempton (1959) suggested a semi-empirical value of Nc = 9, although Cooke and Price (1973) found Nc to vary with depth. The coefficient of earth pressure on the pile in equation 2.14 for calculating the skin friction resistance on a pile has been given by Meyerhof (1951) to be between 0.5 for a loose sand and 1.0 for a dense sand. Coyle and Reese (1966)

stated that the value of Ks is a function of the soil shear strength, overburden pressure and the method of installation. Broms and Silberman (1964), Ismael and Klym (1979) and others have found Ks to be greater than one and to increase with increasing density and pile penetration. Brinch Hansen (1968) found the skin friction on a pile to be dependent on the absolute displacement and direction of the pile movement, Tejchman (1969) confirmed this and showed that the sequence of testing influenced the skin friction resistance that developed.

The changes in the soil properties due to the installation of a pile can be accounted for by :

1. finding methods of measuring the new soil properties or,

2. introducing factors into the equations to account for the different methods of installation.

The pile loading test is the most accurate method of determining the load/settlement behaviour of a pile in the field. However, the high cost of conducting loading tests on large caissons, piers, and pile groups make these tests impractical.

From the previous discussion it is apparent that to understand and describe the soil-pile interaction completely it is necessary to measure the forces and displacements on the pile and in the surrounding soil mass. This is a difficult task to perform but one that must be carried out both in the laboratory and in the field, if reliable and realistic predictions of the pile behaviour are to be made.

For a pile founded in a sand mass, it is clear that the movement of the pile base will influence the development of skin friction along the sides of the pile. Terzaghi (1943) has shown that for piles in sand a cone of sand is compressed in front of the pile as it is driven. This movement of sand is likely to loosen the overlying sand which is in contact with the sides of the pile. Consequently there is very little skin friction developed and an arching ring will form around the lower portion of the pile. This has been confirmed by Vesic (1963), Robinsky and Morrison (1964), Meyerhof and Valsangkar (1977) and others.

With regards to clay soils, there is very little evidence to show that the end bearing influences the wall adhesion. Tomlinson (1977), however, suggested that for under-reamed piles the wall adhesion should be disregarded for a distance of two pile diameters above the top of the under-reaming. In layered soils it is generally assumed, for design purposes (Tomlinson 1977), that the skin friction resistance will develop through the whole granular soil layer and is not influenced by the underlying clay layer.

The situation of a pile penetrating into a clay stratum, as investigated by the candidate, presents a different problem. The end bearing resistance that is developed is likely to be quite small compared to the skin friction resistance. Also, the movement of the clay is far more likely to be in an upward direction in the form of a heave rather than downwards as in the case of a pile end bearing in sand. This will influence the development of the skin friction. Tomlinson (1977) contends that the sand is likely to be drawn down with the pile. This is likely to be the case particularly with driven

piles. These soil movements could also be influenced by the shape of the pile toe. It is the considered view of the candidate that initially in this investigation, it is necessary to examine the development of skin friction in the sand assuming that no heave develops at the clay-sand interface and that no sand is drawn down with the pile (see section 1.1). This situation was simulated by driving the base of the pile into a frictionless cylinder as indicated in Chapter 1 and described in detail in Chapter 3.

Chapter 3

Description and Development of Testing Apparatus and Monitoring Systems

CHAPTER 3

DESCRIPTION AND DEVELOPMENT OF TESTING APPARATUS AND MONITORING SYSTEMS

3.1 Sand Tanks

The pile loading tests were carried out in the soils laboratory at the Polytechnic of Wales. The facilities available included two 3m. diameter by 3m. deep concrete tanks. The tanks are fitted with a Redler Conveyor System for transferring the sand from one tank to the other as shown in Figure 3.1. Elevations were marked on the inside surface of the tank to allow for control of the depth of each layer of sand poured. A system of step brackets has been mounted to the inside wall of the testing tank (see Figure 3.1). Wooden scaffolding planks were placed on the step brackets at four different elevations on the inside wall of the tank. This is used as a walkway from which the operator can work, while pouring sand or placing equipment in the tank. This would minimise the disturbance to the soil.

3.2 Loading Frame

A loading frame has been mounted to the top of the testing tank as shown in Figure 3.2 and Plate 3.1. The frame has been designed to allow for easy access to the tank for filling, and for the positioning of the testing and recording equipment. It consists of a stiffened

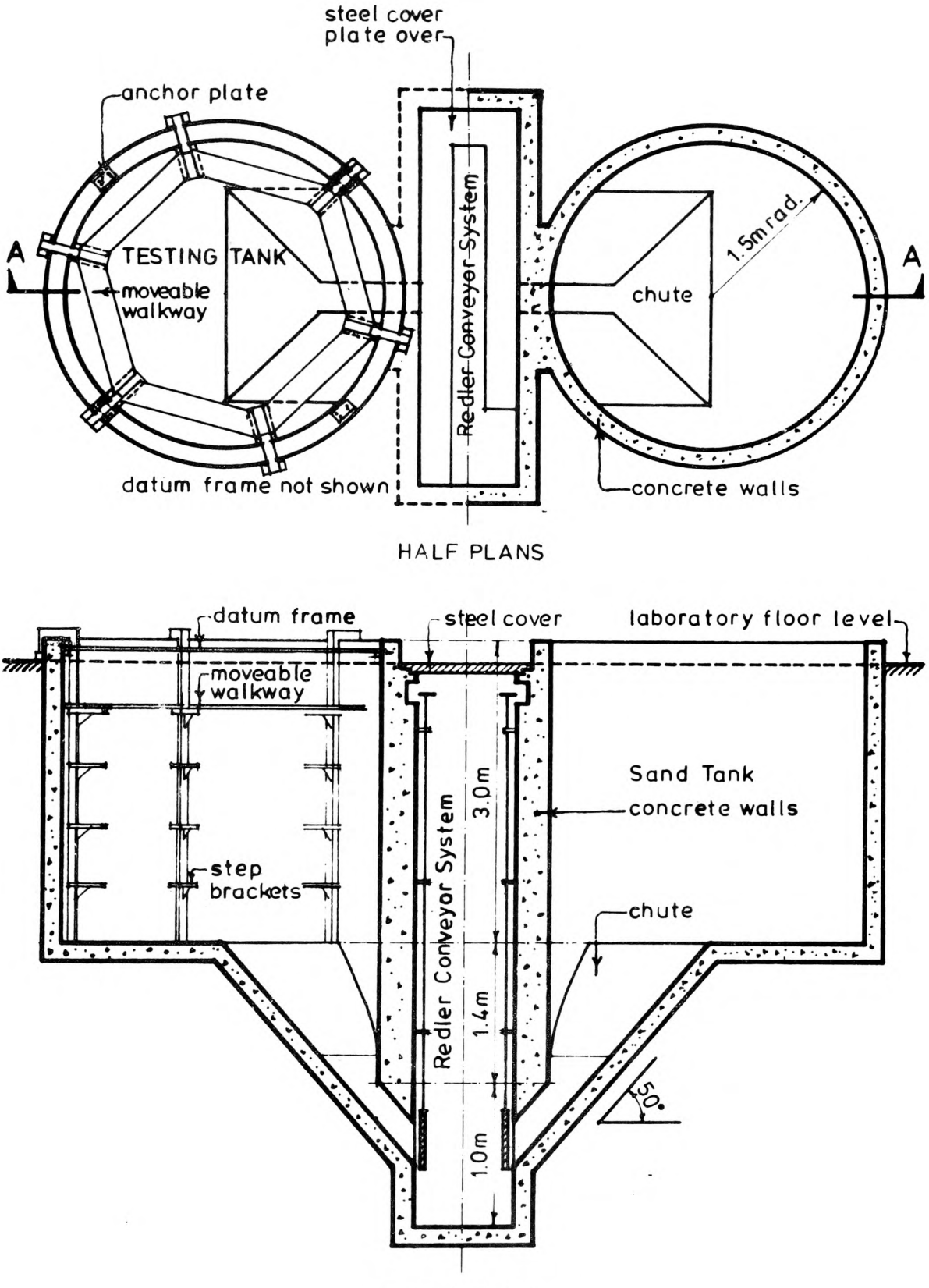

FIGURE 3.1

SAND TANKS AND REDLER CONVEYOR SYSTEM

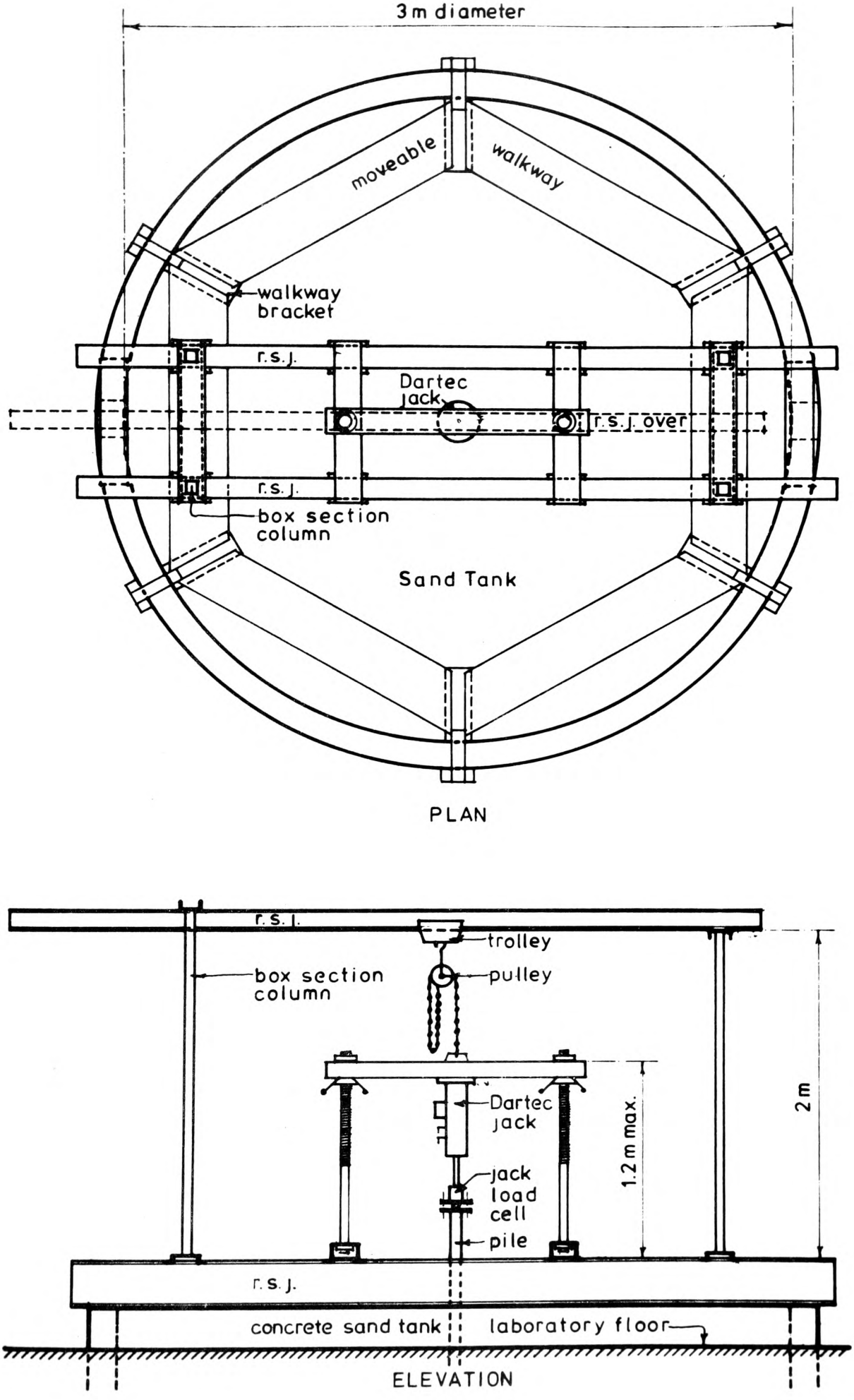

FIGURE 3.2

LOADING FRAME AND GANTRY

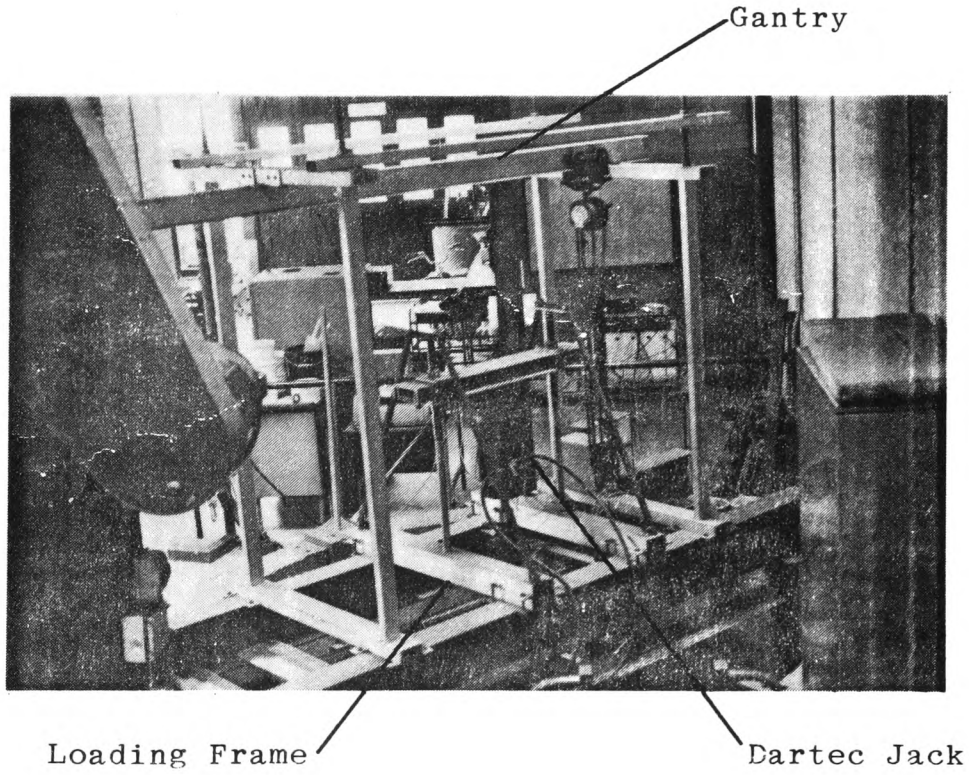

PLATE 3.1

LOADING FRAME AND GANTRY

channel crosshead mounted on two Rolled Steel Joists. The crosshead is attached to the Rolled Steel Joists via two threaded steel pillars. The crosshead can be positioned at any elevation along the threaded section of the pillars. The 50kN hydraulic jack which was used to load the pile is bolted to the crosshead.

3.3 Gantry

To allow for the manipulation of heavy equipment, such as the loading jack and the frictionless cylinder, a gantry was designed and fixed to the top of the superstructure (see Figure 3.2). The gantry consists of a 500 kg block and tackle which travels along an I-section rail supported by a frame constructed of rolled hollow section. The rail runs across the entire length of the tank and extends beyond the edge to enable the equipment to be hoisted off the laboratory floor to its final position above, or in the testing tank.

3.4 Datum Frame

A datum frame, independent of the loading frame, constructed of dexion, was fixed to the inside wall of the testing tank below the loading frame (see Figure 3.1).

The equipment necessary for monitoring the movement and density of the sand was linked to the datum frame.

3.5 Dust Extraction and Sand Placement

It was felt that the dust created in the transfer of sand was a potential health hazard and could adversly influence the function of the mechanical and electrical equipment. Therefore, a dust extraction unit was designed by the candidate and installed by an outside contractor. The dust extraction unit was found to reduce the dust to an acceptable level. At the same time the sand placement machinery was modified to ensure a more uniform placement of sand (see Plate 3.2).

The Redler Conveyor lifts the sand from the bottom of one tank to a maximum height of 5m, from which it flows through a combination of tubes and is poured into the other tank. The last of these tubes is flexible and thus enables the placement of sand to any location in the tank.

The dust extraction unit is connected to these flexible sections of tube so that the dust created by the movement of sand is removed before the sand leaves the tubes. The end of the tube is controlled so that the sand falls freely approximately 150 to 200 mm. The end of the tube was fitted with a .35m diameter conical hood and a brass 2.36 mm sieve to evenly disperse the sand, producing a more uniform placement. This arrangement is shown in Figure 3.3. It assists greater uniformity of the density of the sand and extracts any dust caused by the final fall of sand from the end of the tube to the sand surface.

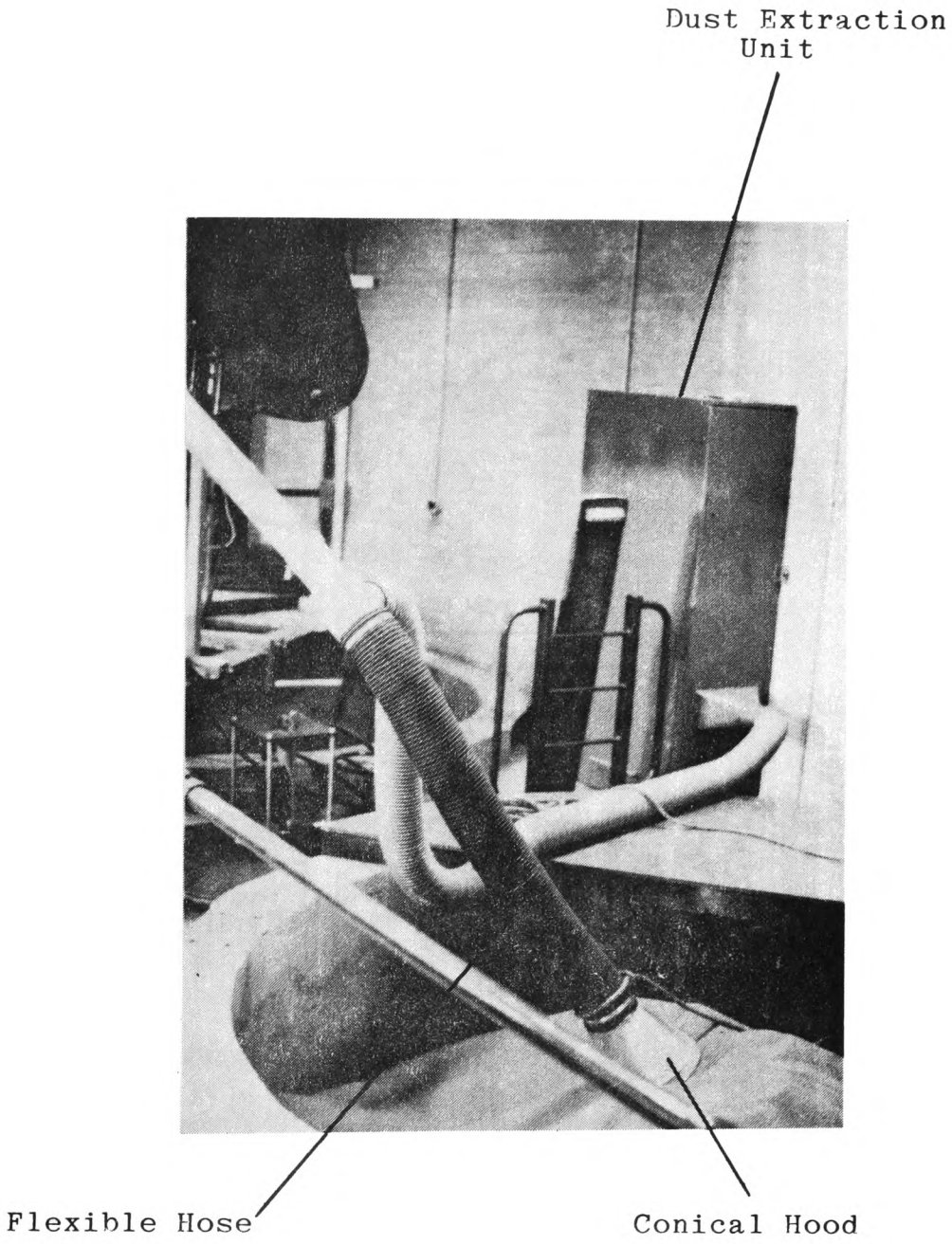

PLATE 3.2

DUST EXTRACTION UNIT AND SAND PLACEMENT APPARATUS

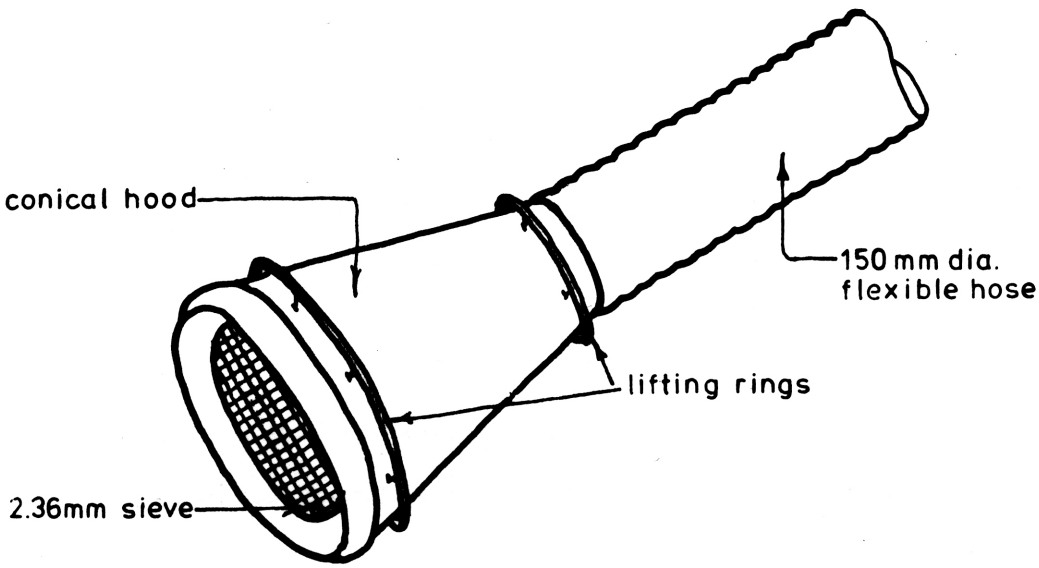

FIGURE 3.3

SKETCH OF SAND POURING ATTACHMENTS

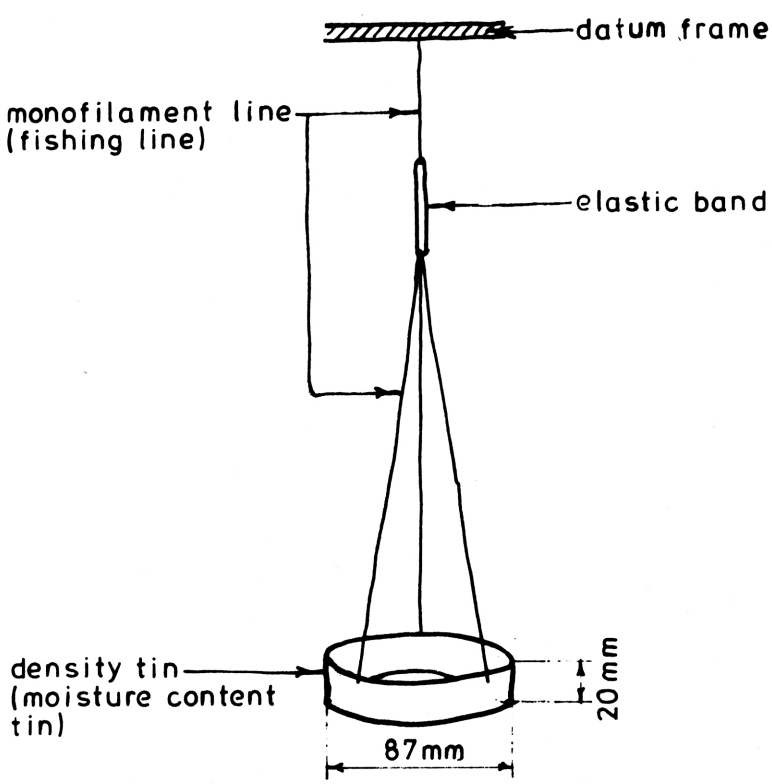

FIGURE 3.4

SKETCH OF DENSITY TIN AND ATTACHMENTS

It was considered that the fines removed by the dust extraction unit would not materially alter the properties of the soil during the testing programme. But the grading of the sand was monitored at regular intervals throughout the testing programme. The results of this are given in section 6.1.

3.6 Measurement and Control of Sand Density

The ability to measure the in-situ density, of purely granular soil, is a field of soil mechanics in which much work has been done, but no absolute practical solution has been found.

In the course of the present study the candidate monitored the uniformity of placement by estimating the relative density of the soil in the following manner :

1. By consistency in the placement and compaction of sand, a uniform sand density should have been achieved. To monitor relative density of the soil a small version of the Mackintosh Prospector probe has been developed and proved successful (see Plate 3.3).

2. Tins were placed at designated positions during sand placement as shown in Plate 3.4. They were connected to the datum frame at the top of the tank by a set of three lengths of monofilament fishing line. These lines are sufficiently elastic to allow movement of the tins due to soil compaction (see Figure 3.4).

3. After testing the pile the tins were manually retrieved as the tank was being emptied via the Redler Conveyor system. Since the tank is emptied from the bottom, the tins were left suspended

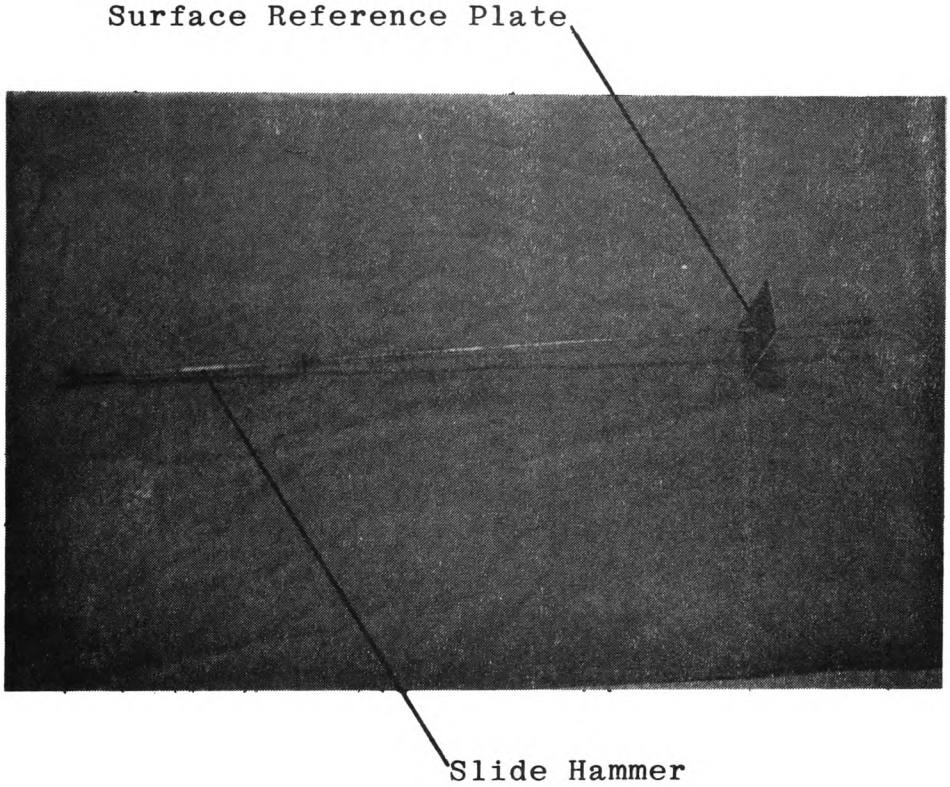

PLATE 3.3

MINI-MACKINTOSH DYNAMIC
PENETRATION PROBE

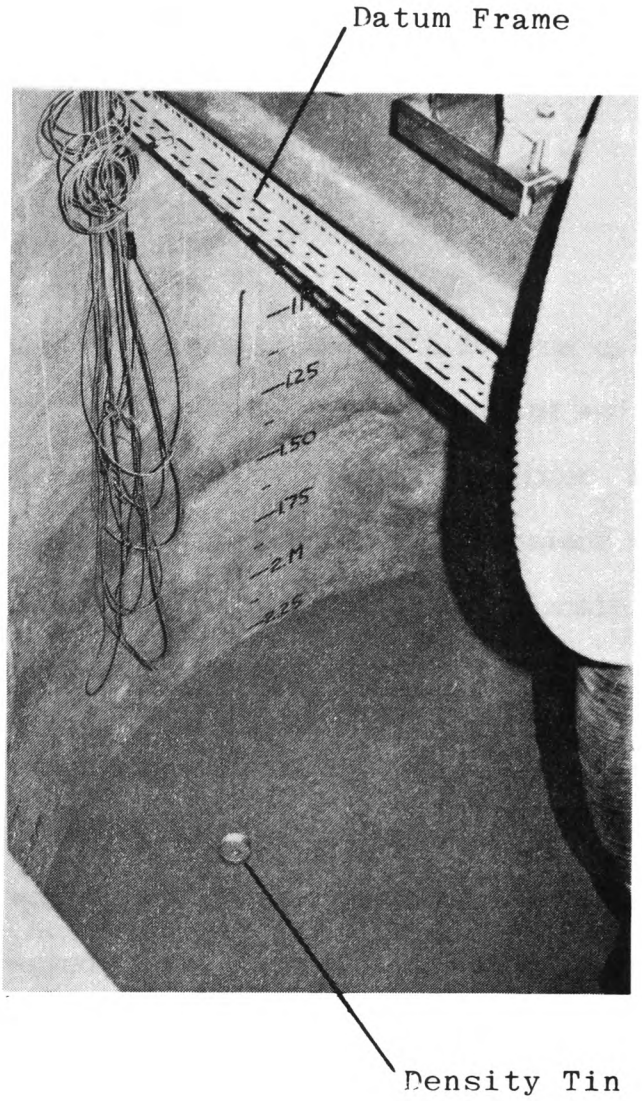

PLATE 3.4

DENSITY TIN

horizontally so they could be retrieved and the density of the sand could be determined as described in section 7.3.4.

The possibility of using a Nuclear Density Meter for measuring changes in the relative density of the sand was explored, but due to safety and economic reasons this method was abandoned.

3.7 Frictionless Cylinder

Following the success of the frictionless cylinder in the pilot study, for the elimination of end bearing and the simulation of an underlying clay stratum, a larger cylinder was manufactured to accommodate the 114 mm diameter pile sections which was used in the present semi-fullscale study. The semi-fullscale pile and cylinder configuration are shown in Figure 3.5.

Consideration was also given to the future modification of the cylinder to simulate the movement of an underlying clay stratum. This modification would simulate the process where a skin of the overlying layer is dragged down into the underlying stratum (as described by Tomlinson 1977).

3.8 Dartec Hydraulic Jacking System

The loading equipment consisted of a 50kN Dartec servo hydraulic jack with a stroke of 100 mm. A load cell and displacement transducer are fitted to the jack shaft. The load cell has an accuracy of 1% of

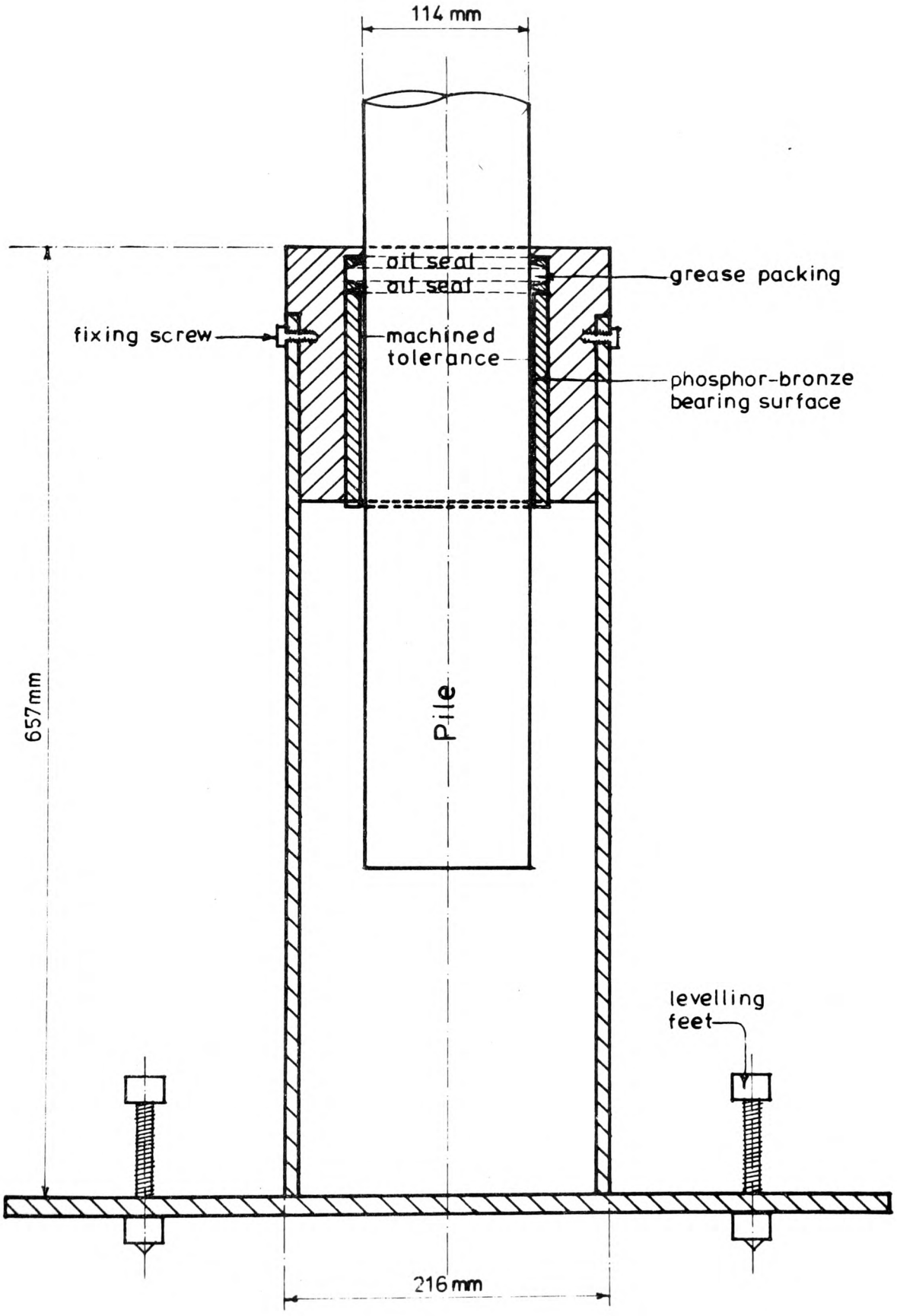

FIGURE 3.5

FRICTIONLESS CYLINDER

the reading down to 1/100 of its capacity.

The jack is driven by a frequency generator capable of driving the pile in load or displacement control in either a static or dynamic mode.

To produce the compatibility necessary between the voltages of the Dartec jack and the strain gauges, for recording on the Mycalex data logger, a reducer conditioning unit was built with a gain of ten to one. This unit reduced the range of the output voltages of the ram displacement and load, from 0-10 volts to 0-1 volt.

A two channel chart recorder was used to record both the displacement and the load of the ram during testing.

3.9 Mycalex Data Logging System

The permanent record of all data was compiled by a Mycalex Data Logger with a 100 channel capacity. All voltage readings of strain, load, and displacement measured by the strain gauges, load cells, and transducers were fed into the data logger and stored on punched tape by a teletype facility as shown in Figure 3.6.

The output from the Mycalex data logger was punched on a standard eight track paper tape which was subsequently fed to the DECsystem-20 computer located in the Computer Centre of the Polytechnic. Computer programs were written to allow the DECsystem-20 to read and store the data in a file form prior to processing. After processing the data, the results were outputted in both numerical and graphical forms. These were analysed and the results are shown subsequently in Chapter 7.

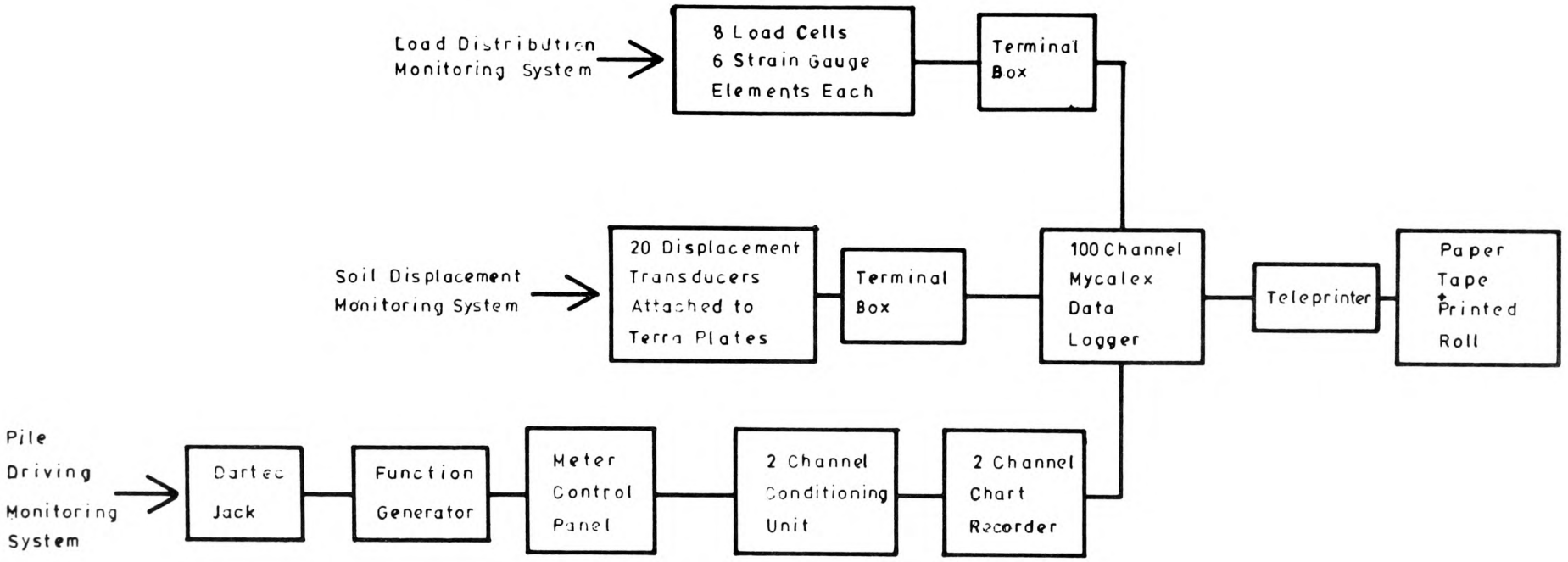

FIGURE 3.6

SCHEMATIC DIAGRAM SHOWING RECORDING EQUIPMENT CONNECTIONS

Chapter 4

Load Transfer Mechanism : Principles and Monitoring Systems

CHAPTER 4

LOAD TRANSFER MECHANISM : PRINCIPLES AND MONITORING SYSTEMS

4.1 Transfer of Load from the Jack to the Top of the Pile

The pile loading arrangement is shown in Figure 4.1. The load was applied to the pile through a steel ball via the two plates which were attached to the jack ram and to the top of the pile. The ball seatings had been machined into the plates to accommodate the steel ball which allowed for centralization of the load. The plates were connected by fixing bolts, to allow the pile to be raised during assembling and dismantling of the apparatus, and to form a continuous member so that pulling tests could be performed.

After the pile had been assembled in position under the jack and checked for verticality, the upper plate which was fixed to the jack was brought into contact with the steel ball, which was seated on the bottom plate which was attached to the top of the pile. The fixing bolts between the two plates were then systematically tightened so that the pile remained in a truely vertical position. This was checked with a theodolite. The pile was thus rigidly fixed to the jack and as far as possible any misalignment or eccentricity was eliminated.

During compression testing the load was applied to the pile solely through the steel ball, but during pulling tests the load was applied via the four fixing bolts.

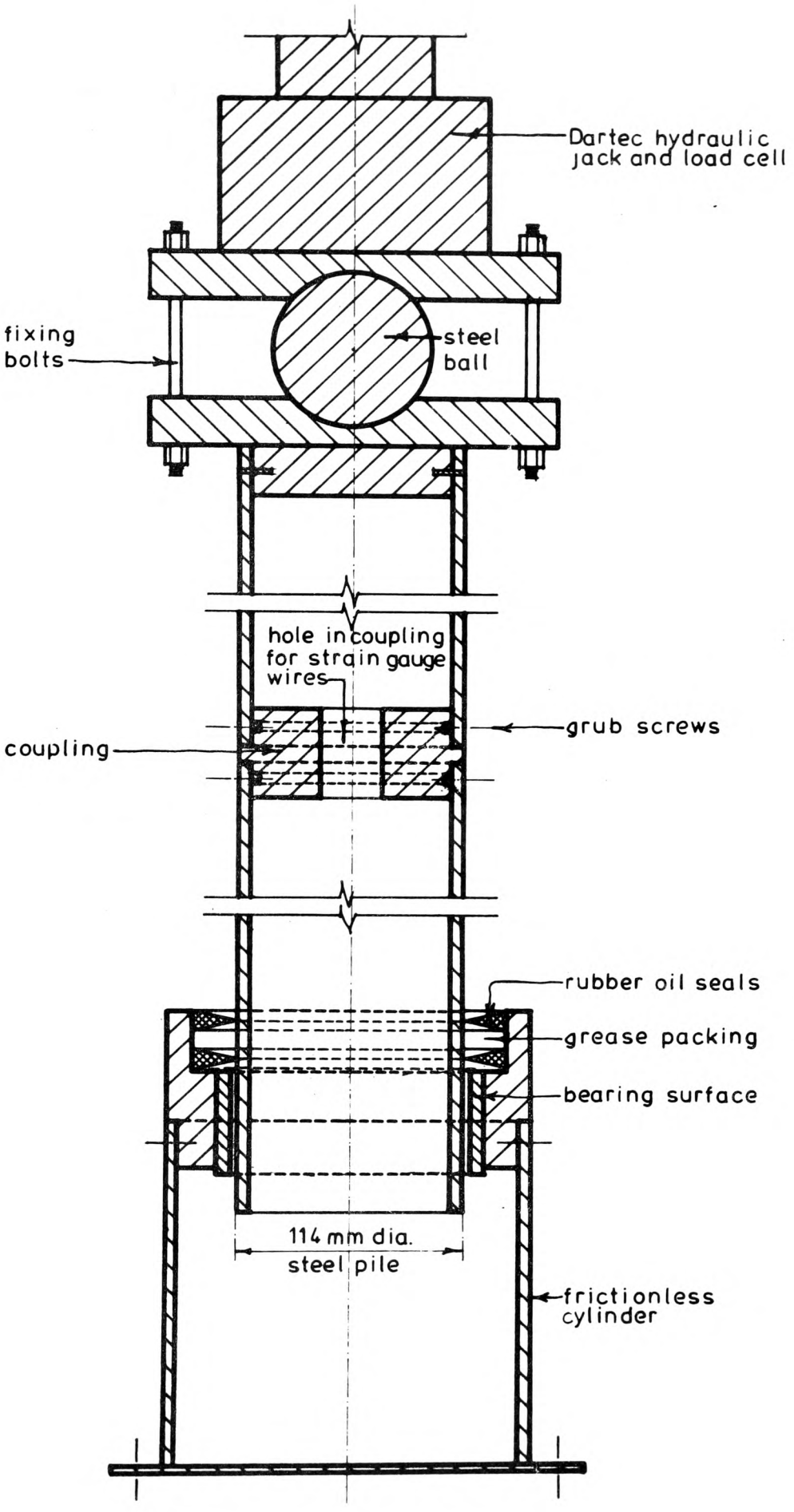

FIGURE 4.1

SEMI-FULL SCALE TEST ARRANGEMENT

4.1.1 Dartec Load Cell

An integral 50 kN load cell is attached to the ram of the Dartec jack (see section 3.8 for detail). This cell was used to measure the total load applied to the pile during the testing programme.

4.2 The Transmission and Dissipation of Load along the Length of the Pile

A review of the proportion of load carried by skin friction and end bearing has been discussed in section 2.6.

The present research work is the investigation of the behaviour of a pile, in a granular medium, which is end bearing in an underlying cohesive soil.

If the pile punches into the clay stratum, the end bearing resistance of the clay acting on the base of the pile is thought to influence the development of skin friction in the granular layer above. This is likely to affect the creation of a 'bin effect' as described by Terzaghi (1936), and the development of the subsequent 'arching ring'.

In order to investigate the behaviour of the pile in the granular medium, for the present study, the end bearing was eliminated.The load was transferred to the surrounding soil medium entirely through skin friction.

A larger model of the frictionless cylinder, which was developed following the promising results of the pilot study, was used in the semi-fullscale testing programme to eliminate skin friction and to simulate the pile punching into an underlying clay layer (see Figure 4.2).

4.2.1 Test Pile Load Cells

The load along the test pile was measured at eight different locations by the eight load cells. The proportion of load transferred to the soil between any two load cells is the difference in load measured by each cell.

The specifications and descriptions of the types of load cells used are given in Chapter 5.

4.2.2 Lateral Pile Displacements : Preventative and Remedial Measures

If, the loading jack is not positioned truly vertical and directly over the pile, eccentricities and bending movements will be created in the pile.

Berezantzev et al. (1961) have shown that the bearing capacity of piles, subject to a combination of axial force and bending movements, can be greater than that of piles subjected to axial forces alone.

To eliminate this complication arising, the jack and the pile were carefully aligned using a theodolite.

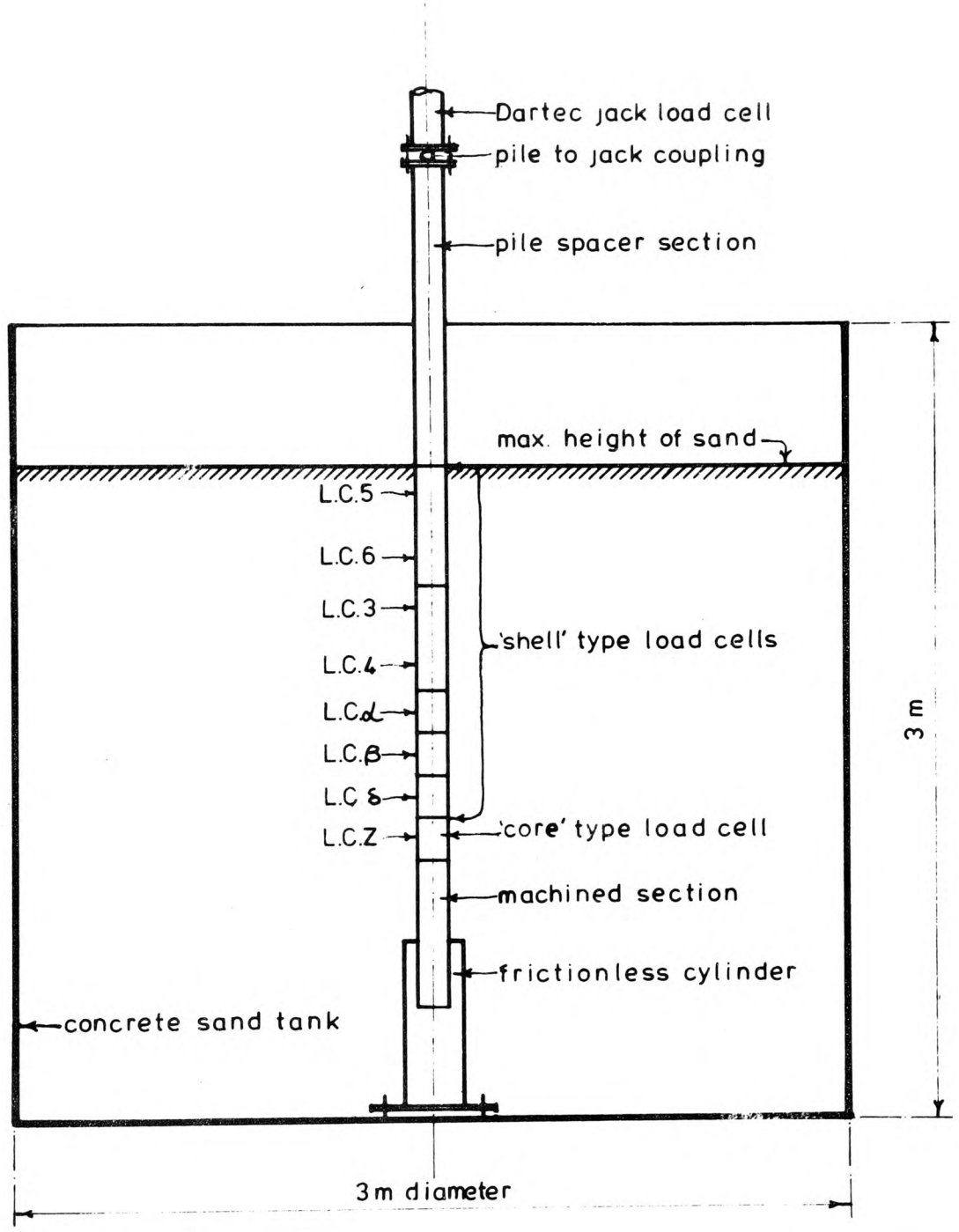

FIGURE 4.2

SKETCH OF SAND TANK AND PILE

Displacement of the pile during driving is further complicated by the fact that the pile is of a composite construction. This type of design tends to cause differential movements of the individual sections. To overcome this problem a load of 25 kN was applied to the pile while the connections between the sections were tightened. This ensured a tight connection between sections, and created initial stresses in the pile which were taken as the reference point for all subsequent tests performed on the pile following this assembly.

A measurement of the lateral displacements and bending of the pile was performed in-situ, and the results are given in section 6.4.3.

4.2.3 Influence of Confinement of the Test Pile in the Granular Medium

The confinement of the pile could influence the results due to the fact that the pile was calibrated in air without any lateral confinement, while during testing some of the load cells were embedded in the sand. This confining lateral force is likely to affect the development of hoop stresses. The influence of this confinement on the testing results is a complicated matter, and requires further investigation. A comparison between the insitu calibration test in air, and one done with the pile embedded in the soil has been carried out and the results are presented in section 6.4.4.

4.3 Transmission of Load from the Test Pile to the Granular Medium

As stated previously the load applied to the pile was transmitted to the soil solely by skin friction, as end bearing had been eliminated. The pile was driven at a constant rate of penetration to allow the build up and mobilization of skin friction.

After the skin friction had been mobilised, further pile penetration was achieved without any perceptible increase in load. It is this load transfer mechanism and its effects on the surrounding soil conditions that the present study intends to determine.

4.3.1 Terra Plates for Measurement of Soil Displacements

As the load on a pile is transferred to the soil, the skin friction is mobilized causing the adjacent soil to move downwards. Piles subjected to both skin friction and end bearing in the same granular stratum create an 'arching ring' and 'bin effect' as described by Terzaghi (1936) and others (discussed previously). The movement of the soil around piles driven through a granular stratum overlying clay, however, is not fully understood as the work in this area is limited.

To measure these small movements of soil, encountered in piling in layered stratum, the candidate has employed a system using 25 mm square aluminium plates (Terra Plates) linked by steel wire (piano wire) to displacement transducers (see Plate 4.1).

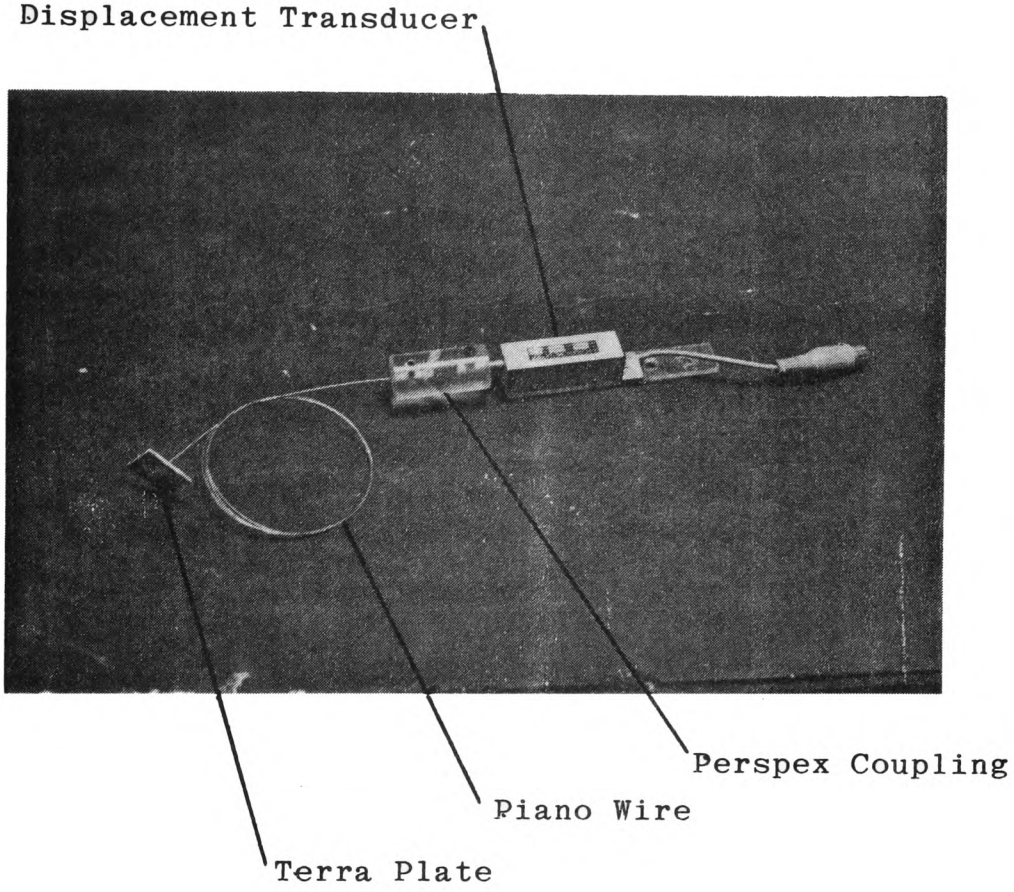

PLATE 4.1

SAND DISPLACEMENT
MONITORING EQUIPMENT

The Terra Plates were placed in the sand at designated positions around the pile. A displacement transducer was mounted to the datum frame directly above each Terra Plate. Steel piano wire was used to connect the Terra Plates to the transducers.

Consideration was also given to incorporate the Terra Plates to monitor horizontal as well as vertical soil movements. However, to safeguard against the possibility of creating a reinforced soil condition, due to an overabundance of instrumentation, the decision was made to postpone this for the present.

The possibility of measuring the actual pressures in the soil has also been considered. Small pressure cells, similar to those developed by Khafagy (1967) at The University of Leeds, could have been incorporated into the soil monitoring system. However, as stated previously, the objective was to use the instrumentation to monitor the soil behaviour and not to influence it in any way. Therefore, the decision was made to limit the instrumentation to monitor vertical soil displacements only for the present study.

4.3.2 Monitoring Soil Density and Density Changes

As discussed in section 2.16 one of the effects of pile driving on soil properties is the changing of the soil density. Compaction of the soil due to skin friction and end bearing resistances increases the soil density, while, 'arching' and the 'bin-effect', which were described earlier, reduce the density in the immediate vicinity of the pile shaft. All these density changes are accompanied by a displacement of the soil. It was these soil displacements that were

monitored during pile driving, using the Terra Plates described in the previous section. It was expected that with the measurement of : the final soil density after testing (using density tins), relative changes in density before and after testing (Mini-Mackintosh Probe) (section 3.6), and the soil displacements during driving (Terra Plates), an overall pattern of the changes in the state of the soil during testing, with a minimum amount of interference due to the presence of the instrumentation, would be achieved.

Chapter 5

Description of the Test Pile

CHAPTER 5

DESCRIPTION OF THE TEST PILE

5.1 Load Cell Development and Investigation

The main objective of the project was to determine the load transfer mechanism.

There are two current methods of measuring loads along a pile. The first is, to instrument one continuous pile, and the second is, to incorporate individual load cells as sections of the pile.

A method of instrumenting a continuous pile is by mounting dial gauges or displacement transducers to the inside of the pile to measure pile deformation. To accomplish this, small tabs are fixed to the inside of the pile and dial gauges or displacement transducers are fixed at other locations on the inside surface. A steel rod is then used to connect the tabs to the displacement measuring instruments. As the pile is stressed, due to loading, the recording device measures the change in length of the pile between the ends of the rod fixed to the tabs and the ends fixed to the dial gauges or transducers (for further details see Hanna 1973). This method was abandoned due to foreseeable difficulties in attaching the equipment to the inside of the pile.

An alternative method is to attach strain gauges along the inside and/or outside of the pile. Due to the unacceptable level of abrasion observed between the outside pile surface and sand during driving, it

was thought that, the strain gauges and their leads if mounted on the outside of the pile would be damaged. Subsequently, this method was also abandoned. Because the equipment required for mounting strain gauges inside the pile, as opposed to manual fixing was not available, a continuous pile was determined inappropriate for the work needed. Therefore, it was decided to use a composite pile. This pile was composed of individual load cells connected by an appropriate coupling.

5.2 Material used for the Manufacture of the Test Pile and the 'Shell' Type Load Cell

The pile was fabricated from 114 mm diameter circular hollow mild steel section, with a wall thickness of 4.5 mm and a continuous weld. The first type of load cell designed was the 'Shell' type. This load cell consisted of a 150 mm length of the 114 mm diameter pipe with internally mounted strain gauges (L.C.α,L.C.β, and L.C.δ) (Section 6.3.1). The 400 mm lengths of pile which were initially positioned between the 'Shell' load cells were later instrumented (L.C.3 and 4 and L.C.5 and 6), increasing the number of load cells by four.

A welded circular tube is not the ideal section to use as the basis for a load cell due to the nonuniform stress distribution. However, the purpose of this investigation was to best model the behaviour of full-scale piles in the field, and hollow steel rolled pipe is in common usage. Therefore, although this does introduce a number of problems into the interpretation of the test results, these problems are present in full-scale piles as well.

5.3 'Core' Type Load Cell

The need for a more sensitive load cell to measure the low strains present at the base of the pile led to the development of the 'Core' type load cell. This load cell as shown in Figure 5.1 and Plates 5.1 and 5.2, consisted of a section of the 114 mm diameter steel pipe surrounding a central core with a coupling at either end. The bottom coupling and core were machined from the same piece of steel. A section of the 114 mm diameter pipe slid over the core and rested on a rubber o - ring on the bottom coupling. The top coupling was threaded onto the central core and fixed to the outer sleeve. Since the outer sleeve was not fastened to the lower coupling, any load carried through the load cell was transmitted via the central core. The core was instrumented with strain gauges, and since it was hollow its cross-section could be machined to correspond to a set sensitivity. In this way a set of 'Core' load cells could be manufactured with varying sensitivities, depending on the size of the central hole and the wall thickness.

5.4 Strain Gauges

The instrumentation of each 'Shell' load cell consisted of two rosette strain gauges (see Appendix 5A) mounted diametrically opposite on the inside surface of the pipe section as shown in Figure 5.2. On the 150 mm length 'Shell' load cells the gauges are located at the centres on the inside surface (75 mm from either end). On the 400 mm lengths, which were developed later, the gauges are located on the inside surface 75 mm from either end. The gauges were positioned so

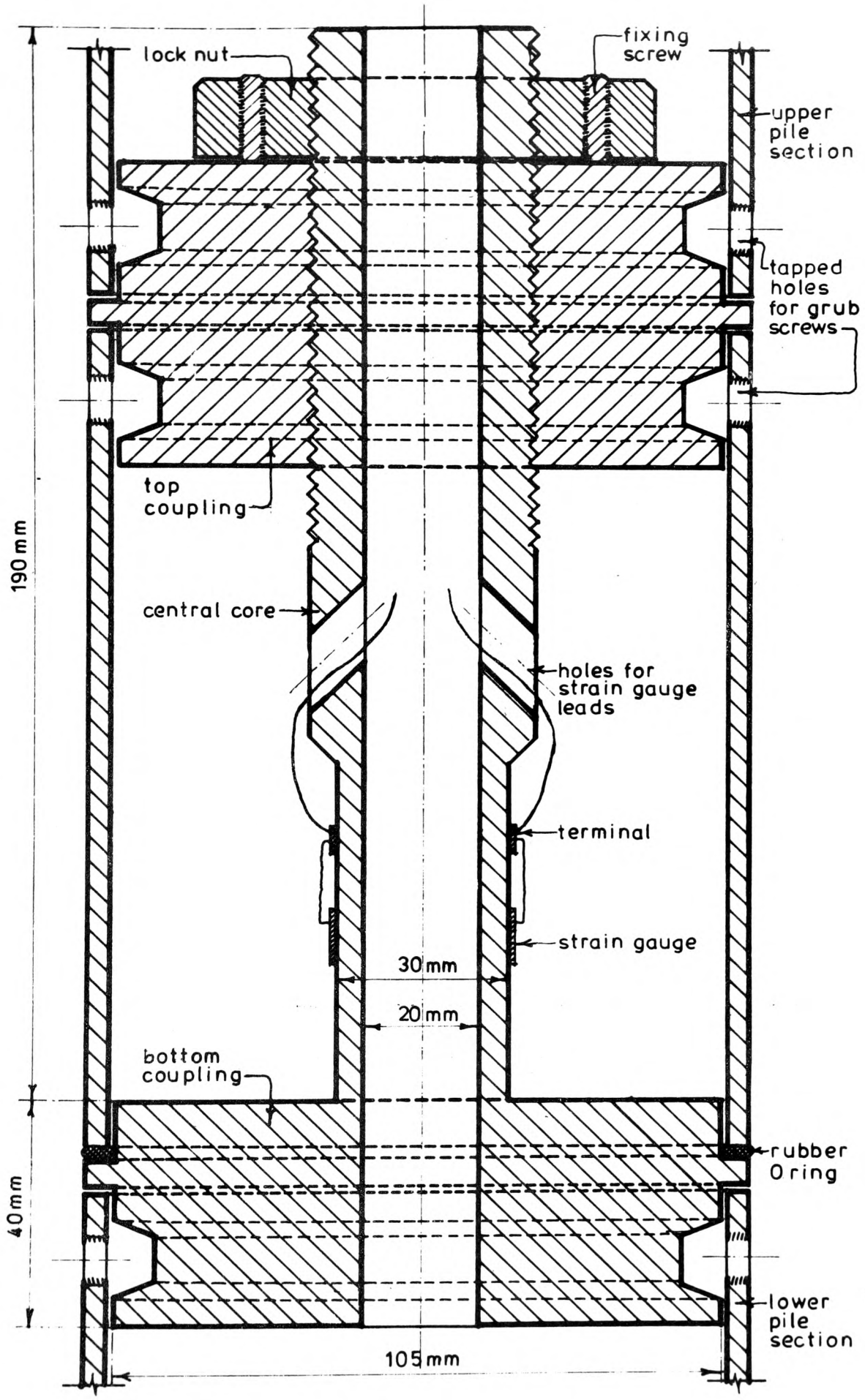

FIGURE 5.1

'CORE' LOAD CELL

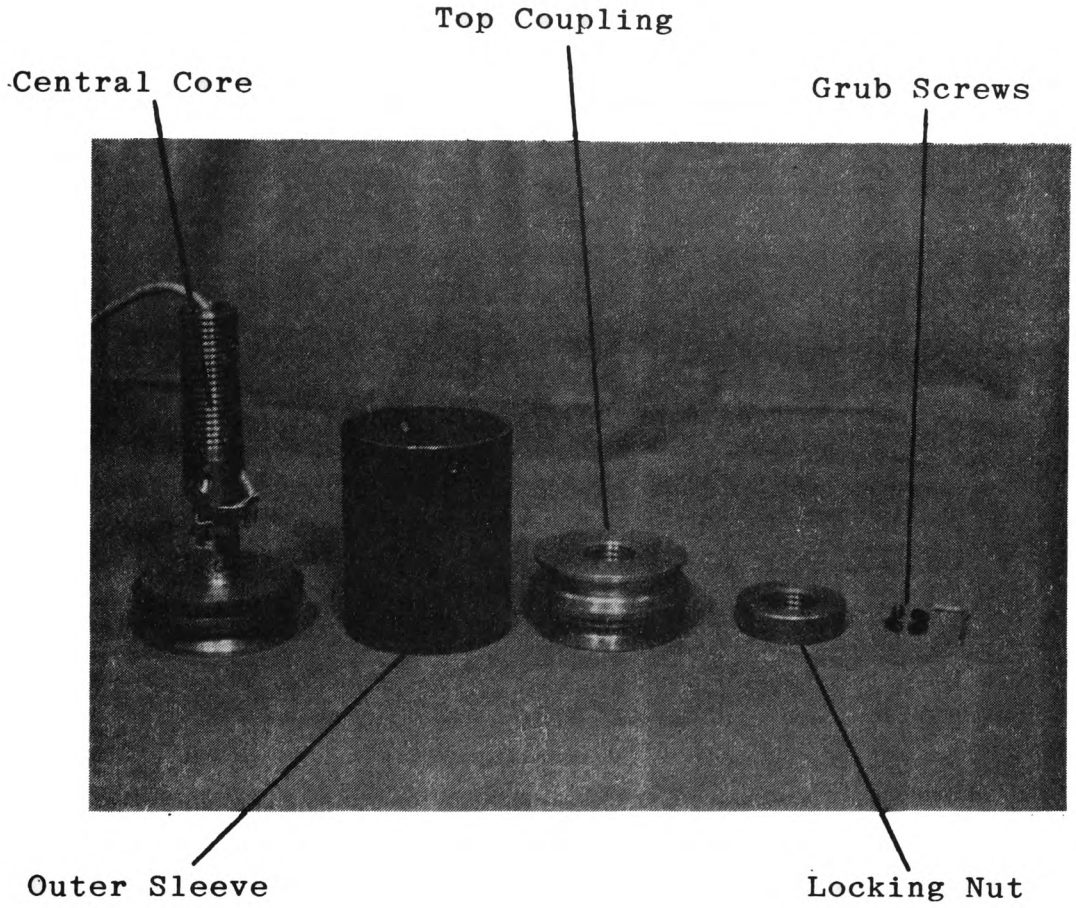

PLATE 5.1

'CORE' TYPE LOAD CELL

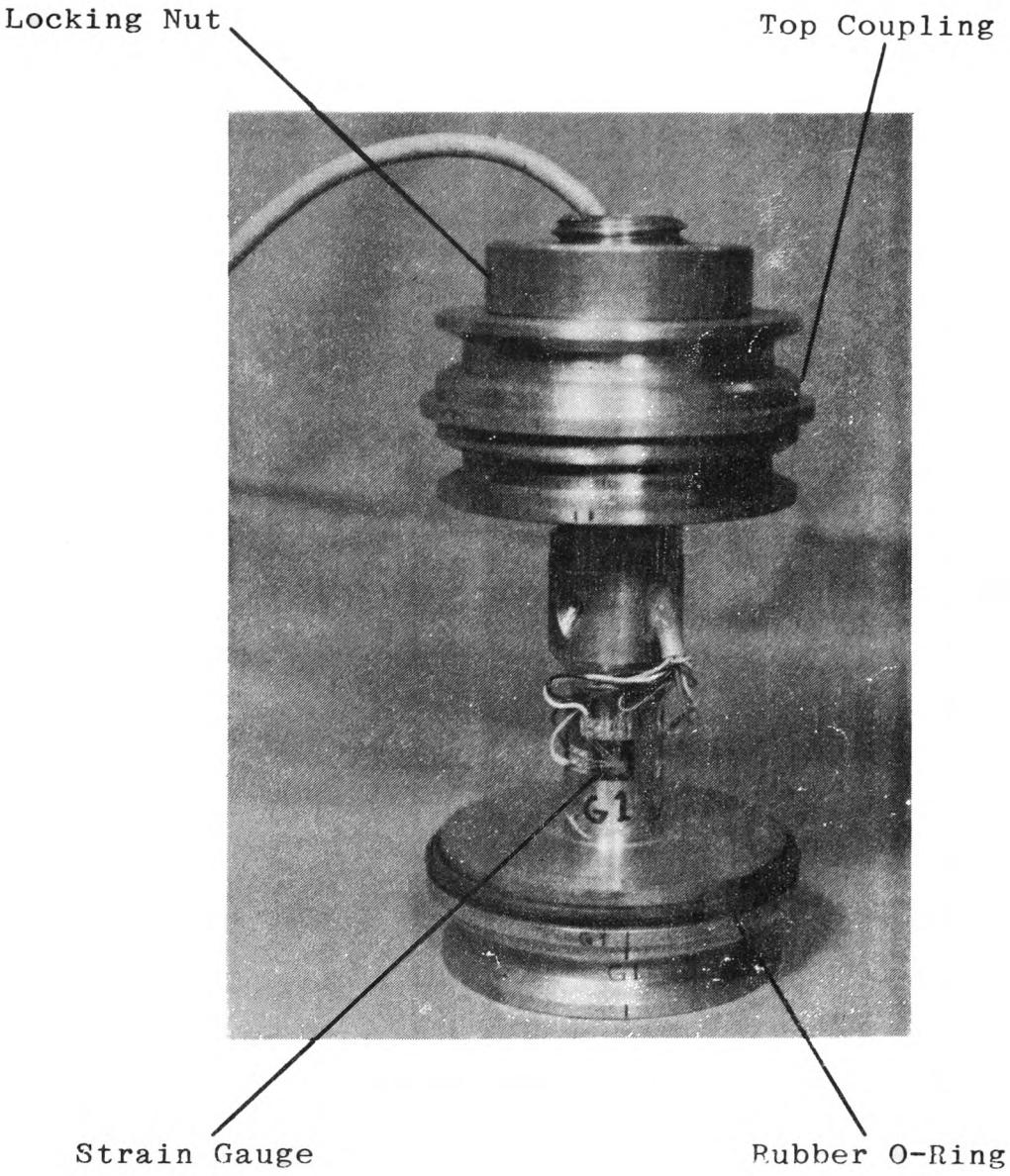

PLATE 5.2

'CORE' TYPE LOAD CELL

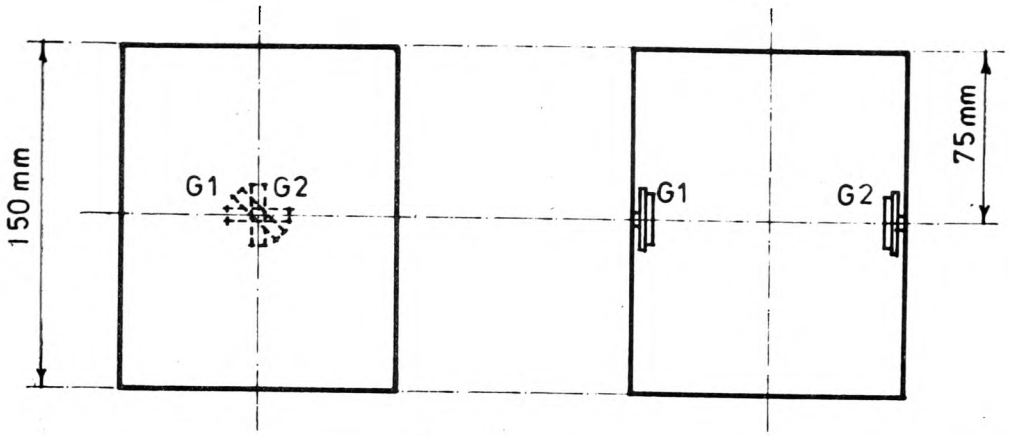

150 mm LOADCELL

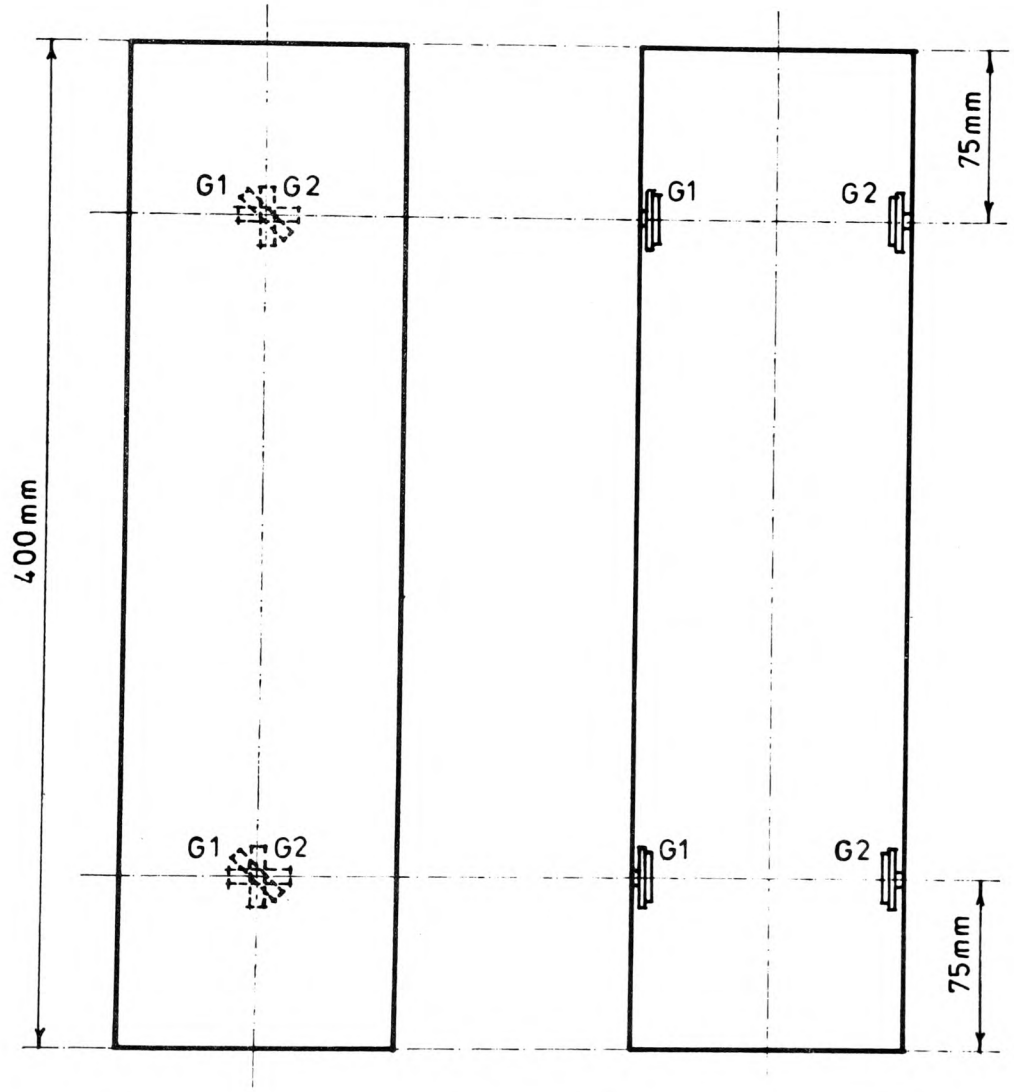

400 mm LOADCELL

FIGURE 5.2

LOCATION OF STRAIN GAUGES
ON 'SHELL' LOAD CELL

that they were each the same distance from the welded seam.

On the 'Core' load cells two rosette strain gauges were mounted diametrically opposite on the central core (see Figure 5.1, Plate 5.2).

5.4.1 Strain Gauge Electrical Circuitry

Each strain gauge contains 3 elements; one vertical, one horizontal, and one at 45°. Initially, the vertical and horizontal elements were connected in an arrangement that formed the four arms of a full Wheatstone-Bridge circuit. The advantage of using a full bridge over a quarter bridge is that the latter arrangement (which incorporates the 2 vertical and 2 horizontal elements in the bridge circuit) increases the sensitivity by a factor of approximately 2.6, and is temperature compensated which eliminates the need for dummy gauges.

One disadvantage of using a full bridge is that any inherent eccentricity will not be shown in the results, since a full bridge will average these strain differences. Another disadvantage in using a full bridge is that if one of the gauges in the bridge develops a fault it would not necessarily show up in the results, since the strain reading from this faulty gauge would still be averaged with the other gauges in the bridge. The results of this could lead to a misleading evaluation of the conditions present. If, however, the gauges are connected in the quarter bridge configuration, a faulty gauge should be detected immediately since the strain measured by each gauge is recorded individually.

Therefore, to produce results which can aid in interpreting any pile bending, the strain gauges were connected in a quarter bridge and incorporated temperature compensating dummy gauges.

A set of 45° elements have been incorporated in the gauges to allow the detection of any pile bending in the plane normal to the vertical plane which intersects the gauges on both sides of the pile (see Figure 5.2). Bending in any other plane will be detected in the vertical and horizontal elements as the strains in one would be greater than in the gauge opposite.

The 45° elements could also be used to measure any torsion in the pile.

5.4.2 Strain Gauge Bonding

In the early stages of the load cells development the problem of finding a reliable method of evaluating the efficiency of the bonding of the strain gauges to the specimen was investigated.

The first method attempted was to run a rubber eraser over the surface of the strain gauge and note any change in strain. This method was abandoned since it was felt that this check in itself could possibly damage the gauge and a new procedure was adopted. This method requires, placing a finger in close proximity (1 - 2 mm) to the gauge, which is connected to a strain recorder, and noting any change in the strain reading. If the gauge is not properly bonded this thermal change caused by body temperature will cause the gauge to expand, which in turn will cause a tensile strain reading to be registered on the recorder.

Advantages of this method are that no pressure is exerted upon the gauge, and the changes in temperature are unlikely to cause overtstressing.

After the strain gauges were fixed in place, a final check on the gauge resistance was performed. By checking the gauges deviation from the set gauge resistance, a faulty gauge, the element of which had been damaged, could be detected. This check will also confirm whether or not a good soldered joint has been made between the gauge and wire leads. Measuring the resistance between the gauge and the pile section, will indicate whether the gauge is 'shorting' against the section. This could be caused by a poor soldering joint, where the solder is in contact with the pile, or by the gauge wires (leads or element) touching the section.

The gauge, terminal, and leads were all covered with a coating of silicone rubber to protect them from moisture and to insulate them from the pile sections.

This resistance test was used to check suspected faulty gauges after the pile had been assembled, since this procedure could be carried out externally at the ends of the gauge leads where they were connected to the terminal box.

5.5 Pile Sections and Attachments

Since the pile was of composite construction (comprised of individual load cell sections connected together) a coupling was designed to connect these sections (see Figure 4.1).

One of the main factors concerning the design of the load cells was whether the local stresses created at the ends of the section around the grub screws, or in the vacinity of the fixing bolts or seam, would affect the performance of the load cell.

The results of the investigation into the influence of these anomalies on the operation of the load cell is described in sections 6.3.

A 114 mm diameter pile section, 700 mm long, with a smooth machined outer surface, was manufactured for attachment to the base of the pile. The frictionless cylinder was designed to take this section of pile.

A 1.1 m long section of the same pipe was attached to the top of the pile, this connected the top load cell to the jack-pile coupling (see Figure 4.1).

The total mass of the pile, including all attachments and couplings was 78.2 Kg (767N).

APPENDIX 5A

Strain Gauge Information and Circuitry

Type : TML/FRA-6-11

Resistance = 120 Ohms

Strain gauge factor K_h = 2.14, K_v=2.15, K_{45}=2.16

Gauge length = 6 mm

To facilitate the easy interpretation of the strain gauge data the voltage applied to the quarter Wheatstone-Bridge circuit (Figure 5A.1) was set so that a change in strain of 1 μstrain produced a change in voltage of 1 μvolt ($1x10^{-6}$). The equation for the relationship between the applied bridge voltage E and the output voltage v, for a quarter-bridge circuit is (Vaughan 1975).

$$E = 4V/\varepsilon K \qquad (5A.1)$$

where ε = strain.

Setting ε = V, K = 2.15, and solving for E yields a value for E, the applied bridge voltage, of 1.86 volts.

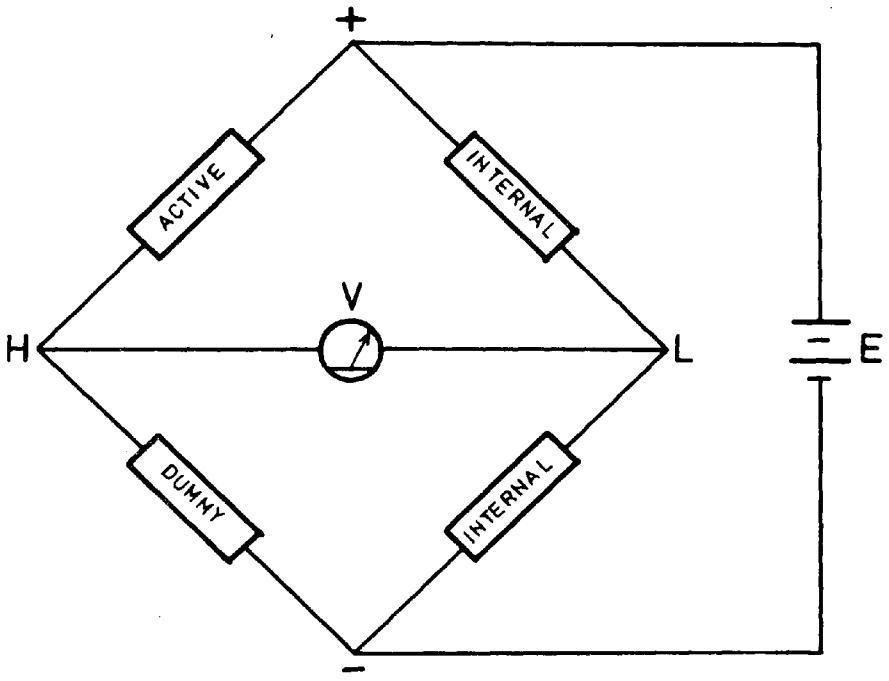

FIGURE 5A1

WHEATSTONE QUARTER-BRIDGE CIRCUIT DIAGRAM
(from drawing titled 'STRAIN GAUGE UNIT' by
MYCALEX INSTRUMENTS, LTD.)

Chapter 6

Sand Properties and Preliminary Tests

CHAPTER 6

SOIL PROPERTIES AND PRELIMINARY TESTS

6.1 Physical and Mechanical Properties of the Test Sand

6.1.1 General Description

It was decided to conduct the experiments using 'Leighton Buzzard Sand'. This particular sand was chosen for its relative uniformity.

It was important that over the duration of the testing programme any changes in the index properties of the test soil should be monitored. Since, it was felt that the extraction of dust and possible grinding of the individual sand grains in the Redlar conveyer could alter the index properties of the sand, five samples were taken during the sequence of testing. The results presented in this section are the average values from the samples taken, except where noted, and any significant differences will be stated.

The procedures for determining the index properties are presented in full when they vary from the methods described in B.S.1377 or any other accepted laboratory testing procedure.

Prior to testing, the entire quantity of sand used was passed through the 2.36mm sieve attached to the hood at the end of the sand pouring apparatus. As well as aiding in the creation of a uniform mass of sand, by a raining technique, the sieve removed any larger

sized materials.

6.1.2 Particle Size Distribution

The mechanical analysis test was performed according to B.S.1377 using the method of coarse analysis by dry sieving. The average grading curve of the five samples tested is given in Figure 6.1 along with the range of results. From the grading curve, it can be seen that the test sand is a medium sand with an effective grain size (D_{10}) of 0.28mm, a Hazen's Uniformity Coefficient ($Cu=D_{60}/D_{10}$) of 1.79 and a coefficient of curvature ($Cz=D_{30}^2/D_{60}D_{10}$) = 1.14. Therefore, the sand is relatively uniform. This uniformity of particle size is desirable in test sand as it helps in depositing a relatively homogeneous sand mass.

It appeared that the variation in the test results obtained from the five samples was quite random and did not indicate any particular trends.

6.1.3 Moisture Content

The moisture content was determined, according to B.S.1377 using the standard method, for 15 air dry samples (three specimens from each of the five samples taken). The moisture content for sample S5, the last sample taken, was found to be approximately 0.2 per cent, while, the moisture content for the remaining samples showed a zero percent moisture content.

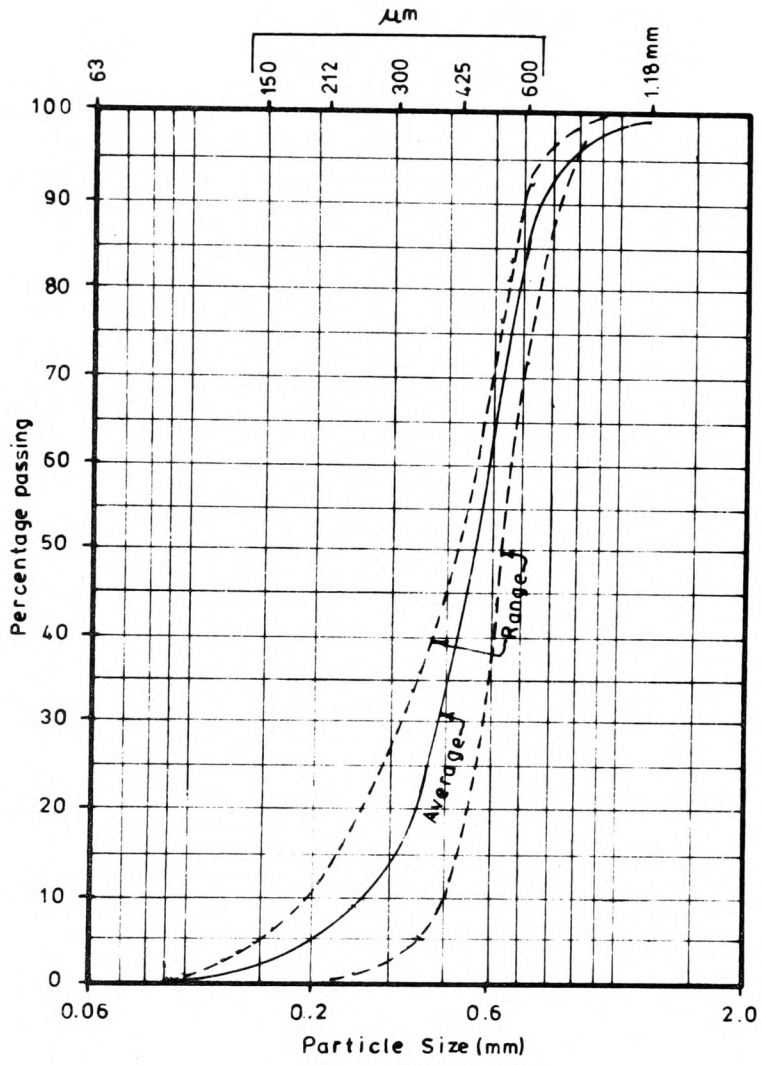

FINE	MEDIUM	COARSE
SAND FRACTION		

FIGURE 6.1

PARTICLE SIZE DISTRIBUTION

6.1.4 Specific Gravity

The specific gravity of the sand particles was determined according to B.S.1377 using the method for fine grained soils. By testing two representative samples from each of the five samples obtained during the testing programme the average value for the specific gravity was determined to be 2.66.

The values obtained for the five samples (S1-S5) were respectively 2.70,2.68,2.66,2.62, and 2.65. This implies that the specific gravity of the sand particles was decreasing during the testing programme. This suggests that during the testing programme the weight of particles removed (i.e. by the dust extractor) was not proportional to the decrease in the volume. Therefore, the amount of dust size particles removed by the dust extration unit appeared to be greater than the amount, if any, created in the transfer of the sand.

6.1.5 Maximum and Minimum Porosity

A number of methods were tested to achieve the loosest possible deposition for the determination of the maximum porosity. The method found most successful was one similar to the "Tilting Test" presented by Kolbuszewski (1948).

In this test, 1kg of dry sand was placed in a 2000ml, 70mm diameter graduated glass cylinder. A stopper was placed in the end of the cylinder, the cylinder held in the horizontal plane, and rotated about its central axis, thus loosening the sand grains. Next, the cylinder was brought to a vertical position while continuing to rotate

it about its central axis. In this way the grains rolled over one another avoiding any free fall of the particles. This prevents compaction due to impact. It was necessary to bring the cylinder slightly through the vertical to acquire a horizontal, level top surface. The volume of the soil was measured and its density determined.

The above procedure was carried out on three representative samples, of each of the five samples taken during the testing programme. The mean value for the maximum porosity was 41.8 percent. This corresponds to a minimum dry density of 1547 kg/m^3.

The method employed for determining the minimum porosity was to pour a weighed quantity of dry sand into a glass cylinder containing water and vibrating this until a maximum density was obtained. The vibration was carried out by the use of a vibrating table and the time needed to reach a maximum density was found to be approximately three minutes. After this time the surface of the sand was observed to be "bubbling up" and no further compaction took place. One advantage of this method is that the compaction and grain migration can be observed during vibration through the glass cylinder, and the final volume of sand can be easily observed.

The results of the five tests performed using this method yielded a minimum porosity of 34.1 percent, corresponding to a maximum dry density of 1754 kg/m^3.

6.1.6 Shear Strength

The shear strength of the test sand was determined by the direct shear test. For this test, the 100mm square standard shear box apparatus was used. Six air dry samples were tested, under three different normal pressures, and at two ranges of bulk density.

The lower density samples were achieved by loosely pouring the sand into the box, while the denser samples were prepared by placing the sand in five layers and tamping each layer.

The purpose of this procedure was to determine the relationship between the angle of internal friction (ϕ) and the sand bulk density (ρ). The results of these tests are presented in Figure 6.2 together with the equation suggested by Meyerhof (1956), $\phi = 28+15Dr$.

An interesting point to be noted here is that during the emptying of the sand tank the angle of repose of the soil was monitored. The average angle was judged to be 30° with only a slight variation.

6.1.6.1 Shear Modulus

The shear modulus (G) of the test sand was determined in the following manner using the 100mm square shear box apparatus.

1. The test sand was placed in the shear box and its density was determined.

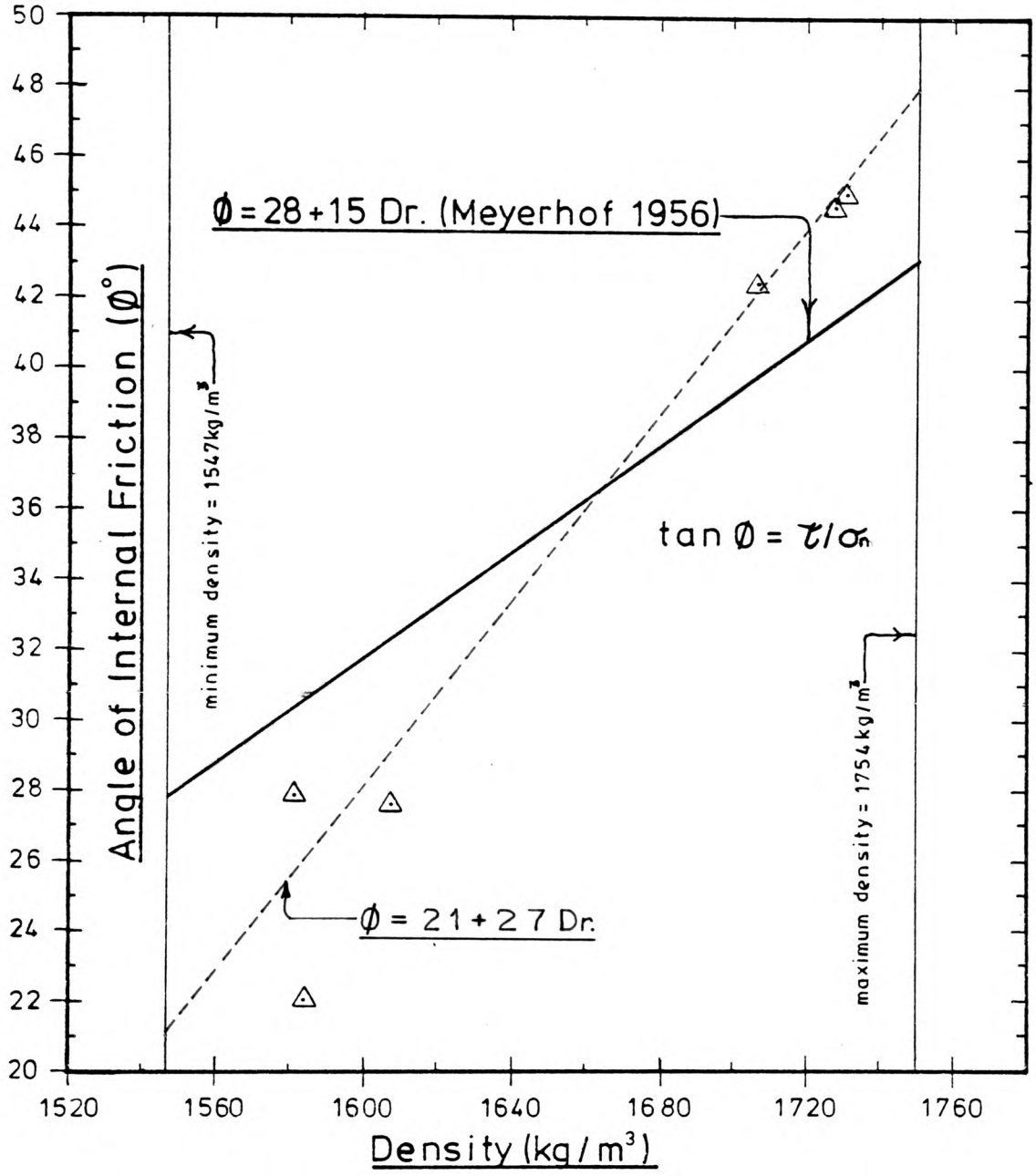

FIGURE 6.2

ANGLE OF INTERNAL FRICTION VERSUS SAND DENSITY FROM SHEARBOX TEST RESULT

2. From the density gradiant determined during the testing programme (section 7.3.4), the depth corresponding to this density was obtained and the overburden pressure at this depth was based on the average density of the soil above.

3. A normal pressure, equal to the overburden determined in step 2, was applied and a check was made for any changes in density. If the density changed (the sand in the box compacted by normal pressure), steps 1,2, and 3 were repeated until the additional normal pressure did not produce any significant change in the sand density.

4. The shear box test was carried out.

5. From the results of the shear box test the stress-strain curve was plotted. The shear modulus was obtained from the slope of the initial linear portion of the curve.

This procedure was conducted on six samples with different densities and the resultant plot of shear modulus versus density is shown in Figure 6.3.

With the exception of two of the six samples tested, there seems to be a steady increase in shear modulus as the density increases (with depth)[1]. as shown in Figure 6.3.

Vesic (1964) has presented similar results for shear modulus versus density for piles buried, driven and jacked into sand.

[1]. Banerjee and Davis (1977) have obtained solutions for calculating the settlement of piles and pile groups in a "Gibson" soil.

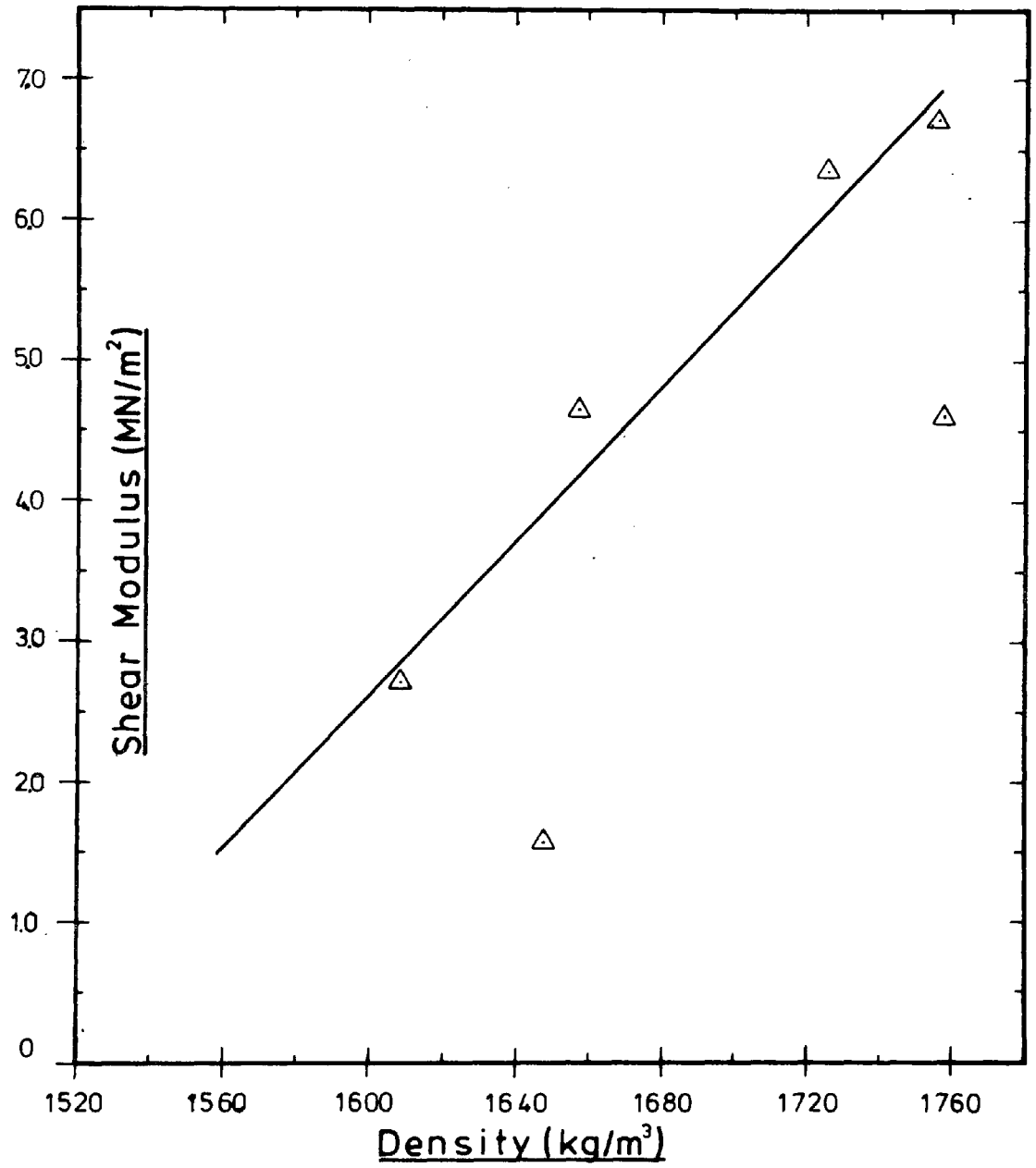

FIGURE 6.3

SHEAR MODULUS VERSUS SAND DENSITY

FROM SHEARBOX TEST RESULTS

6.2 Investigation of the Prototype Load Cell

6.2.1 General

For the purpose of conducting an extensive investigation into the characteristics of the 'Shell' type load cell, under closely controlled conditions, an extensively instrumented prototype was assembled. The amount and extent of instrumentation mounted to the prototype increased as the testing warranted. The additional instrumentation will be described as it is introduced in the following sections.

The basic prototype consisted of a section of the 114 mm diameter pipe which was described in section 5.2. The length of the prototype was 400 mm, the same length as L.C. 3 and 4 and L.C. 5 and 6.

The initial difference between this load cell and the other two was that the prototype had six rosette strain gauges mounted to the inside surface at either end instead of two (see Figure 6.4). These strain gauges were mounted in sets of two, diametrically opposite, and at distances of 50, 75, and 100 mm from the ends of the load cell.

The purpose of the 12 rosette strain gauges were :

1. to study the effects of local stresses induced at the extremities of the load cell during loading,

2. to determine a suitable location for the strain gauges, and

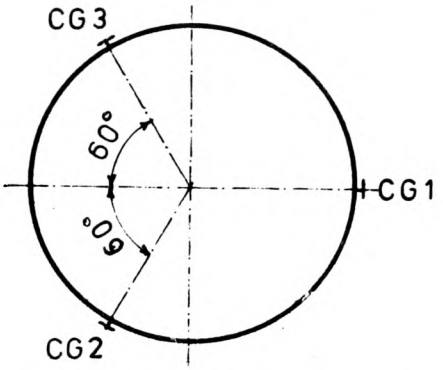

Centrally Located Strain Gauges

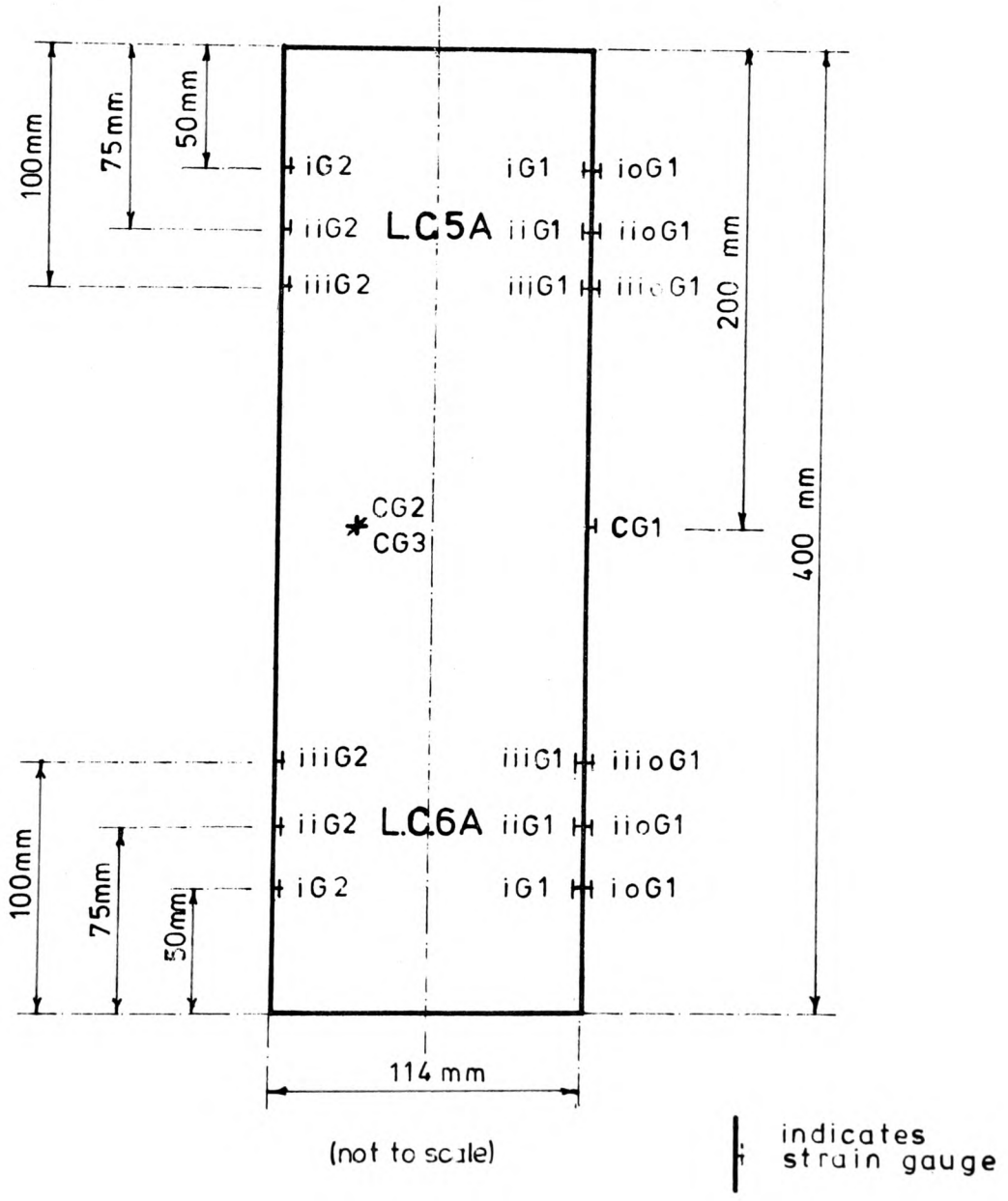

FIGURE 6.4

PROTOTYPE LOAD CELL - STRAIN GAUGE LOCATIONS

3. to investigate the behaviour of the 'Shell' type load cell under load.

The distance that the strain gauges were mounted from the ends of the sections was limited by the distance that a strain gauge could be properly hand mounted to the inside surface of the pipe. In practice, this limiting distance was found to be 100 mm for the 114 mm diameter pipe.

Mechanical mounting of the strain gauges at further distances inside the pipe was not feasible for two reasons :

1. the inside surface of the pipe was rough and needed considerable preparation before mounting the gauges, and

2. the presence of the seam inside the pipe, and the fact that the pipe did not have a true circular cross-section, meant that machining the inside surface was not possible with any of the mechanical equipment available.

6.2.2 Loading Arrangement and Testing

The prototype load cell was calibrated as shown in Figure 6.5 and Plate 6.1 in the Instron Universal dynamic/static materials testing machine, series 1251 (Instron 1251). The steel ball bearing was incorporated to minimise any end fixity and moments present.

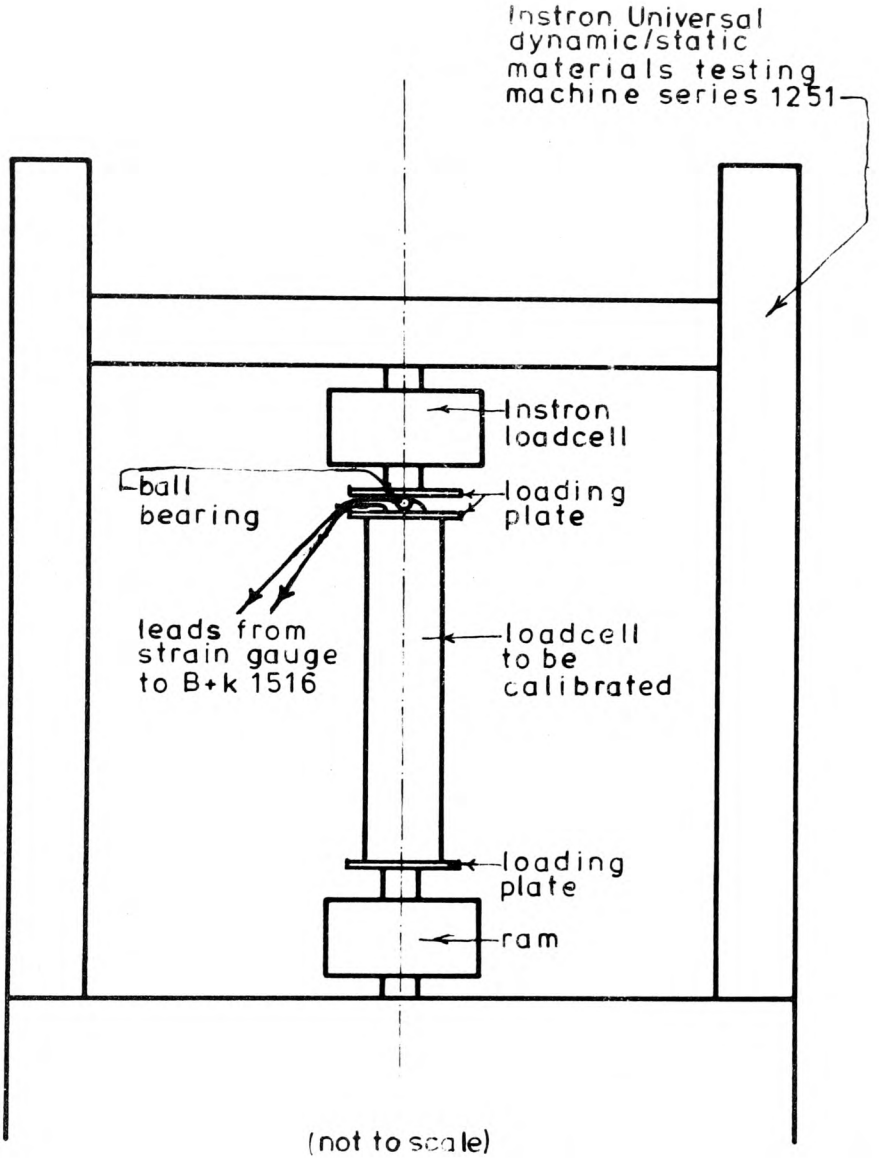

FIGURE 6.5

LOAD CELL CALIBRATION ARRANGEMENT IN THE INSTRON TESTING MACHINE 1251

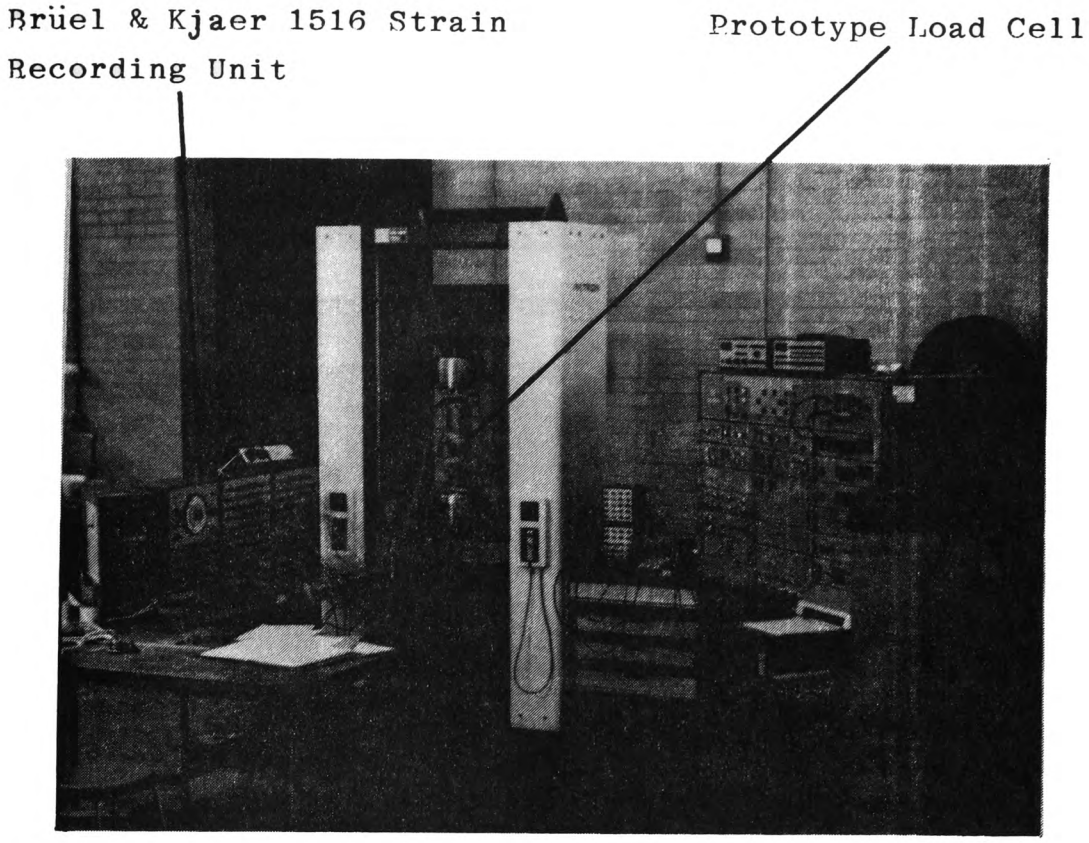

PLATE 6.1

TESTING ARRANGEMENT FOR THE PROTOTYPE LOAD CELL
IN THE INSTRON UNIVERSAL DYNAMIC/STATIC MATERIALS
TESTING MACHINE SERIES 1251

The strain gauges were monitored on a Brüel and Kjaer 1516 strain recording unit.

Before measurements were taken for each calibration test, the load cell was loaded to the maximum test load at least three times. These pretest loading cycles were performed to allow proper seating of the apparatus and to allow the equipment and strain gauges to settle into equilibrium before calibration.

On placing the prototype load cell into the Instron 1251 the cut extremities of the section were found to be not properly machined, and therefore, they were neither flat nor normal to the central axis of the load cell. The fault was found to lie in the method of manufacturing the pile sections. The method was modified and the load cell was properly machined.

The standard workshop procedure was adopted, to check the trueness of the end machining. This involved using a plane table and a set of feeler gauges to check the surface unevenness and a square to check that the ends were normal to the central axis.

To check for any eccentricity caused by the loading arrangement on the load cell, the calibration was repeated after rotating the load cell by 180° about its central axis. The difference in individual strain readings for the two tests was less than 3 per cent of the maximum value.

As a means of further assessing whether the loading arrangement was causing any eccentricity, three further strain gauges were mounted on the outside surface of the load cell. These were located and installed at the centre of the load cell 120° apart as shown in Figure

6.4. Since mounting gauges on the outside surface of the pipe was much easier, better control could be exercised in the bonding of the gauges. The subsequent readings from these gauges also proved useful as a check on the strain readings of the internally mounted gauges.

Two further steps were taken to check and confirm the calibration results :

1. additional gauges were bonded externally at locations corresponding to the internal ones (see Figure 6.4), and

2. an extensometer was mounted to the outside surface of the load cell over the externally mounted central gauges as shown on Plate 6.2.

Initially the calibration curves for the extensometer showed some hysteresis. It was discovered that this was being caused by the 'knife edge' of the extensometer, slipping along the surface of the pipe. This problem was rectified by first placing a small piece of cellophane tape on the metal surface of the pipe before fixing the extensometer in place. The tape helped to hold the 'knife edge' of the extensometer in place and eliminated this hysteresis.

6.2.2.1 Test Results

The results of the Instron calibration tests carried out on the prototype load cell, each test being performed at least twice to assure repeatability, were as follows :

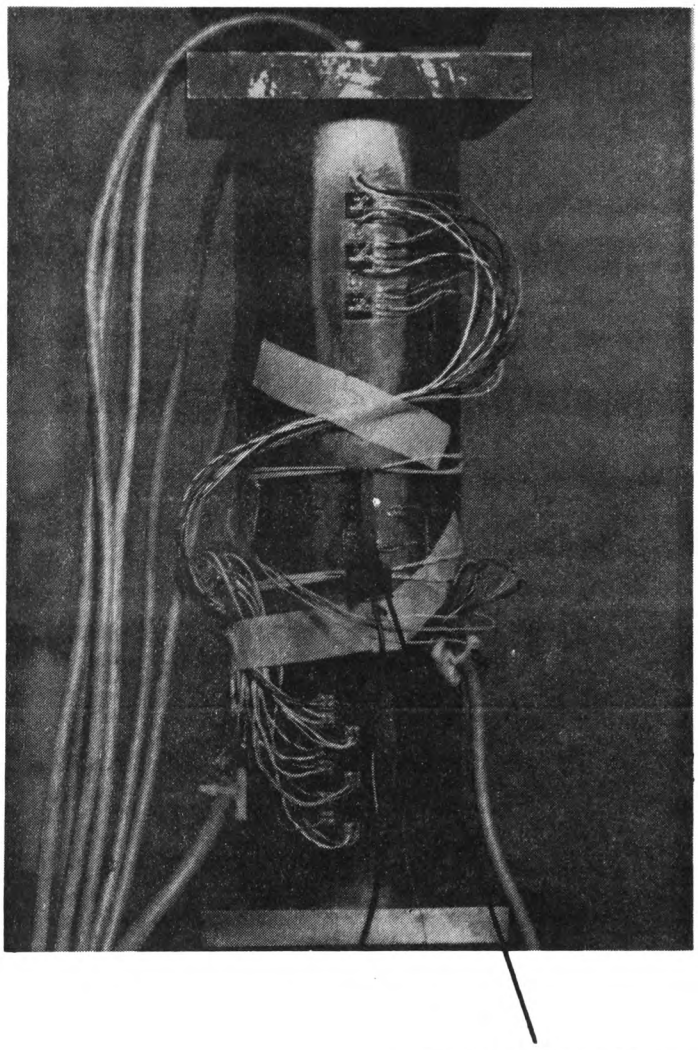

PLATE 6.2

PROTOTYPE LOAD CELL PLACED IN THE INSTRON 1251

1. The calibration curves for ten of the twelve internally mounted gauges (two of which were found to be faulty) were all found to be lower than the theoretical curve as shown in Figure 6.6.

2. The calibration curves for the gauges at the L.C.5A end of the load cell were all less than those at the other end of the load cell as shown in Figure 6.6.

3. The initial portion of the calibration curves displayed non-linearity, while the latter portion was linear.

4. No appreciable changesin the curves were found by either rotating the load cell about its central axis or turning it over, so that the strain gauges at the bottom for one test were located, at the top for another.

5. As the distance between the strain gauges and the end of the load cell increased the calibration curves approached the theoretical values. This is shown in the calibration curves of Figure 6.6.

6. The average slope of the calibration curves for the externally mounted central strain gauges (CG1,CG2 and CG3) were found to be approximately 80 percent of the slope of the theoretical curve as shown in Figure 6.7.

7. With the exception of one of the three central gauges, the strains measured with the extensometer were close to those measured by the strain gauges, the variation being approximately 4 percent of the maximum value (see Figure 6.7).

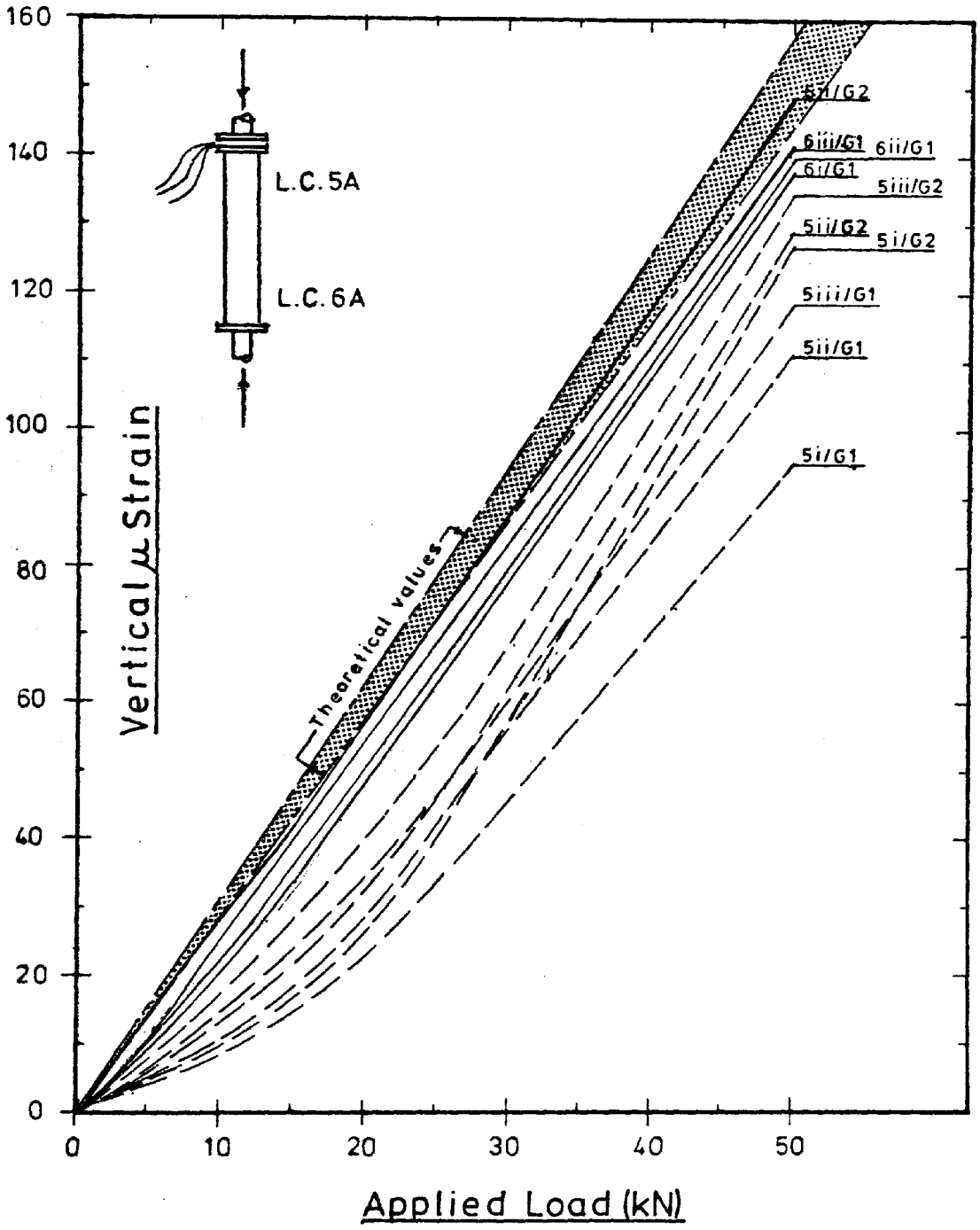

FIGURE 6.6

AVERAGE OF THREE CALIBRATION TESTS OF THE PROTOTYPE LOAD CELL IN THE INSTRON 1251

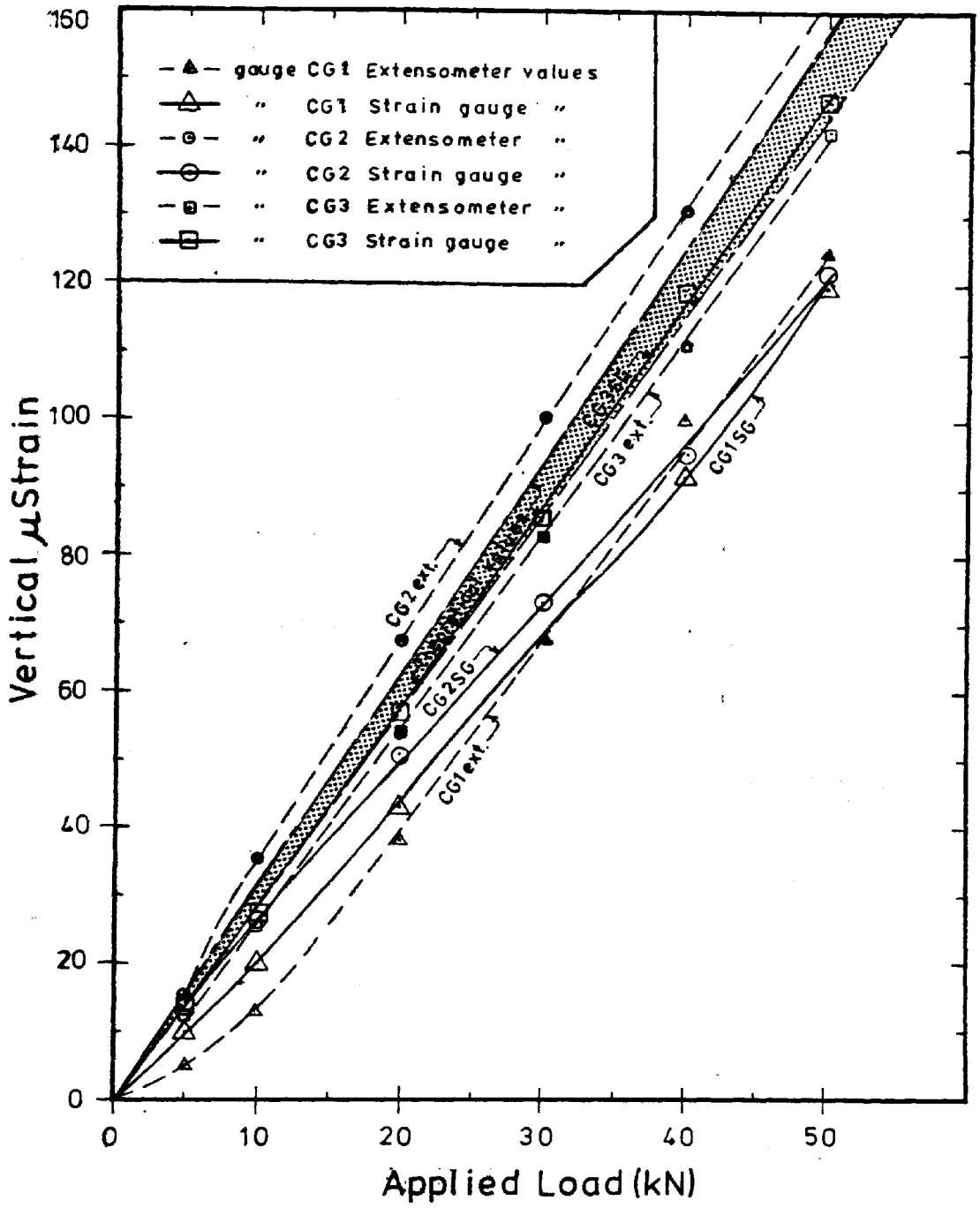

FIGURE 6.7

COMPARISON BETWEEN THE VALUES OBTAINED FROM THE VERTICAL ELEMEMENTS OF THREE EXTERNALLY MOUNTED STRAIN GAUGES AND AN EXTENSOMETER FIXED OVER THE THREE GAUGES ON THE PROTOTYPE LOAD CELL

8. For four of the six gauges mounted on the G1 side of the load cell (see Figure 6.4), the difference in recorded vertical strain measured between the gauges mounted on the inside surface and those mounted externally was approximately 7% of the maximum value as shown in Figure 6.8. The difference between gauges 6Aii/G1 and 6Aiio/G1 was quite large. Gauge 5Ai/G1 was found to be faulty.

9. All of the calibration curves were repeatable and showed no hysteresis.

6.2.3 Conclusions

The investigation and calibration of the prototype load cell in the Instron testing machine highlighted a number of points.

The correct fabrication and machining process of the pipe sections proved to be critical. It was found that if the section ends were not perfectly flat or coincided with the plane normal to the central axis, local bending movements or unwanted stresses would be induced in the pile.

It was shown (Figure 6.6) that the departure in strain readings from the theoretically predicted values decreased with increasing distance from the section ends. This phenomenon which was caused by local stresses set-up at the pile ends was verified by locating gauges at varying distances from the pile section ends.

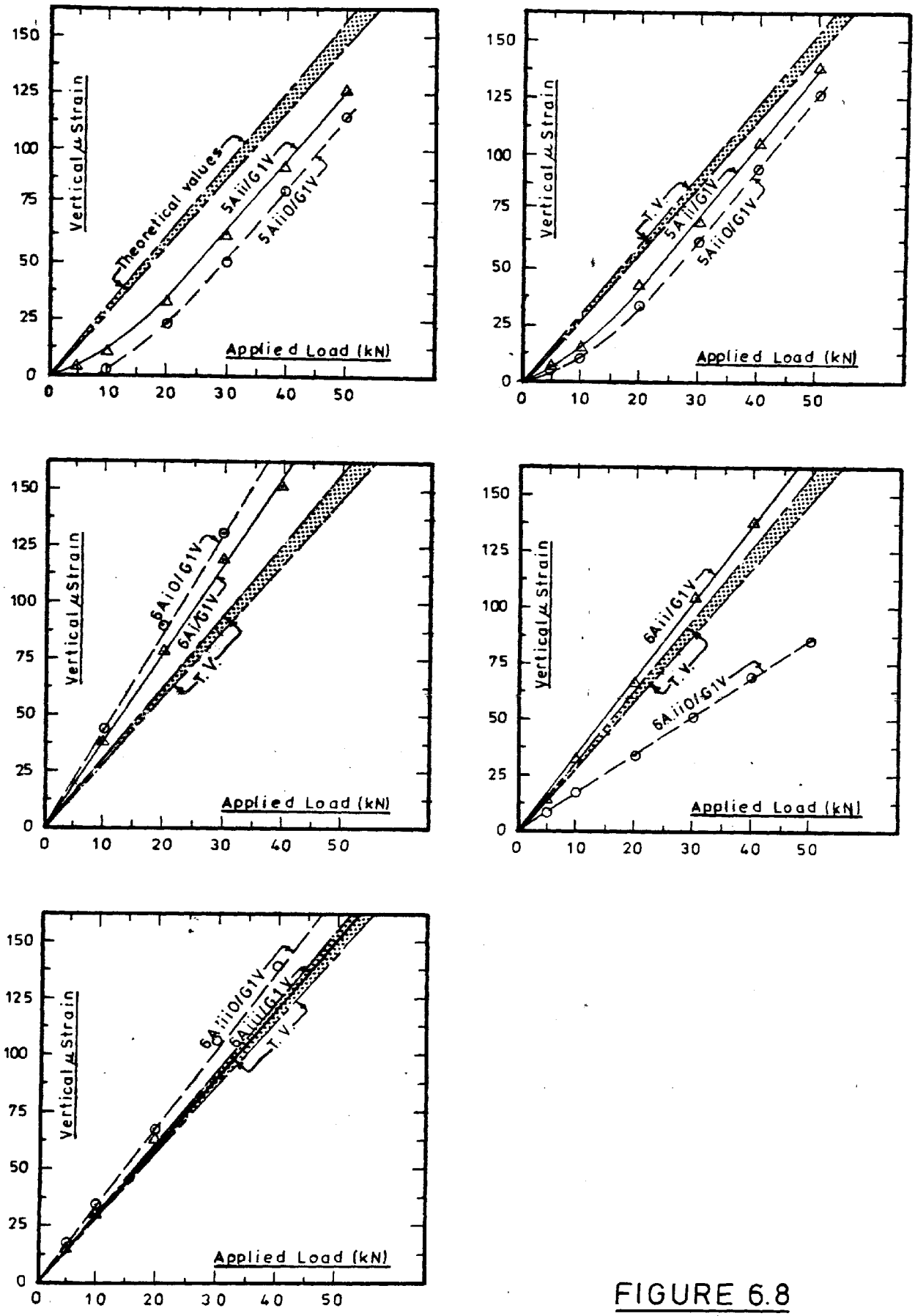

FIGURE 6.8

COMPARISON OF VERTICAL STRAINS MEASURED ON STRAIN GAUGES FIXED TO THE INTERNAL AND EXTERNAL SURFACES OF THE PROTOTYPE LOAD CELL SHOWING THE AVERAGE OF THREE TESTS IN EACH CASE

A distance of 75 mm from the section ends was found to be a suitable distance for the location of the strain gauges for the following reasons :

1. on the average, the difference between the calibration curves of the gauges mounted at 75 mm and 100 mm from the section ends was less than the difference of the gauges mounted at 50 mm and 75 mm from the ends, and

2. the extent of the accessibility for mounting strain gauges was improved significantly at distances of 75 mm or less.

The location of the strain gauges in relation to the seam is also critical, since local stresses are likely to be induced in the vicinity of the seam during loading.

The mounting of the strain gauges is of the utmost importance and must be carried out in a meticulous manner, by an experienced technician. If, the surface of the specimen to which the gauge is to be fixed is not properly prepared, if the surface of the specimen or gauge is not kept clean, or if the cleaning fluid or adhesive is contaminated to any extent, the reliability of the readings becomes doubtful.

Eccentricities could also be induced in the load cell if the loading machine had not been properly aligned.

The investigation of this type of load cell has shown that the calibration curves are reproducible and show no hysteresis. However, for some gauges the initial portion of the calibration curve displays

non-linearity. It was speculated that this non-linearity could be due to the following factors :

1. the manufacturing process of the tube (being rolled),

2. the possible variation in wall thickness,

3. the departure from a true circular cross-section, and

4. the seating of the couplings.

6.3 Calibration of the Test Pile Load Cells in the Instron 1251

6.3.1 Calibration of the 'Shell' Type Load Cells

The 'Shell' type load cells described in section 5.2 were calibrated in the Instron 1251 stiff testing machine in the same manner as the prototype load cell (see Figure 6.5).

The strains were recorded on the Brüel and Kjaer 1516 strain recording equipment which was used for the calibration of the prototype, and were checked by attaching an extensometer to the outside surface of the load cells.

Figure 6.9 shows the calibration curves obtained from the testing of the load cells in the Instron 1251. Each load cell was loaded to the maximum test load. This was repeated a minimum of three times to allow proper seating of the cells and to allow the equipment and strain gauges to settle into equilibrium before testing. Each calibration curve, shown in Figure 6.9, is the average value of the

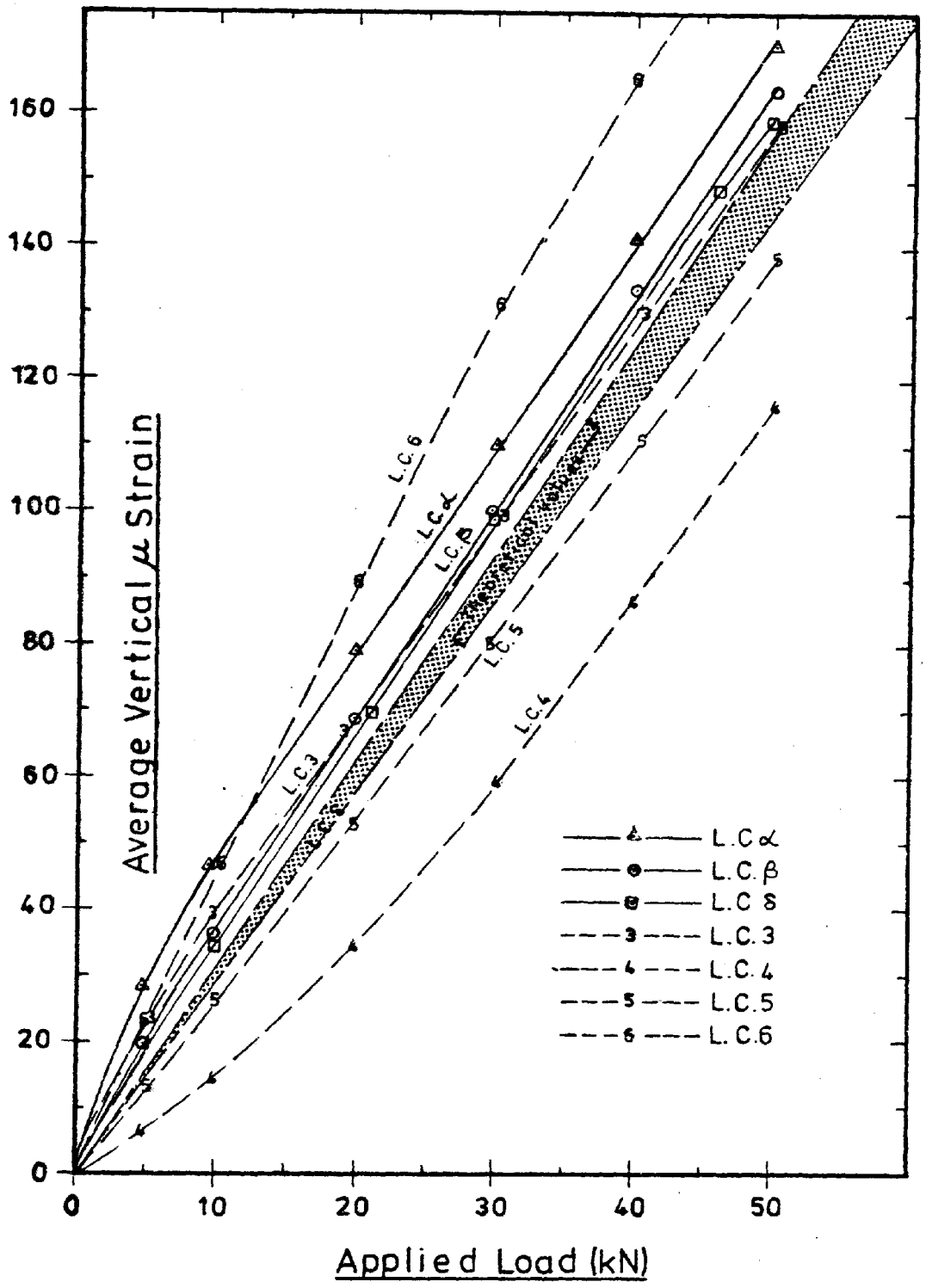

FIGURE 6.9

CALIBRATION CURVES OBTAINED FROM TESTING IN THE INSTRON 1251 SHOWING THE AVERAGE VERTICAL STRAIN VERSUS APPLIED LOAD FOR EACH LOADCELL

mean vertical strain obtained from four independently performed loading tests.

From the Instron calibration tests and the subsequent plot of the calibration curves presented in Figure 6.9, the following observations have been made :

1. the strain-load characteristics for the seven load cells were found to be reproducible and showed no measurable hysteresis.

2. The calibration curves of the 150 mm length load cells (L.C.α,β andδ) were found to be grouped closer to the theoretically predicted curve than the 400 mm length cells (L.C.3 and 4 and L.C.5 and 6).

3. The calibration curves for the pile load cells showed the same characteristic of nonlinearity for the lower range of applied loads as the prototype load cell. The magnitude of this nonlinearity was, however, not as large as for the corresponding values of the prototype load cell.

This nonlinearity together with the accuracy needed for measurement of the smaller strains at the lower range of the applied loads necessitated the development of the more sensitive 'Core' type load cells; since it was anticipated that the lower sections of the test pile would be transmitting smaller loads. With the latter design, shown in Figure 5.1, the load can be measured more accurately through a carefully machined central core.

6.3.2 Calibration of the 'Core' Type Load Cell

A series of calibration tests was carried out on the 'Core' type load cell (L.C.Z) in the Instron 1251 and the strains were measured on the Brüel and Kjaer 1516 strain recording equipment.

The calibration curve for the 'Core' load cell is shown in Figure 6.10. This figure exhibits a slight difference between the theoretical and measured strain values. As experienced with the 'Shell' load cells the response of the 'Core' load cell at its lower range of applied load was found to be nonlinear. However, the linear portion of the calibration curve extended to a much lower applied load than with the 'Shell' load cells.

To assure that none of the applied load was being transmitted through the rubber o-ring, calibration tests were carried out on the load cell with the outer sleeve removed as shown in Figure 6.10. It was found that less than 0.5 percent of the maximum test load was being transmitted through the o-ring.

6.3.3 Investigation of the Influence of the Assembly

An investigation of the influence of the assembly (couplings and grubscrews) on the response of the load cell was carried out in the Instron 1251. The loading arrangement for this investigation is shown in Figure 6.11.

A series of three loading tests was performed with the three load cells linked together. The first test was done with the grubscrews removed, the second with the grubscrews loosely in place,

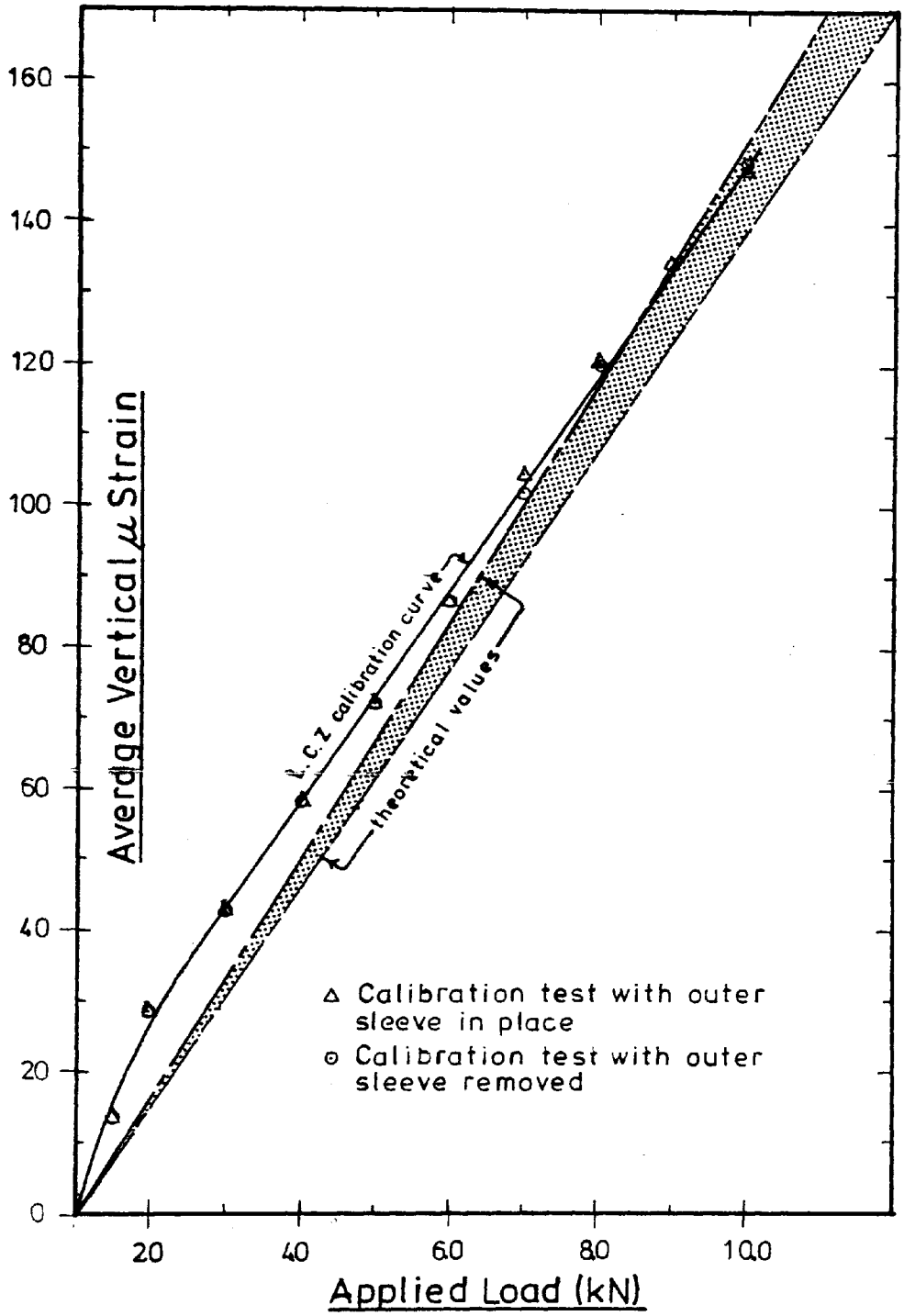

FIGURE 6.10

CALIBRATION CURVE OBTAINED FROM TESTING IN THE INSTRON 1251 SHOWING THE AVERAGE VERTICAL STRAIN VERSUS APPLIED LOAD FOR THE 'CORE' LOAD CELL

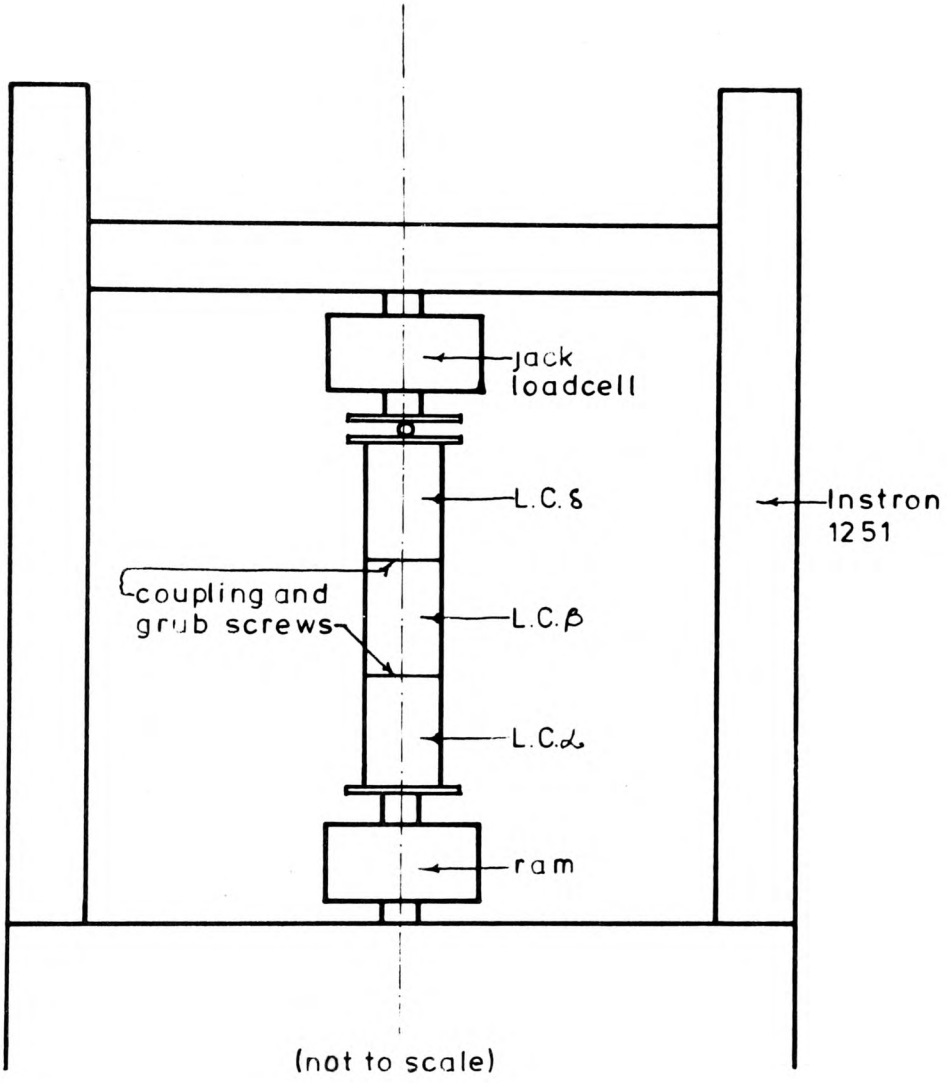

FIGURE 6.11

APPARATUS FOR MEASURING INFLUENCE OF LOAD CELL COUPLING FIXING SCREWS

and the third with the screws tightened.

No measurable differences in strain readings were recorded between the test performed without the grubscrews and the one with the grubscrews loosely in place. When the grubscrews were tightened a slight change in strain reading was recorded (approximately 1.5 per cent of the maximum test load, see Figure 6.12). This response was reproducible and any further loading performed on the cell produced the same strain results. Hence, it was essential that the pile sections be fixed rigidly together before calibration.

It was therefore decided to perform an in-situ calibration test on the entire pile assembly before testing, and to use this as the calibration for the load cells.

The Instron calibration confirmed the reliability of the load cells and helped to identify any faulty strain gauges before the pile was assembled in the testing tanks.

6.3.4 Conclusions

The calibration tests performed on the individual test pile load cells, both 'Shell' and 'Core' types, in the Instron 1251 stiff testing machine brought a number of points to light.

As long as the calibration test was conducted after the pile sections had been rigidly fixed together, the curves were reproducible and showed no hysteresis; even though they were all different (some curves were non-linear at lower applied loads) and all were scattered around the theoretical curve.

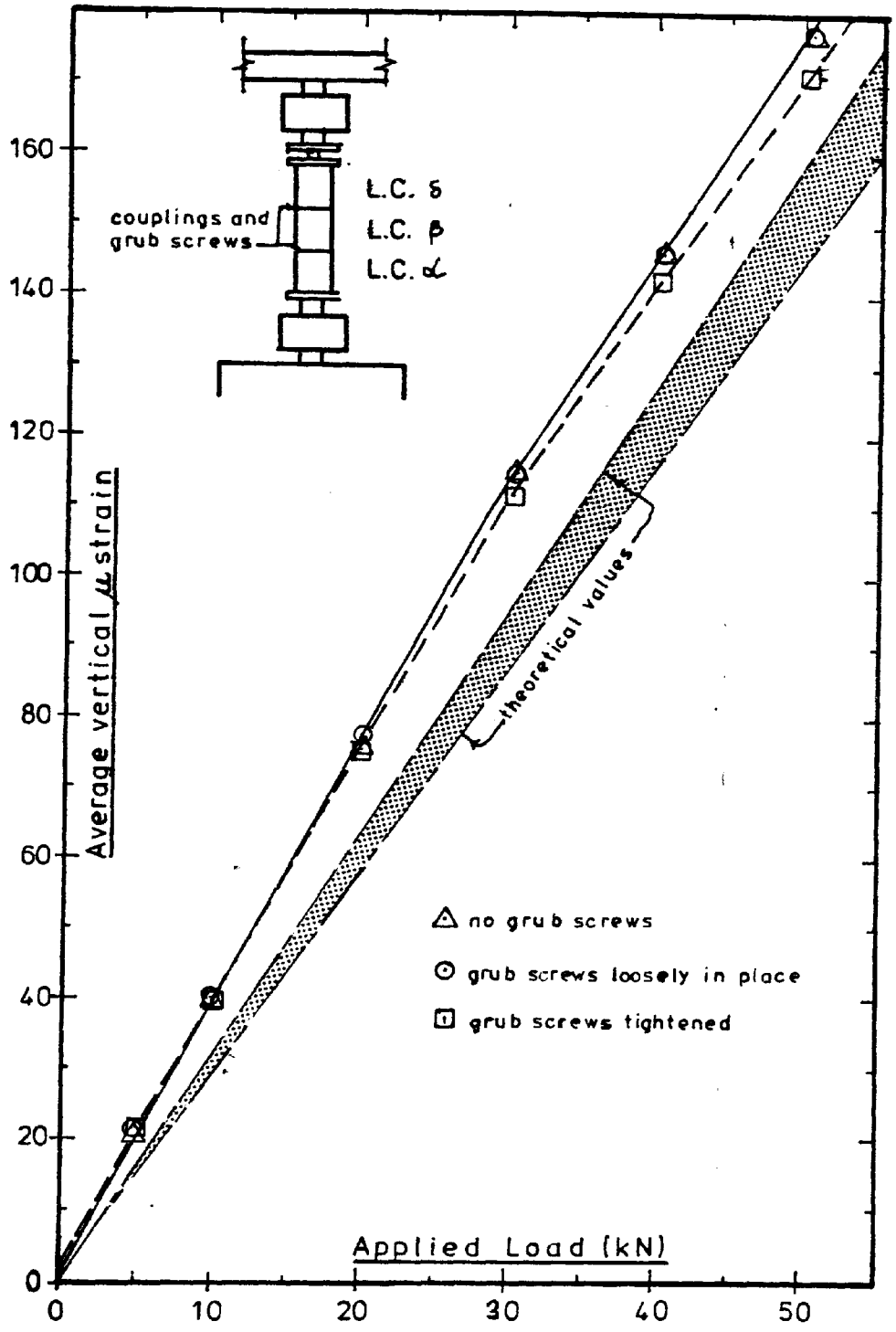

FIGURE 6.12

CALIBRATION CURVES SHOWING THE INFLUENCE OF THE ASSEMBLY ON THE LOAD CELL RESPONSE TO LOADING. EACH CURVE REPRESENTS THE AVERAGE OF TWO INDEPENDENT TESTS

For the analysis of the semi-fullscale testing results, an in-situ calibration test was conducted in the testing tank after the pile had been fully assembled. This calibration was used for all subsequent analysis of the strain readings for this assembly. If the pile was disassembled in any way it would have necessitated a new in-situ calibration test to be performed.

Details of the in-situ calibration test are given in the next section.

6.4 In-Situ Calibration of the Test Pile Load Cells

6.4.1 Pile Assembly and Alignment

The pile assembly is shown in Figure 4.2 and Plate 6.3. The pile was assembled in the following manner :

1. The frictionless cylinder was positioned in the correct location in the bottom of the tank so that the central axis of the cylinder and jack ram were congruous This was checked with a theodolite at two perpendicular locations.

2. An electrolevel was used to check that the top of the cylinder was level. This would ensure that the central axis of the cylinder would be truly vertical.

3. Step 1 was rechecked.

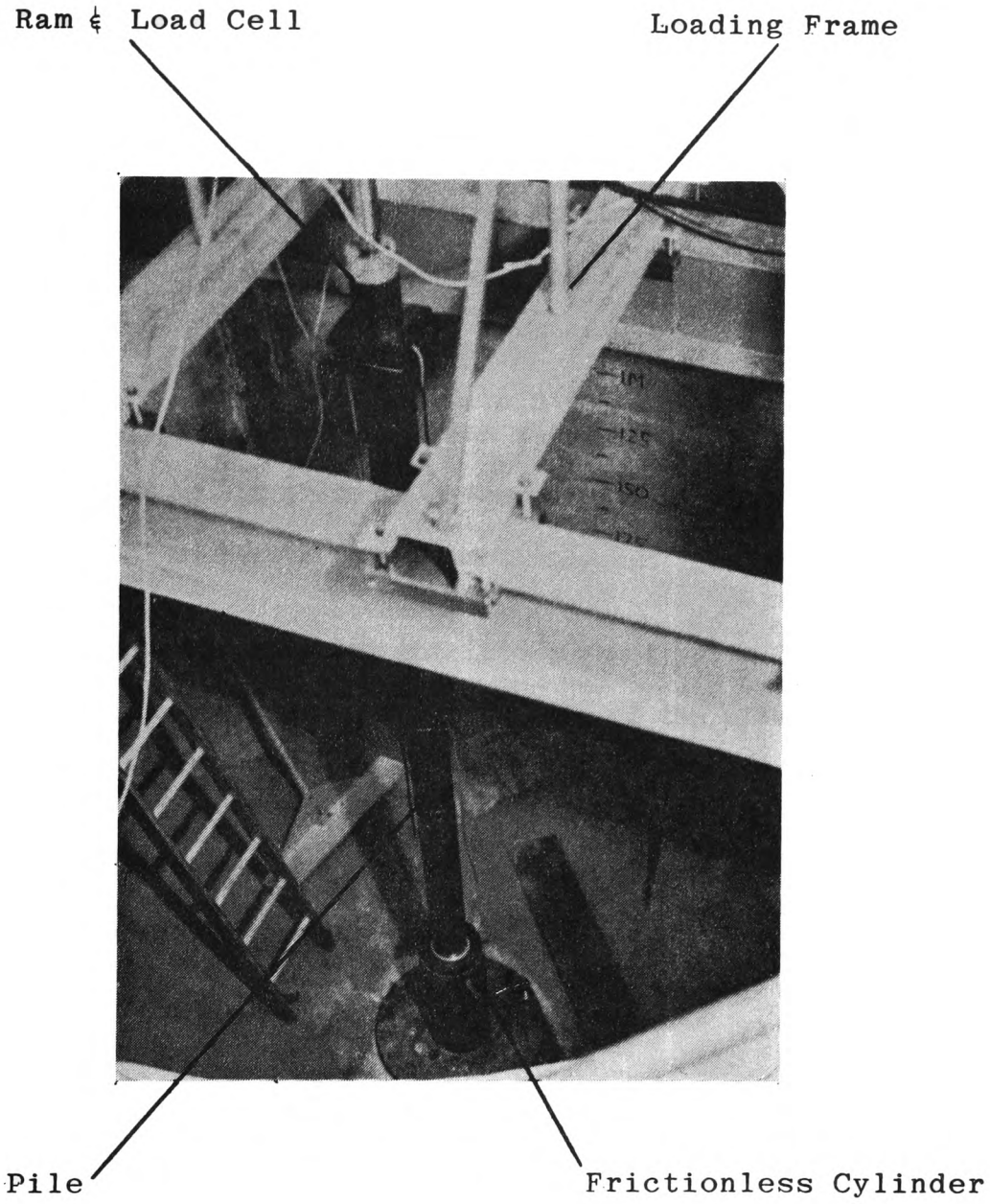

PLATE 6.3

PILE ASSEMBLY

4. The machined 700 mm length section of pile was placed in the frictionless cylinder.

5. The pile was loosely assembled, one section on top of another, threading the strain gauge leads through each section. Each lead was rigidly fixed to the coupling above it to safeguard against the possibility of the wires being pulled from the gauge terminals. Finally, the 1100 mm length spacer section of pile was attached.

6. The strain gauge leads were then fed through the eight holes in the top plate and this plate was brought into position on the top of the 1100 mm length spacer section.

7. The jack ram was then brought into contact with the steel ball which had been placed on the top plate of the pile.

8. A load of 25 kN was applied to the pile while the couplings were tightened. Then the load was removed and the verticality of the pile was checked.

To check that the pile was not adhering to the inside of the cylinder the pile was moved up and down and the load measured. It was thought that there was no friction between the pile and the cylinder, since the load measured by the jack load cell during this movement was only the self weight of the pile and did not vary.

At this point the resistance and insulation resistance of each strain gauge element was checked to assure that no gauges had been damaged or gauge leads pulled off during assembly.

The initial method of conducting the in-situ calibration test, was to drive the pile against the bottom of the frictionless cylinder. However, since the end of the machined section of pile and cylinder bottom had not been designed with this in mind, it could not be assumed that they were parallel. If, this was the case, bending moments and local stresses could be created in the pile during loading. This could lead to damage of the machined surface of the pile which was in contact with the bearing surface of the cylinder. Therefore, the following procedure was adopted.

The machined section of pile was detached and removed, and two steel plates separated by a steel ball bearing were positioned on the top of the cylinder. Next, the pile was brought into contact with the top plate as shown in Figure 6.13. The steel ball was used to eliminate any bending moments. The pile was calibrated by loading it against this arrangement. After calibration the two plates and steel ball were removed, the machined section of pile placed in the cylinder and reattached to the pile, and the pile was ready for testing.

6.4.2 Calibration Tests: Before, During, and After the Testing Programme

To verify and measure any variation in the calibration characteristics of the load cells during the seven month testing programme, the in-situ calibration tests were performed on the pile before testing commenced, half-way through the testing programme, and at the completion of testing.

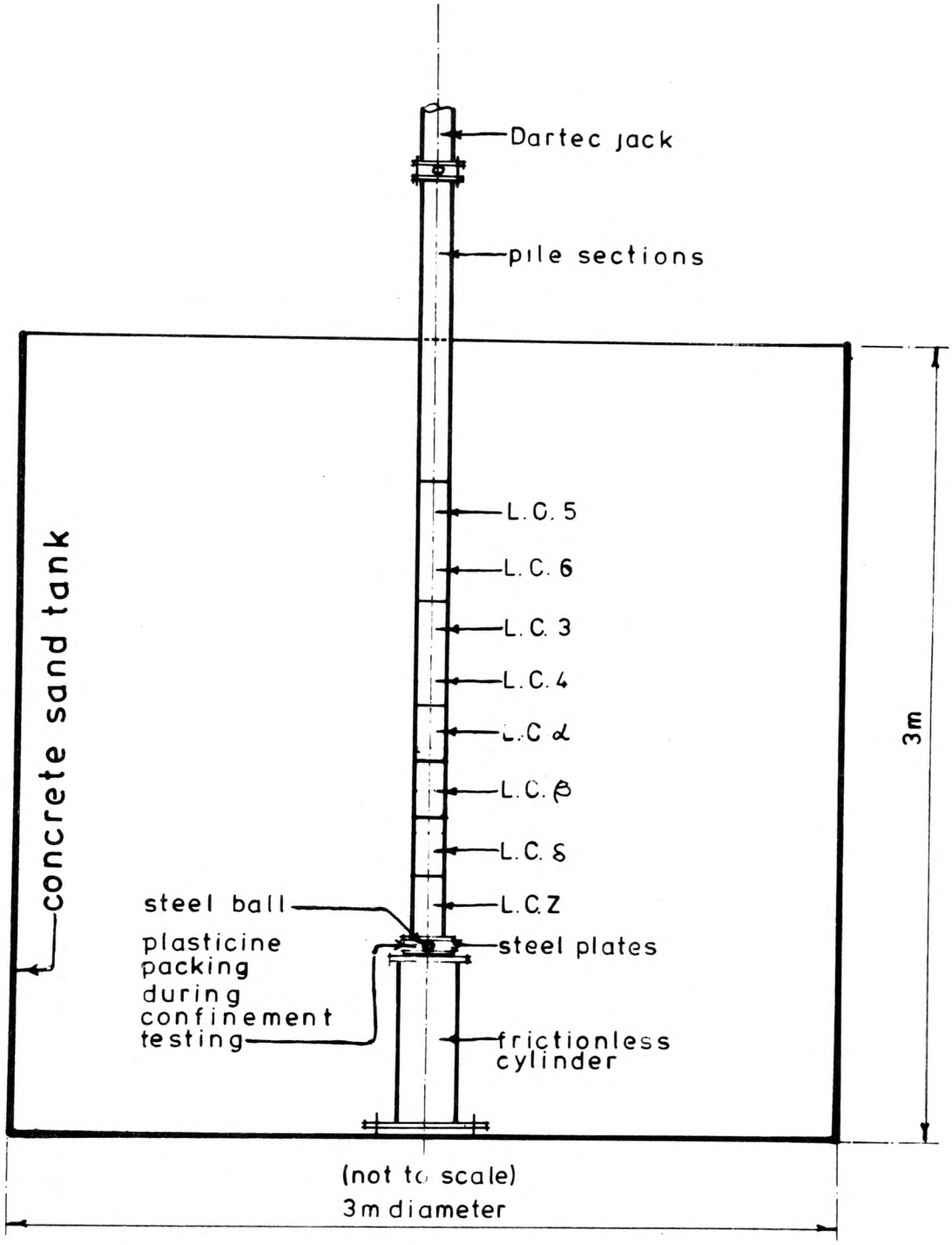

FIGURE 6.13

ARRANGEMENT FOR IN-SITU CALIBRATION TEST

The individual calibration curves of the average vertical strain vs. applied load, for each of these three calibration tests are shown in Figures 6.14. As with the calibration tests performed in the Instron 1251, the curves for the in-situ tests show no hysteresis. With the exception of L.C.4 and L.C.5 in Figure 6.14 the calibration curves appear to be linear, and with the exception of L.C.3 and L.C.5 did not vary to any extent during the testing programme.

A more sensitive calibration test with a loading range of 0-10 kN was conducted at the same time as the calibration checks carried out halfway through, and at the end of the testing programme. This is the maximum range over which the load cells would be subjected to in this testing programme. The load cell calibration curves for these tests are shown in Figure 6.15. The variation of the results of these tests are less than those for the 0-40 kN calibration tests, and are very small with the exception of L.C.3.

For the purpose of analysing the test data, the results of the calibration test 2A (0-10 kN) were used as the calibration curves for the individual load cells. The method with which these curves were used to process the test results is described in Chapter 7.

6.4.3 Detection of Lateral Displacements and Bending

Lateral displacement and bending of the pile during the in-situ calibration tests before the start of the testing programmme were monitored by displacement transducers as shown in Plates 6.4 and 6.5.

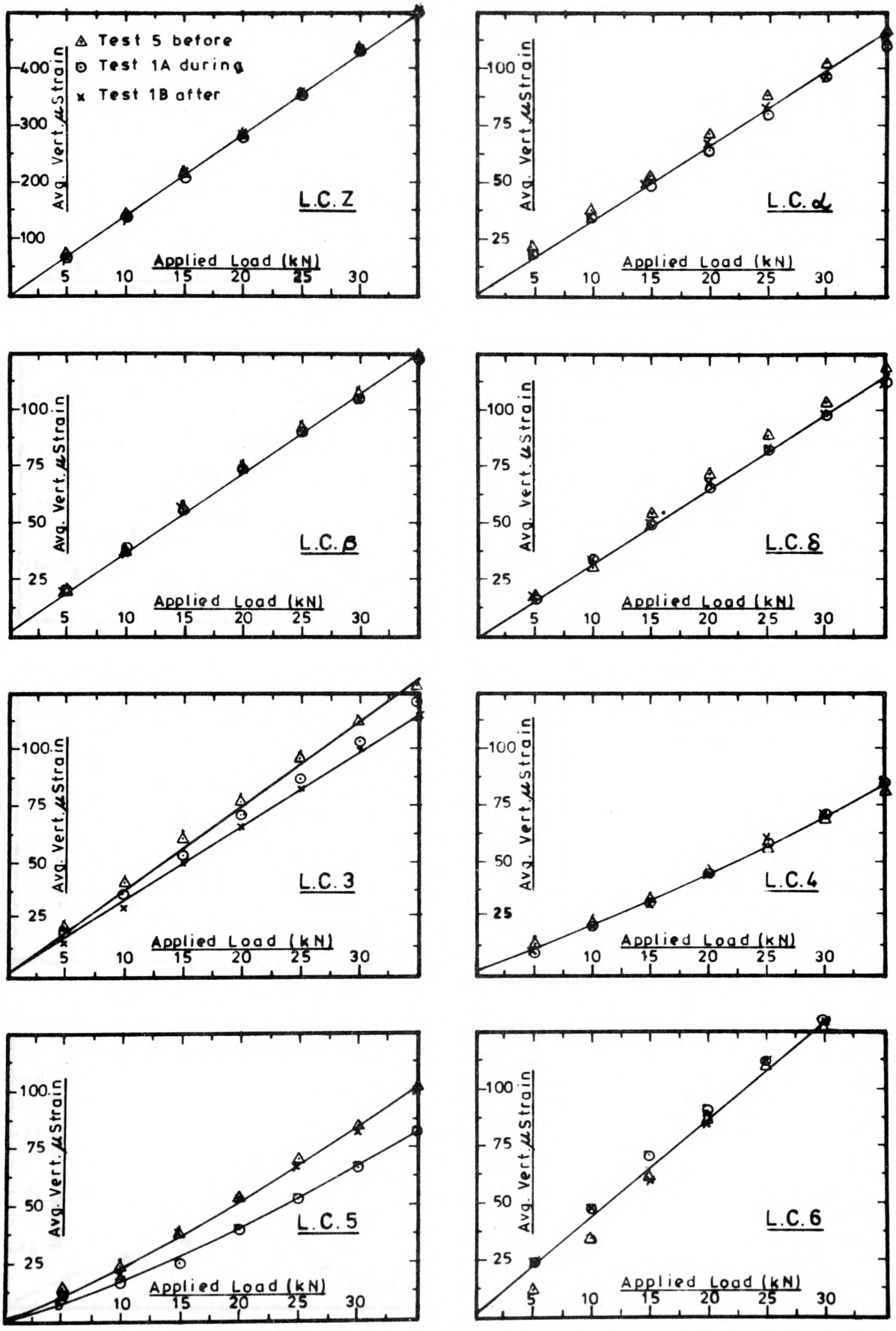

FIGURE 6.14

IN-SITU LOAD CELL CALIBRATION TEST BEFORE, DURING AND AFTER THE TESTING PROGRAMME

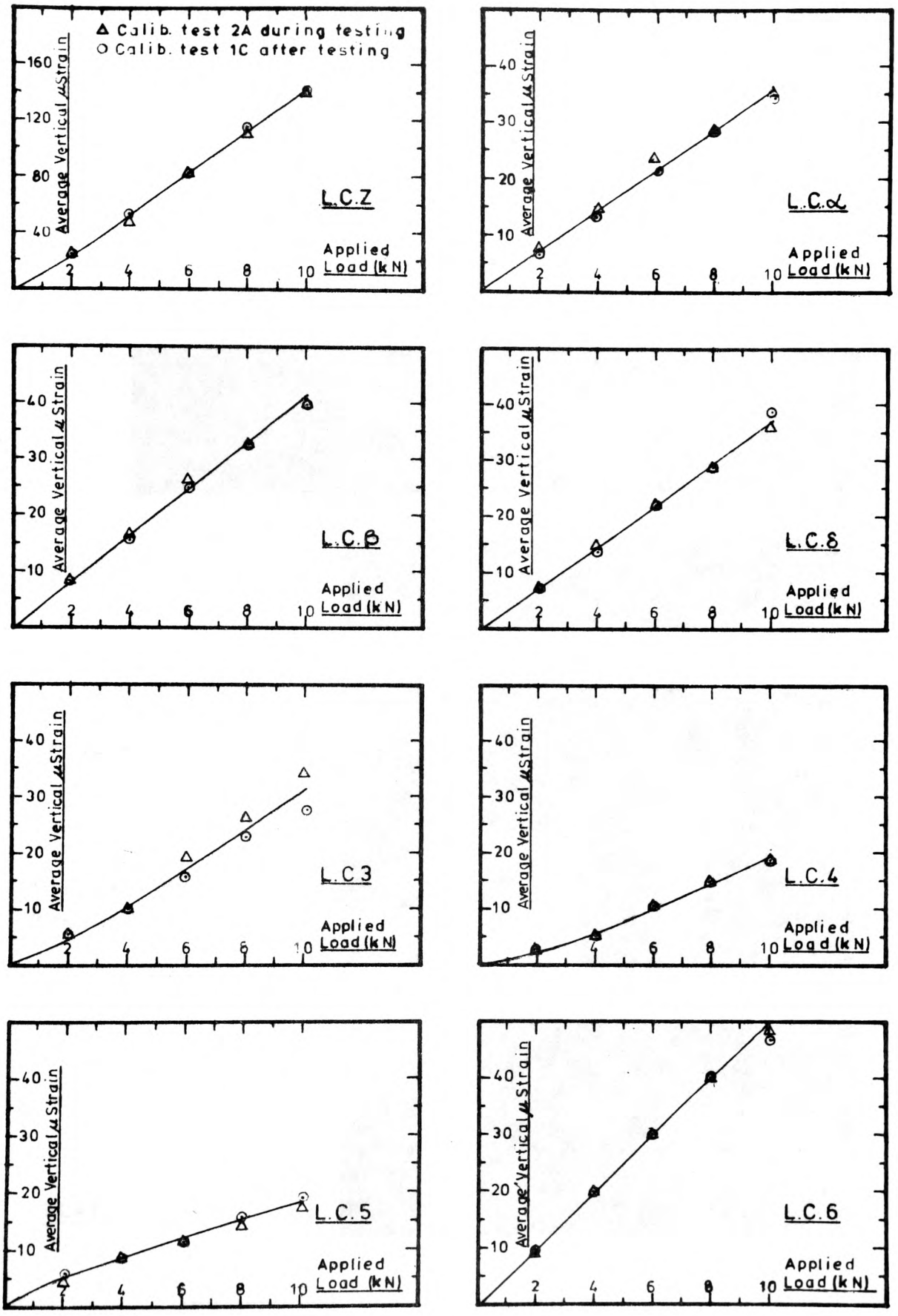

FIGURE 6.15

IN-SITU LOAD CELL CALIBRATION TESTS DURING AND AFTER THE TESTING PROGRAMME

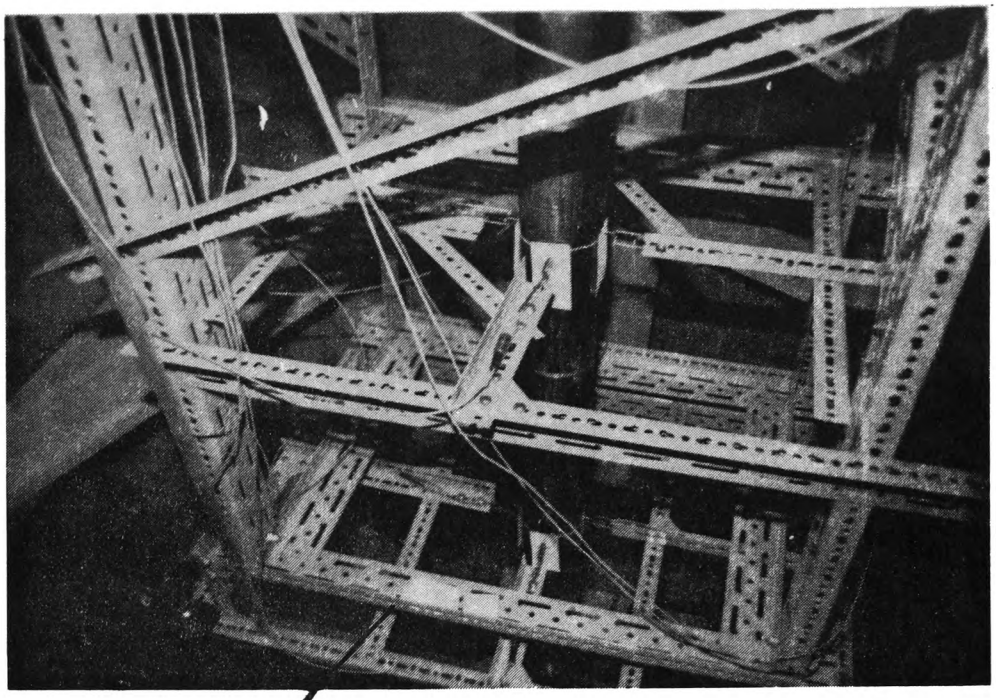

PLATE 6.4

Datum Frame

Pile

Displacement
Transducer

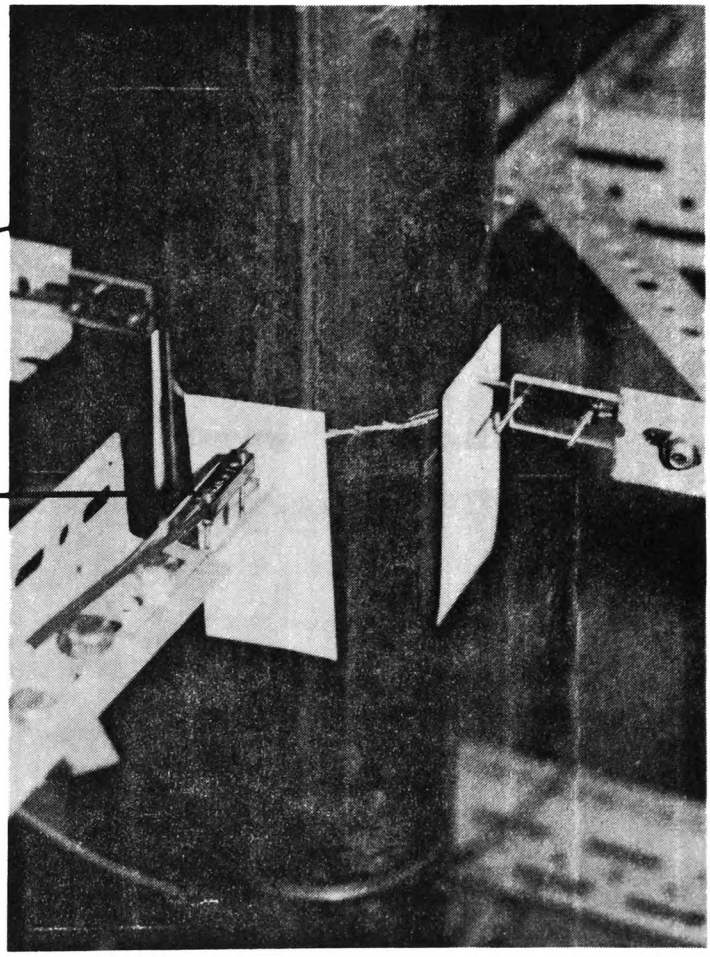

PLATE 6.5

ARRANGEMENT FOR MONITORING THE
LATERAL DISPLACEMENTS AND BENDING
OF THE TEST PILE

The dexion frame was constructed around the pile and connected to the datum frame. The displacement transducers measured the extent and direction of the lateral movements of the pile at three locations on the pile shaft (midpoint (L/2) and at one-quarter of the pile length (L/4) from each end).

The maximum lateral displacements measured at 10 kN applied load were 0.36mm at L/4 from the top of the pile, 0.29mm at the midpoint and 0.046mm at 3L/4 from the top of the pile.

These displacements were measured without any confinement around the pile during testing. The added restraint caused by the sand around the pile should restrict these small lateral displacements.

6.4.4 Influence of Confinement on Calibration

The three sets of in-situ calibration tests performed on the test pile, were carried out in the sand tank in the absence of any confining pressures on the pile. During the testing programme (described in Chapter 7) the pile was confined laterally by the sand placed around it.

To investigate the influence of this confinement on the pile (in particular the strain gauges response) a series of in-situ calibration tests were performed.

The pile was set up as described in section 6.4.1, with the addition of the space around the steel ball, between the pile and the frictionless cylinder, being packed with plasticine (see Figure 6.13). This was done to avoid getting the sand in between the two plates and

interfering with the test results. Next, sand was placed in the tank in three equal layers and each layer was vibrated; bringing the surface of the sand to the elevation of the top of the cylinder. At this point an in-situ calibration test was performed (no confinement on the pile). A 250mm layer of sand was then poured into the tank around the pile following the same procedure used during the testing programme described in Chapter 7. Another calibration test was performed with the pile embedded in the 250mm layer of sand. Next, the layer of sand was compacted using the surface vibrator and the calibration test was repeated. A total of seven, 250mm layers of sand were placed around the pile and two calibration tests carried out on each, one before and one after vibraton.

Figure 6.16 shows the range of values for the 15 calibration tests described above, for each load cell. No significant trends in the results could be established. For one-half of the load cells (L.C.γ,L.C.β,L.C.δ and L.C.4) the strains tended to decrease as the piles embedded length increased, while for the other four load cells the opposite appeared to be the case.

Also plotted on the graphs of Figure 6.16are the values obtained from the in-situ calibration test performed halfway through the testing programme. These are the calibration values used for analyzing the test data. As can be seen from Figure 6.16, with the exception of load cells L.C.3 and L.C.5, these values coincide with the average of the range.

The influence of confinement on the pile behaviour and calibration, is an interesting subject. The candidate has not come across any formal investigations into this aspect of testing. Due to

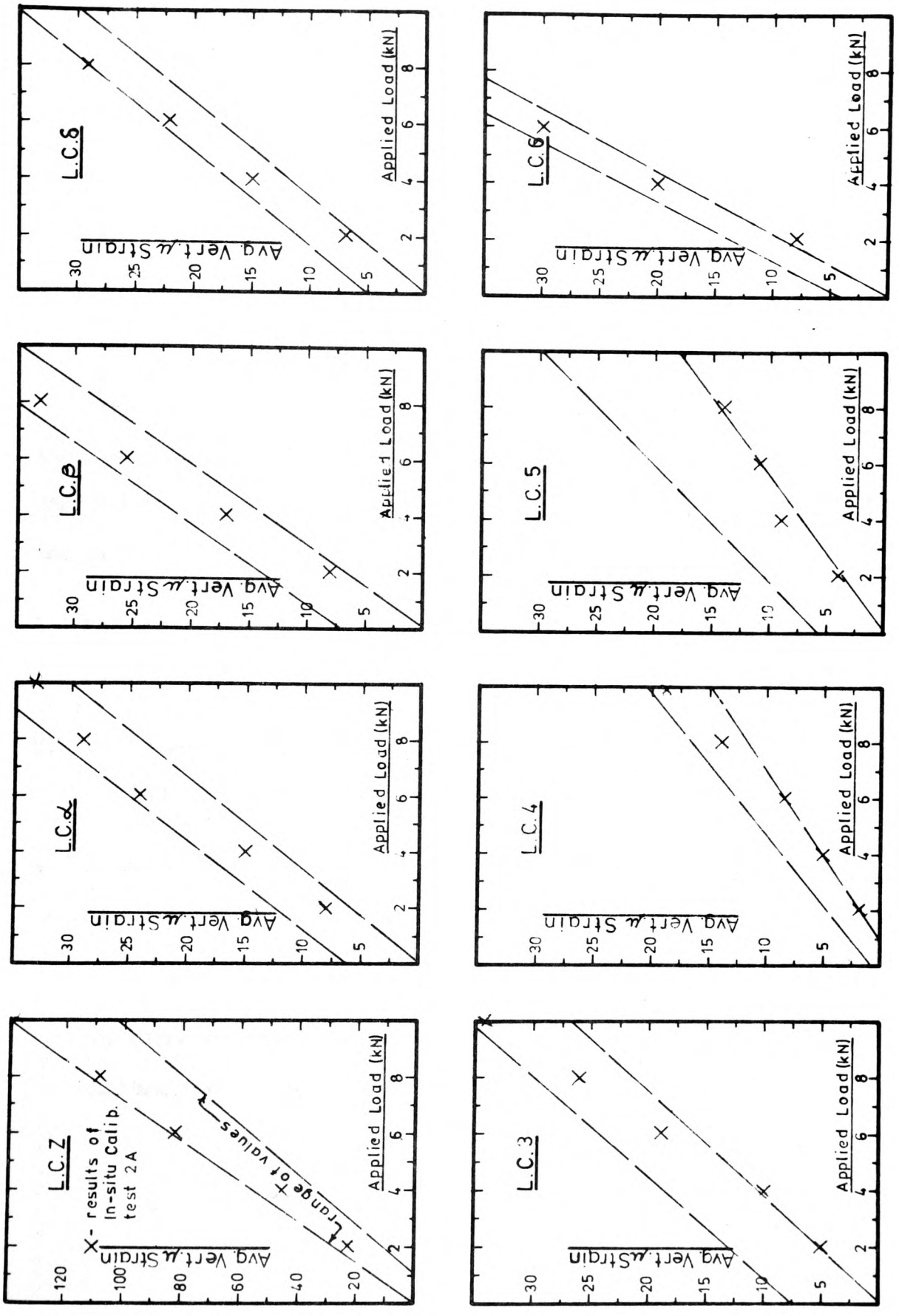

FIGURE 6.16

INFLUENCE OF CONFINEMENT ON IN-SITU CALIBRATION TESTS

the lack of time available, the candidate was unable to investigate this any further, however, he feels this limited data shows that this subject needs further investigation and should be considered by investigators who calibrate their equipment in one state and test them in another.

6.4.5 Conclusions

The in-situ calibration tests conducted before, during and after the testing programme, and the investigation of the influence of the confinement of the test pile in the sand medium, during testing, on the pile load cell response, have highlighted the following points.

1. The variation in the calibration over the duration of the testing programme was insignificant.

2. The order of magnitude of the lateral displacements measured with the pile free of any confinement was very small.

3. Further experimentation is needed to investigate the influence of confinement on the load cell calibration.

4. The calibration values used for the analysis of the data, coincided with the average of the range of values, obtained for calibration during confinement of the pile in the sand medium.

6.5 Preliminary Testing of the Sand Displacement Monitoring System

6.5.1 General

A description of the Terra Plate-wire-transducer system for monitoring the vertical soil displacement has been given in section 4.3.1 and is shown on Plate 4.1. The purpose of this system was to measure the sand displacement during pile loading.

6.5.2 Terra Plates

The main concern in the design of the system was to insure that the presence of the instrumentation in the soil would cause the least amount of influence on the soil displacement. The two main considerations in deciding on the size of the plates were :

1. to make them large enough so that they would move with the sand, and

2. that they would be small enough to cause no influence on the soil behaviour (i.e. create a reinforced earth).

The Terra Plates were 25mm square by 1.5mm thick aluminium plates. These were similar to the settlement plates used by Denman, Nicholls, and Symons (1977) for measurement of the consolidation of a weak clay stratum which induced a negative skin friction on a group of model piles.

6.5.3 Displacement Transducers

The pilot study described in Chapter 1 enabled the candidate to rectify a number of difficulties with the equipment before commencing on the much larger semi-fullscale testing programme. Among the problems which came to light in the pilot study were those encountered with the displacement transducers. The type of transducer initially used was of the wire wound type. However, difficulties were found in obtaining a holder that would not cause any electrical interference and would not distort the transducer body, thus giving a linear response. A holder was designed and manufactured from Tufnel industrial laminated plastic which met these requirements. Unfortunately, in practice this holder was found to be bulky and difficult to set up.

At this stage a new type of displacement transducer was investigated. This was a conductive plastic linear-motion potentiometer. These rectilinear potentiometers provide an electrical signal directly proportional to a linear mechanical movement of the potentiometer shaft.

The conductive plastic resistive element provides virtually infinite resolution. Since, the potentiometric transducer provided a full scale output equal to the applied voltage, there was no need for amplifiers, conditioning units, or other complex electronic circuitry.

The potentiometric transducers used were equipped with mounting holes which enabled easy mounting to a simple perspex holder.

The manufacturers specified linearity of the two types of potentiometric transducers used is 1%, however, the candidates calibration of the transducers (see Plate 6.6) found values much better than this. For the 30mm displacement transducer a value of 0.2% was obtained while for the smaller 11mm displacement transducer a value of 0.4% was recorded.

6.5.4 Piano Wire and Connections

As a means of connecting the displacement transducer to the Terra Plate the candidate chose to use steel 'piano' wire (Denman, Nicholls and Symons (1977) used inelastic glass fibre threads). The essential factors to be considered in the choice of a wire were that :

1. it was inelastic at the small loads which would be imposed on it,
2. it had a small cross section, and
3. it did not have to be rigid, since the transducer provided the necessary tension to keep the wire taut.

Loading tests performed on the 'music spring steel wire of grade piano supreme' produced an elongation of 6.8×10^{-4}mm for a 1.0mm transducer movement (see Appendix 6A), and a failure load of 490N. The maximum load applied to the piano wire by the transducer during pile loading was approximately 0.18N and the small elongation this would cause (6.8×10^{-4}mm) was insignificant.

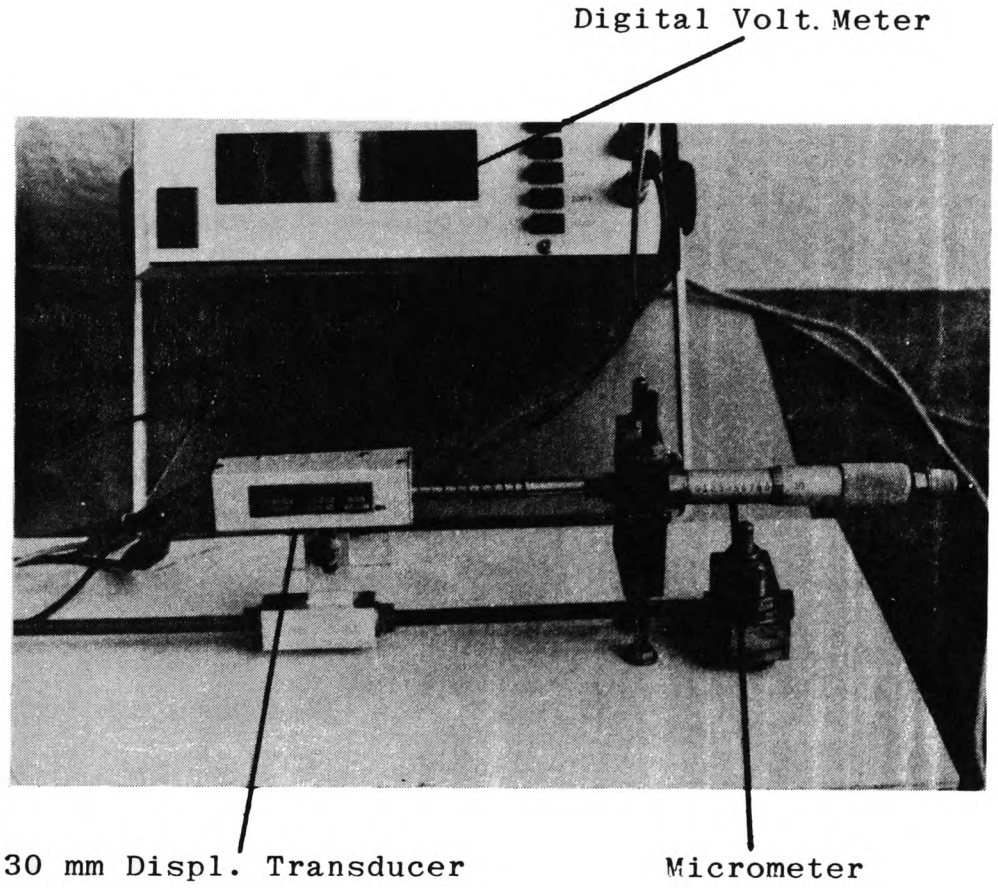

PLATE 6.6

APPARATUS FOR CALIBRATION OF
DISPLACEMENT TRANSDUCERS

The piano wire was fixed to the Terra Plate by passing the end of the wire through a hole in the centre of the Plate, looping it around a 10mm length of 1.0mm diameter wire (paper clip), and bonding this to the back of the Plate with Araldite epoxy adhesive. This connection was found to withstand a load of 22kg without failing.

The piano wire was connected to the displacement transducer by a simple perspex coupling with grub screw fasteners (see Plate 4.1).

6.6 Sand Compaction

The method employed for compaction of the sand was by surface vibration of each layer.

Consideration was given to the possibility of using a poker vibrator for soil compaction. However, owing to the possibility of the disturbance of the instruments (i.e. density tins and Terra Plates), this method was abandoned.

The compressed air vibrator adapted for surface vibration is shown in Plate 6.7.

The compaction was performed by: placing the (0.44mx1.0m) vibrating board of the vibrator on the surface of the sand, placing the two 15kg sandbags on the board, to act as a surcharge, and vibrating for three minutes. The board was subsequently moved to the next location and vibrated for a further 3 minutes. The locations of the board were such that the entire surface would be vibrated, working from the side of the tank inwards towards the pile.

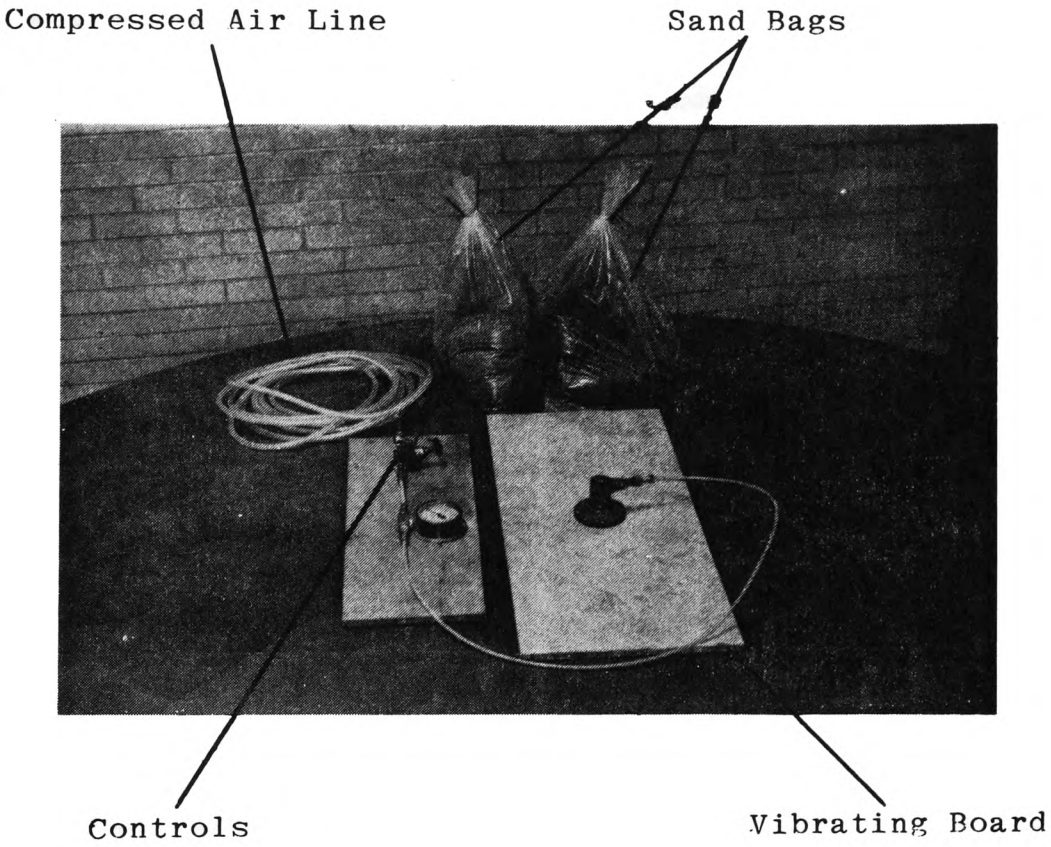

PLATE 6.7

SURFACE VIBRATOR

A smaller (285mmx115mm) board was fitted to the vibrator for compaction of the area between the wires connected to the density tins and Terra Plates. This vibrator was held in place by hand for the required three minutes.

The three minute vibration time was decided upon from the results of a preliminary vibration test which was conducted employing the perspex tank which was used in the pilot study. This arrangement is shown on Plate 6.8.

A circular board was manufactured and attached to the vibrator. This board which fitted inside the perspex tank had sufficient clearance to avoid contact with the inside surface of the tank. Two 250mm layers of sand were each vibrated for 12 minutes with the two 15kg sandbags placed on the board. This test was repeated three times for a total of six layers.

The results of this preliminary test showed that an average of 70% of the total compaction achieved for 12 minutes was reached after three minutes vibration.

Since, each layer of sand would have to be vibrated in a minimum of 16 locations, and time was an important consideration, it was decided to vibrate for a period of three minutes in each location.

The main concern with the compaction of the sand was to reach a uniform density and to formulate a set procedure for compaction that would be consistent and repeatable.

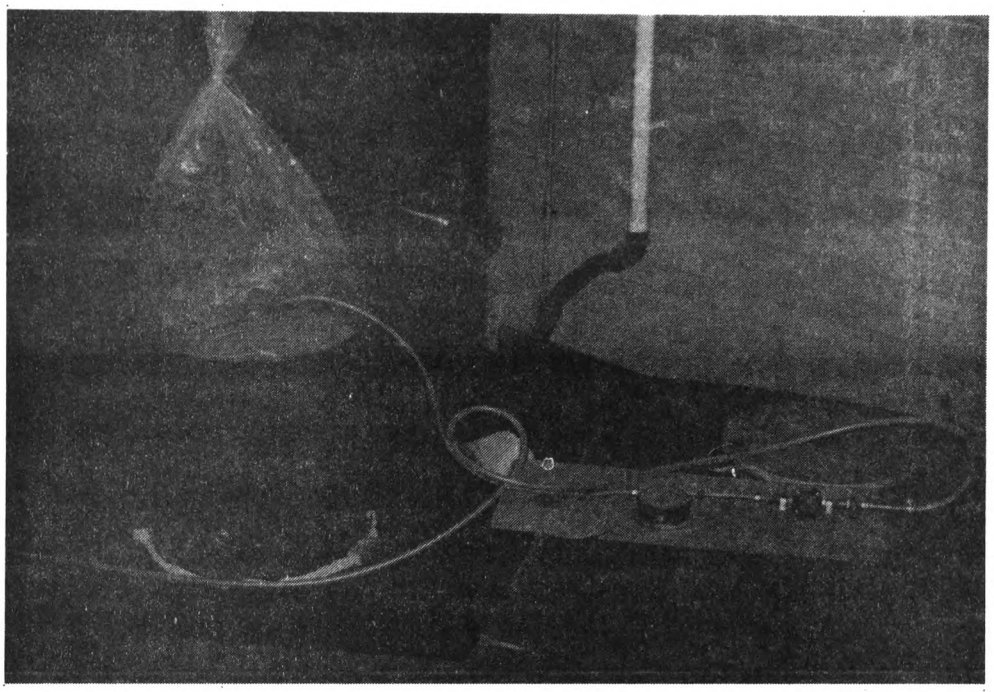

PLATE 6.8

ARRANGEMENT FOR TESTING VIBRATION TIME USING
THE SURFACE VIBRATOR

APPENDIX 6A

Piano Wire Elongation

From the loading test performed on the 0.5mm diameter steel piano wire the slope of the load-deflection curve was 3.73×10^{-5} mm/g.

Another loading test was carried out on the stiffer 30mm displacement transducer and it was found that the slope of the load deflection curve was 18.22 g/mm.

For a maximum transducer movement of 1.0mm (the assumed maximum Terra Plate settlement during a pile loading test) the additional load applied to the piano wire was

$$1.0\text{mm} \times 18.22\ \text{g/mm} = 18.22\text{g}.$$

Therefore, the elongation of the piano wire for an additional load of 18.22g is

$$18.22\text{g} \times 3.73 \times 10^{-5}\text{mm/g} = 6.8 \times 10^{-4}\text{mm}$$

Hence, it was unlikely to interfere with the displacement measurements.

APPENDIX 6B

Expected Values of Maximum Load on the Test Pile

The skin friction resistance (Q_s) of a pile in a cohesionless soil is equal to

$$K s \tan \delta q s A s \quad \text{(Vesic 1963)}$$

where Ks = coefficient of skin pressure

δ = friction angle between soil and pile

qs = average overburden pressure

As = area of the pile shaft

For a smooth (0.114m diameter) steel pile bored into 2m of dry, dense sand, assuming :

$\phi = 45^{\circ}$ from Potyondy (1961)

Ks = 1.0 from Meyerhof (1951)

$\delta = 27^{\circ}$ from Potyondy (1961)

$qs = \frac{1}{2}\gamma D_f = \frac{1}{2}(1750)(9.807 \times 10^{-3})(2) = 17.2 kN/m^2$

$As = 2\pi r D_f = 2\ (0.057)(2) = 0.72 m^2$

$Qs = (1.0)(\tan 27^{\circ})(17.2)(0.72)$

Q_s = 6.3kN

The load cells and pile were designed to facilitate at a later date, the base of the pile to be driven into a clay layer. Cooke, Price and Tarr (1979) drove 168mm diameter 5m long steel piles into London clay. On testing the piles in compression after installation they measured a unit base bearing capacity of 1985kN/m^2. Applying this unit resistance to the 114mm diameter test pile used in the candidates testing programme accounts for an ultimate base resistance of 20kN. Adding to this the expected skin friction on the pile shaft of 6.3kN the expected maximum load on the pile is 26.3kN. Since the maximum load that the jacking system was rated at was 50kN the test pile was designed and calibrated for this maximum load. This allowed for a factor of safety of approximately 2 against the expected maximum total load and would allow the driving of the pile while end bearing in a loose sand layer.

APPENDIX 6C

Theoretical Calibration Values for the 'Shell' Type Load Cell

$$\varepsilon = \frac{P}{AE} \qquad (6C.1)$$

where ε = Strain

P = applied load

A = cross sectional area = $1583mm^2$

E = Youngs Modulus of the material

The value of Youngs Modulus for mild steel varies from 200 to $220GN/m^2$. Therefore for an applied load of 50kN, the theoretical value of strain is

158μ strains for E = $200GN/m^2$ and

144μ strains for E = $220GN/m^2$.

Chapter 7

Testing of the Semi-Fullscale Pile

CHAPTER 7

TESTING OF THE SEMI-FULLSCALE PILES

7.1 Pile Assembly

The pile was assembled in the testing tank as described in section 6.4.1. The wire leads for both the strain gauges and displacement transducers were connected as shown in Figure 3.6.

7.2 Testing Programme

The sand tank was filled and the subsequent testing was carried out in the following sequence :

1. A clamp was designed and attached to the top of the superstructure to allow the pile to be secured so that it would not move between driving tests. The pile was raised and secured.

2. Three equal layers of sand (foundation layers) were placed in the tank and compacted with the surface vibrator which was described in section 6.6. The locations for the vibrator corresponded to the 16 positions shown in Figure 7.1. This brought the level of the surface of the sand up to the level of the top of the frictionless cylinder and the base of the first test layer (T1), as shown on Figure 7.9.

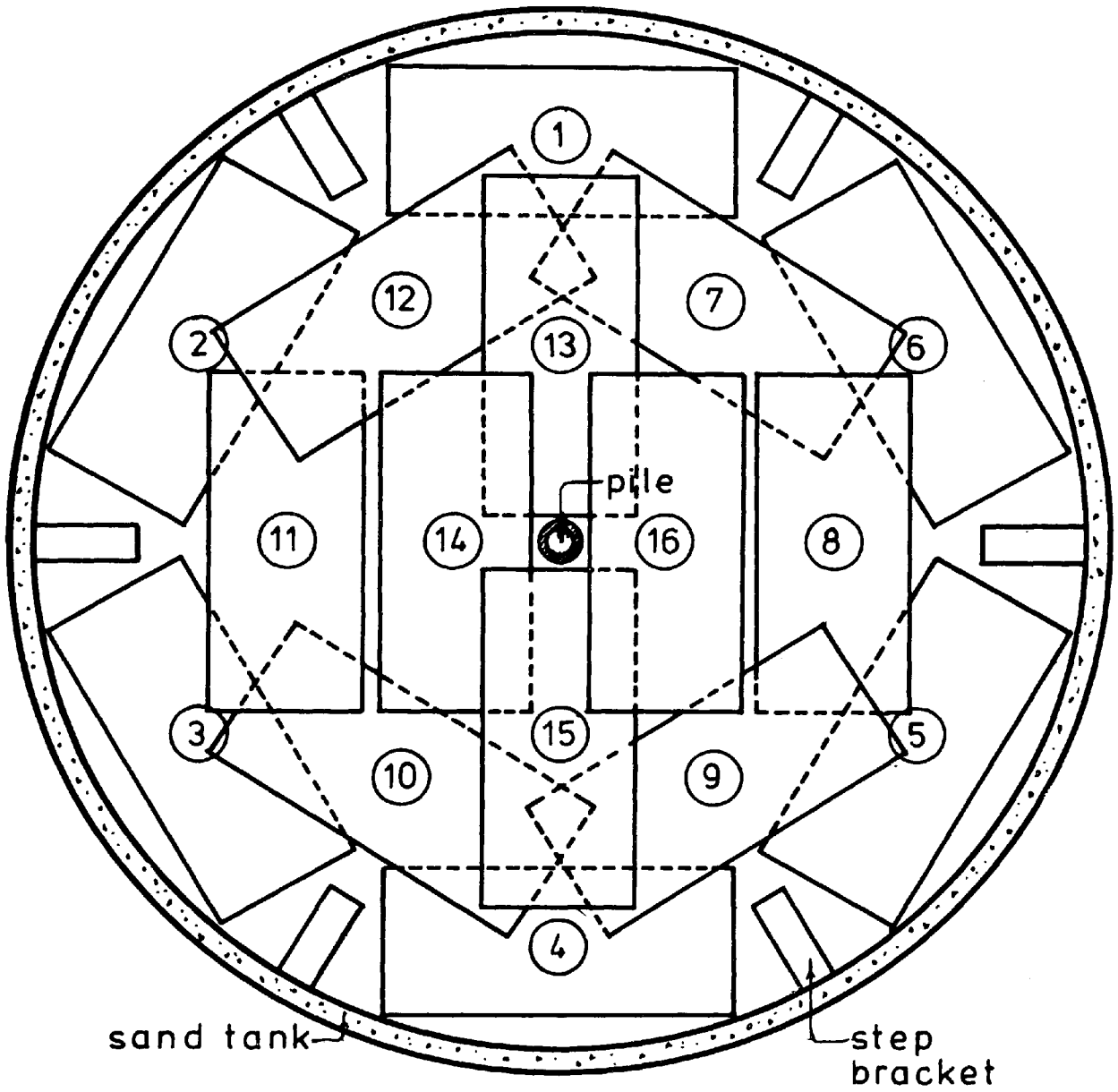

FIGURE 7.1

SURFACE VIBRATOR LOCATIONS

3. Two density tins were then placed into position on the top of the third foundation level (base of layer T1).

4. The first test layer was poured to a depth of 0.25m, while care was taken to produce a uniform, homogeneous mass of soil.

5. A Mini-Mackintosh dynamic probe penetration test was conducted to a depth of 0.5m, at two locations.

6. The first test layer of soil was then compacted using the surface vibrator which was located at the 16 positions which were described earlier.

7. The Mini-Mackintosh penetration test was repeated on the compacted layer. Again the probe was driven to a depth of 0.5m. In this way the resistance to penetration of the last two layers poured was measured.

8. The hydraulic jacking system was then switched on and the pile was unclamped.

9. The pile was then driven, at a constant rate of penetration of 0.6mm per minute, for a distance of 12mm. During pile driving the load cell strains, soil displacements, total applied load, and pile top movement were monitored by the Mycalex Data Logger and recorded on punched paper tape via the teleprinter.

10. At the completion of this driving test the pile was secured at this position and the hydraulic jacking system was switched off.

11. For the next layer the Terra Plates and Density Tins were positioned in place, the sand layer was poured, a Mini-Mackintosh penetration test was carried out, the layer vibrated, another Mini-Mackintosh test performed, and the pile was driven for a further 12mm.

12. Step 11 was repeated for each of the seven test layers.

Each layer was instrumented, poured, compacted and tested according to a set time schedule. By following this schedule :

1. compaction due to the self weight of the sand, and

2. any stress relief which was likely to take place within the pile-soil system would have taken place over the same duration of time for repeated fillings of the tank.

The total pile penetration of 12mm for each test layer was found to be sufficient to fully mobilize the skin friction during each test. This is in agreement with other researchers such as Tomlinson (1977) who suggested that the skin friction is fully mobilized after a settlement of 10% of the pile diameter.

The testing programme consisted of four independent fillings of the tank. The second filling was a repeat of the first and was carried out under the same testing sequence. The third and fourth fillings of the tank were conducted in the same manner as the first two, with the exception that the seven test layers were not vibrated. Thus, the results obtained were representative of testing at two

different values of soil density.

The reason for repeating the two tests were :

1. to aid in identifying any anomalies in the test results, and

2. it was felt that by taking the average values of two independently performed tests, a better understanding of the actual soil displacements and load transfer would be obtained.

After the completion of the testing of test layer T7, and prior to emptying the tank, a series of loading tests were carried out on the entire depth of soil in the following sequence :

1. C.R.P.1 - a constant rate of penetration test driving the pile a further 12mm. This test was a repeat of the CRP test performed on the final test layer of soil T7.

2. P.O.T.1 - a pull-out test was carried out extracting the pile at a constant rate.

3. M.L.T. - a maintained load test was performed loading the pile in increments until failure occured by plunging.

4. C.R.P.2 - another constant rate of penetration test was performed driving the pile until the penetration resistance reached a maximum.

5. P.O.T.2 - a final pull-out test, withdrawing the pile at a constant rate until the resistance reached its maximum value.

The results of these five loading tests are presented in section 7.3.5.

7.3 Test Results

In the sections to follow the results of the semi-fullscale pile tests are presented together with an explanation of the procedures for obtaining these results and a discussion of any implications and anomalies.

7.3.1 Load-Penetration Curves

The load-penetration relationship was derived from the total applied load, measured by the Dartec jack load cell, and the pile top displacement recorded by the ram displacement transducer (see section 3.8).

The total load versus pile penetration curves of the seven test layers, for each of the four fillings of the tank, are shown in Figure 7.2.

These curves represent the skin friction component of the load-settlement relationship of a pile passing through a granular stratum. The curves are similar to the shaft load component of the curves presented by Poulos (1974) for the construction of a load-settlement curve as shown in Figure 2.7.

The curves obtained from the test results possessed an initial linear relationship between load and pile penetration for a penetration of approximately 1% of the pile diameter for the denser

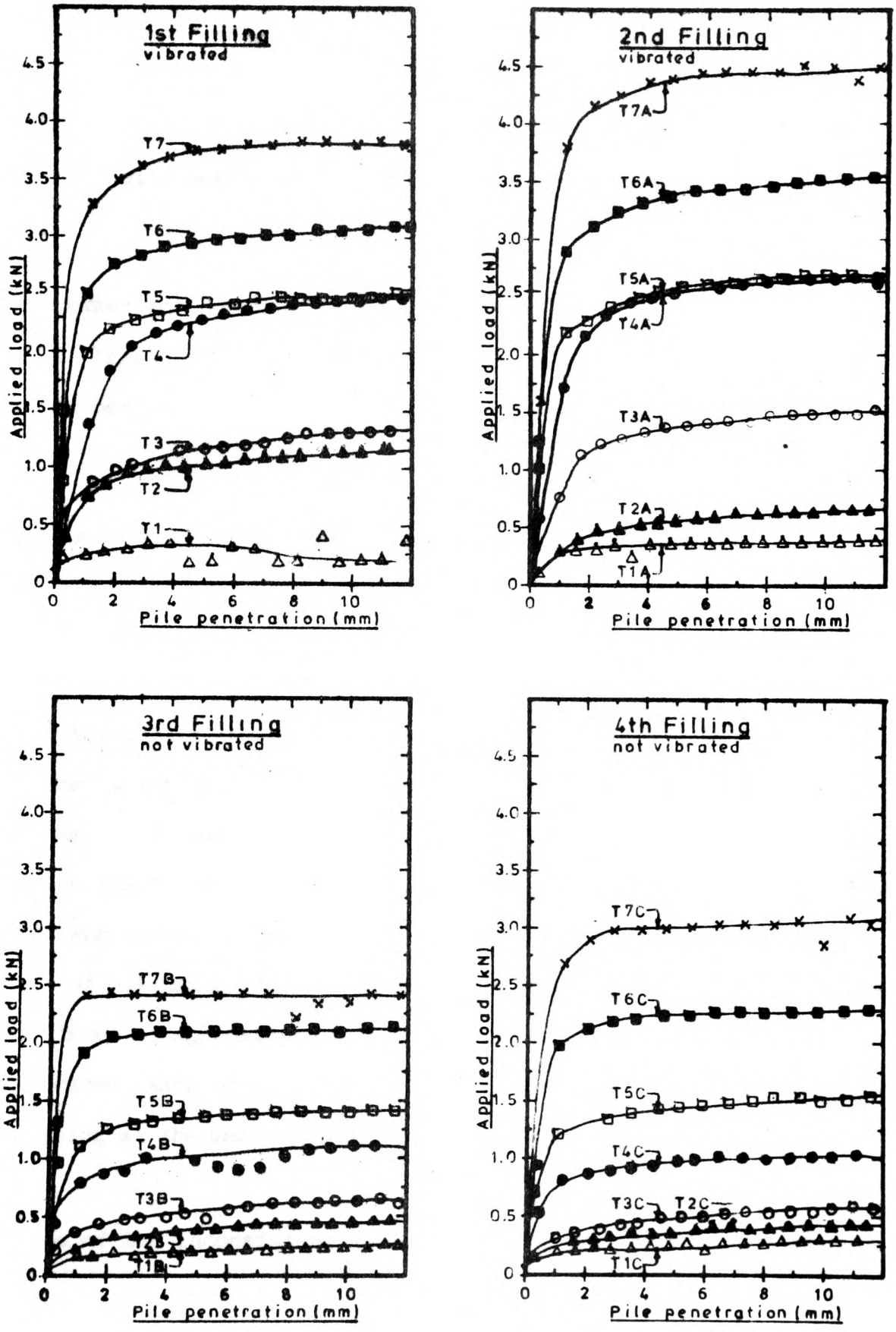

FIGURE 7.2

APPLIED LOAD VERSUS PILE PENETRATION CURVES FOR 4 FILLINGS OF THE TANK - 7 TEST LAYERS FOR EACH FILLING

fillings and slightly less than this for the looser fillings. Further penetration of the pile was accomplished with only a slight, if any, increase in the applied load. This suggests that the skin friction was almost fully mobilized after a penetration of 1% of the pile diameter.

As expected and shown in the curves of Figure 7.2, as the embedded length of the pile increased, the skin friction which had developed between the pile and the sand also increased.

Figure 7.3 shows the relationship between the average skin friction which was developed along the pile shaft and the piles embedded length. The average skin friction was calculated by dividing the total load applied to the pile by the embedded area (see Table 7.1). The values shown in Figure 7.3 represent the average skin friction which was developed at 1mm pile penetration and the ultimate or maximum values obtained at 12mm pile penetration. The skin friction was found to increase with embedded length of pile at shallow depths approaching a constant value at greater depths. The maximum value of ultimate skin friction for the vibrated sand layers was encountered at approximately twelve pile diameters, while for the notvibrated sand the value of the ultimate skin friction was still increasing at the maximum embedded pile length of 1.75m.

Some of the inconsistencies in the test results presented in this section could have been caused by problems occurring with the testing equipment. During the time when the first filling of the tank was being carried out, a fault was found with the hydraulic cooling system

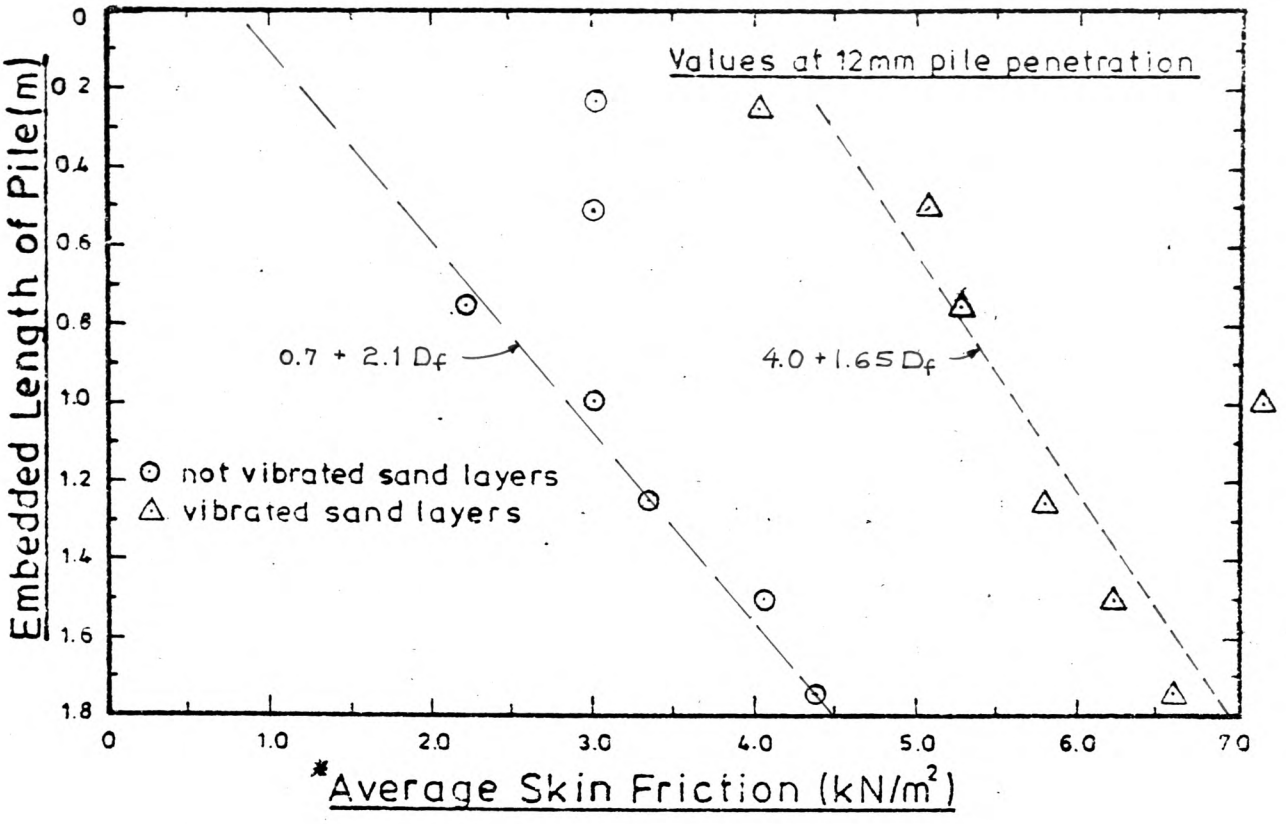

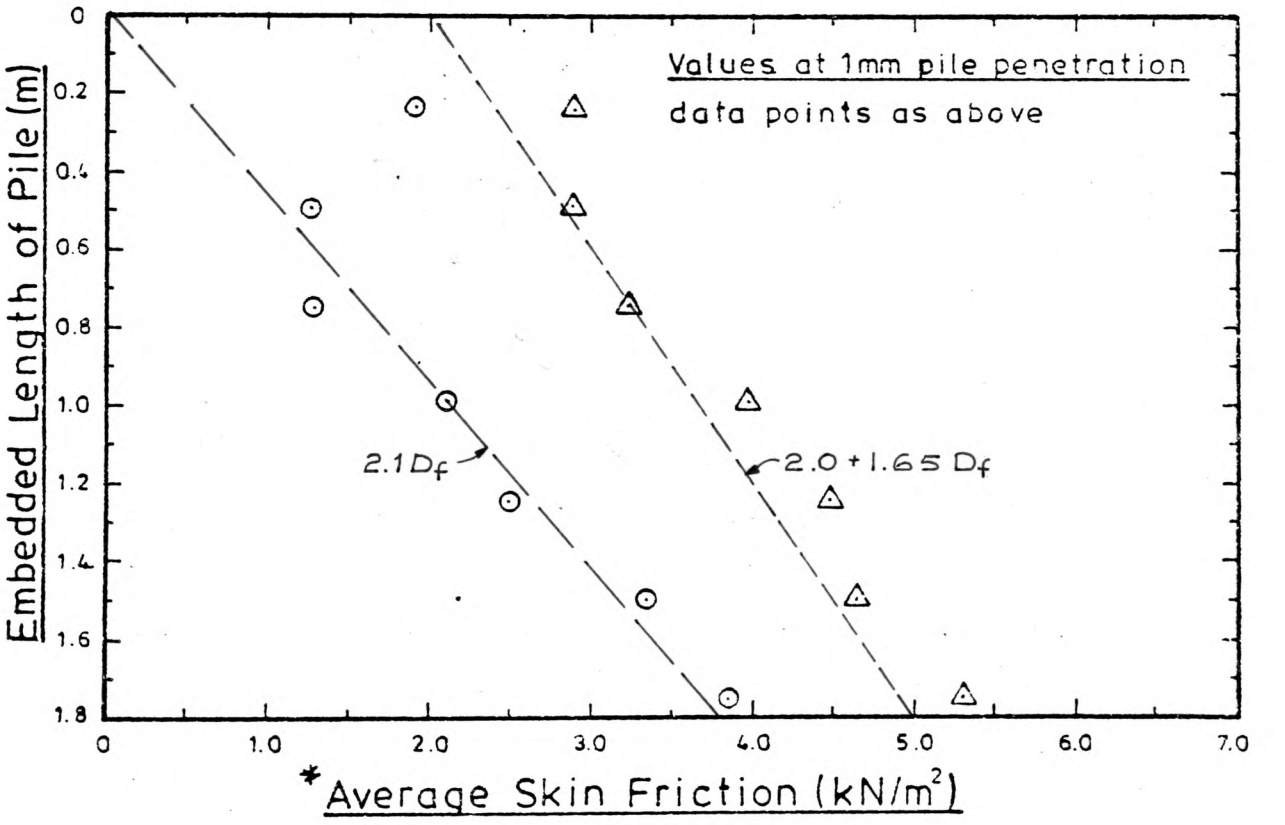

* Average Skin Friction = Total applied load divided by embedded pile area

FIGURE 7.3

AVERAGE SKIN FRICTION VERSUS EMBEDDED LENGTH OF PILE

Applied Load (kN)

Layers		T1		T2		T3		T4		T5		T6		T7	
Pile Pen.(mm)		1mm	12mm	1mm	12mm	1mm	12mm	1mm	12mm	1mm	12mm	1mm	12mm	1mm	12mm
Loading Stage	1st	.23	.32	.71	1.14	.80	1.34	1.16	2.44	1.92	2.51	2.37	3.11	3.17	3.85
	2nd	.28	.39	.33	.67	.94	1.50	1.67	2.65	2.13	2.69	2.61	3.56	3.49	4.43
	Avg.	.26	.36	.52	.91	.87	1.42	1.42	2.55	2.03	2.60	2.49	3.34	3.33	4.14
	3rd	.16	.24	.25	.45	.37	.65	.77	1.10	1.08	1.40	1.80	2.11	2.27	2.40
	4th	.18	.29	.20	.43	.30	.53	.76	1.06	1.16	1.59	1.79	2.28	2.56	3.05
	Avg.	.17	.27	.23	.44	.34	.59	.77	1.08	1.12	1.50	1.80	2.20	2.42	2.73

Average Skin Friction (kN/m^2) *

Layer		T1		T2		T3		T4		T5		T6		T7	
Embedded Pile Area (m^2)		8.95×10^{-1}		1.79×10^{-1}		2.69×10^{-1}		3.58×10^{-1}		4.48×10^{-1}		5.37×10^{-1}		6.27×10^{-1}	
Pile Pen.(mm)		1mm	12mm	1mm	12mm	1mm	12mm	1mm	12mm	1mm	12mm	1mm	12mm	1mm	12mm
Loading Stage	1st	2.57	3.57	3.96	6.37	2.98	4.99	3.24	6.81	4.29	5.61	4.41	5.79	5.05	6.14
	2nd	3.13	4.36	1.84	3.74	3.50	5.58	4.66	7.40	4.76	6.01	4.86	6.63	5.57	7.07
	Avg.	2.90	4.02	2.90	5.08	3.24	5.29	3.96	7.12	4.53	5.81	4.64	6.22	5.31	6.61
	3rd	1.79	2.68	1.40	2.51	1.38	2.42	2.15	3.07	2.41	3.13	3.35	3.93	3.62	3.83
	4th	2.01	3.24	1.12	2.40	1.12	1.97	2.12	2.96	2.59	3.55	3.33	4.24	4.08	4.87
	Avg.	1.90	3.02	1.28	3.02	1.27	2.20	2.13	3.02	2.50	3.35	3.34	4.09	3.86	4.36

* Average skin friction = total applied load divided by embedded pile area

TABLE 7.1

Values of Total Applied Load taken at 1mm and 12mm Pile Penetration

for the M.T.S. pump, which supplies the oil to the Dartec jack. At the start of driving the pile for test T3 the system overheated and shut down. Subsequently, the only force holding the pile in place vertically, was the skin friction between the pile and the sand. This premature development of skin friction and subsequent soil disturbance could have caused the smaller than expected skin resistance which developed during the testing of T3 which followed.

When the driving of the pile for test T4 commenced the pile moved in an upwards rather than downwards direction. This was not noticed until the pile had been withdrawn a distance of 2.82mm. The pile was then stopped, clamped and the hydraulic controls were switched off. When the jack was later turned on an instantaneous movement of 12.74mm of the jack ram occurred driving the pile this distance through the sand. The system was serviced and these problems were eliminated. However, it can be appreciated that the controlled progress of the skin friction development which followed these disturbances would have been adversely affected. This is reflected in the load-penetration curves for these two tests (T3 and T4, first filling).

It should be also mentioned that test layer T4 was the first layer where the smaller vibrating board was employed for vibration of the soil in the vicinity of the pile and wires (see Section 6.6).

7.3.2 Load Distribution along the Pile

The load distributions and stress transfers presented in this section were obtained from a set of computer graphs of load cell load versus pile penetration plotted on the DECsystem-20 Tektronix 4662

flat-bed plotter. A computer program was written which used the calibration data, obtained from the in-situ calibration test, to calculate the individual load cell loads from the recorded strains. For each of the seven tests carried out on each filling of the tank a set of eight curves were plotted corresponding to the eight load cells comprising the pile. A total of 224 curves were plotted for the four fillings of the tank.

From each of these graphs the values of the ultimate or maximum load and the load measured at 1mm pile penetration by each load cell were tabulated. These values were plotted against the load cell depth and are shown in Figures 7.4 through 7.7. These graphs show the distribution of load along the pile for each layer tested in the testing programme.

The curves for the first test layer of each of the four fillings have been omitted because the skin friction developed for these tests was found to be negligable.

Also plotted on the above mentioned graphs are the curves showing the stress transfer developed along the pile. The stress transfer τ has been calculated by dividing the load transferred between two points along the embedded length of the pile by the area of the pile shaft between these two points. The load transferred is equal to p_1, the load measured at the top of the pile segment of length l, minus p_2, the load measured at the bottom of the segment. This gives the value of stress transfer at the midpoint of the segment. Therefore,

$$\tau = (p_1 - p_2)/cl \qquad (7.1)$$

where c = circumference of the pile

The curves showing the average stress transfer developed along the pile at 1mm pile penetration are shown in Figure 7.8. These curves have been compiled by averaging the curves of stress transfer versus depth for the dense fillings (Figures 7.4 and 7.5), and for the loose fillings (Figures 7.6 and 7.7).

Since, the value of the stress transfer at the frictionless cylinder was determined to be zero, the speculated extentions below the limit of the instrumentation have been included in Figure 7.8. This figure suggests that the density of the testing medium had two effects on the stress distribution :

1. the magnitude of the stress transfer was less for the looser material, and

2. the stress transfer developed at a lower elevation in the looser sand stratum.

The depths at which the stress transfer begins to develop and reaches its peak value are shown in Table 7.2. Also included in this table are the values of the peak stress transfer developed during the testing of layers T3 through T7.

7.3.3 Sand Displacements

As discussed in section 4.3.1 the candidate has employed a system using 25mm square aluminium plates (Terra Plates) linked to displacement transducers for monitoring the sand displacement at

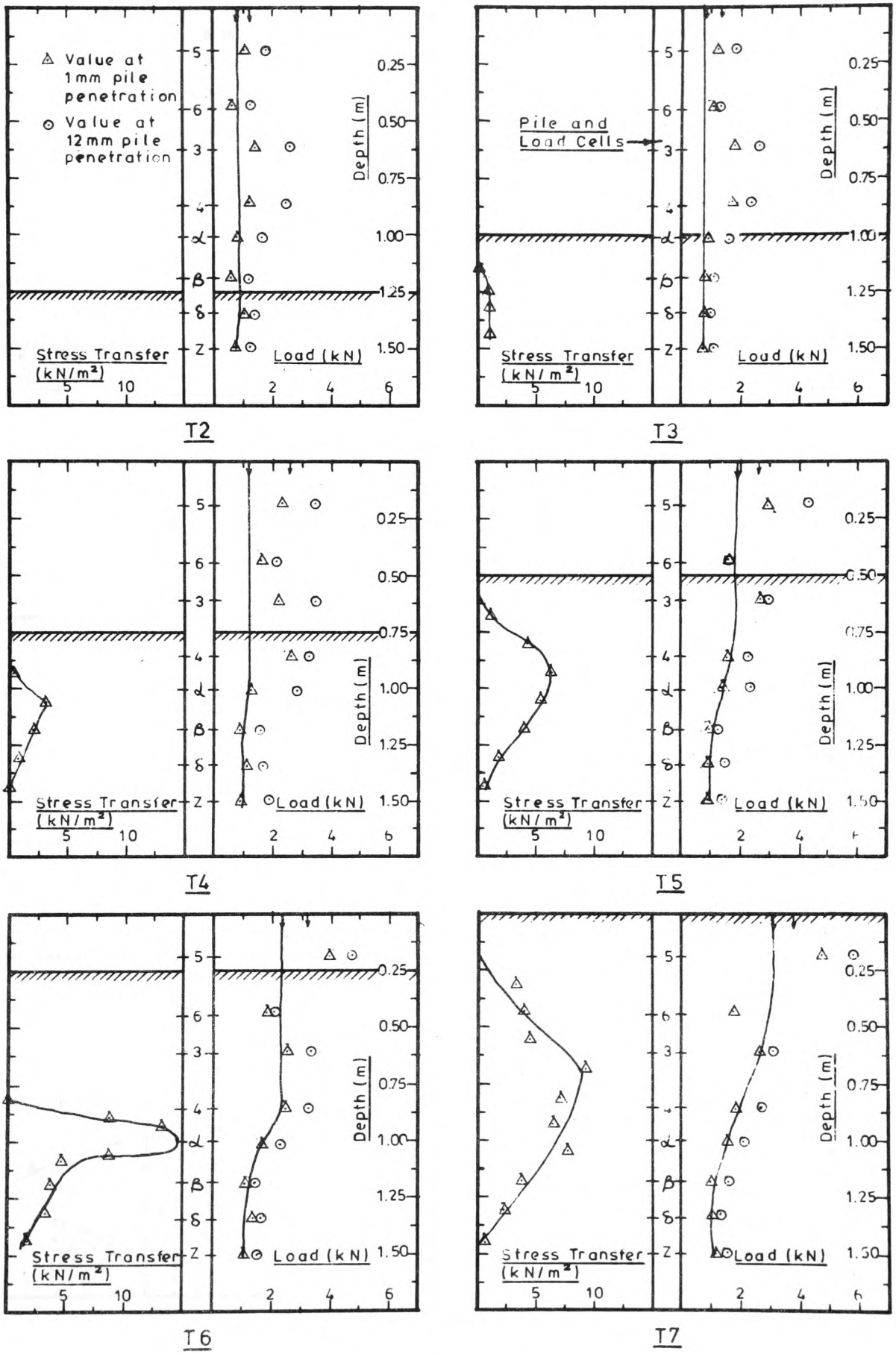

FIGURE 7.4

STRESS AND LOAD DISTRIBUTION CURVES-1st FILLING

VIBRATED

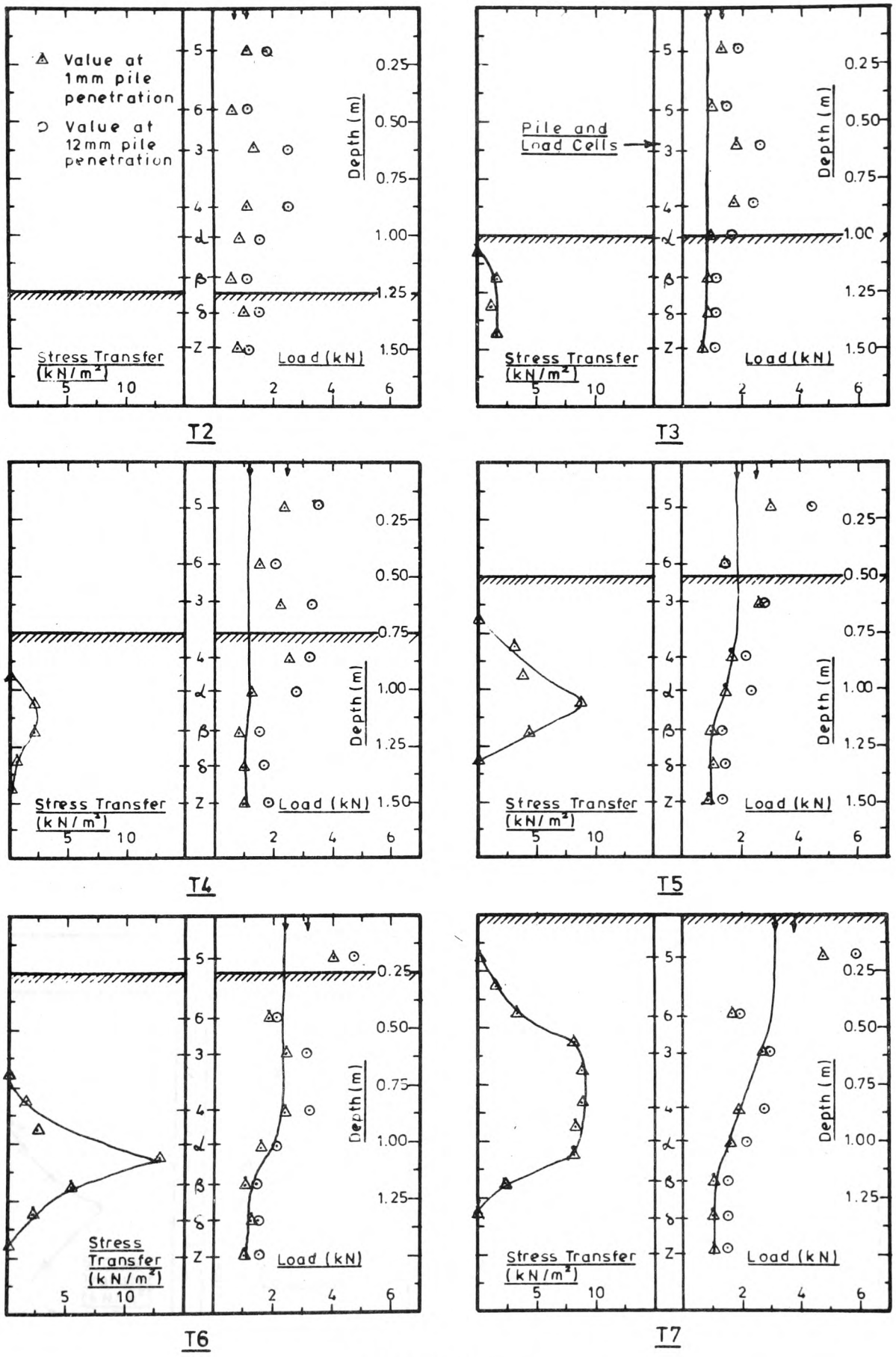

FIGURE 7.5

STRESS AND LOAD DISTRIBUTION CURVES-2nd FILLING

VIBRATED

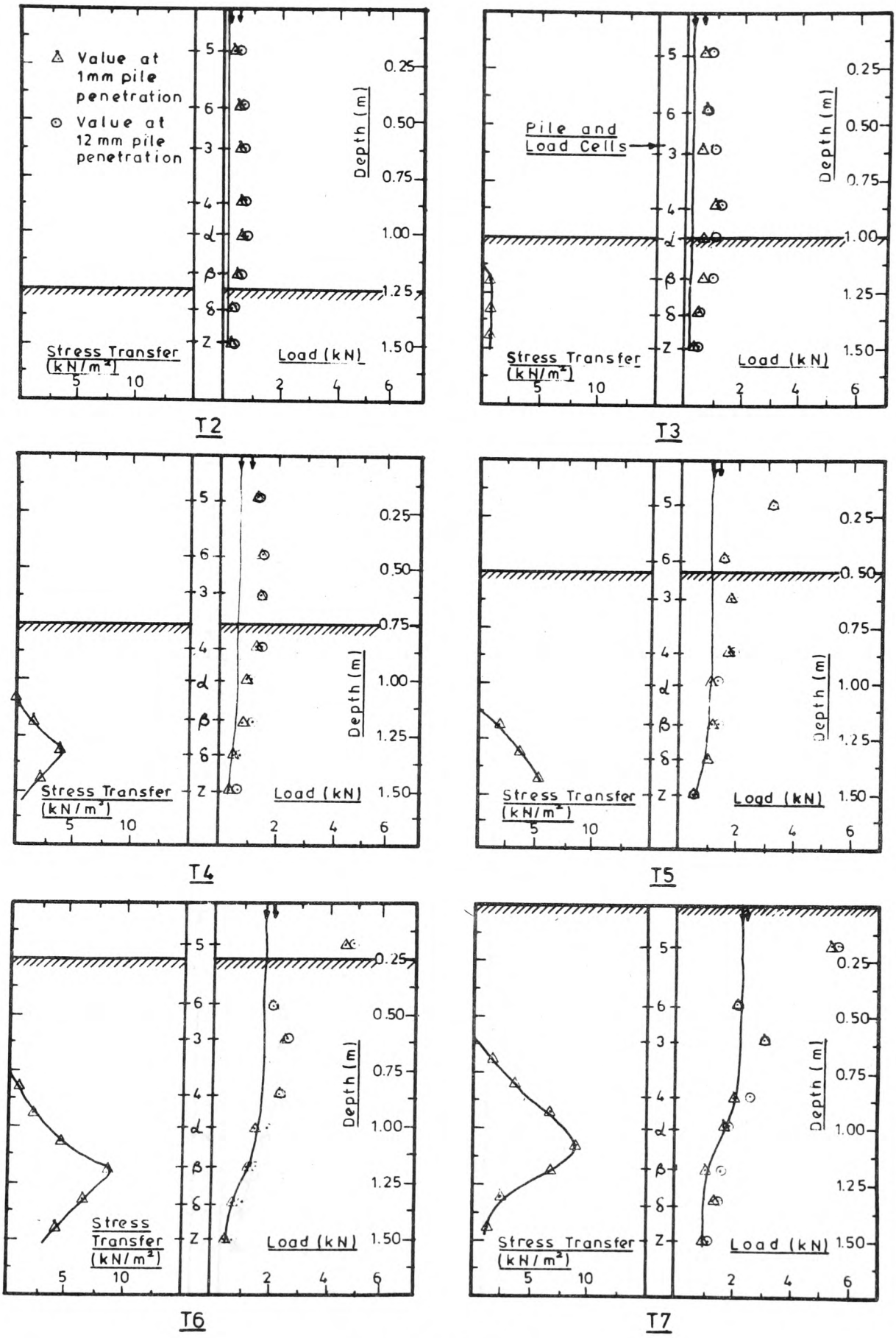

FIGURE 7.6

STRESS AND LOAD DISTRIBUTION CURVES-3rd FILLING

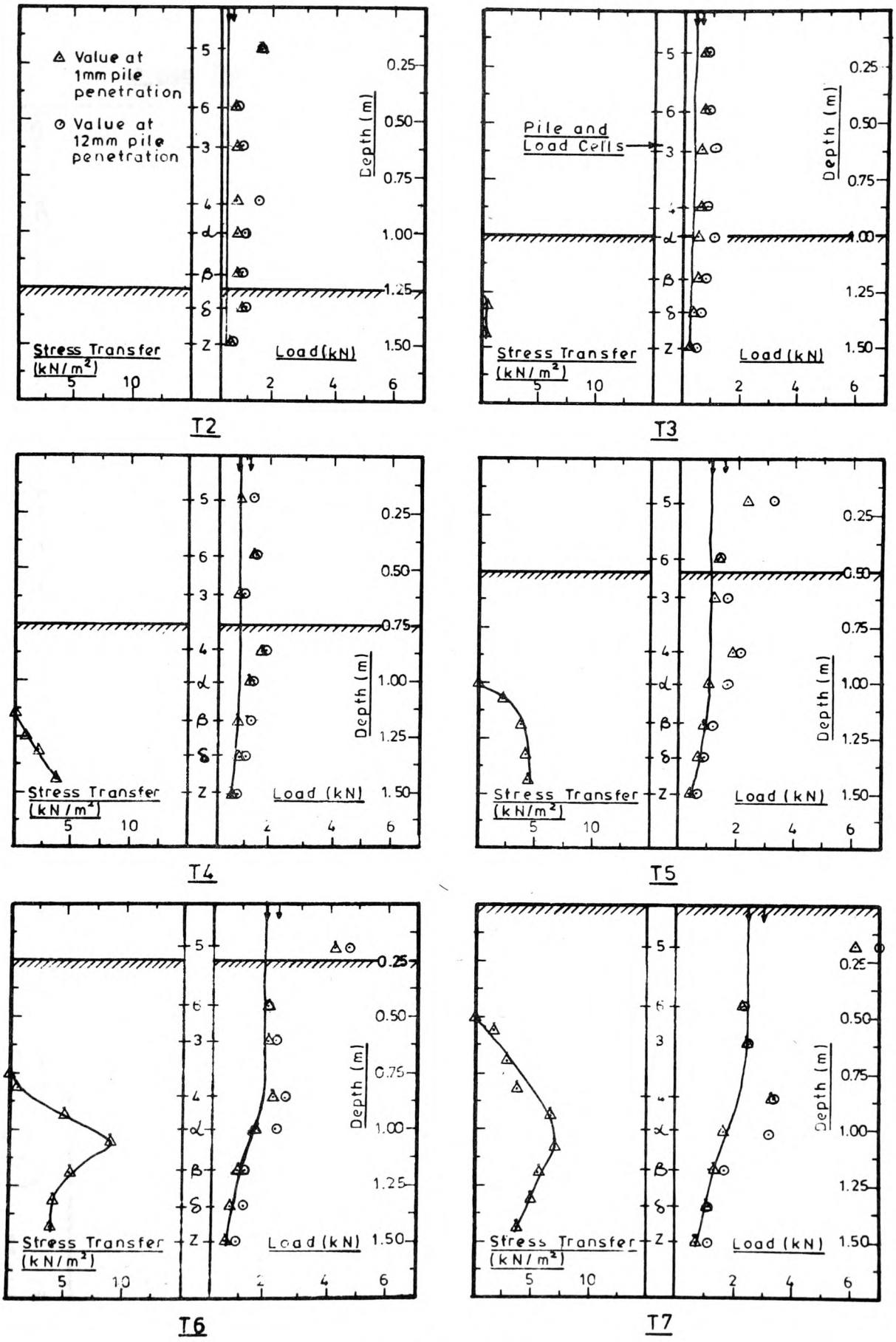

FIGURE 7.7

STRESS AND LOAD DISTRIBUTION CURVES-4th FILLING

NOTVIBRATED

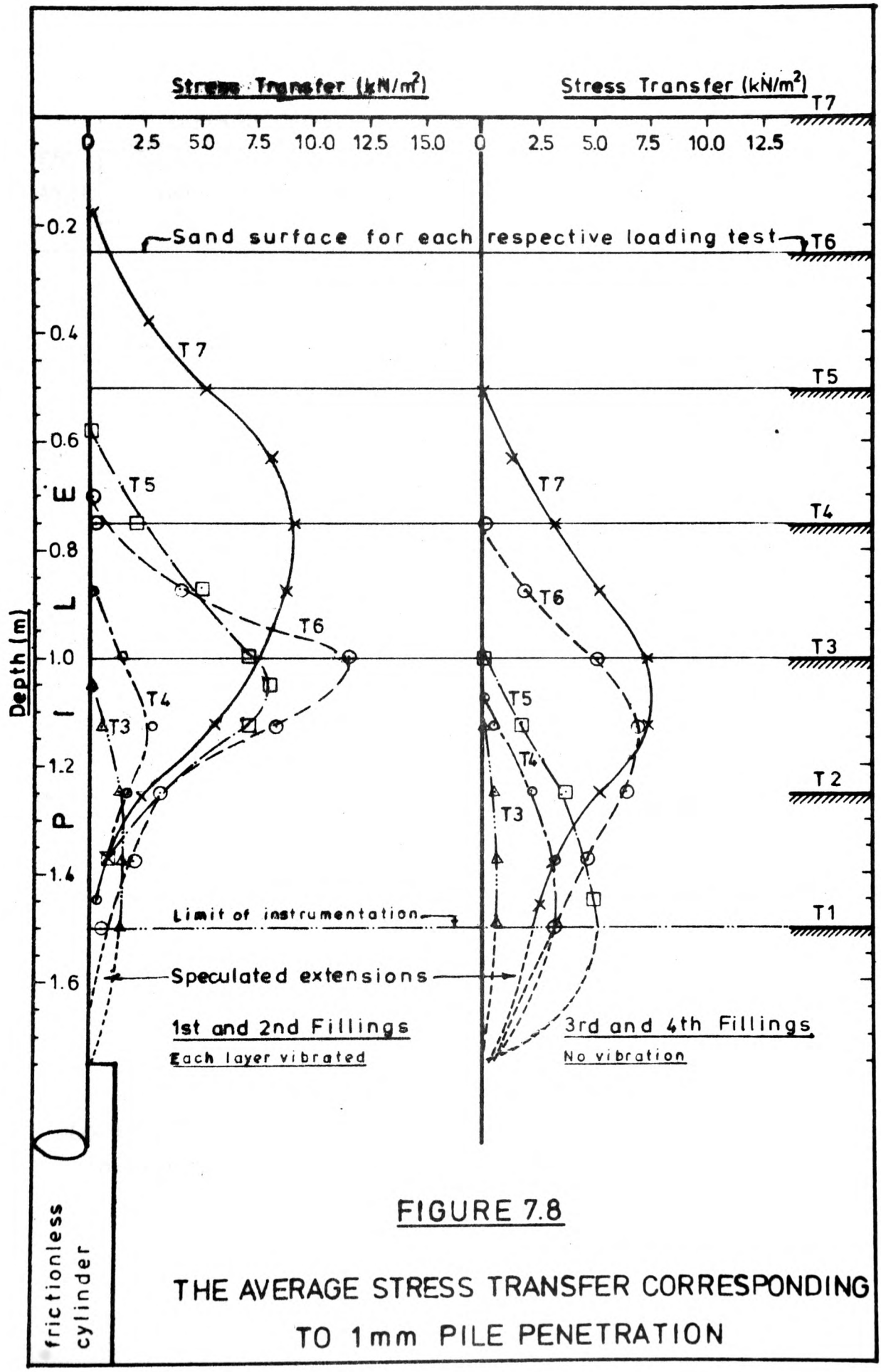

FIGURE 7.8

THE AVERAGE STRESS TRANSFER CORRESPONDING TO 1mm PILE PENETRATION

TEST LAYER	Depth at which Stress Transfer begins		Depth at which Stress Transfer peaks		Max.Stress Transfer (kN/m^2)
	(m)	No. of pile dia.	(m)	No. of pile dia.	
	Average of 1st and 2nd Fillings (vibrated)				
T3	0.05	0.4	0.45	3.9	1.4
T4	0.13	1.1	0.38	3.3	2.7
T5	0.08	0.7	0.56	4.9	8.0
T6	0.46	4.0	0.76	6.7	11.5
T7	0.17	1.5	0.76	6.7	9.0
Average		1.5D		5.1D	
	Average of 3rd and 4th Fillings (notvibrated)				
T3	0.12	1.1	0.50	4.4	0.7
T4	0.32	2.8	0.75	6.6	3.8
T5	0.50	4.4	1.00	8.8	5.2
T6	0.50	4.4	0.90	7.9	7.0
T7	0.50	4.4	1.07	9.4	7.7
Average		3.4D		7.4D	

TABLE 7.2

LOCATION AND MAXIMUM VALUE OF STRESS TRANSFER DEVELOPMENT ALONG THE PILE DURING DRIVING

various depths.

One of the main considerations in deciding on the locations for the Terra Plates was, as mentioned earlier, to avoid creating a reinforced earth caused by a multitude of instrumentation. The candidate designed a configuration for the installation of the Terra Plates which positioned them in two sets of diametrically opposite spirals surrounding the pile. One spiral set starts at a depth of 1.5m below the final sand surface and a distance of one pile diameter from the piles central axis. The Terra Plates in this set were located so that as the depth below the final sand surface decreased the radial distance from the piles central axis increased. The final Terra Plates were positioned a distance of 3.5 pile diameters from the central axis. The other spiral set started at a distance of 3.5 pile diameters from the central axis, at a depth of 1.25m below the final sand surface, and finished at a distance of one pile diameter from the central axis. Figure 7.9 shows the location of the Terra Plates in both plan and elevation.

Following this procedure, all the Terra Plates except the top two were used to measure sand displacements for more than one pile driving test. Each time a Terra Plate was used, it was located at a different depth from the surface of the sand, though its radial distance remained the same.

Each Terra Plate had a counterpart diametrically opposite and at the same depth and radial distance from the pile. It was the average of these two Terra Plate displacements which was used in the analysis.

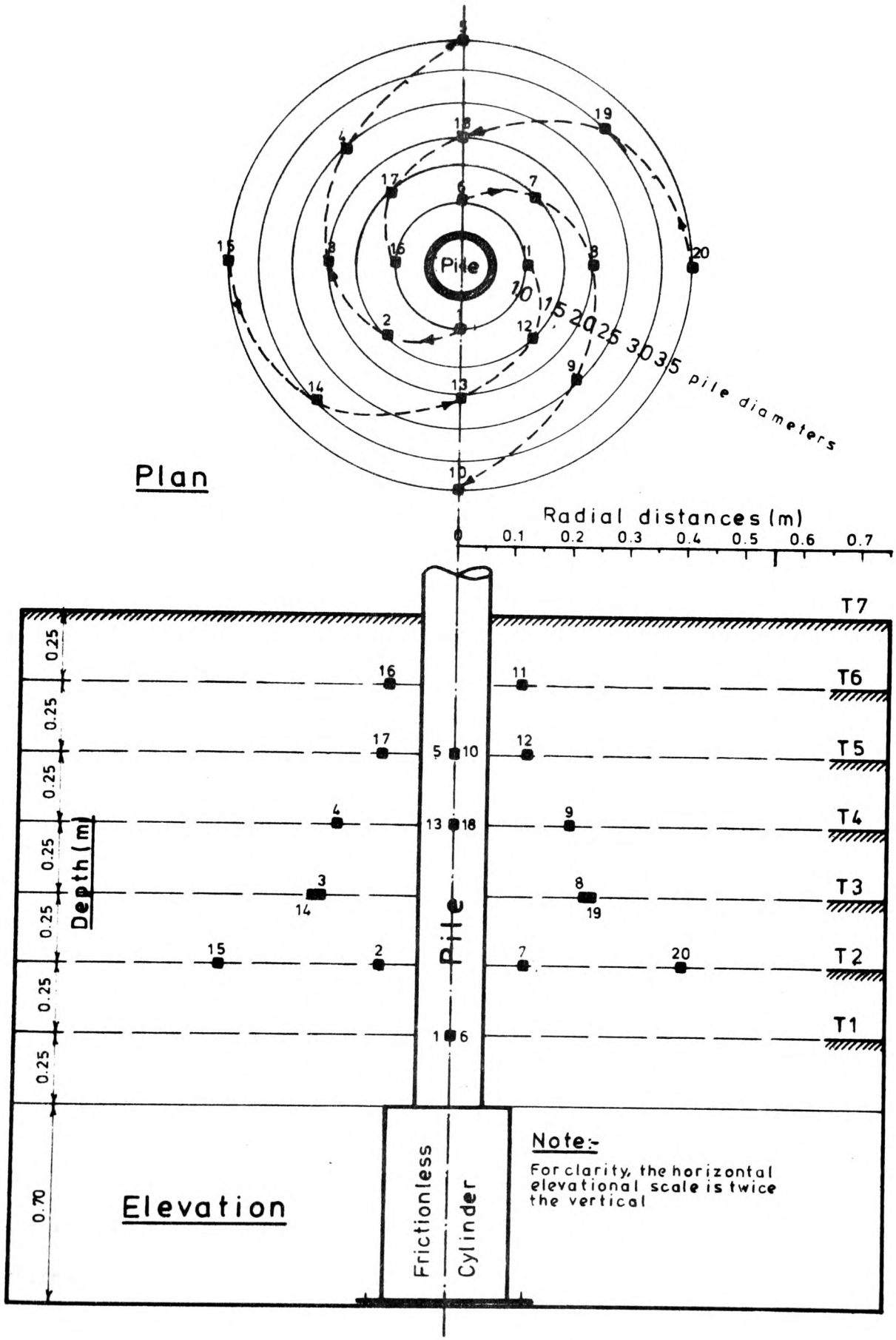

FIGURE 7.9

LOCATION OF TERRA PLATES

The computer programs mentioned previously processed, compiled and plotted the soil displacements of the diametrically opposite Terra Plates as well as the average of the two against the pile penetration. Therefore, although the average displacements were used for the analysis, the actual displacements were also available to check any anomalies.

The average vertical sand displacements have been compiled for varying depths and radial distances from the pile. The mean values for the two dense and two loose fillings of the tank are shown in Table 7.3. The soil displacements presented are those which were measured corresponding to 1mm, 6mm, and 12mm pile penetration.

From this data the average vertical sand displacements during pile driving have been plotted at various depths for the dense and loose fillings of the tank. These are shown in Figures 7.10 and 7.11. These figures illustrate the vertical sand displacements at six different depths caused by pile penetrations of 1mm, 6mm, and 12mm respectively. To show how the vertical sand displacement varied with depth, graphs of vertical sand displacement versus depth have been plotted on Figures 7.12 and 7.13. The sand displacements corresponding to pile penetrations of 1mm, 6mm, and 12mm have been plotted on these graphs.

As expected, the graphs of Figures 7.12 and 7.13 show that the magnitude of the vertical soil displacements decreases with depth. This was more pronounced than the values obtained from the loose fillings of the tank.

Fillings	T.P. Depth (m) ↓ / Pile Pen. (mm) →	1.0 Dia.			1.5 Dia.			2.0 Dia.			2.5 Dia.			3.0 Dia.			3.5 Dia.		
		1mm	6mm	12mm	1mm	6mm	12mm	1mm	6mm	12mm	1mm	6mm	12mm	1mm	6mm	12mm	1mm	6mm	12mm
1&2	.25m	.010	.052	.073	0	.025	.041	.002	.012	.021	.006	.018	.028	0	.008	.023	0	.001	.004
3&4		.050	.122	.164	.046	.100	.137	.019	.052	.072	.002	.011	.023	.004	.015	.022	.002	.015	.038
1&2	.50m	.009	.043	.068	.005	.025	.038	.008	.025	.050	.001	.005	.014	.008	.020	.036	.001	.004	.012
3&4		.040	.094	.134	.042	.088	.111	.030	.071	.094	.022	.046	.065	.001	.003	.020	.004	.015	.025
1&2	.75m	.014	.060	.079	.013	.038	.056	.001	.006	.012	0	.001	.002	0	.002	.013	.007	.020	.030
3&4		.041	.088	.112	.008	.037	.067	.022	.046	.069	.014	.031	.050	.005	.020	.036	.001	.002	.008
1&2	1.00m	.019	.043	.065	.008	.018	.033	0	0	.008				0	0	.008	0	.003	.007
3&4		.011	.045	.071	.017	.044	.068	.007	.018	.022				.005	.007	.014	.006	.015	.026
1&2	1.25m	.009	.033	.055	.004	.012	.030										.001	.001	.011
3&4		.011	.047	.061	.019	.045	.066										.004	.011	.016
1&2	1.50m	.005	.023	.041															
3&4		.005	.019	.032															

TABLE 7.3

COMPOSITE AVERAGE TERRA PLATE DISPLACEMENTS FOR VIBRATED & UNVIBRATED SAND LAYERS AT VARIOUS PILE DIAMETERS FROM CENTRAL AXIS OF THE PILE

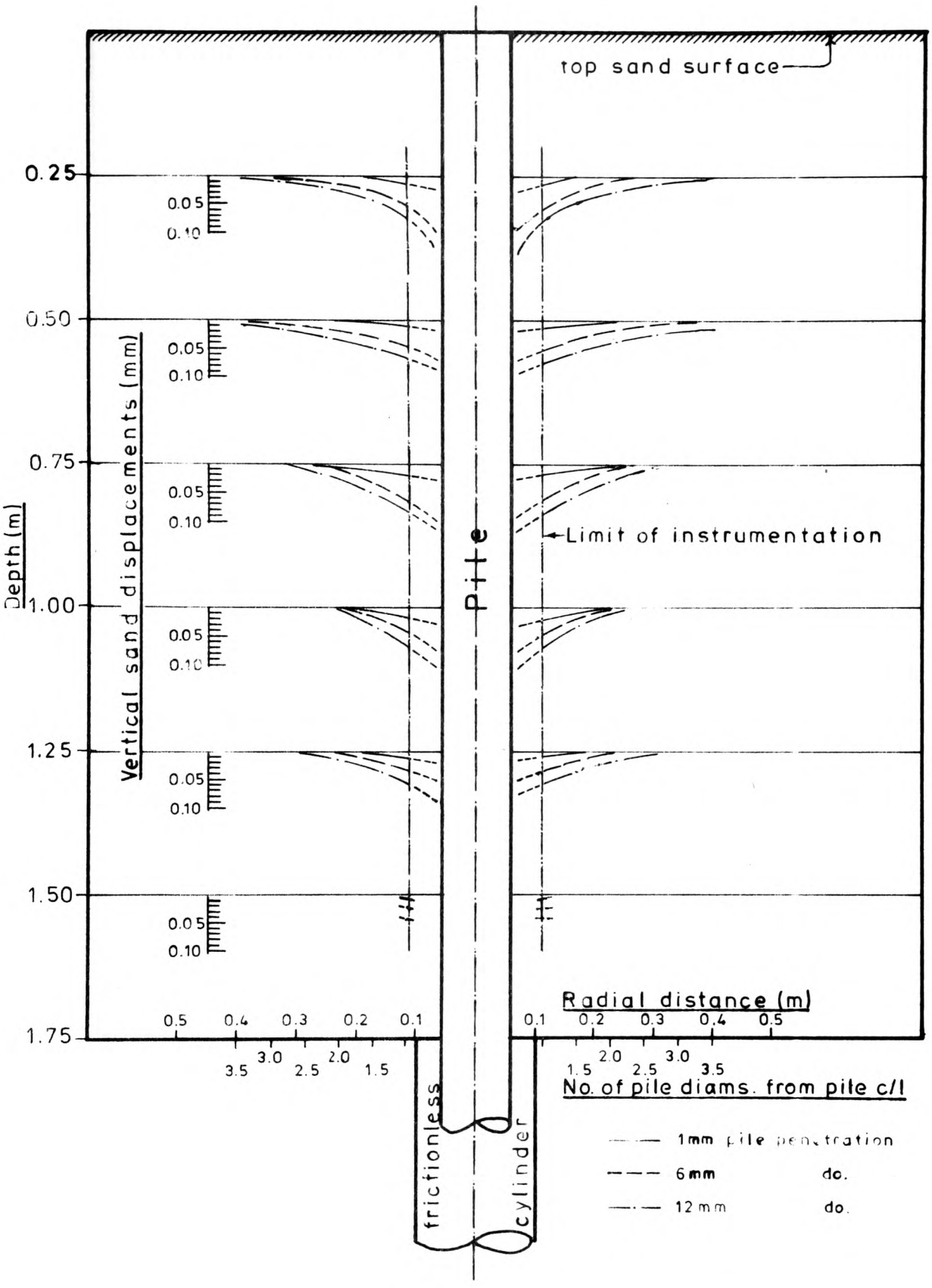

FIGURE 7.10

AVERAGE VERTICAL SAND DISPLACEMENTS OF THE 1st AND 2nd FILLINGS (VIBRATED SAND) AT VARIOUS DEPTHS COMPILED FROM TERRA PLATE DISPLACEMENTS

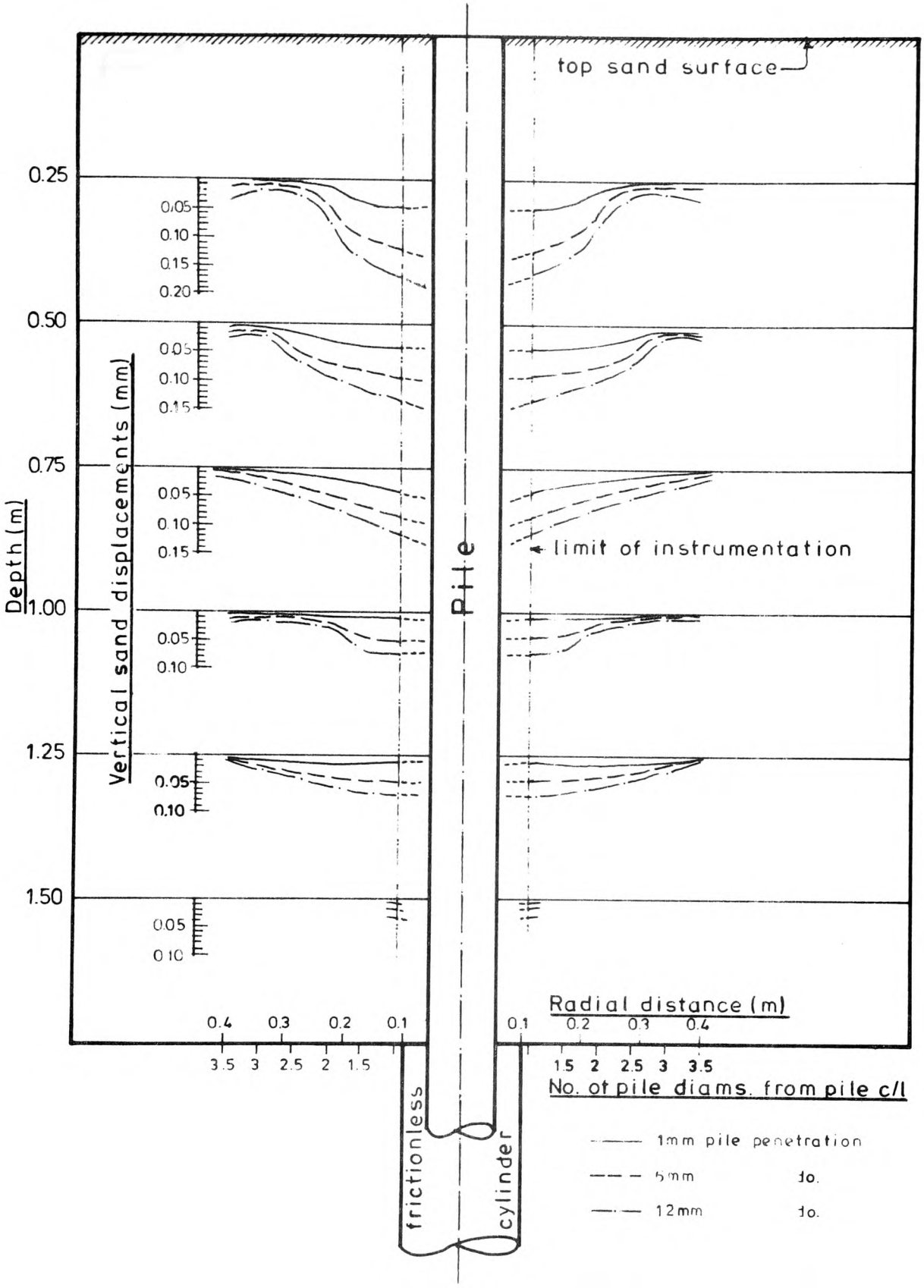

FIGURE 7.11

AVERAGE VERTICAL SAND DISPLACEMENTS OF THE 3rd AND 4th FILLINGS (NOTVIB. SAND) AT VARIOUS DEPTHS COMPILED FROM TERRA PLATE DISPLACEMENTS

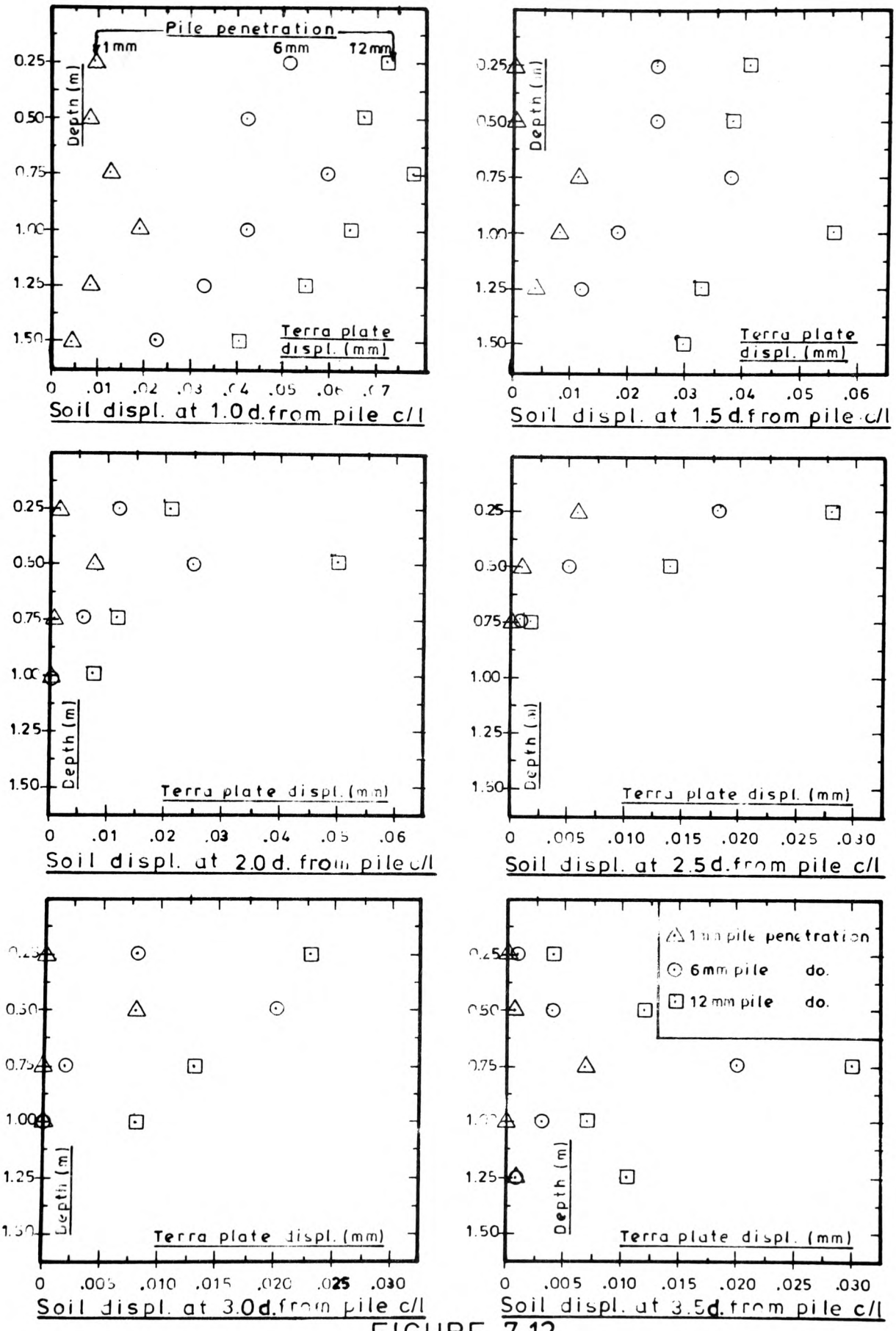

FIGURE 7.12

AVERAGE VERTICAL SAND DISPLACEMENTS VERSUS DEPTH (VIBRATED SAND)

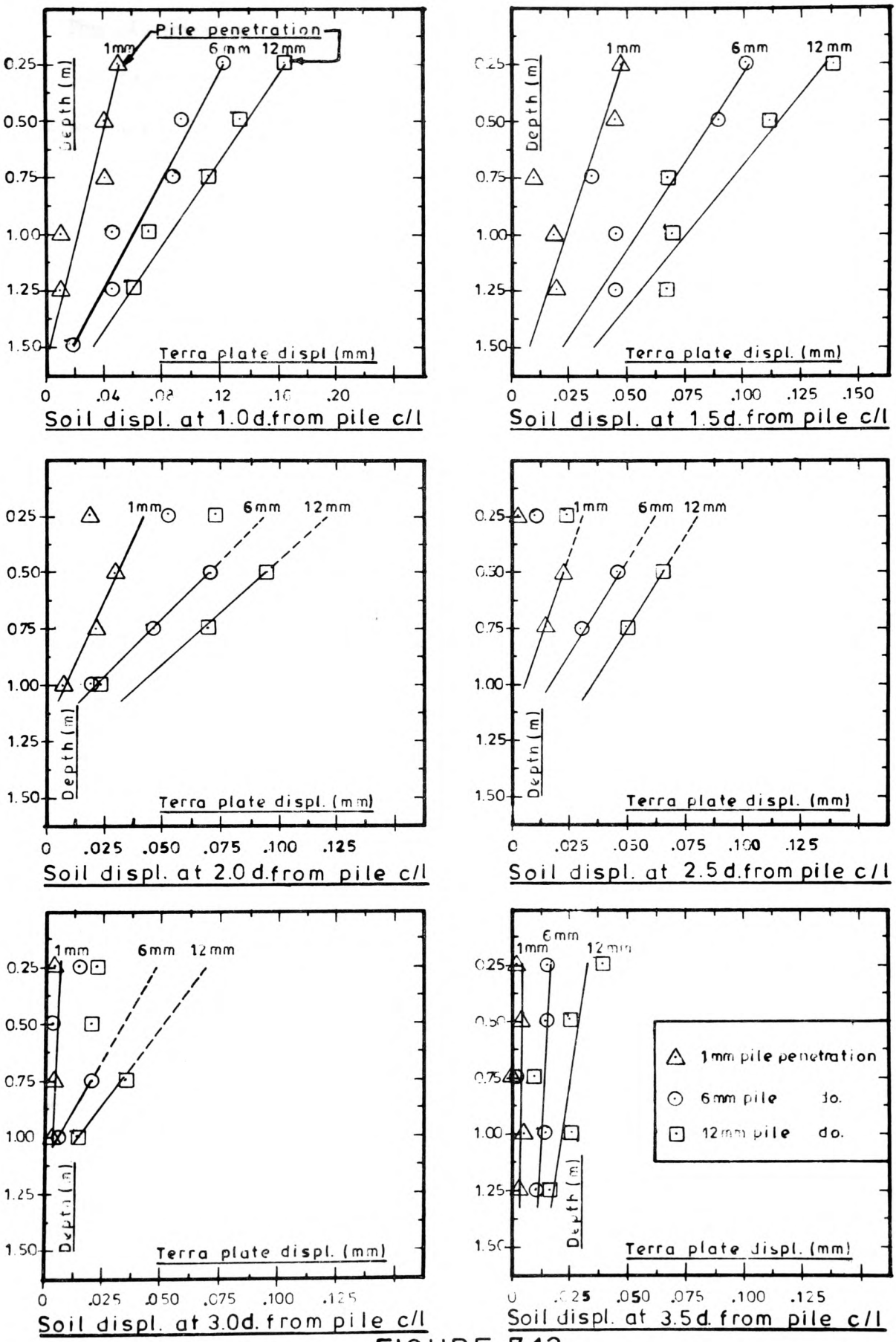

FIGURE 7.13

AVERAGE VERTICAL SAND DISPLACEMENTS VERSUS DEPTH (NOTVIB. SAND)

The observed soil displacements measured at 0.25m below the final soil surface were found to be smaller than expected since these were in some cases (see Figures 7.12 and 7.13) less than the values at a depth of 0.50m. A possible explanation for this is that in the case of the displacements at this depth, the Terra Plate was being used for the first time in that particular testing sequence, and any 'slack' in the Terra Plate - wire-transducer system would have been taken up at this time. Also and possibly more important was the fact that the soil at this depth had less overburden pressure exerted on it than at any other Terra Plate depth. Thus, less vertical force was acting on the sand causing it to move downward as the soil below it moved downward as well, due to the friction which was exerted on the sand by pile driving. It will, however, be noted from Figure 7.13 that this phenomenon was experienced at a radial distance greater than 1.5 pile diameters from the central axis of the pile. At distances closer to the pile a seemingly linear decrease of sand displacement with depth was observed.

From the data presented in this section on vertical sand displacement due to pile driving, the following observations can be made :

1. the magnitude of the vertical soil displacement decreases with depth and radial distance from the pile.

2. The magnitudes of the vertical soil displacements were larger for the pile driving tests carried out in the looser sand medium.

3. The maximum value of the soil displacement measured was 0.16mm.

The object of this exercise was to obtain the largest amount of data in the time available while causing the least possible disturbance to the soil with the necessary instrumentation. In the candidates opinion this has been achieved. However, it must be remembered that the data presented here is a compilation of seven pile driving tests for each filling of the sand tank. Therefore, the results of this exercise should only be accepted and used in the light of this. The candidates intention was to establish the trends and orders of magnitude of the sand displacement.

A more extensive programme will have to be undertaken to form a better understanding of how a granular medium moves during pile penetration and how this movement affects the piles behaviour under load. This should include the measurement of horizontal as well as vertical soil displacements.

7.3.4 Sand Density

As discussed in section 3.6 the relative uniformity of the density of the sand was monitored using the Mini-Mackintosh Penetration Probe after the placement of each sand layer and by carrying out a full size Mackintosh Prospector Probe penetration test, on the entire depth of sand, at the completion of testing. For the two denser fillings of the tank a Mini-Mackintosh (Mini-Mac) test was carried out on each layer before and after compaction.

Figures 7.14 to 7.17 show the results of the 'Mini-Mac' tests for each of the seven test layers of the four fillings of the tank. For each 'Mini-Mac' test the probe was driven by the impact of the drop of the falling weight (29 grams) a total distance of 0.5m or until the resistance to penetration was such that more than 100 blows were needed to drive the probe 10mm.

By driving the probe to a depth of 0.5m, the penetration resistances of the last two 0.25m thick layers of sand were measured. Plotted on the graphs of Figures 7.14 to 7.15 are the results of the 'Mini-Mac' test before and after vibration of the sand (for the two dense fillings of the tank). These figures illustrate the increase in penetration resistance (and thus density) caused by the surface vibration.

In the graphs of Figures 7.14 to 7.17 the interface between the last two layers poured can be identified by the point on the curves where there is a marked change in slope. This suggests that the top portion of each layer is in a denser state than the lower region. This would be expected to be the case with compaction by surface vibration.

The graphs of Figures 7.14 and 7.17 also show the larger penetration resistance for the first and second fillings of the tank. This indicates the extent of compaction created by vibrating the sand layers. This fact is also illustrated in Figure 7.18 which is the results of the full-size Mackintosh Prospector Probe test for three fillings of the tank. Unfortunately, the results of a full-size Mackintosh Probe test for the third filling, which is needed to confirm the results of the fourth filling, are not available. The

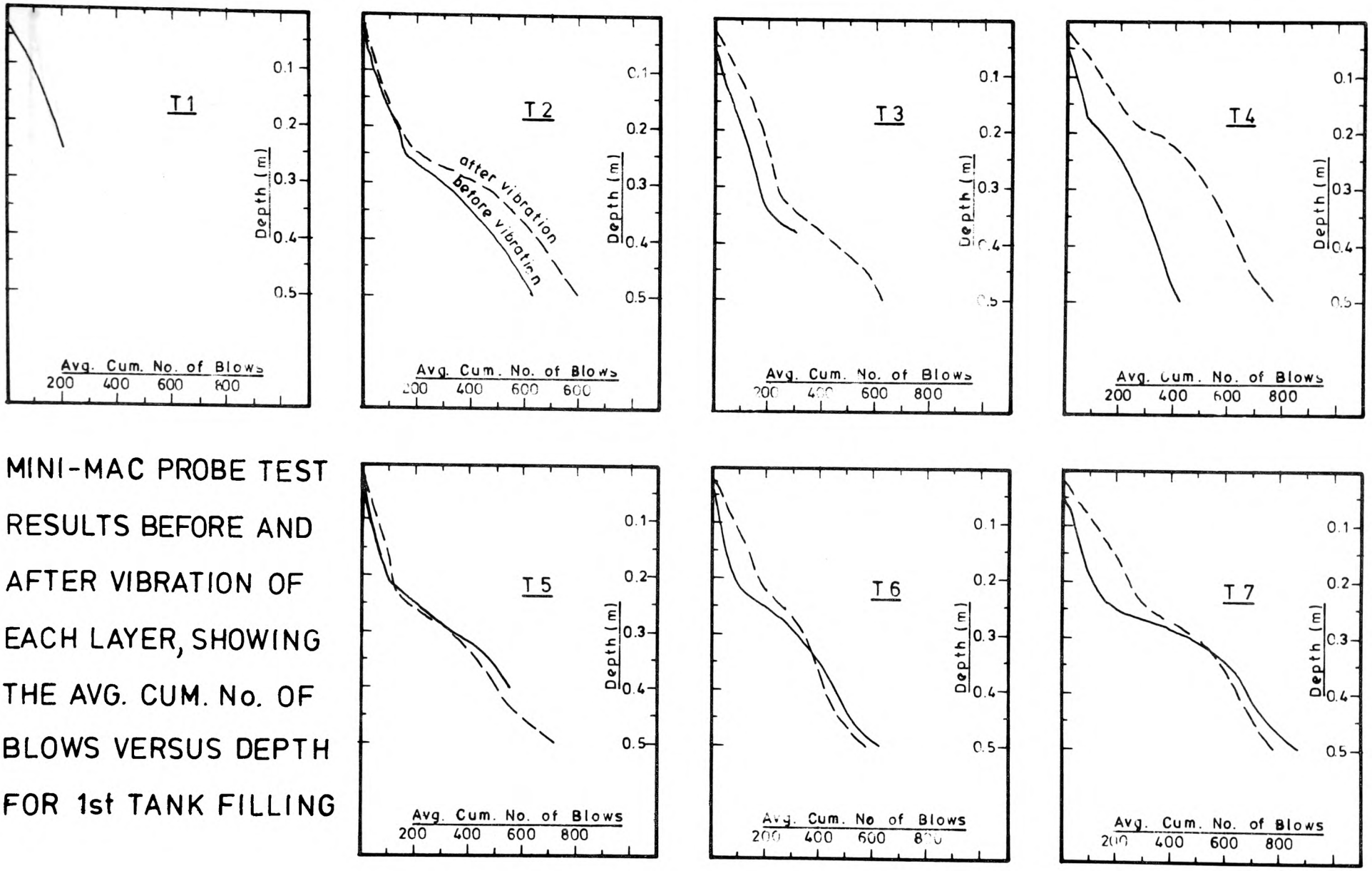

FIGURE 7.14

MINI-MAC PROBE TEST RESULTS BEFORE AND AFTER VIBRATION OF EACH LAYER, SHOWING THE AVG. CUM. No. OF BLOWS VERSUS DEPTH FOR 1st TANK FILLING

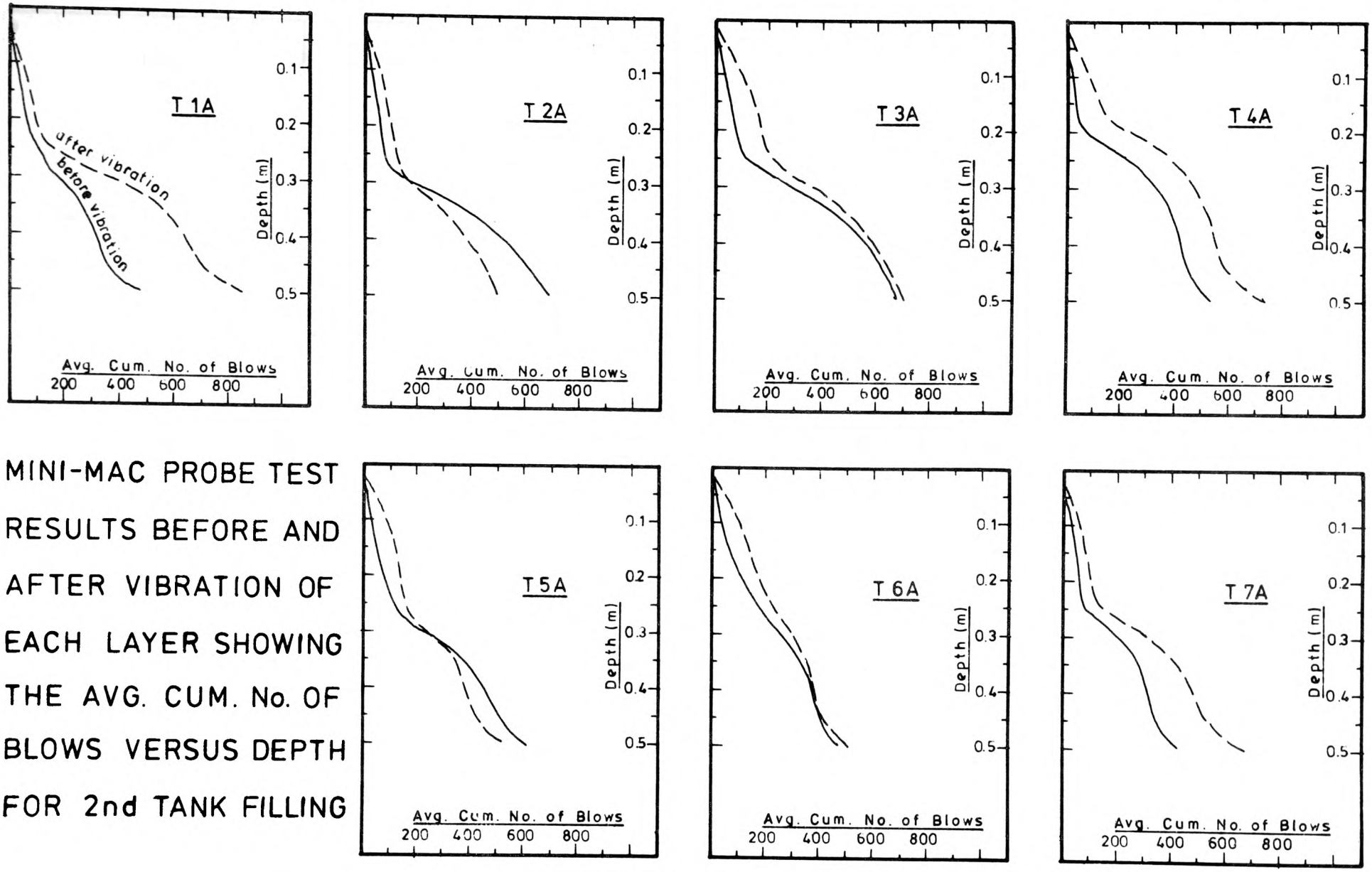

FIGURE 7.15

MINI-MAC PROBE TEST RESULTS BEFORE AND AFTER VIBRATION OF EACH LAYER SHOWING THE AVG. CUM. No. OF BLOWS VERSUS DEPTH FOR 2nd TANK FILLING

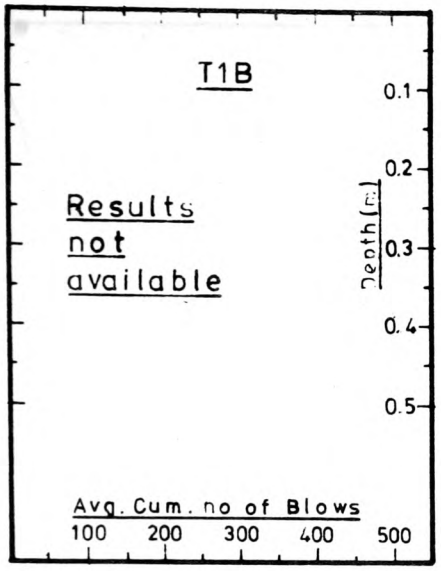

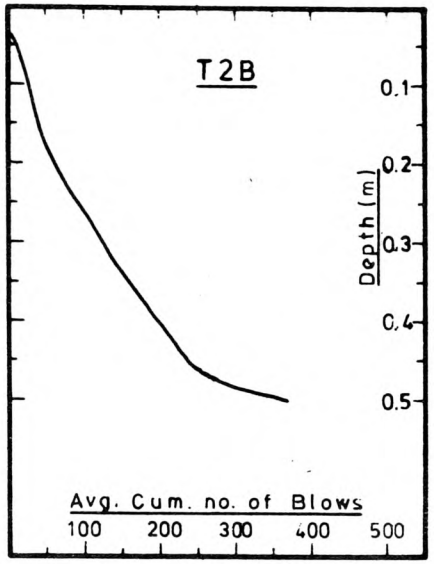

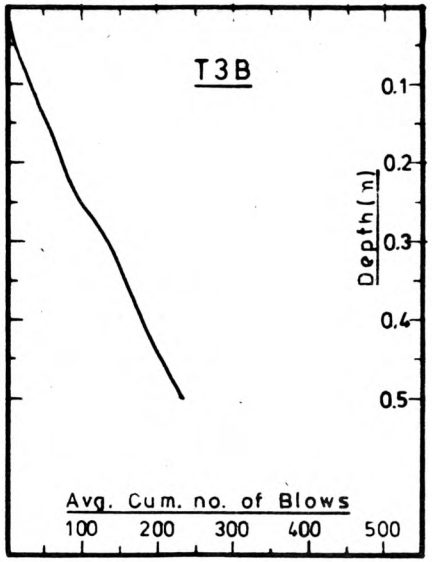

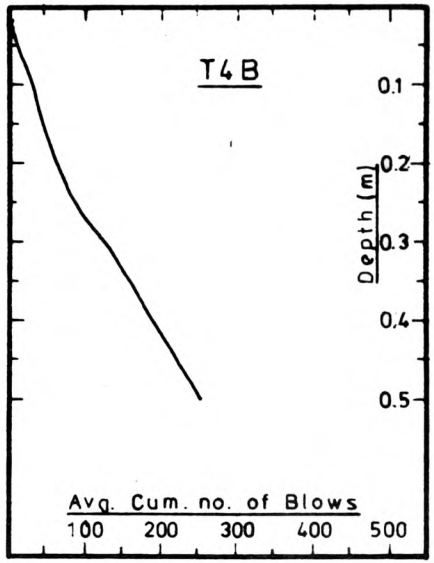

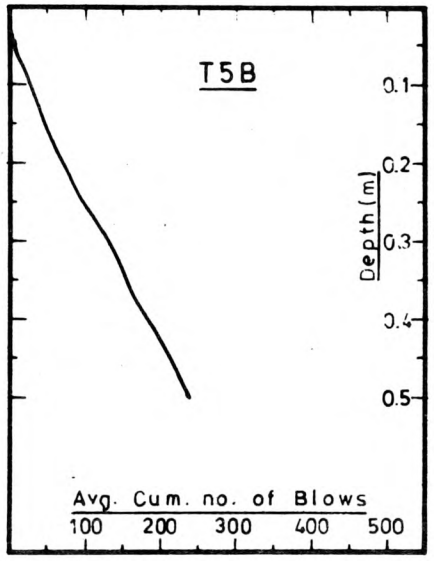

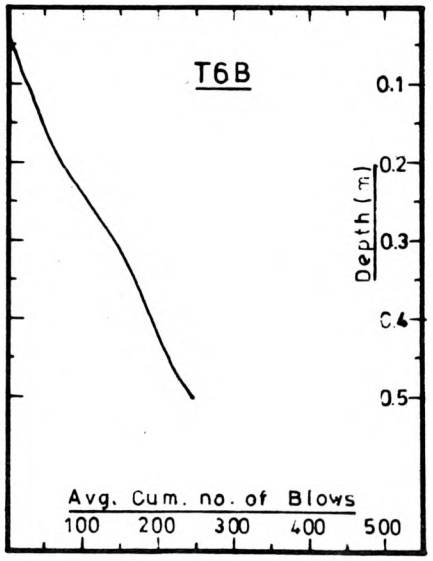

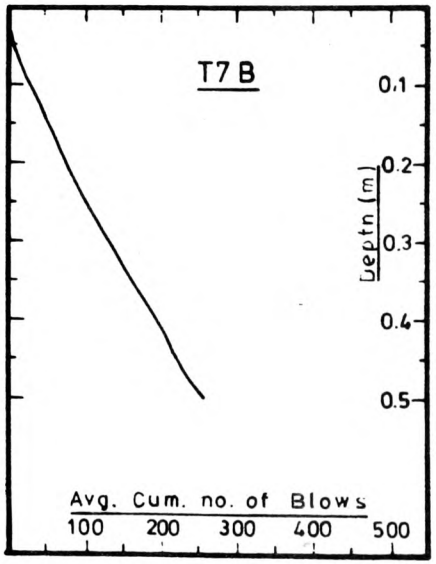

FIGURE 7.16

MINI-MAC PROBE RESULTS FOR EACH LAYER OF THE THIRD FILLING OF THE TANK SHOWING THE AVERAGE CUMULATIVE NUMBER OF BLOWS VERSUS DEPTH

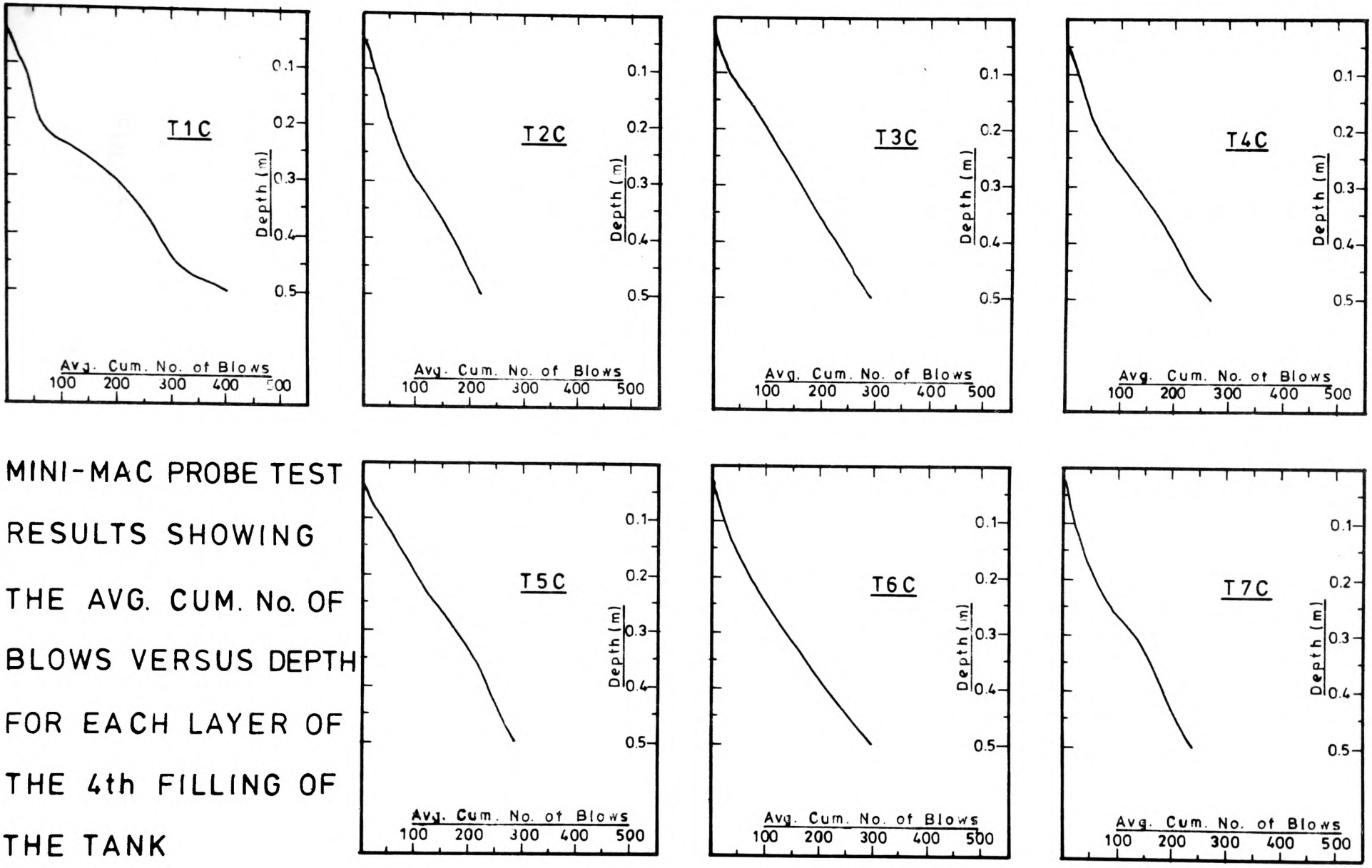

FIGURE 7.17

MINI-MAC PROBE TEST RESULTS SHOWING THE AVG. CUM. No. OF BLOWS VERSUS DEPTH FOR EACH LAYER OF THE 4th FILLING OF THE TANK

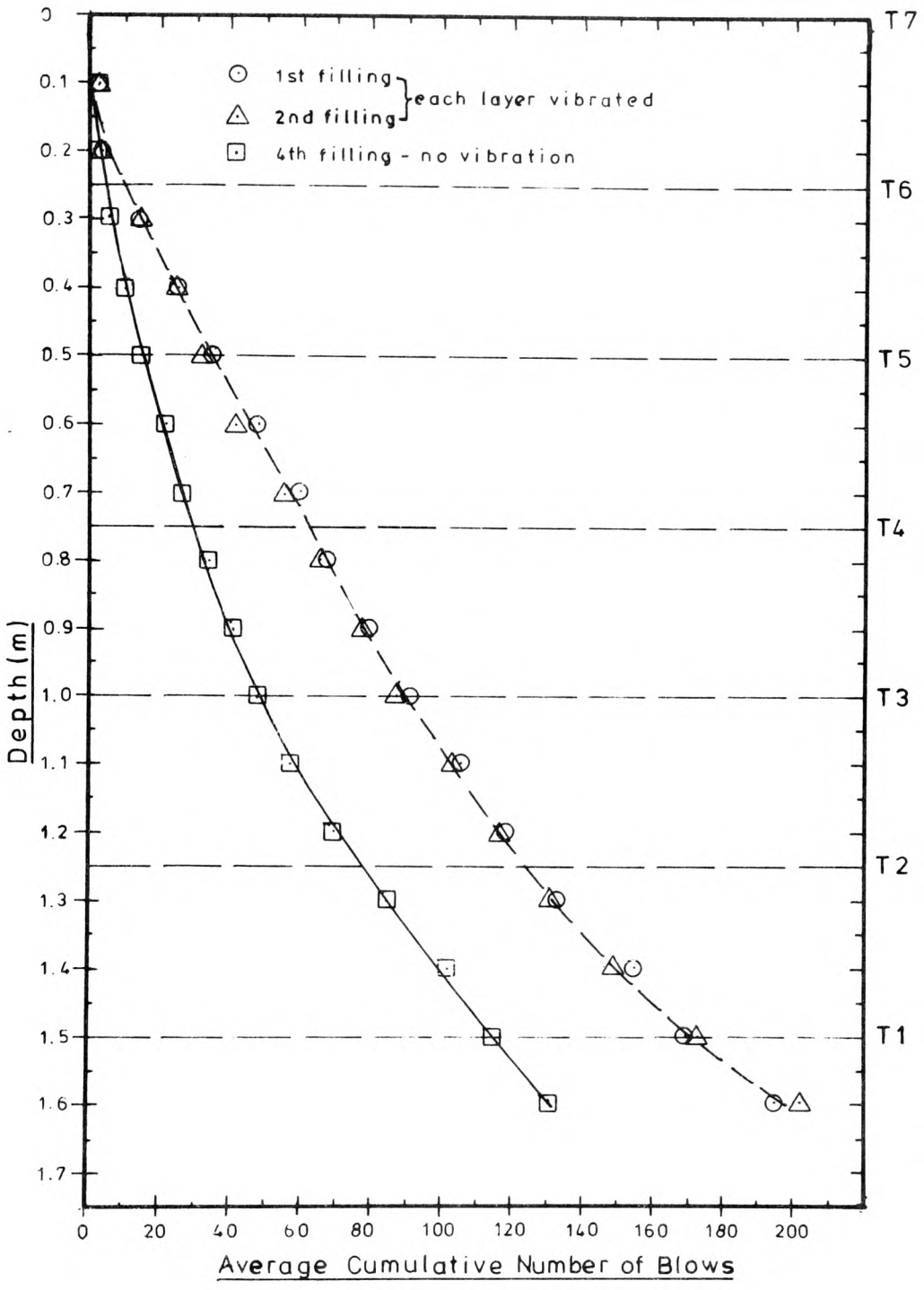

FIGURE 7.18

FULL-SIZE MACKINTOSH PROSPECTOR PROBE TEST RESULTS

results presented in Figure 7.18 do however, show the increase in penetration resistance of the entire depth of sand caused by the surface vibration of each layer.

The purpose of carrying out these Mackintosh Probe tests was to help identify the possible explanation for any anomalies of the test results.

As discussed in section 3.6, density tins (see Figure 3.4) were placed in the sand tank during the filling process. After the sand had been removed from the tank (from the bottom via the Redler Conveyor) the tins were left suspended from the datum frame by the monofilament fishing lines. These tins were carefully retrieved and the density of the sand in each tin was determined.

The procedure for calculating the density of the sand in each tin was :

1. with the straight edge of a spatula the sand was carefully levelled off to the top of the tin,

2. the mass of the sand in the tin was determined, and

3. the volume of the tin was ascertained by filling the tin with water from a graduated pipette.

The density of the sand was calulated from its mass and volume and plotted against the depth at which the tin was located in the testing tank. The results of this are shown in Figure 7.19 and 7.20.

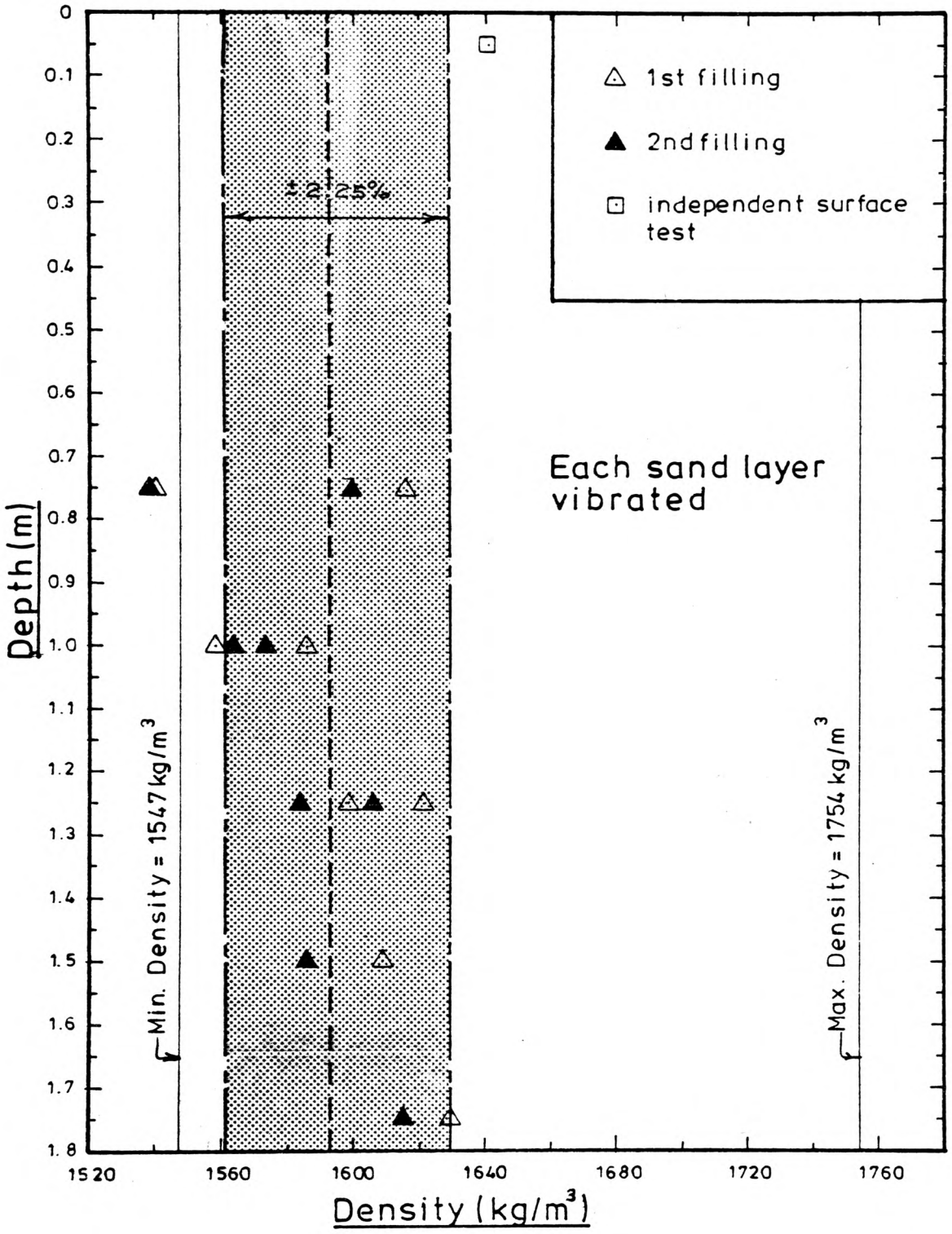

FIGURE 7.19

SAND DENSITY DETERMINED FROM DENSITY TIN RESULTS FIRST AND SECOND FILLINGS

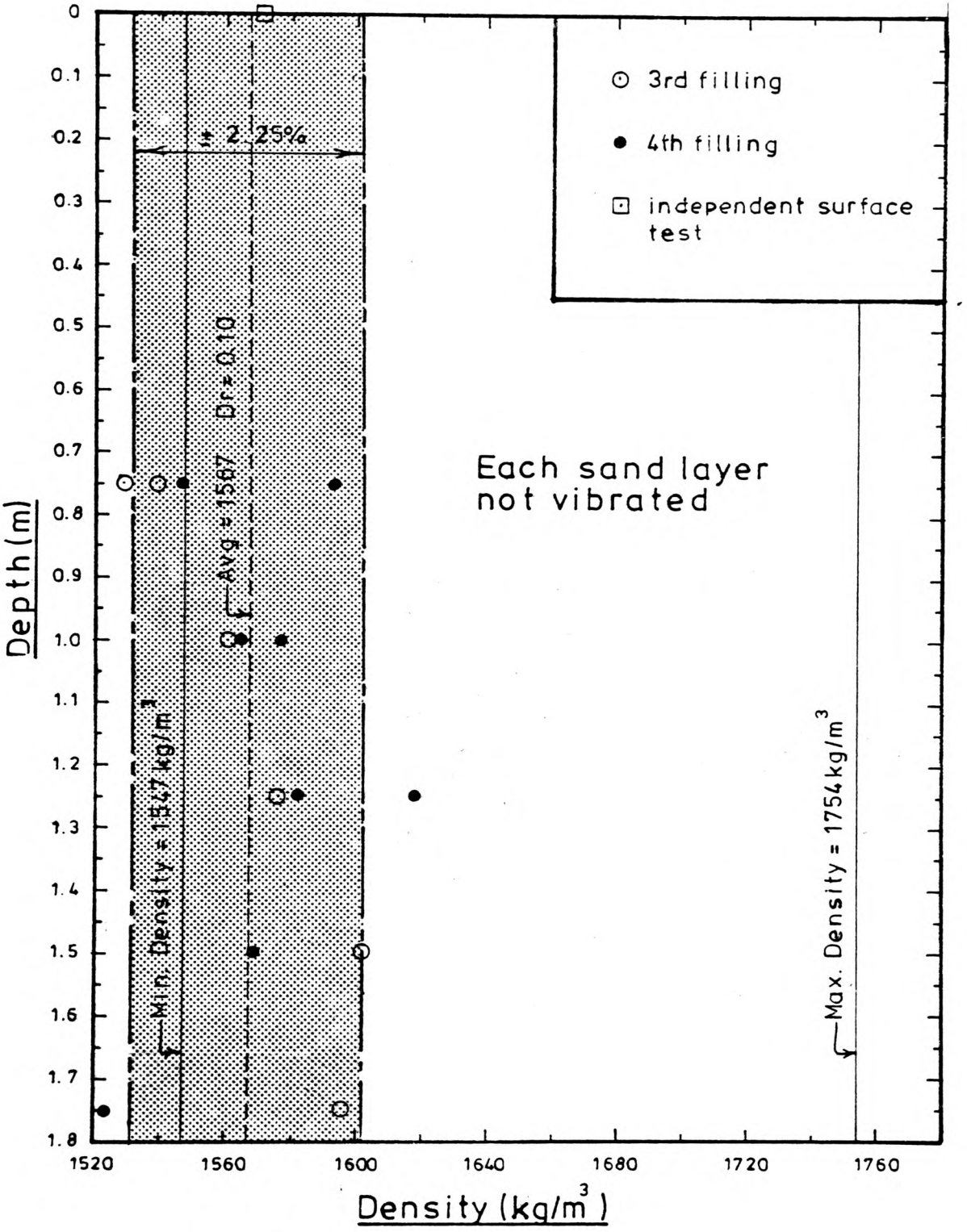

FIGURE 7.20

SAND DENSITY DETERMINED FROM DENSITY TIN RESULTS THIRD AND FOURTH FILLINGS

The results from one of the density tins has been omitted for the following reason. Three tins were located in the vicinity of the emptying chute of the sand tank. Two of the tins were lost during the emptying of the tank because as the sand flowed from the bottom of the tank the sand above it fell onto this void, the tins moving with it. There were failures in the monofilament line and rubber band when they reached large strains. The monofilament line of the tin nearest the surface did not break owing to insufficient weight of sand above the tin. However, the density of the sand in this tin was extremely high. This could have been caused by the emptying process and therefore would not reflect the density of the sand during testing. For this reason the results from this tin were ignored.

From the results of the density measurements shown in Figures 7.19 and 7.20 the average sand densities for the vibrated and not vibrated sand layers are 1593kg/m^3 (Dr=0.22) and 1567kg/m^3 (Dr.=0.10) respectively. The sand in both cases was found to be in a relatively loose state and the effect of the surface vibration only produced a marginal increase in density. Due to the large amount of instrumentation located in the sand mass, further compaction by other means (e.g. poker vibrator) was not possible since it was felt that this would disturb the instruments.

The possible error of under 3% in determining the sand density was arrived at as follows :

1. the height of the density tins was 20mm (Figure 3.4),

2. the mean particle size of the test sand was 0.45mm (Figure 6.1), therefore

3. while levelling the tin for density determination, an error of plus or minus one grain size was possible corresponding to an error of 0.45/20 = ±2.25%.

7.3.5 CRP, MLT and Pull-Out Tests Carried Out on the Final Depth of Sand

As mentioned in section 7.2 after the completion of the testing of test layer T7, for each filling of the tank, a series of loading tests were carried out on the entire depth of sand. This series consisted of :

1. a repetition of test T7, driving the pile at a constant rate, a further 12mm (T7 secondary, Figure 7.21),

2. a pull-out test fully extracting the pile at a constant rate until the pile was at its zero position (pull-out 1, Figure 7.22),

3. a maintained load test (MLT), loading the pile incrementally (Figures 7.23 and 7.24),

4. another constant rate of penetration test (CRP3, Figure 7.25), and finally

5. a second pull-out test (pull-out 2, Figure 7.22).

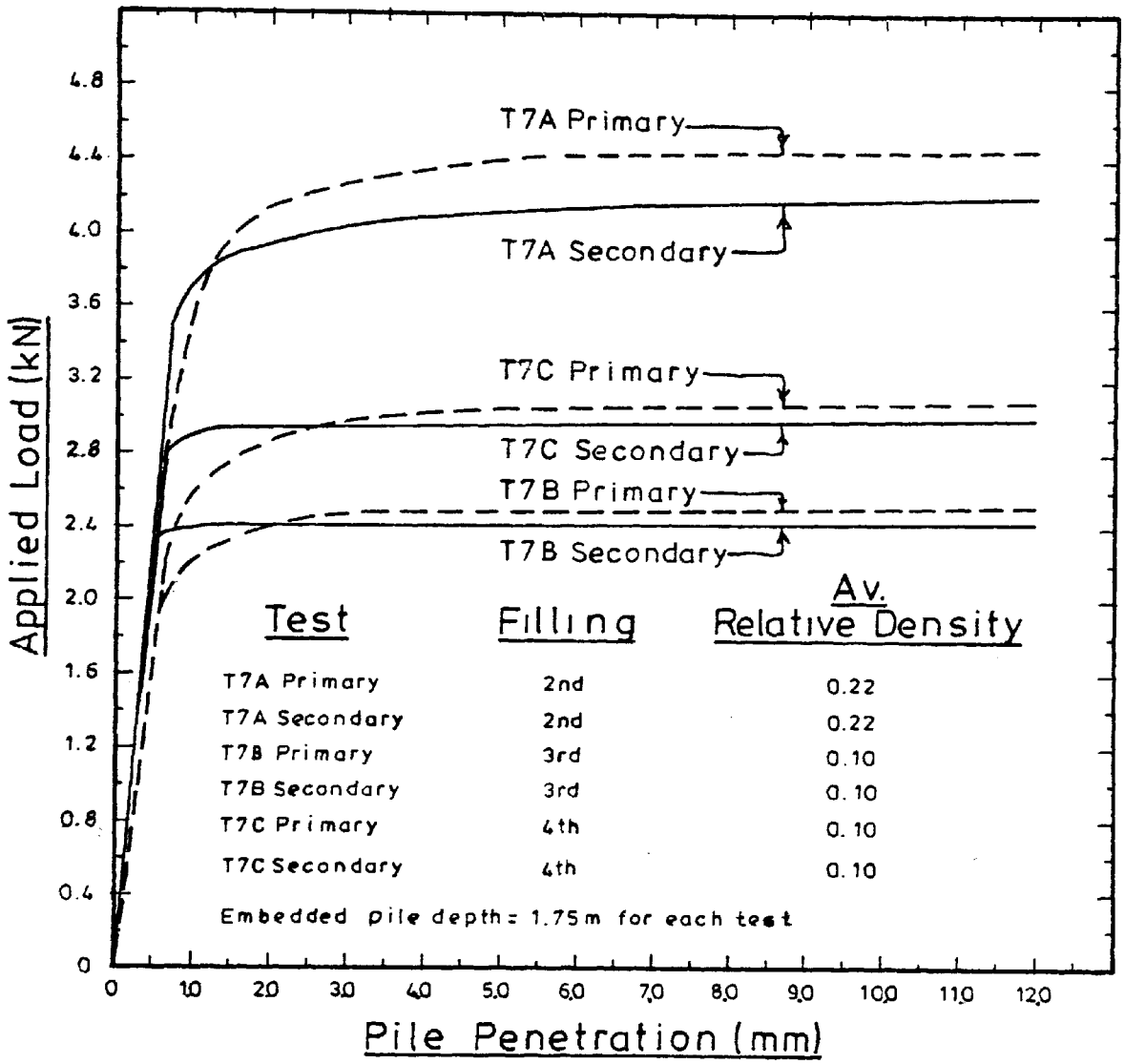

FIGURE 7.21

PRIMARY AND SECONDARY LOAD/PENETRATION CURVES

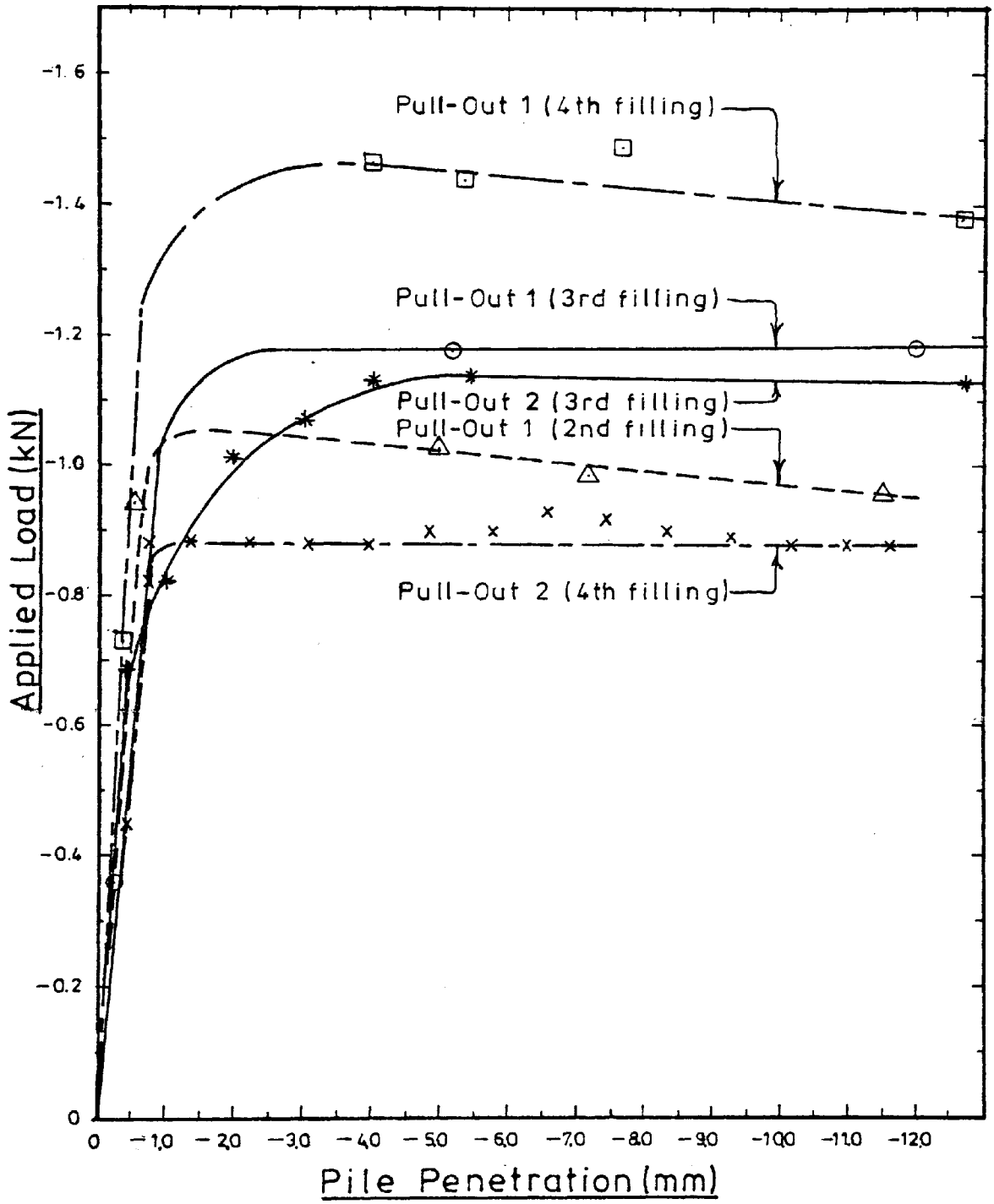

FIGURE 7.22

PILE PULL-OUT TESTS

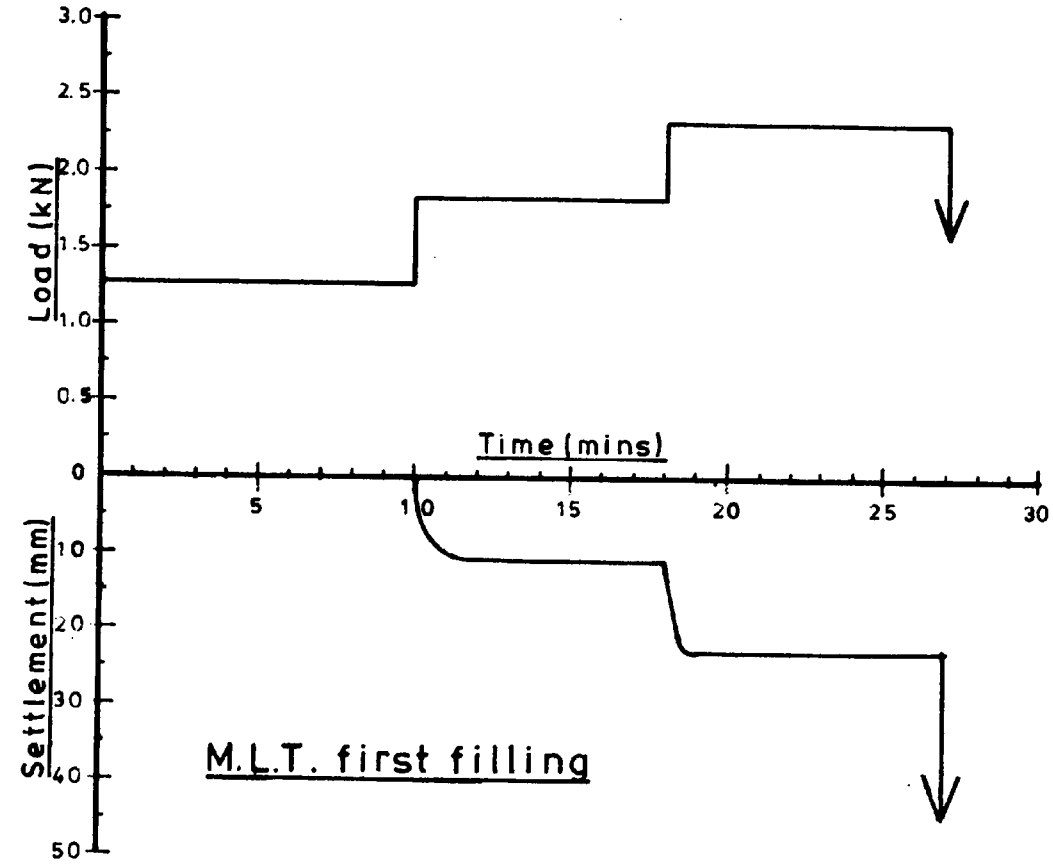

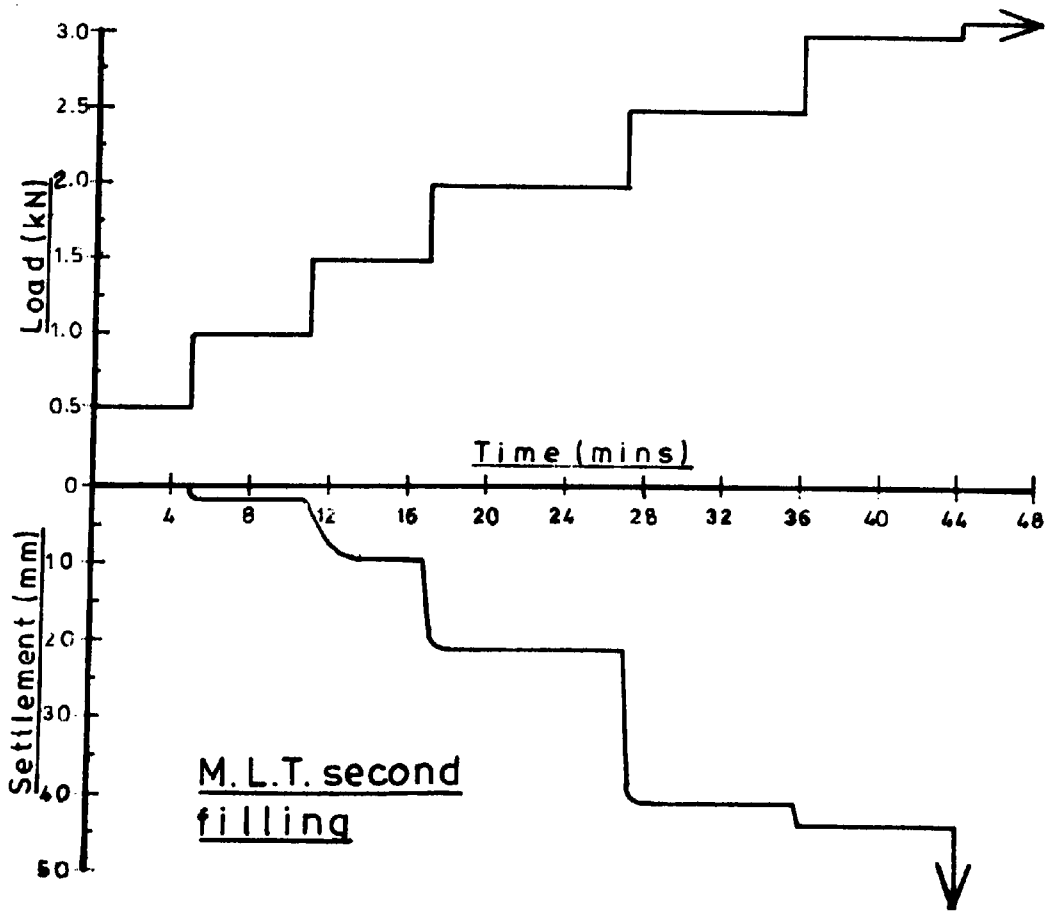

FIGURE 7.23

MAINTAINED LOAD TEST RESULTS FOR FIRST AND SECOND FILLING

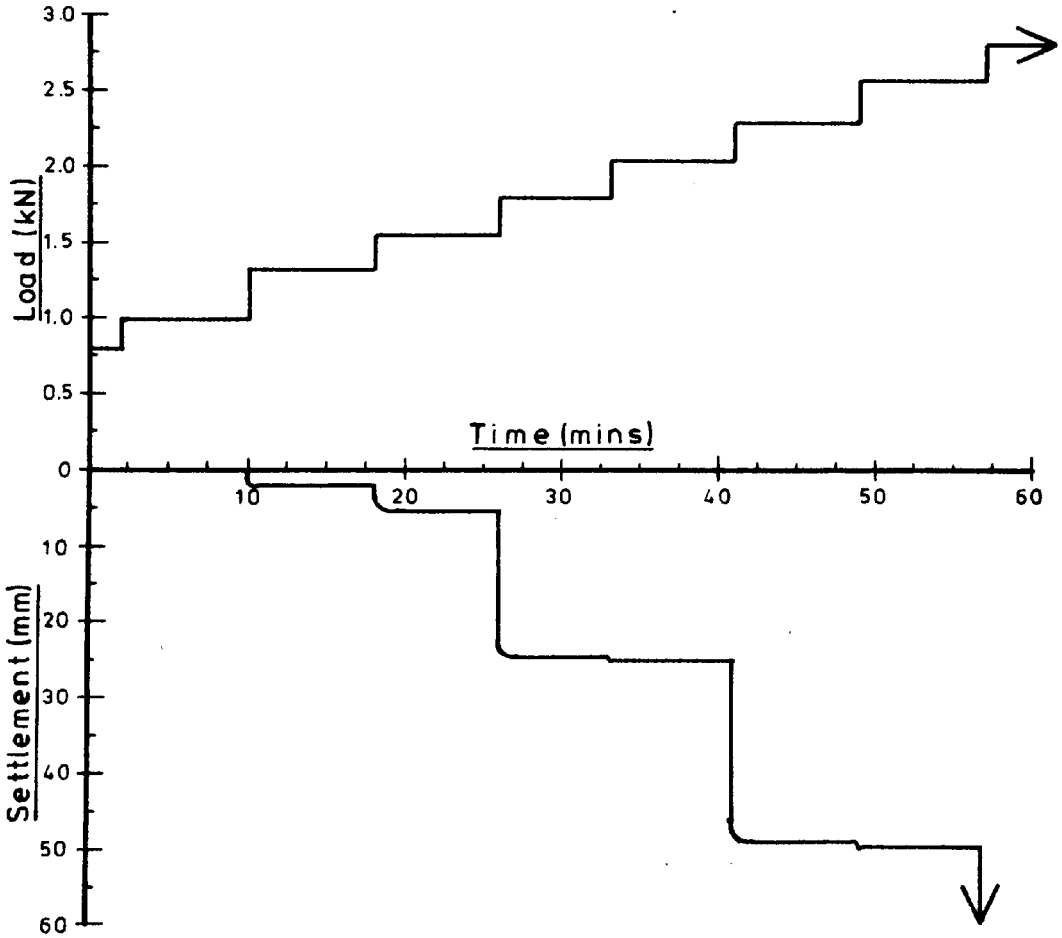

FIGURE 7.24

MAINTAINED LOAD TEST RESULTS FOR FOURTH FILLING

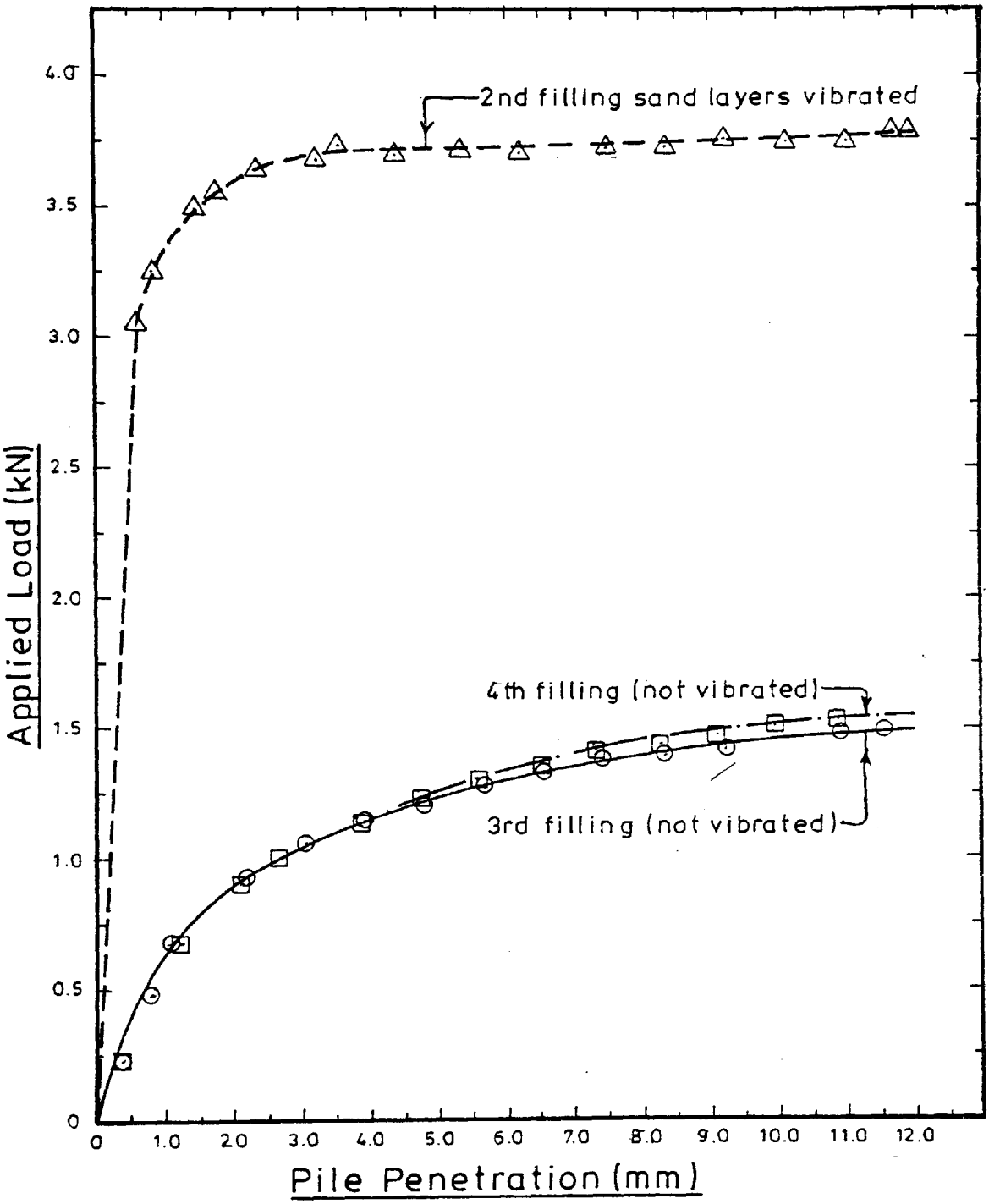

FIGURE 7.25

CONSTANT RATE OF PENETRATION TEST

C.R.P 3

The failure load for each test together with the ratios of the failure loads for the initial T7 test to each of the other loading test are presented in Table 7.4. Included in the table is the day and time at which each test commenced in relation to the date of test T7.

The criteria for determining the failure loads for the different loading tests were as follows. For the CRP tests the failure load was chosen to be either the ultimate load (a peak in the load-penetration curve) or the maximum load at 12mm pile penetration if the load was still slightly increasing. The failure load for the MLT was the maximum load recorded prior to the pile failing by plunging. The criterion for the pull-out test was the same as for the CRP test, though in each case the load reached a peak value after only a small pile movement and then continued to decrease slightly with further extraction of the pile (see Figure 7.21).

The values of ultimate skin resistance for the secondary CRP tests were slightly less than for the primary CRP tests and this resistance was mobilized at a lower pile penetration. This was possibly due to the compaction of the soil during the primary loading tests. However, it appears that the disturbance of the sand caused by the primary test reduced the ultimate load attained during any further testing. The ultimate skin resistance for the CRP 3 test was further reduced. This may have been due to the fact that the sand had been disturbed even more and the sand grains had been re-orientated during the pull-out and maintained loading tests (see Figure 7.25).

The results of three maintained load tests are shown in Figures 7.23 and 7.24. No appreciable skin friction developed for the MLT performed on the third filling of the tank. The reasons for this

Filling →	Vibrated Sand				Notvibrated Sand			
	1st		2nd		3rd		4th	
Test	Failure Load (kN)	Day and Time of Commencement of test	Failure Load (kN)	Day and Time of Commencement of test	Failure Load (kN)	Day and Time of Commencement of test	Failure Load (kN)	Day and Time of Commencement of test
T7	3.85	1/1544	4.43	1/1431	2.47	1/929	3.06	1/923
T7 repeat	a	-	4.17	7/1424	2.40	1/1123	3.00	1/1133
Pull-Out 1	b	8/1117	-1.03	9/1013	-1.19	1/1436	-1.45	1/1428
M.L.T.	2.85	9/1415	3.10	9/1355	b	2/958	2.83	2/914
C.R.P.3	c	11/953	3.78	12/943	1.48	2/1524	1.58	2/1410
Pull-Out 2	a	-	-1.43	12/1338	-1.14	3/947	-1.18	3/952

a - This test was not performed.

b - No appreciable skin friction developed.

c - Load steadily increasing over the entire travel of the jack (100mm) no ultimate load obtained.

Ratio of Loading Test/T7

Filling	1st	2nd	3rd	4th
T7 repeat/T7	-	.94	0.97	.98
Pull-Out 1/T7	-	.23	.50	.48
MLT/T7	.74	.70	-	.93
CRP3/T7	-	.85	.62	.52
Pull-Out 2/T7	-	.32	.48	.39

TABLE 7.4

FAILURE LOADS OBTAINED FROM VARIOUS LOADING TESTS CARRIED OUT ON ENTIRE DEPTH OF SAND

could not be ascertained from the available data. Another irregularity experienced was the decrease in load accompanying the failure of the pile for the MLT carried out on the first filling. Normally the load remains constant as the pile plunges through the soil at failure for an MLT. This was experienced with the maintained load tests performed on the second and fourth fillings.

The data presented in this section is only for general interest as it was not one of the specific objectives of the research work. It does however, confirm that the sequence of loading (Tejchman 1969) and the direction of loading (Tejchman 1969 and Broms and Silberman 1964) influence the carrying capacity of a pile. Tejchman suggested that tests performed previously on a pile can create residual stresses on the pile which would have the same effect as the development of negative skin friction on the pile shaft. In the case of a pull-out test the effects are to relieve part of the effective overburden pressures while a compression test increases the effective overburden pressures and lateral forces acting normal to the pile surface (Broms and Silberman 1964). However, there was no evidence, in the candidates series of tests, of any peak or residual stresses related to strain as in the conventional triaxial tests.

7.4 General Discussion and Analysis of Test Results

7.4.1 Load/Penetration Data

The load/penetration curves for the twenty eight pile loading tests are presented in Figure 7.2. The analysis described in this section was carried out to normalize the curves so that :

1. any inherent trends in the test data would be more easily identified, and

2. the results could be extrapolated and compared with other test data.

The curves possessed two distinct features :

1. the load/penetration curve commenced with a linear characteristic from the origin and continued almost linearly for a substantial portion of the total load, OA (see Figure 7.26), and

2. from point A there was a significant change in the gradient of the tangent where the slope asymptotically approached the horizontal. This portion of the curve AB was approximated by an exponential curve, the construction of which is discussed below.

To obtain the equation for the exponential portion of the load/penetration curves the data points were plotted to a log-log scale and the equation of the line through the points (with the exception of the first few points for each test) was determined. The plot of these curves is shown in Figures 7.26 to 7.29 together with

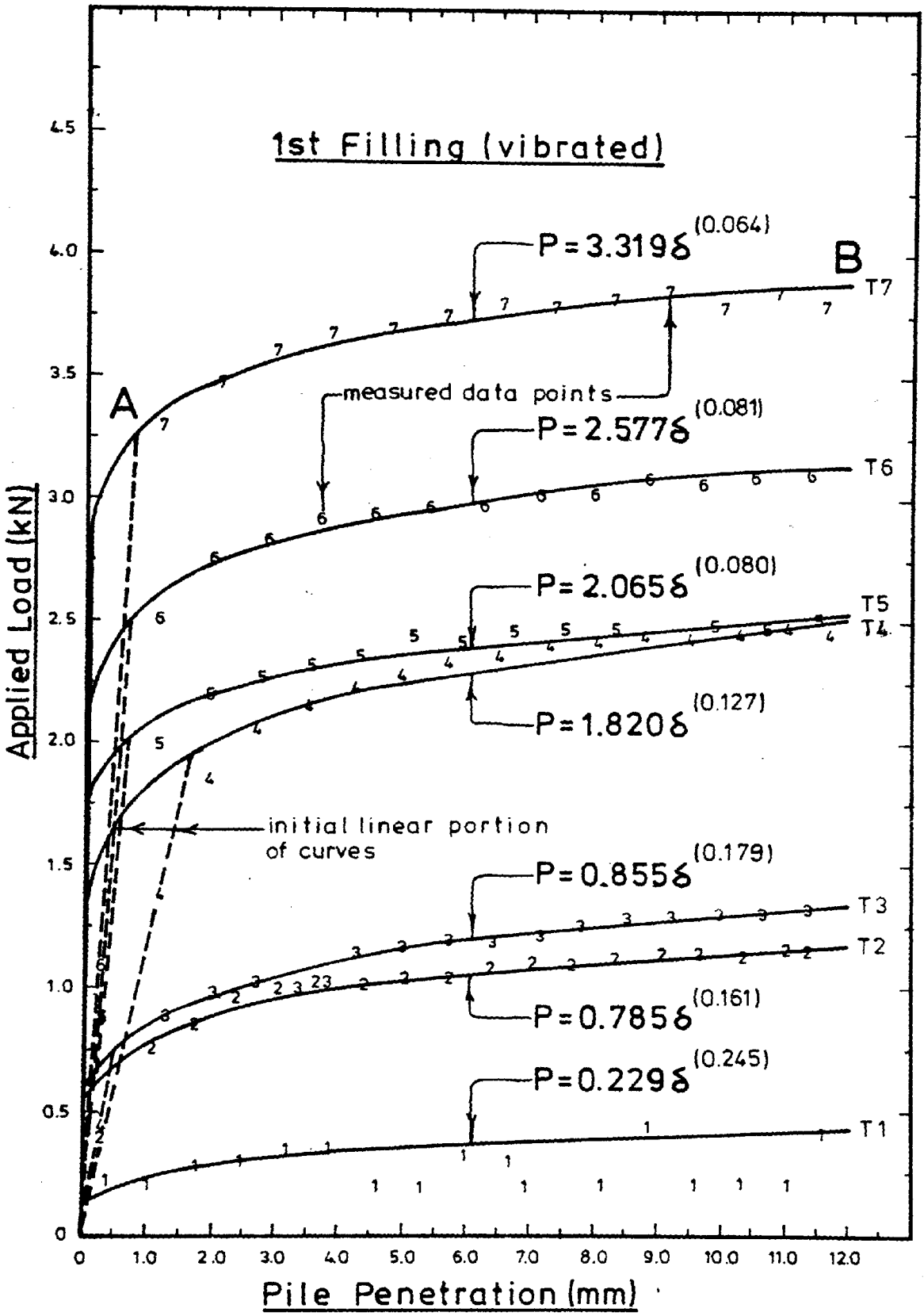

FIGURE 7.26

LOAD / PENETRATION CURVES

FIRST FILLING

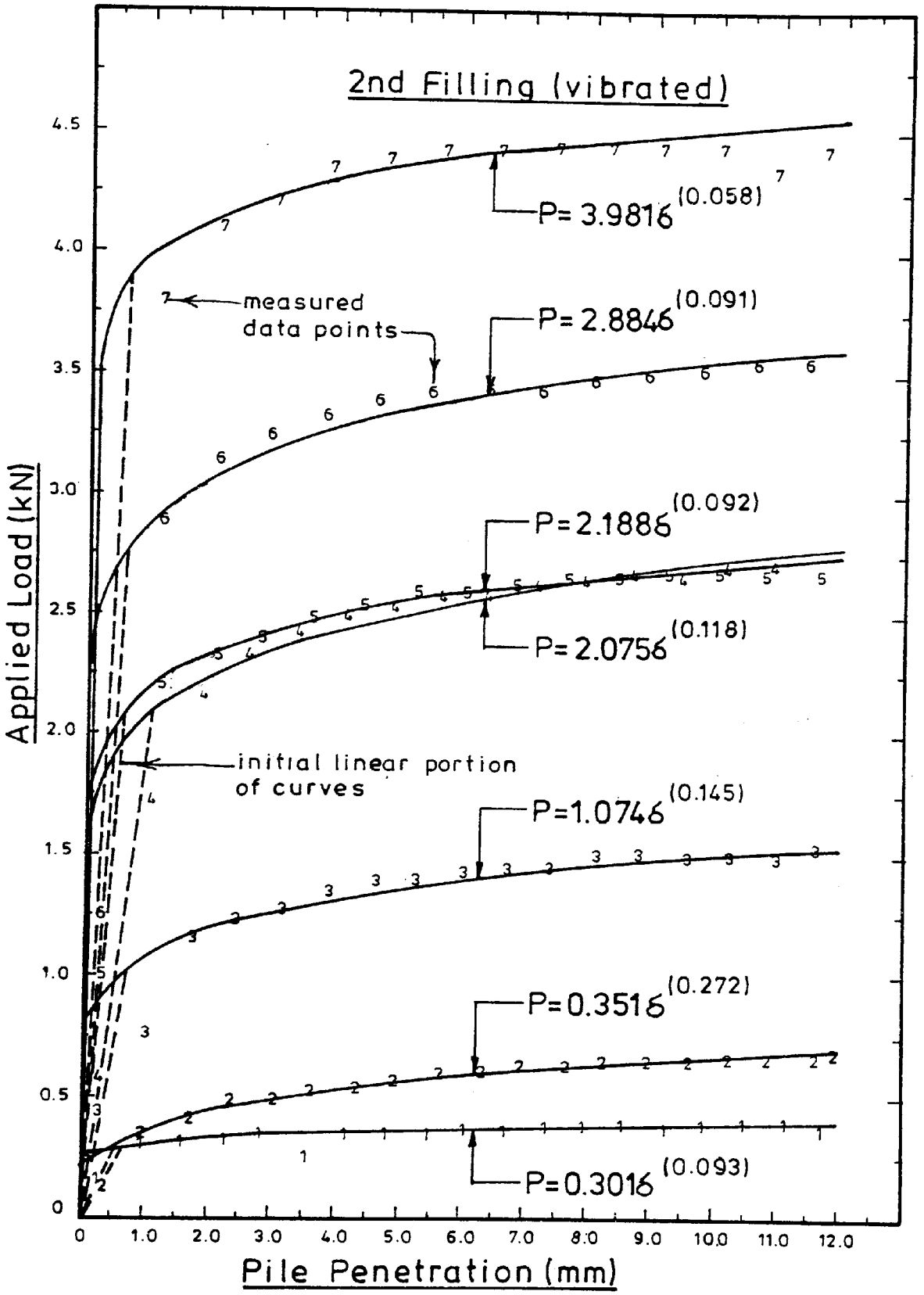

FIGURE 7.27

LOAD/PENETRATION CURVES

SECOND FILLING

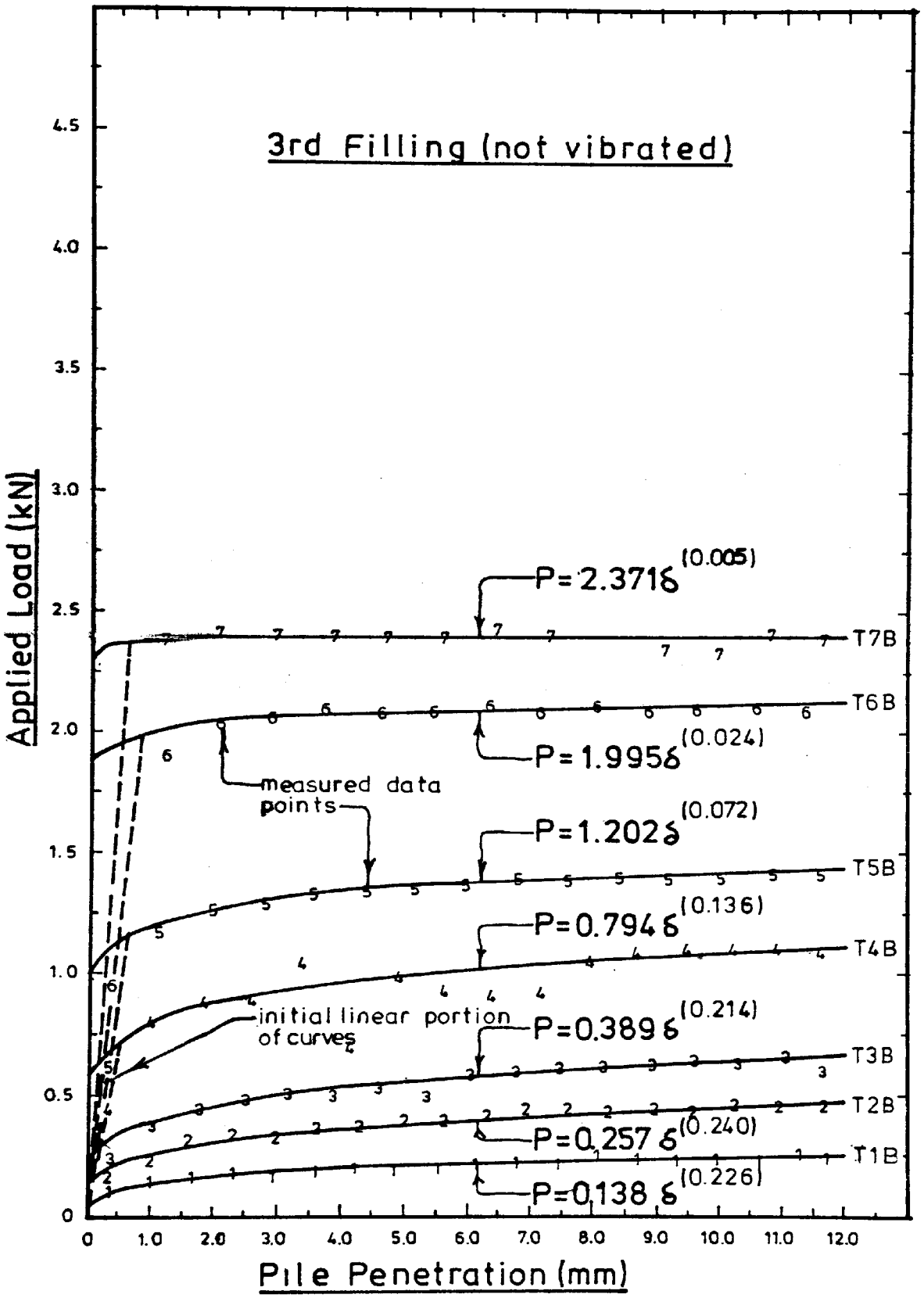

FIGURE 7.28

LOAD/PENETRATION CURVES

THIRD FILLING

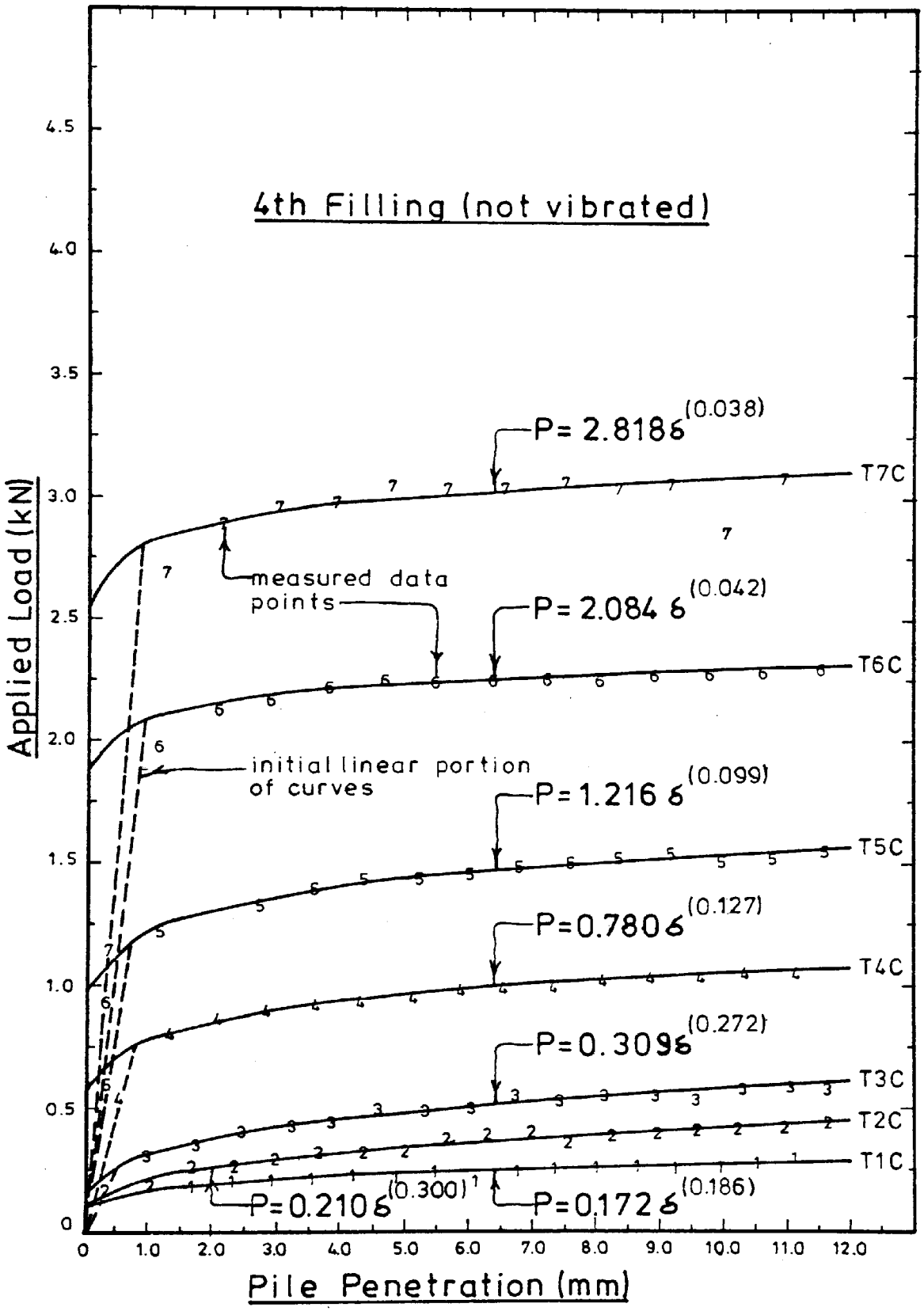

FIGURE 7.29

LOAD / PENETRATION CURVES

FOURTH FILLING

the measured data points. The equations for the exponential curves are of the form $P = A\delta^B$ where P is the applied load in kN, δ is the pile penetration in mm, and A and B are factors to be determined. The constants A and B have been plotted against the embedded length of the pile and are shown in Figures 7.30 and 7.31. The values of the constant A, which are plotted in Figure 7.30, appear to be increasing linearly for embedded lengths of pile with lengths in excess of 0.6m or five pile diameters. From Figure 7.30 the constant A is shown to be dependent on density, since the value of A is consistently higher for the vibrated sand layers than for the sand layers which were not vibrated.

The exponential coefficient (B) of the equation was found to be less dependent on the sand density. Figure 7.31 shows the values of B to be scattered around a mean line through the points. No apparent difference was found for the data points for the vibrated and notvibrated tests.

The following exercise was carried out to determine if any relationship existed between the extent of the initial linear portion of the load-penetration curves and the embedded length of pile. A straight line OA (Figure 7.26) was drawn from the origin through the initial data points for each curve and the values of the pile penetration at which these lines intersected the exponential curves AB, along with the slopes of these lines, have been plotted against pile embedded length and are shown in Figures 7.32 and 7.33 respectively. Figure 7.32 is similar to Figure 7.30 in that the slope appears to increase linearly for embedded lengths of pile greater than five to six pile diameters. From Figure 7.33 it can be assumed that

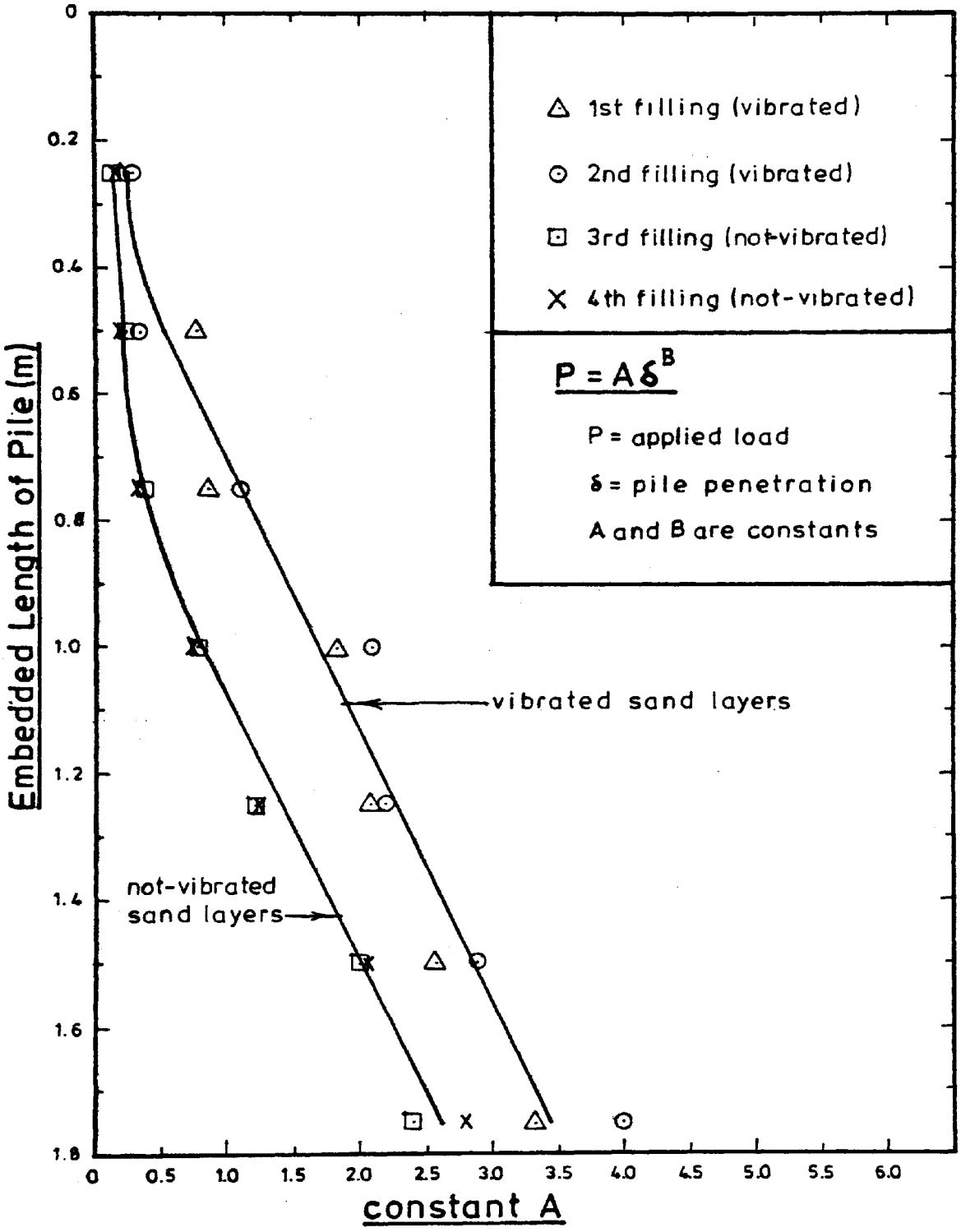

FIGURE 7.30

VARIATION OF CONSTANT A WITH EMBEDDED LENGTH OF PILE

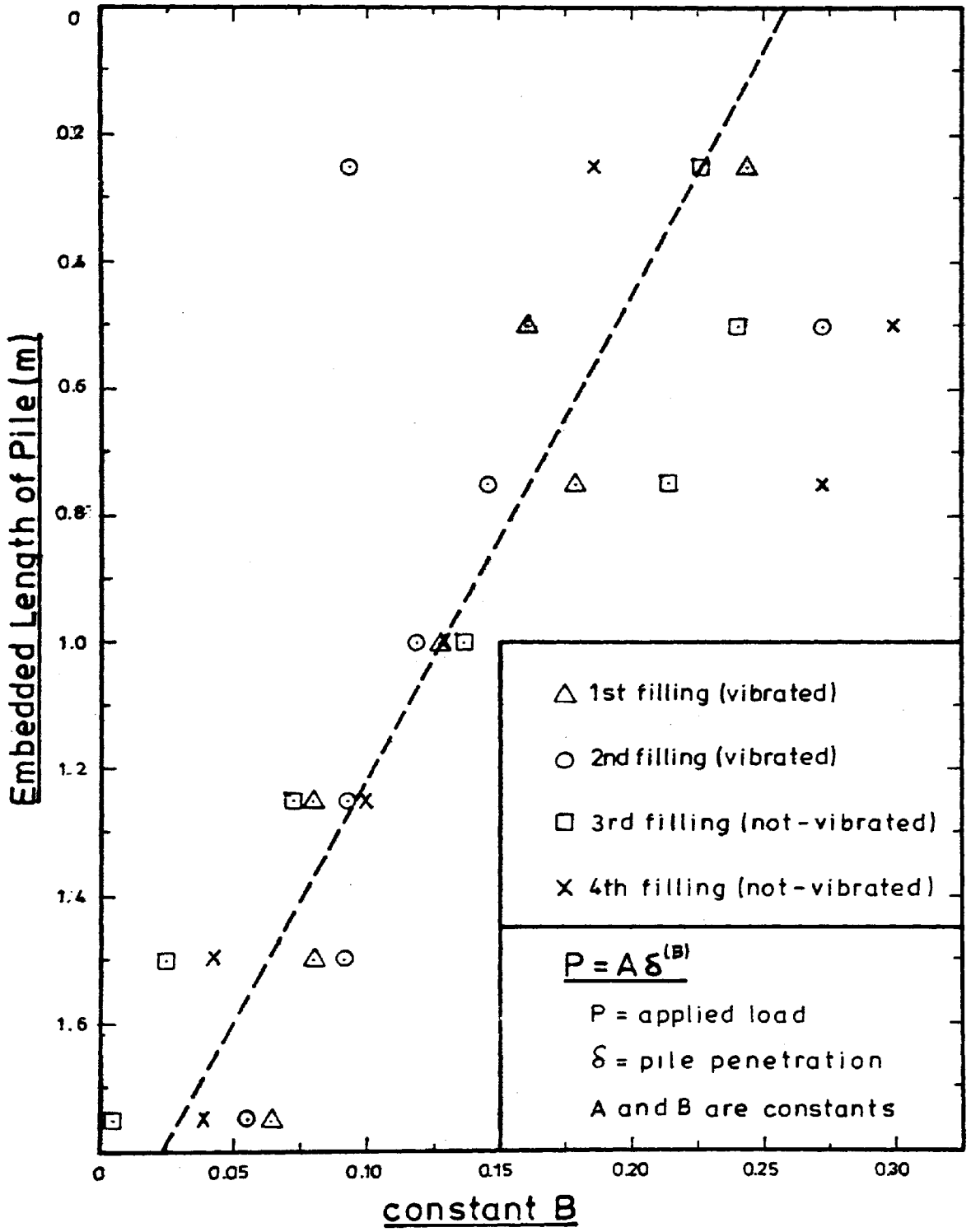

FIGURE 7.31

VARIATION OF CONSTANT B
WITH EMBEDDED LENGTH OF PILE

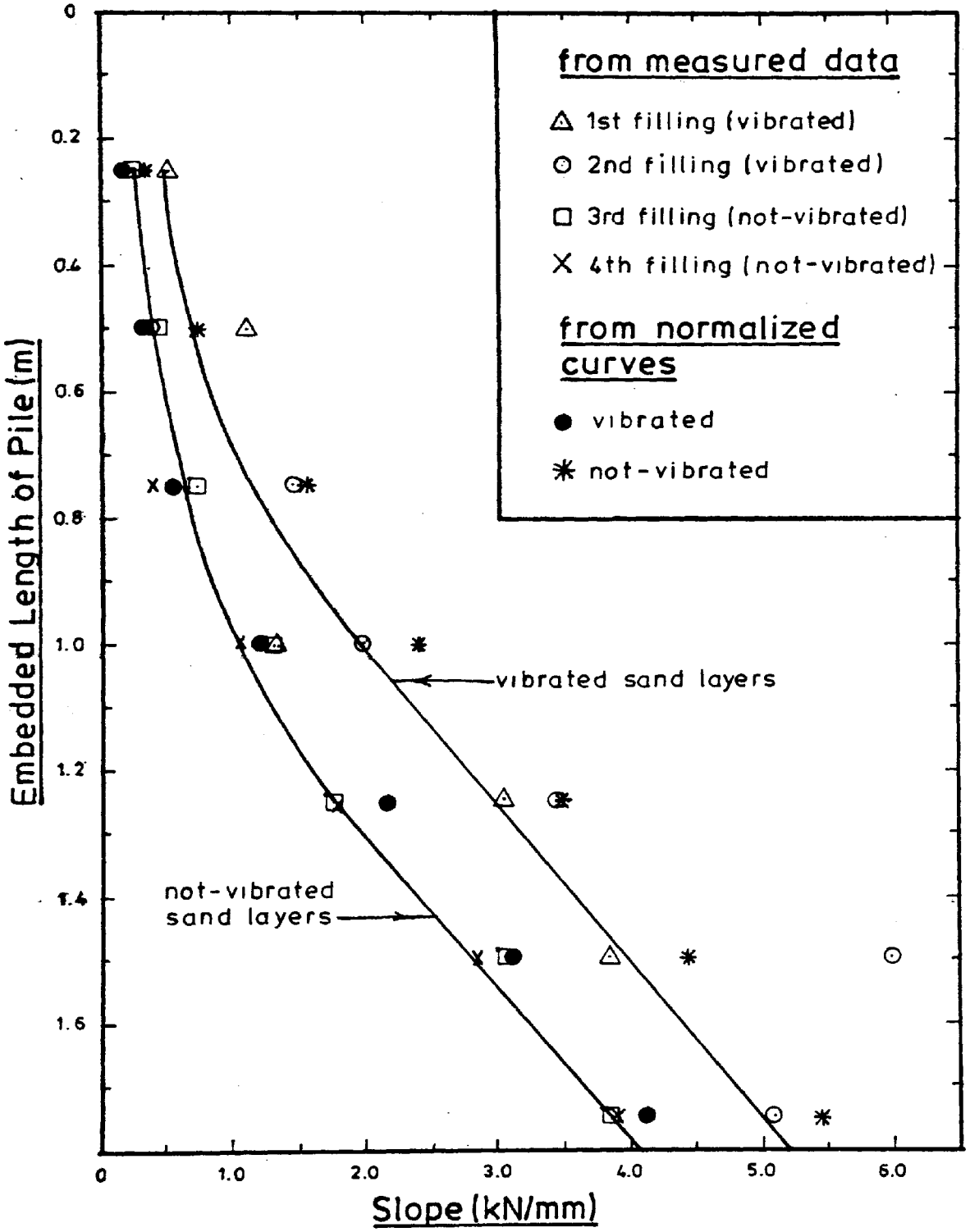

FIGURE 7.32

SLOPE OF INITIAL LINEAR PORTION OF LOAD/PENETRATION CURVE VERSUS EMBEDDED LENGTH OF PILE

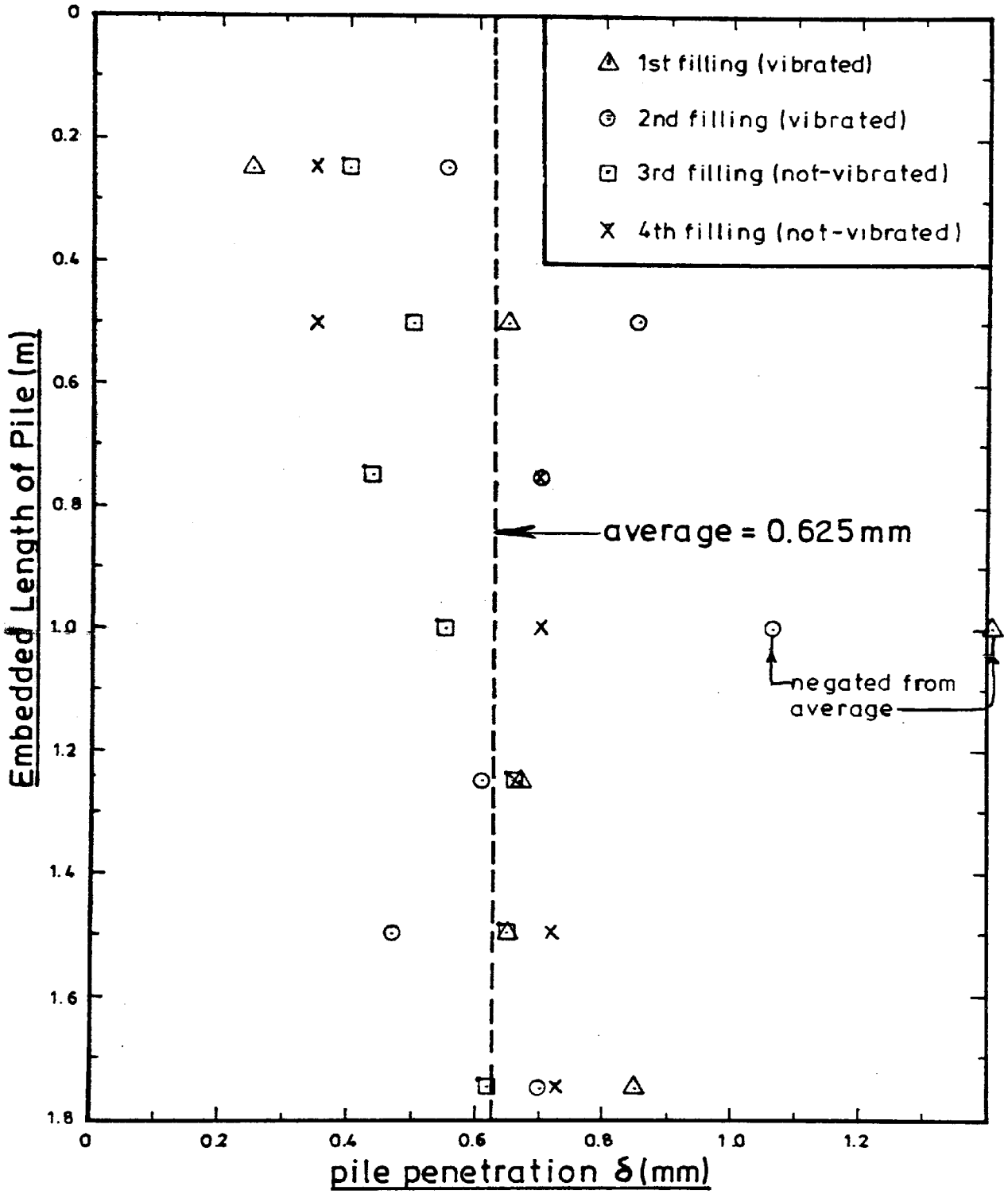

FIGURE 7.33

PILE PENETRATION AT THE END OF THE INITIAL LINEAR PORTION OF THE LOAD/PENETRATION CURVES

the extent of the initial linear portion of the curves is independent of the embedded length of the pile and the sand density. This agrees with the findings of Vesic (1963) who drove 51mm, 102mm, and 171mm diameter piles into dry sand and found the shaft displacements needed to reach ultimate skin resistance were independent of foundation width, foundation depth and of the sand density. Vesic (1963) also stated that his findings confirmed the belief that the mobilization of shear strength along a fixed rupture surface is governed by the absolute displacement along that surface.

For the 114mm diameter steel pile used in the candidates experiments, the average displacement δ needed to mobilize a substantial portion of the skin friction was found to be in the order of 0.625mm corresponding to the extent of the initial linear portion of the load/penetration curve (see Figure 7.33).

From the skin friction versus pile penetration curves presented by Vesic (1963), the initial linear portion of the curves extend to an average pile penetration of approximately 1.6mm.

The normalized load/penetration curves for the seven different embedded lengths corresponding to the seven test layers were plotted in the following manner. The constants A and B for the equation of the exponential portion of the curve were obtained from the average values taken from Figures 7.30 and 7.31. The initial linear portion of the curves were obtained by drawing a line from the origin to intersect the exponential curves at 0.625mm pile penetration. These curves are shown on Figures 7.34 and 7.35. The resultant slopes of the initial linear portions of the curves are plotted on Figure 7.32 and show reasonable agreement with the values obtained from the experimental

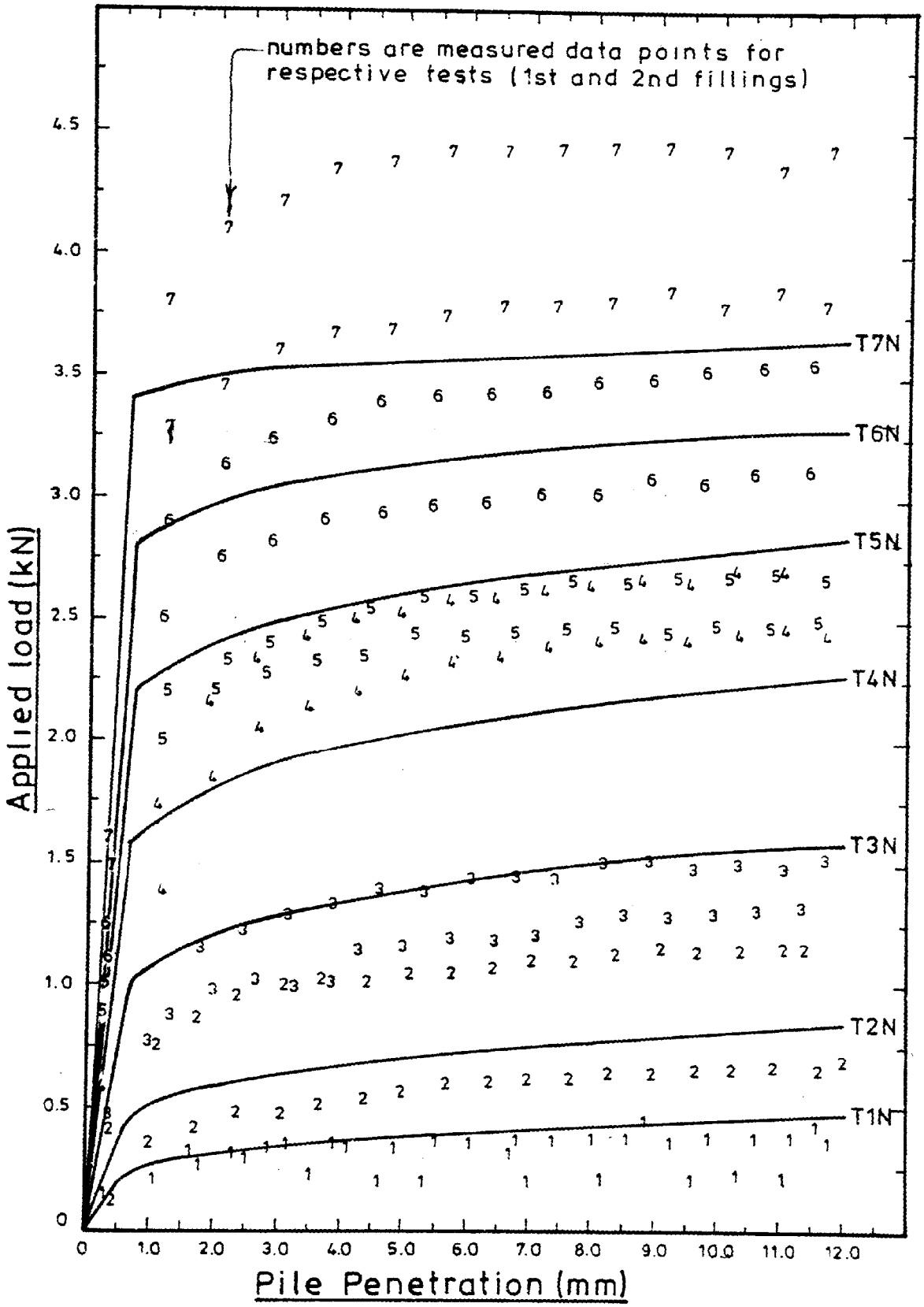

FIGURE 7.34

NORMALIZED LOAD / PENETRATION CURVES FOR VIBRATED SAND LAYERS

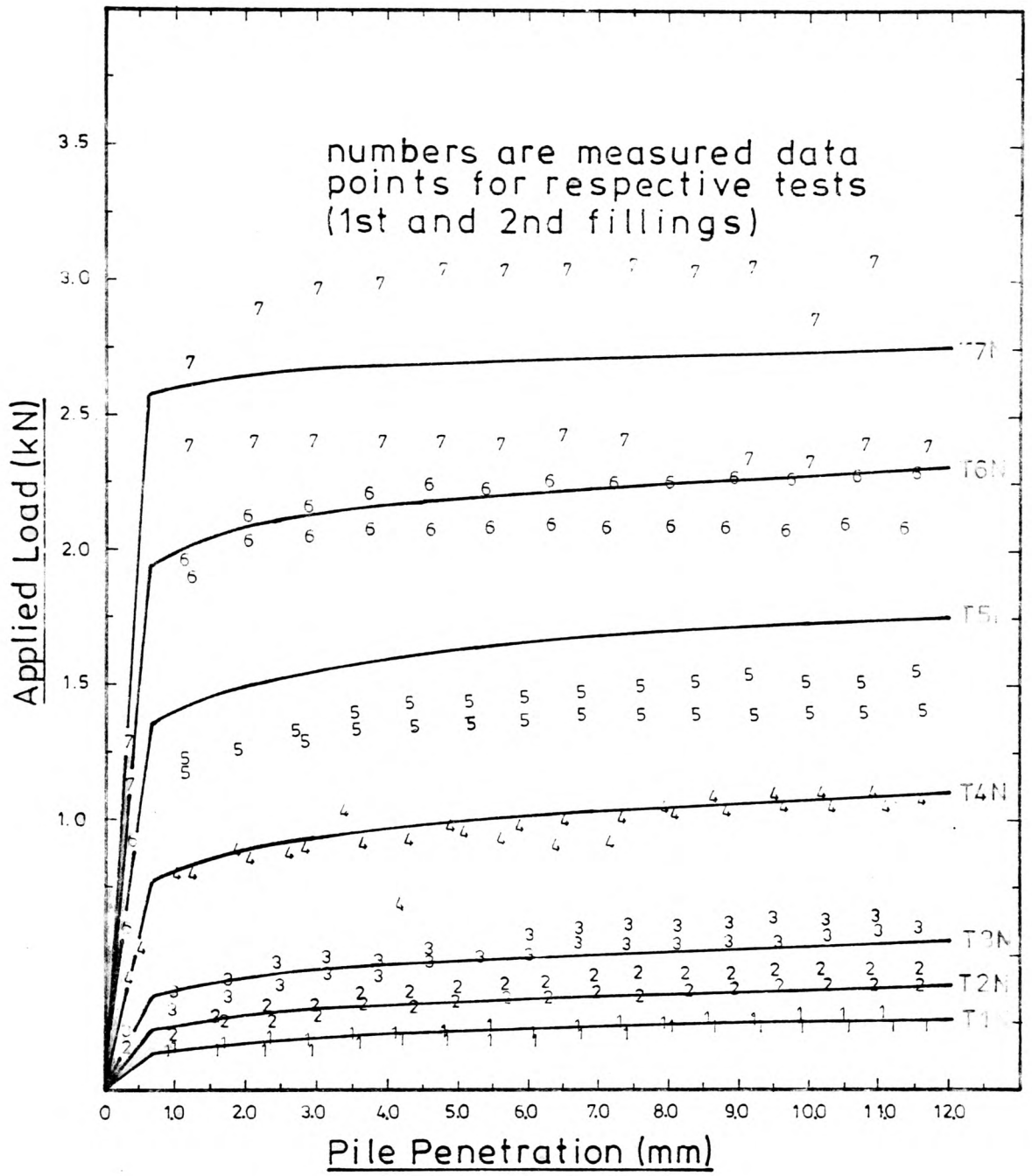

FIGURE 7.35

NORMALIZED LOAD/PENETRATION CURVES FOR NOT-VIBRATED SAND LAYERS

data. Also plotted on Figures 7.34 and 7.35 are the actual data points measured during testing.

The average skin friction versus pile penetration for the seven vibrated and the seven notvibrated embedded lengths of pile are shown in Figures 7.36 and 7.37. These curves were derived by dividing the total applied load by the embedded area of the pile shaft. The curves show an initial decrease followed by an increase in the value of skin friction as the piles embedded length increased.

The skin friction values for the deeper, vibrated sand layers (T3 and T7) increased at a decreasing rate although the difference in the maximum value was slight (see Figure 7.36). This relationship between average skin friction and embedded length of pile is shown in Figure 7.3. With the exception of the first layer for each filling, as the piles embedded length increased the average skin friction on the pile initially increased and then, for the vibrated layers, reached a constant value at approximately 14 to 15 pile diameters. Vesic (1963) and others have found that the skin friction increases with the embedded depth of pile and reaches a constant value at greater depths.

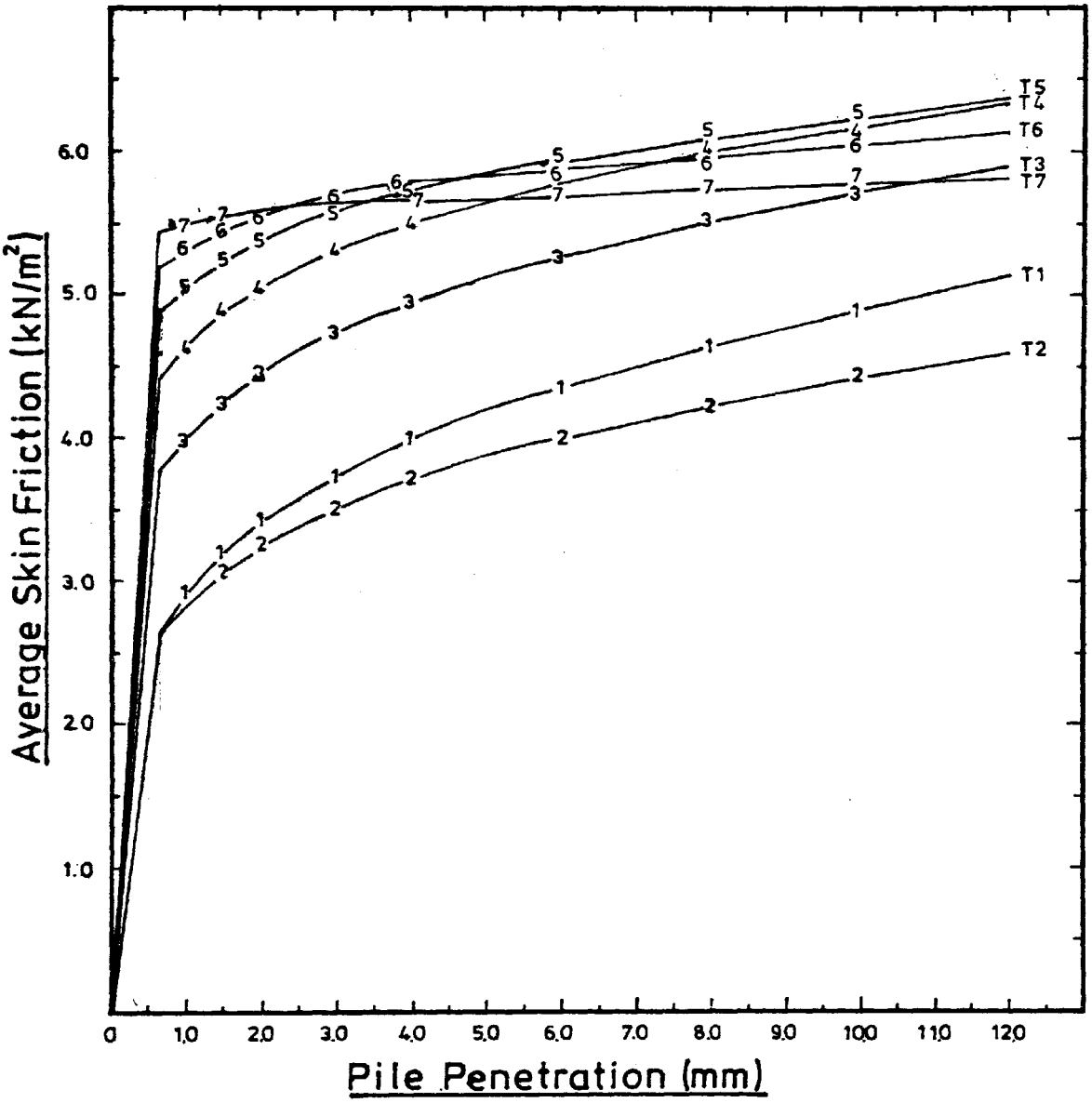

FIGURE 7.36

AVERAGE SKIN FRICTION VERSUS PILE PENETRATION FROM NORMALIZED LOAD/PENETRATION CURVES FOR VIBRATED SAND LAYERS

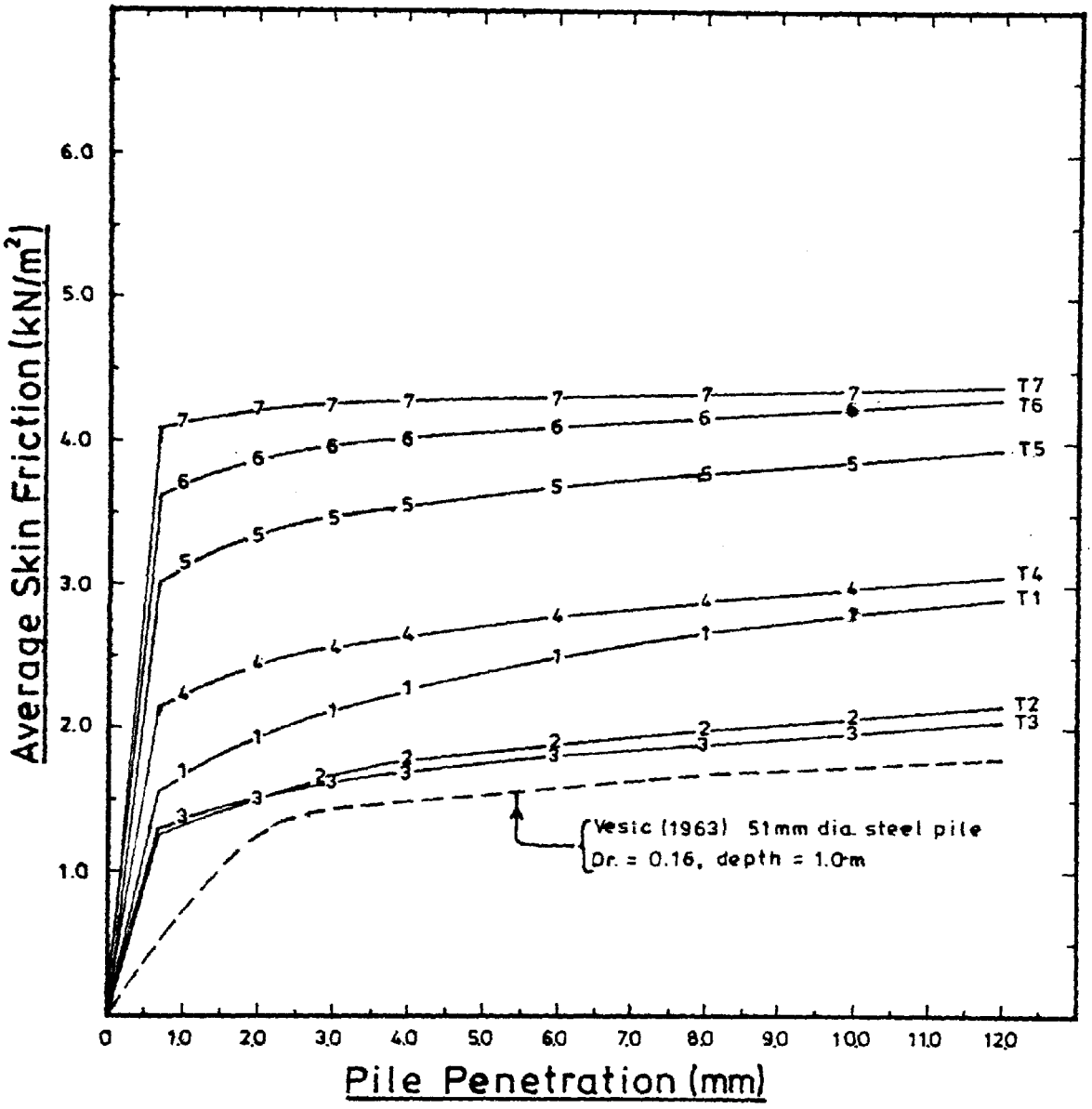

FIGURE 7.37

AVERAGE SKIN FRICTION VERSUS PILE PENETRATION FROM NORMALIZED LOAD/PENETRATION CURVES FOR NOT-VIBRATED SAND LAYERS

7.4.2 Average Skin Friction Versus Pile Length

The relationship between the average skin friction and the embedded length of pile is shown in Figure 7.3. The values of the average skin friction calculated from the normalized load/penetration curves are shown together with the measured values (from Figure 7.3) in Figure 7.38. These results agree with the research performed by Vesic (1963) and others who revealed that the unit shaft resistance of a pile does not necessarily increase linearly with depth, but instead reached almost constant values beyond a certain depth. From the results shown in Figure 7.38 the value of the average skin friction appears to reach a constant value at approximately 1.4m depth (12 pile diameters) for the vibrated sand layers and is still slightly increasing at the maximum depth of 1.75m for the not vibrated sand layers.

The above results indicates that the vertical effective stress adjacent to a pile is not necessarily equal to the effective overburden pressure, but reaches a limiting value at depth. Vesic attributed this phenomenon to arching similar to that described by Terzaghi (1943) in relation to tunnels. The stress disturbed curves of Figure 7.8 support the hypothesis that arching of the sand is taking place near the base of the test pile. This would explain the decrease in stress at greater depths as shown in Figure 7.8.

The processing and normalization of the stress distribution curves together with the implications of this data are given and discussed in the next section.

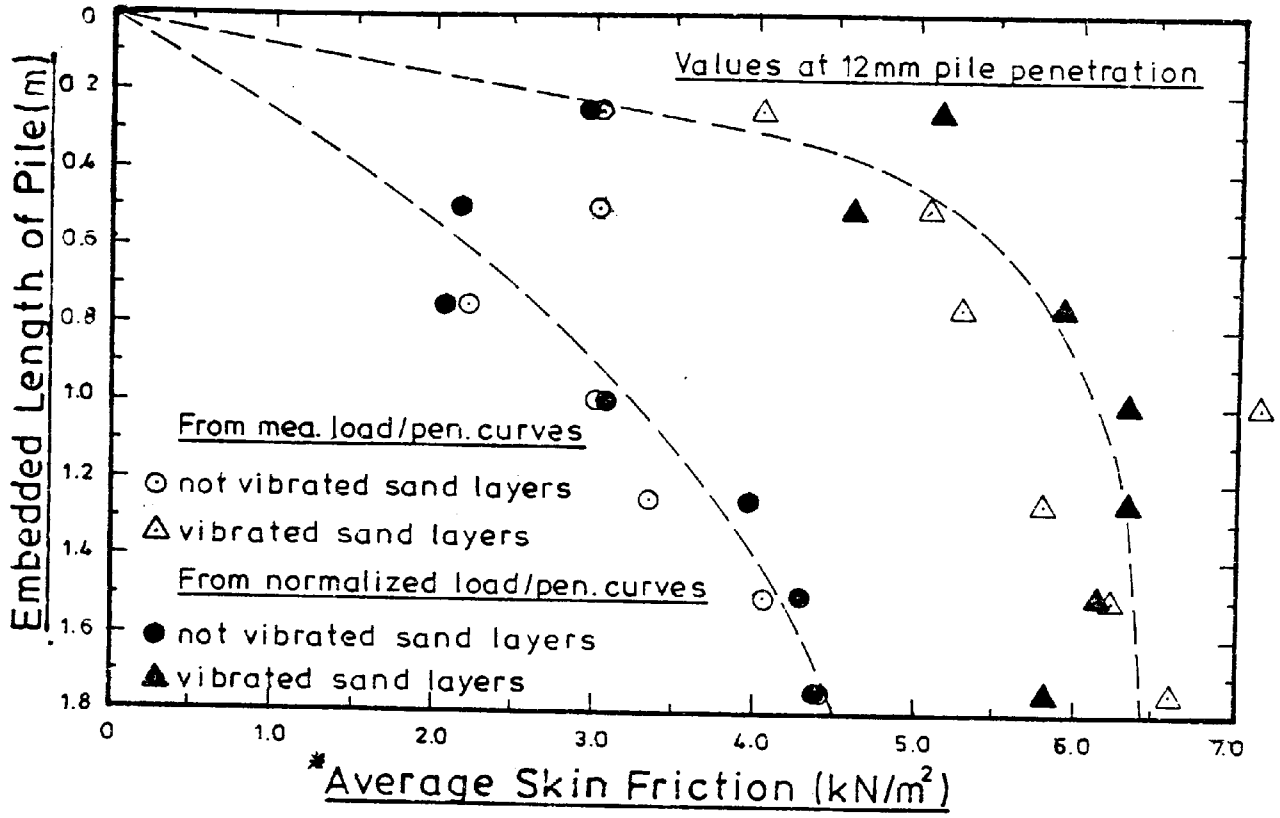

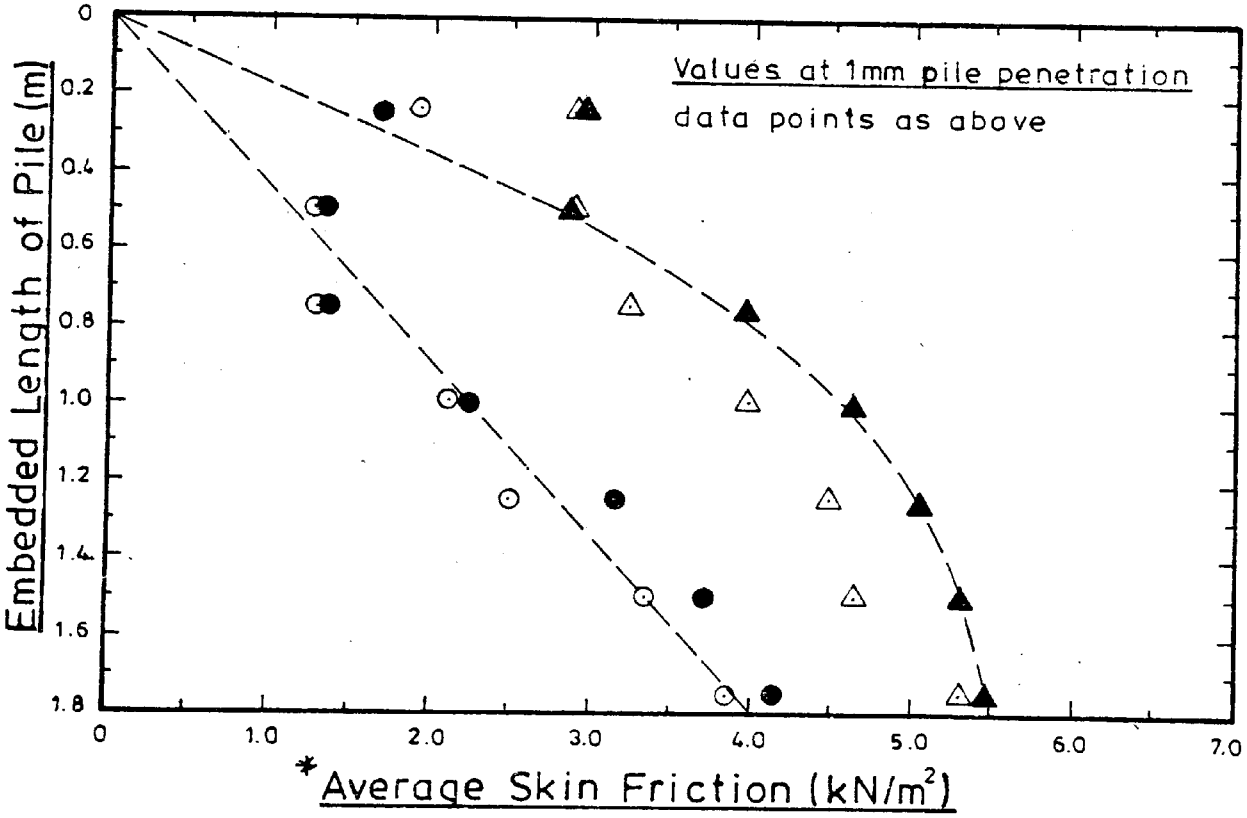

* Average Skin Friction = Total applied load divided by embedded pile area

FIGURE 7.38

AVERAGE SKIN FRICTION VERSUS EMBEDDED LENGTH OF PILE

7.4.3 Distribution of Axial Load and Skin Friction Along the Pile

The testing procedure has been presented in detail in section 7.2. One of the difficulties encountered in interpreting the load distribution data was in determining the residual stresses in the pile, if any. Residual stresses can be caused by :

1. negative skin friction acting on the pile due to soil consolidation, or

2. installation of a pile by driving.

Gregersen and DiBiagio (1973) have shown that the effect of a pile loading test on the residual stresses on a pile is to reduce them considerably.

It was not possible to monitor the residual loads because of the amount of drift in the electrical strain recording equipment over the 30 days testing programme.

The assumption was made that the pile was free from any residual stresses at the start of each loading test since :

1. the pile and sand were disturbed between the testing of each sand layer, due to the clamping and unclamping of the pile and the pouring (and vibrating) of the next sand layer, and

2. the previous loading was likely to reduce any residual stresses in the pile.

The load distribution curves of Figures 7.4 to 7.7 agree with the curves proposed by Tomlinson (1967) and those derived by Mansur and Kaufman (1956) and Gregerson and DiBiagio (1973). Mansur et al. (1956) recorded the load distribution on instrumented field piles in a soil stratum consisting of layers of silty sand and sandy silts overlying a sand. The field loading tests reported by Gregerson et al. (1973) were for instrumented precast concrete piles in loose sand. Typical axial load distribution curves from these two field reports are shown in Figure 7.39.

It is possible that the pile acted as a strut above the sand surface creating stress concentrations at different locations along the pile. This could account for the high loads measured in L.C.5 as shown on Figures 7.4 to 7.7.

To determine the effect of the top 250mm layer of sand on each loading test the following exercise was carried out. From each of the load/penetration curves shown in Figure 7.2 the curve of the previous test was subtracted. The resulting curve was a measure of the additional load due to the placement of the top soil layer. These curves are shown in Figure 7.40. This additional load is caused by the skin friction on the pile in the top layer and the increased overburden on the lower sand layers. From the stress distrution curves (Figure 7.8) it can be seen that the skin friction was very small at shallow depths. Therefore, the prevalent effect of the top layer on the skin friction of the pile was the additional overburden and not the skin friction offered by that layer.

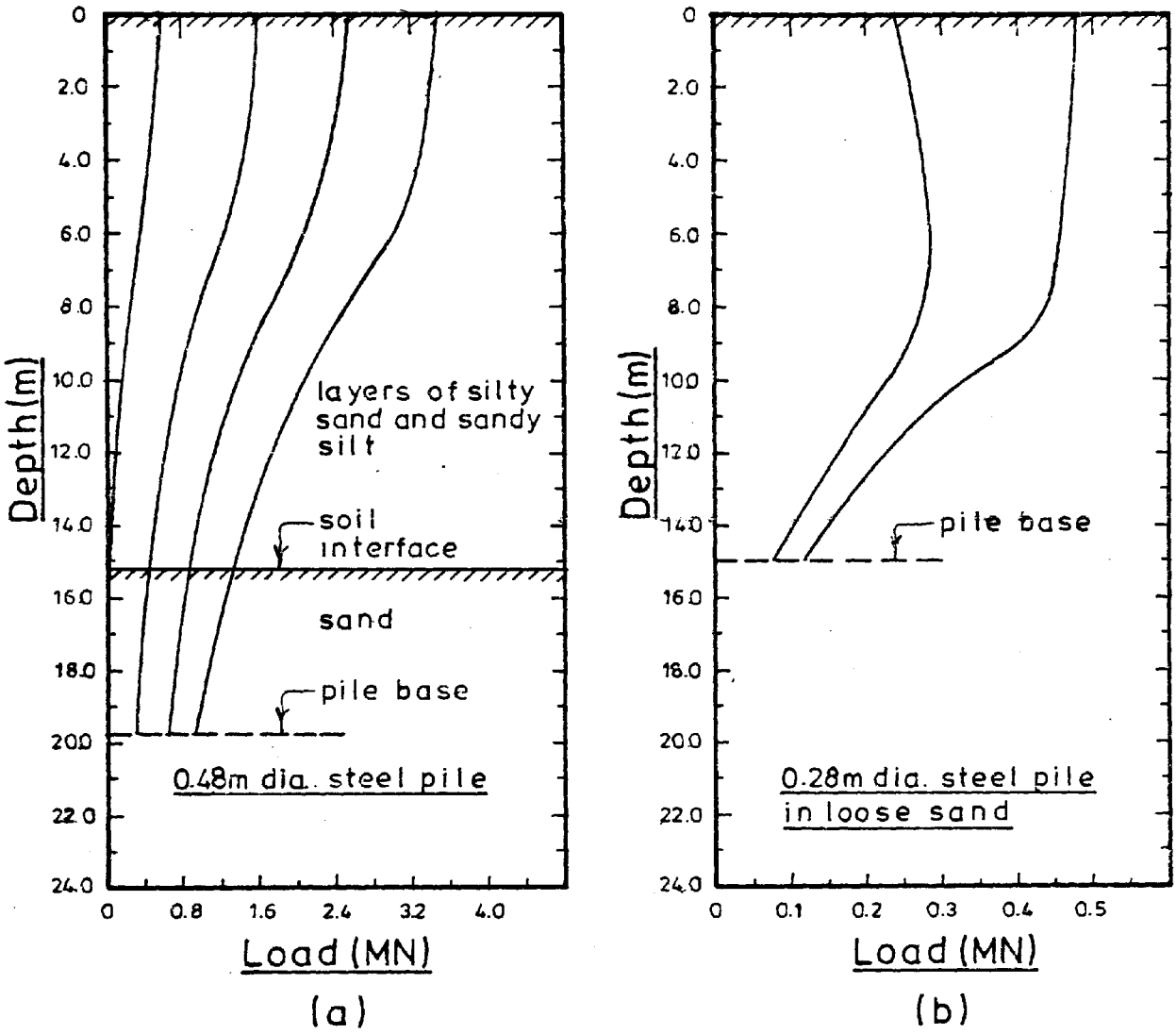

FIGURE 7.39

DISTRIBUTION OF AXIAL LOAD IN INSTRUMENTED TEST PILES IN THE FIELD

(a) MANSUR and KAUFMAN (1956)

(b) GREGERSEN and DIBIAGIO (1973)

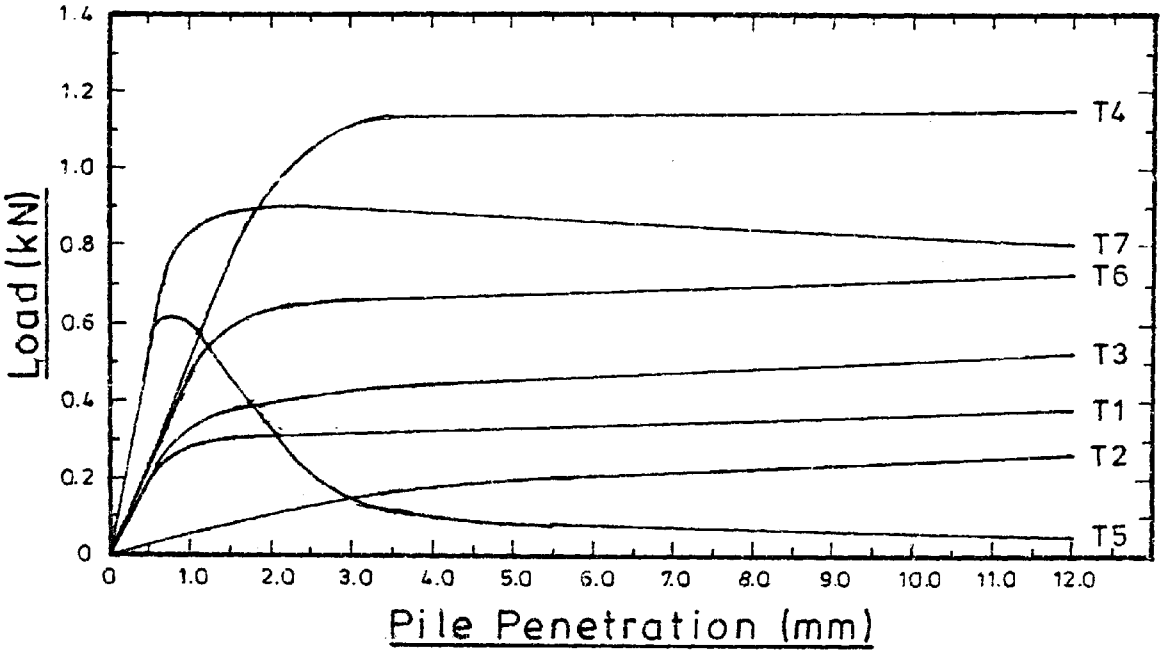

a) Average of 1st and 2nd fillings (vibrated)

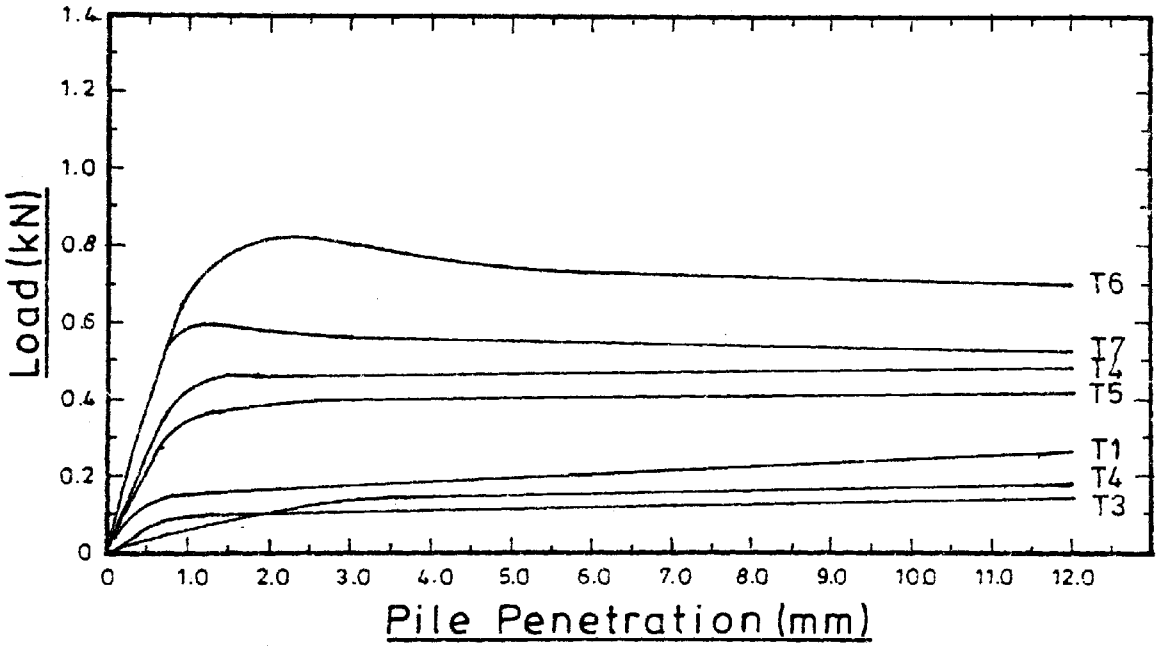

b) Average of 3rd and 4th fillings (not vibrated)

FIGURE 7.40

LOAD/PENETRATION CURVES SHOWING ADDITIONAL LOAD CAUSED BY THE TOP 250mm LAYER OF SAND FOR EACH OF THE SEVEN LOADING TESTS

From Figure 7.40 there does not appear to be any trend in the magnitude of this increase in resistance due to the addition of the top layer of sand. For some of the curves the increased resistance was less than that for the initial 250mm layer of sand (T1) while for the others it was greater.

The stress transfer curves of Figure 7.8 have been normalized for the same reasons as the load/penetration curves mentioned in section 7.4.1. These curves have been approximated by the trigonometric function $\cos^2\phi$. The equation for the curves takes the form

$$y = A \cos^2\left(\frac{\pi}{2r}\right) \cdot x \qquad (7.2)$$

where y = stress transfer

x = distance from centre of curve

A = stress transfer at peak of curve

r = ½ the maximum width of the curve.

The values of A and r taken from the stress distrubtion curves of Figure 7.3 have been plotted against the embedded length of the pile on the graphs of Figure 7.41. The value of n was found to be independent of the sand density while the value of A increased with increasing density as well as depth.

The values of the distance from the top of the final layer of sand to the centre of each stress distribution curve have been plotted against pile embedded length on Figure 7.42. This Figure shows that the maximum stress transfer occurred at lower elevations in the looser sand stratum.

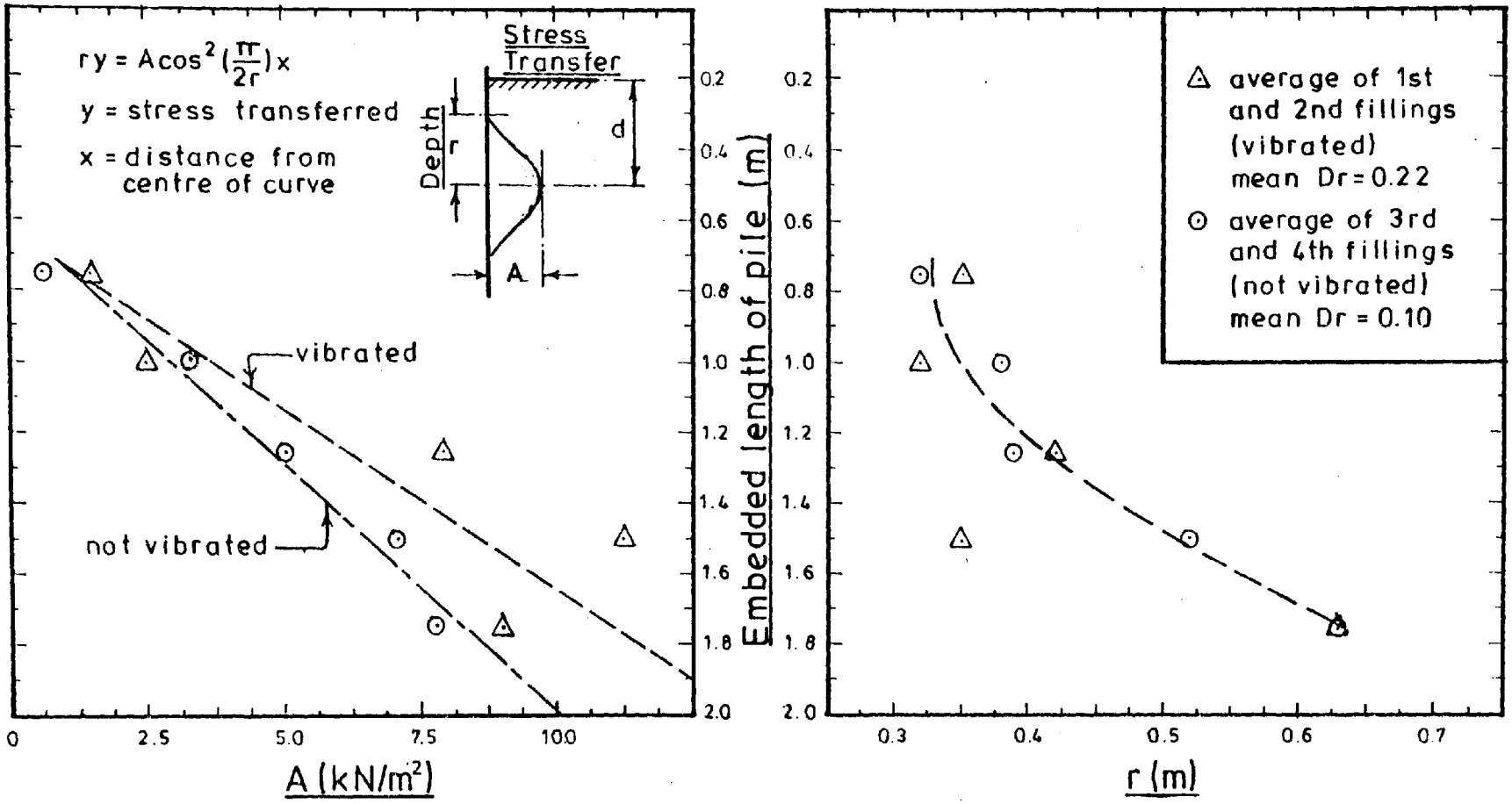

FIGURE 7.41

VARIATION OF CONSTANTS A AND r WITH EMBEDDED LENGTH IN THE EQUATION FOR THE STRESS DISTRIBUTION CURVES

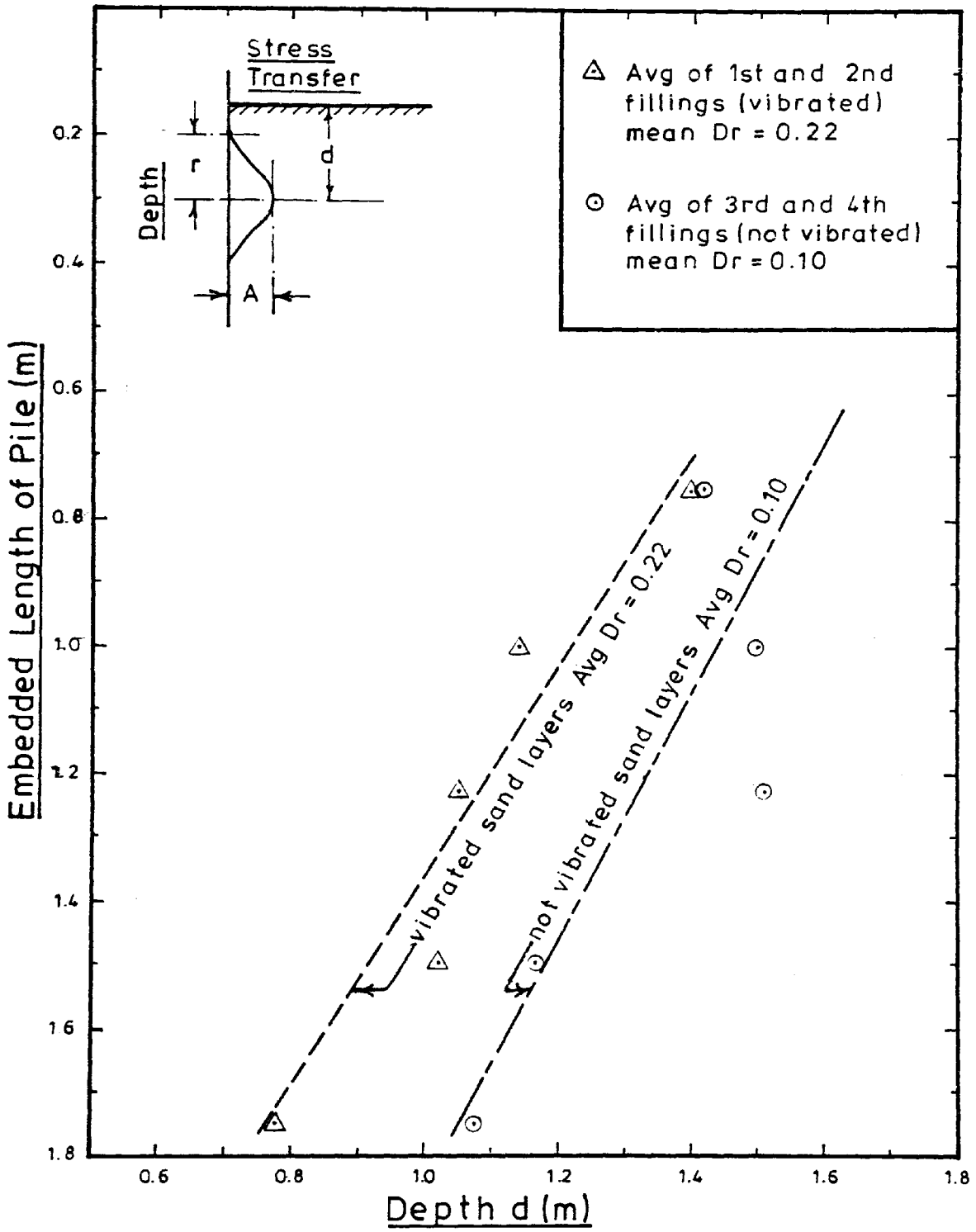

FIGURE 7.42

VARIATION OF THE POINT OF MAXIMUM STRESS TRANSFER WITH LENGTH OF PILE

The equations for the normalized stress distribution curves have been determined from the average values of A,r and d taken from Figures 7.41 and 7.42. These curves have been plotted on Figure 7.43.

The shape of the stress distribution curves shows a gradual increase in skin friction with depth, reaching a peak value and decreasing at further depths. As mentioned previously Meyerhof and Valsangkar (1977) and Meyerhof and Sastry (1978) found this same relationship between the radial stresses acting on the shaft of the pile and depth. However, in both of these investigations the piles were end bearing in an underlying soil layer and a value of radial stress was recorded at the base of the piles. Gregerson and DiBiagio (1973) found this same variation of skin friction along the shaft of a 0.28m diameter steel pile loaded in a loose sand. The skin friction distrubtion for one of the loading tests carried out by Gregerson et al. (1973) has been reproduced and is shown in Figure 7.44.

From the results of the normalization of the stress distribution curves presented in Figures 7.41 and 7.42 stress distribution curves can be predicted (within the limits of this investigation) for different embedded lengths of pile when the total load is carried by the skin friction on the shaft.

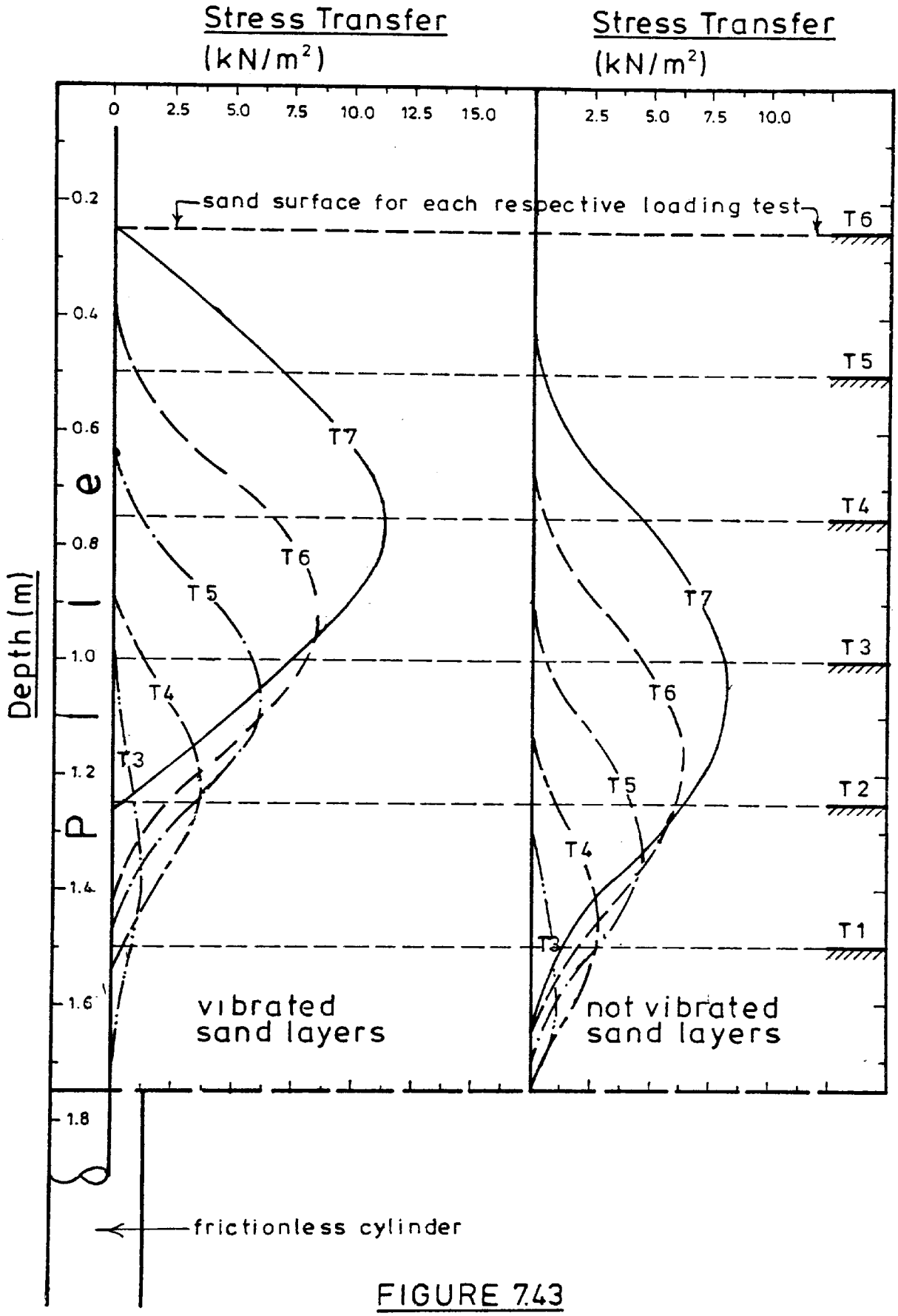

FIGURE 7.43

NORMALIZED STRESS TRANSFER CURVES
FOR 1mm PILE PENETRATION

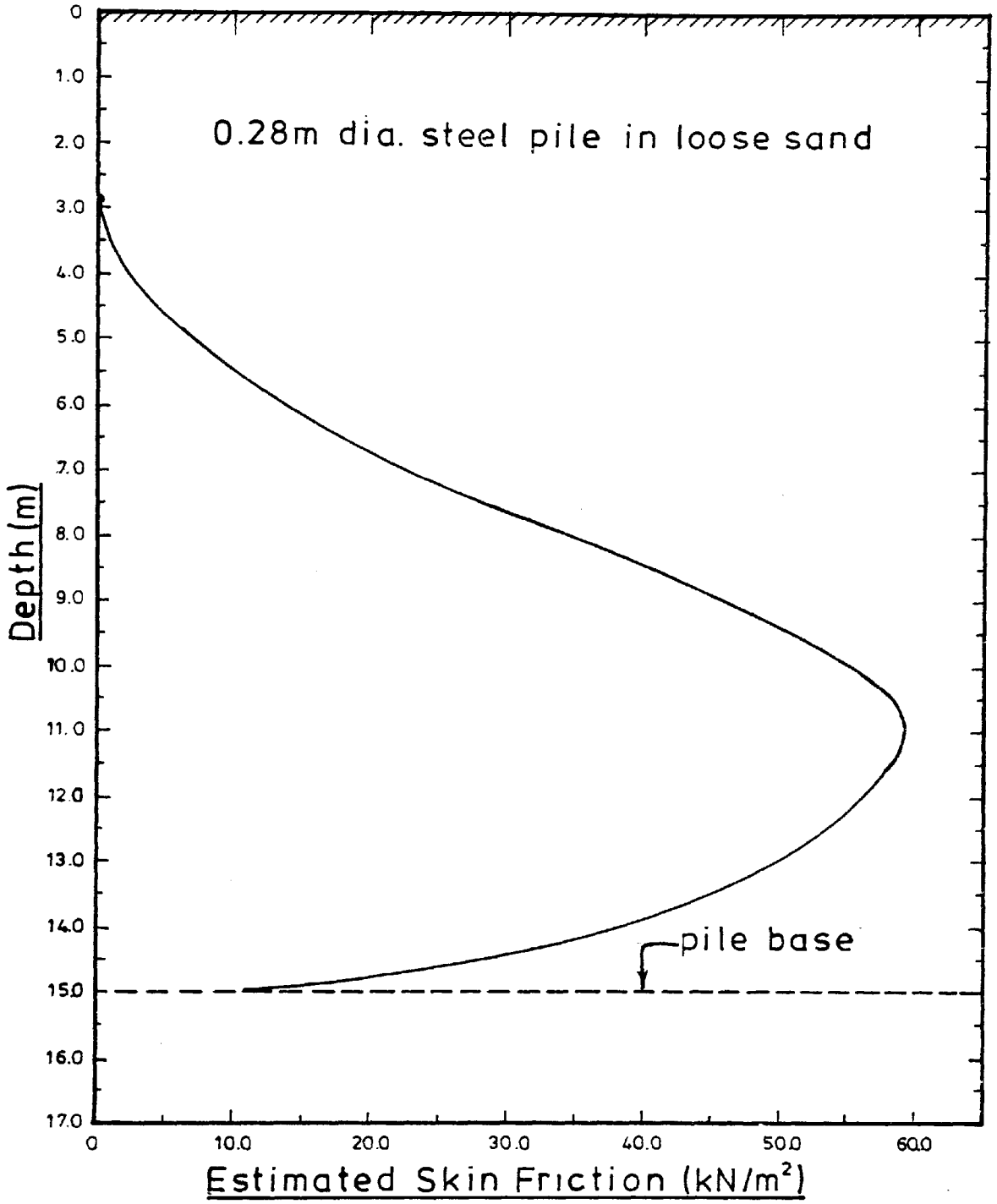

FIGURE 7.44

SKIN FRICTION VALUES ESTIMATED ON THE BASIS OF MEASURED AXIAL LOADS IN INSTRUMENTAL PILES

(from GREGERSEN and DIBIAGIO 1973)

7.4.4 Coefficient of Earth Pressure

The equation presented by Meyerhof (1953) for the tangential force per unit area on a pile shaft in a soil with both cohesion and friction is

$$qs = Ca + Ks\gamma D\tan\delta \qquad (2.4)$$

where Ca = the adhesion per unit area,

Ks = coefficient of earth pressure on the pile shaft, and

δ = the angle of friction of the soil on the pile shaft.

For sands Ca = 0, so that $qs = Ks\gamma D\tan\delta$, therefore

$$Ks = \frac{qs}{\gamma D \tan\delta} \qquad (7.3)$$

Most earlier investigators have assumed average values for qs, γ, and δ when using equation (7.3) in order to calculate Ks, although it is accepted that these parameters will vary with depth along the pile. In this section the candidate has attempted to calculate the value of Ks along the pile based on the experimental results presented in this thesis as well as on other experimental data.

In order to derive a relationship between Ks and depth D, the parameters qs, γ and δ have been expressed in terms of depth.

The relationships between the average unit skin friction on the shaft of the pile and the embedded length of the pile for the cases of the vibrated and notvibrated sand layers have been calculated from the

normalized values of Figure 7.38. The equations relating the average unit skin friction to embedded length were found to be :

$$qsv = 5.53D^{(0.25)} \qquad (7.4)$$

for the vibrated sand layers, and

$$qsn = 3.16D^{(0.75)} \qquad (7.5)$$

for the notvibrated sand layers.

From the graphs of Figures 7.19 and 7.20 the average density gradients were determined to be :

$$\gamma_v = 15.30+0.38D(kN/m^3) \qquad (7.6)$$

for the vibrated sand layers, and

$$\gamma_n = 15.17+0.22D(kN/m^3) \qquad (7.7)$$

for the notvibrated sand layers. In terms of relative density Dr, the gradients are :

$$Drv = 0.06+0.19D \qquad (7.8)$$

for the vibrated and

$$Drn = 0.11D \qquad (7.9)$$

for the notvibrated sand layers.

Potyondy (1961) performed a number of experiments on the measurement of δ for different pile materials and soils. For sands on smooth steel surfaces, the average ratio of $\tan \delta / \tan \phi$ was found to be 0.46. Combining this with Meyerhof's relationship between the angle of internal friction of a sand and the sand's relative density :

$$\phi = 28+15\ Dr \quad \text{(Meyerhof 1956)} \qquad (7.10)$$

yields :

$$\tan \delta = 0.46 \tan (28+15Dr). \qquad (7.11)$$

Therefore, for the vibrated sand layers :

$$qsv = 5.53D^{(0.25)}, \qquad (7.4)$$

$$\gamma_v = 15.30+0.38D, \qquad (7.6)$$

and combining equations (7.11) and (7.8) yields

$$\tan\delta_v = 0.46 \tan (28.9+2.85D) \qquad (7.12)$$

while for the notvibrated sand layers :

$$qsn = 3.16D^{(0.75)}, \qquad (7.5)$$

$$\gamma_n = 15.17+0.22D, \qquad (7.7)$$

and combining equation (7.11) and (7.9) yields

$$\tan \delta_n = 0.46 \tan (28.0+1.65D). \qquad (7.13)$$

Substituting these expressions into equations (7.3) yields for the vibrated sand layers :

$$Ksv = \frac{5.53D^{(0.25)}}{[0.46\tan(28.9+2.85D)][15.30D+0.38D^2]} \qquad (7.14)$$

and for the notvibrated sand layers :

$$Ksn = \frac{3.16D^{(0.75)}}{[0.46\tan(28.0+1.65D)][15.17D+0.22D^2]} \qquad (7.15)$$

These values are plotted for various embedded lengths of pile in Figure 7.45.

Also plotted on Figure 7.45 are the values of Ks calculated from the results of the model pile tests carried out by Vesic (1963).

These results are in broad agreement with the findings of Meyerhof (1951), Coyle and Sulaiman (1967) and others. Meyerhof (1951) stated that the value of Ks varied from 0.5 for a loose sand to 1.0 for a dense sand. Coyle and Sulaiman (1967) found that densification of the sand near the top of a pile during driving, would tend to increase the soils shear strength at shallow depths. If this increased shear strength is not accounted for in the calculations a larger value of Ks would be obtained. It has been shown by Coyle and Sulaiman (1967) that the value of Ks can exceed 1. This would explain the relatively high values of Ks at shallow depths as shown in Figure 7.45. The increased shear strength at the top of each layer caused by

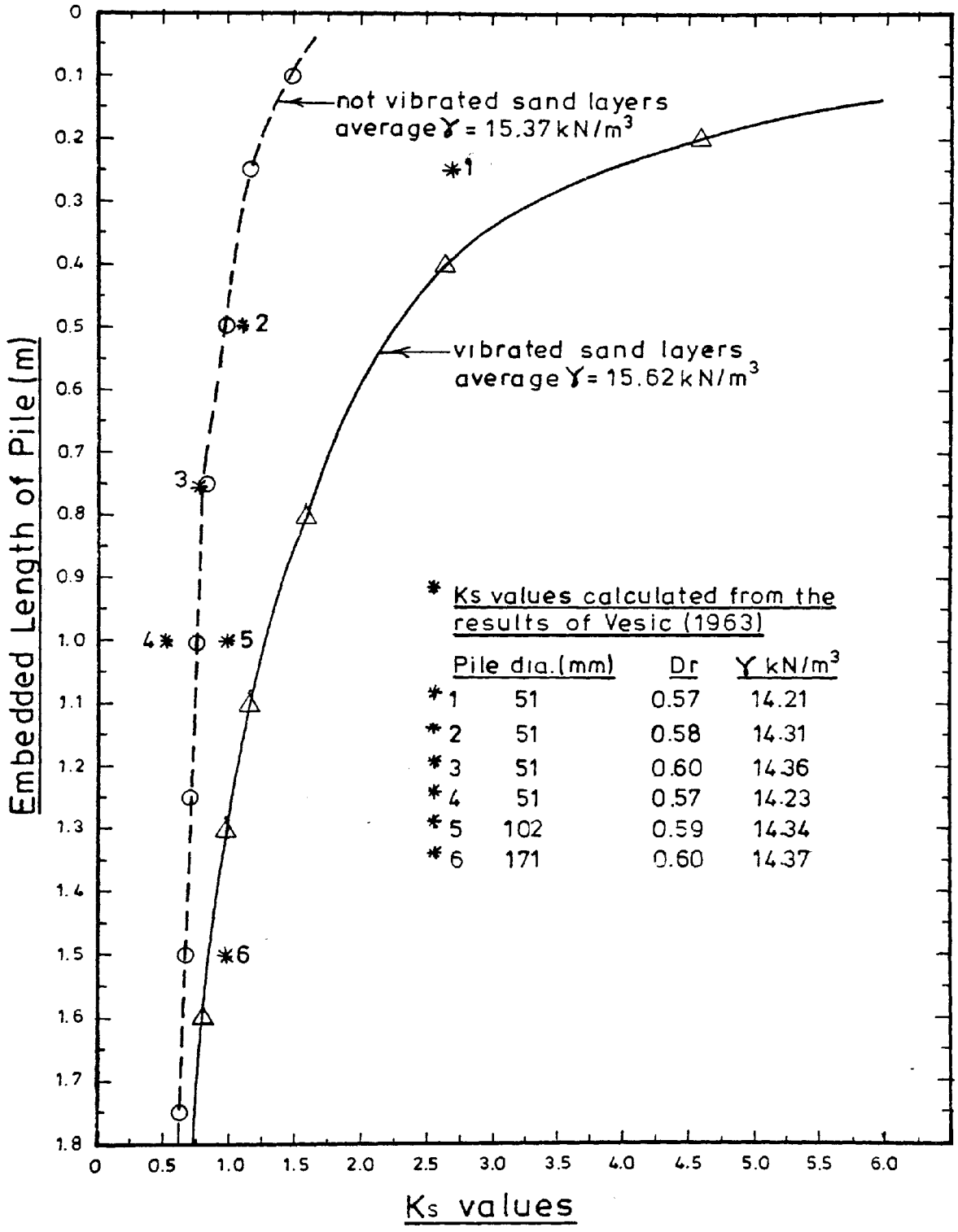

FIGURE 7.45

Ks VALUES CALCULATED FROM PILE LOADING TEST RESULTS

surface vibration has not been accounted for in the calculation of Ks. As the embedded length of pile increases the effect of this dense crust of soil at the surface decreases and the values of Ks approach those derived by Meyerhof (1951). As expected the values of Ks for the vibrated soil layers are higher than those for the soil layers which were not vibrated.

The calculated values of Ks have been plotted against the dimensionless depth (pile length divided by pile diameter) in Figure 7.46. Also plotted on this Figure are the ultimate values of skin friction divided by soil shear strength derived by Coyle and Sulaiman (1967). Coyle et al. (1967) assumed Ks to be a constant when determining the soil shear strength, though they did state that this assumption was not correct at shallow depths where Ks was apparently greater than one. Therefore, assuming Ks to vary with depth, as suggested by Robinsky and Morrison (1964), the ratio of skin friction to soil shear strength presented by Coyle et al. (1967) would represent the value of the earth pressure coefficient Ks.

The values of Ks, calculated from the data presented by Coyle et al. (1967) shown on Figure 7.46 show the same trends as the candidates results; the values are greater than one at shallow depths and approach asymptotically constant values at greater depths. The values at greater depths are again in the range suggested by Meyerhof (1951).

The higher values of Ks determined from Coyle and Sulaiman's (1967) results reflect the higher soil density that is expected with a saturated soil. Unfortunately the value of the relative density of the soil has not been given in the Coyle et al. (1967) report.

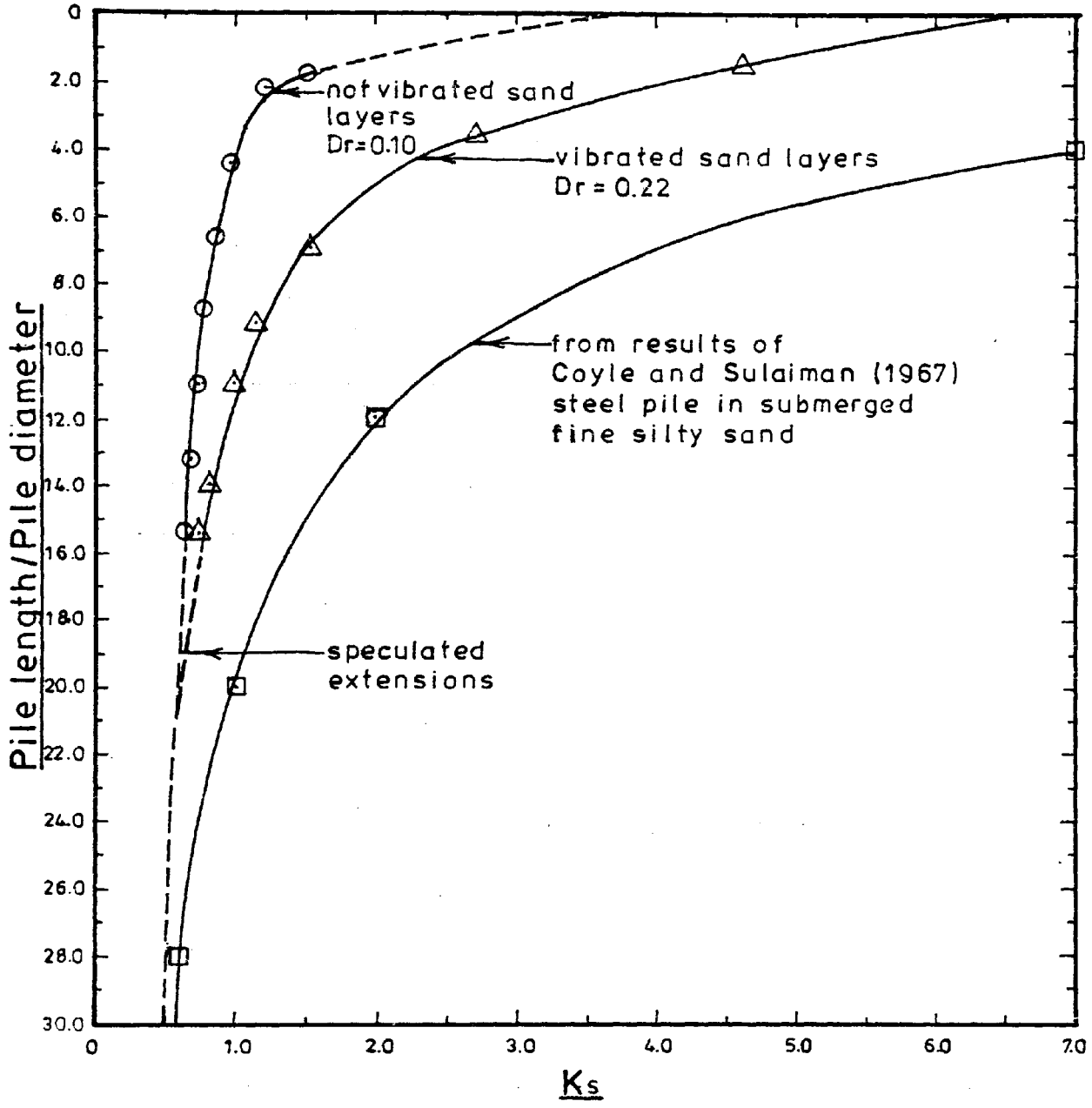

FIGURE 7.46

K_s VERSUS RELATIVE PILE LENGTH

These values of Ks reflect the effect of the installation of a pile on the surrounding soil. The value of the coefficient of earth pressure at rest Ko, determined from the well known relationship suggested by Jaky (1944) for $\phi = 25^{\circ} - 45^{\circ}$

$$Ko = 0.9(1-\sin\phi) \qquad (7.16)$$

yields values of Ko = 0.43 for $\phi = 31.3^{\circ}$ (vibrated sand layers) and Ko = 0.46 for $\phi = 29.5^{\circ}$ (not vibrated sand layers). Budhu (1979) using a modified simple shear apparatus determined the values of Ko for dense and loose Leighton Buzzard sand to be 0.425 and 0.435 respectively.

7.4.5 Backanalysis of Soil Modulus

The candidate has used the method of analysis presented by Poulos (1974) to backfigure the values for the soil modulus of elasticity Es from his pile loading test results. The values used in the analysis were the applied loads at 1mm pile penetration[1]. taken from the normalized load/penetration curves (Figures 7.34 and 7.35).

The results of this analysis are presented in Table 7.5, and a sample calculation is given in Appendix 7A.

From the values of the soil modulus the shear modulus G has been determined using the relationship

$$G = \frac{Es}{2\,(1+\nu)} \qquad (7.17)$$

where ν is Poissons ratio, assumed to be equal to 0.30 for

1. See Appendix 7A

TEST LAYER	P (kN)	L (m)	$L/_d$	I	SOIL MODULUS E_s (MN/M^2)	SHEAR MODULUS G (MN/M^2)
VIBRATED SAND LAYERS						
T1	0.26	0.25	2.19	0.350	0.80	0.31
T2	0.51	0.50	4.39	0.220	0.98	0.38
T3	1.07	0.75	6.58	0.180	1.69	0.65
T4	1.66	1.00	8.77	0.135	1.97	0.76
T5	2.26	1.25	10.96	0.120	2.38	0.92
T6	2.86	1.50	13.16	0.110	2.76	1.06
T7	3.44	1.75	15.35	0.105	3.17	1.22
NOTVIBRATED SAND LAYERS						
T1	0.15	0.25	2.19	0.350	0.46	0.18
T2	0.24	0.50	4.39	0.220	0.46	0.18
T3	0.37	0.75	6.58	0.180	0.58	0.22
T4	0.81	1.00	8.77	0.135	0.96	0.37
T5	1.41	1.25	10.96	0.120	1.48	0.57
T6	2.00	1.50	13.16	0.110	1.93	0.74
T7	2.60	1.75	15.35	0.105	2.39	0.92

TABLE 7.5

DETERMINATION OF SOIL MODULUS
USING THE BACKANALYSIS METHOD
PRESENTED BY POULOS (1974)

the density of the soil used during the pile loading tests (see Appendix 7B).

The values for the settlement correction factors R_h and R_k in the analysis have been taken to be equal to one, due to the assumed infinite distance to a rough rigid base layer and the relatively high value for the pile stiffness factor K.

The candidate realises that he is not totally justified in using the analysis since Poulos (1974) considered the load to be transmitted to the soil by end bearing as well as skin friction. According to the equations presented by Poulos (1974) the proportion of load which would have been transferred to the base, had the pile been end bearing in the sand, would have ranged from 8% to 20%. However, the analysis was carried out as a comparison on the range of values for the shear modulus determined in the shearbox apparatus which is presented in section 6.1.2.2.

The values of G presented in Table 7.5 represent the average shear modulus for each layer of sand. By comparing these values with thoseshown in Figure 6.3 it can be seen that the average values of shear modulus were similar to the values determined from the shearbox test carried out at sand densities approximating the average densities for the test layers. Both of these moduli were derived from tests with a predetermined rupture surface. In the case of the shearbox test, the rupture surface was in the sand at the plane passing through the centre of the shearbox while for the pile loading test the rupture surface was at the pile sand interface, since the angle of friction between the sand and the pile surface (δ) was considerably less than the angle of internal friction of the sand (ϕ).

APPENDIX 7A

Backanalysis of Soil Modulus Es From Poulos (1974)

Example calculation for test layer T7, vibrated sand layers

$$Es = PI_1/\rho d \; R_k \; R_h \quad (7A.1)(\text{Poulos } 1974)$$

where P = applied load (kN)

I_1 = settlement influence factor

ρ = settlement (m)[1]

d = pile diameter (m)

R_k, R_h = settlement correction factors for the effects of pile compressibility and finite layer depth respectively.

For T7 vibrated

P = 3.44kN

ρ = 1×10^{-3}m pile penetration

L = embedded length of pile = 1.75m

d = 0.114m

L/d = 15.35

$d_b/d = 1$

d_b = diameter of pile base (m)

From Figure 7.2 (Poulos 1974), $I_1 = 0.105$ and from Figure 7.4 (Poulos 1974) $R_h = 1$.

1. arbitrary value assumed to be in the elastic region of the load/penetration curve

Assuming $R_k = 1$ (i.e. pile stiffness factor ($K=E_p/E_s$) is very large) then from equation (7A.1)

$$E_s = 3.17 MN/m^2$$

By checking the value of K assuming that $E_p = 2x10^5 MN/m^2$, where E_p is equal to the effective Young's Modulus of the pile section.

Then $K = 2x10^5/3.17 = 6.3x10^4$

Therefore, referring to Figure 7.3 (Poulos 1974) the justification is proven for assuming $R_k = 1$.

APPENDIX 7B

Determination of Poissons ratio

Kezdi (1972) gives a relationship between the coefficient of earth pressure at rest Ko and Poissons ratio (ν) based on the theory of elasticity as,

$$\nu = Ko/1+Ko \qquad (7B.1)$$

Kezdi (1972) has also shown that for the values of ϕ between 20° and 45°

$$Ko = 0.9(1-\sin\phi) \qquad (7B.2)$$

Therefore, for the vibrated sand layers, Dr = 0.22.

$$\phi = 28+15Dr = 31.3^\circ \qquad \text{Meyerhof (1951) (7.9)}$$

and

$$\nu = \frac{0.9(1-\sin 31.3^\circ)}{1+0.9(1-\sin 31.3^\circ)} = 0.30$$

For the notvibrated sand layers, Dr=0.10

$$\phi = 28+15(0.10) = 29.5^\circ \qquad (7.9)$$

and $\nu = 0.31.$

Chapter 8

Conclusions and Proposed Future Work

CHAPTER 8

CONCLUSIONS AND PROPOSED FUTURE WORK

8.1 Conclusions

The conclusions presented in this section are based upon :

1. the literature review carried out,

2. the design, manufacture and subsequent testing of the equipment and monitoring systems, and

3. the analysis of the results of the testing of the semi-fullscale piles.

It is recognised that the results of the research work presented in this thesis are applicable only within the context of the present experiments, i.e. for the two ranges of sand density tested. However, by using a test pile of considerably larger diameter than that which is usually used for laboratory testing the results should reflect more closely the characteristic behaviour of the development of load transfer along the shaft of a pile and the subsequent soil displacemments, for a pile passing through a granular medium.

Therefore, based upon the results presented in this thesis the following conclusions can be drawn :

1. The size of the sand tank was found to be sufficient so as not to interfere with the displacement stresses developed in the sand due to the driving of the test pile. The central axis of the pile was located at a distance of approximately 13 pile diameters from the wall of the tank and 10.5 pile diameters from the closest reaches of the step brackets.

Kishida (1963) observed that the distribution of displacement stresses developed by the displacement of sands due to pile driving extended a distance of approximately four pile diameters from the piles central axis. Meyerhof (1959) found the zone of volume change (see Figure 2.8) to extend to a distance of approximately three to four pile diameters. Robinsky and Morrison (1964) using radiographic techniques observed a visible displacement envelope in sand to extend to three to four pile diameters to the side of the pile in loose sand (Dr = 17%) and 4.5 to 5.5 pile diameters in medium sand (Dr = 37%).

In the course of the present study the maximum vertical sand displacements measured at 3.5 pile diameters from the central axis of the pile were found to be approximately 0.035mm at a depth of 0.25m below the sand surface for the looser fillings of the tank. This is approximately 25% of the value of the displacement measured at a distance of 1.0 pile diameter from the centre of the pile.

2. The dust extraction and sand placement equipment were found to be efficient in practice. The results of the specific gravity test carried out on the five samples, taken during the testing programme, and presented in section 6.1.1.2, did suggest that a small

amount of the lighter dust-size particles had been removed during testing. It is not felt that this small change in the properties of the soil mass had any significant influence on the test results. This does however, show the necessity for monitoring any changes in the properties of the testing medium over the duration of the testing programme.

It appears that the utilization of the 2.36mm sieve, in the conical hood of the sand pouring equipment, as shown in Figure 3.3 and the consistancy in the height of the final free fall of the sand aided in the placement of a uniform mass of sand. This is reflected in the results of the Mini-Mac penetration tests.

3. The density tins proved useful for determining the density gradient of the testing medium at the completion of each testing sequence. Though there was a considerable dispertion in the results, two density gradients of the sand were established. The results of the Mini-Mac penetration test were helpful for checking the uniformity of the testing medium and identifying possible reasons for anomalies in the test results.

4. The elimination of end bearing and simulation of an underlying clay stratum were accomplished with the use of the frictionless cylinder. The pilot study proved this method to be the most efficient of those tested to monitor the development of skin friction and subsequent soil displacements while simulating the conditions of a pile passing through a granular medium and end bearing in an underlying clay stratum. In this study the frictionless cylinder did not allow for the simulation of any movement of the underlying clay stratum caused by pile driving.

However, the adaption of the cylinder to simulate this movement, as described in section 3.7, has been left for a future study.

5. Of the two types of test pile load cells employed in this investigation (described in detail in Chapter 5) the 'Core' type load cell was found to be the more efficient. The problems encountered with the 'Shell' load cell i.e. welded seam, inaccessibility for location of strain gauges, noncircular cross section, and nonuniform wall thickness led to the development of the 'Core' load cell. One of the main advantages of the 'Core' load cell was the greater and controlled sensitivity. The central core of this load cell could be manufactured (within structural limits) to vary the sensitivity of the response of the load cell.

   The investigation and calibration of the prototype 'Shell' type load cell and the test pile load cells in the Instron 1251 stiff testing machine helped to identify the problems inherent in the load cells and appurtenances. These have been discussed and are presented in section 6.2 and 6.3.

6. As described in section 5.4.1 the advantages found in using a quarter Wheatstone-Bridge circuit were that any inherent eccentricities and faulty gauges could be detected in the test results, since the response of each individual gauge element was recorded. Rather than averaging the strains measured by each gauge on either side of the load cell in the bridge circuit, the strains were averaged in the analysis via the computer program. Consequently the average as well as the individual strains were recorded.

The candidate found the best method of checking the efficiency of the bonding of the strain gauges to be that described in section 5.4.2.

7. The shear modulus of the test sand was determined from the results of shearbox tests and backanalysis of the pile loading test results. The values of shear modulus were found to lie in the range of 0.2 to 1.5 MN/m^3.

As pointed out in section 7.4.5 the test procedure in both cases was for a predetermined rupture surface.

8. The in-situ calibration tests carried out on the test pile before, during, and after the testing programme reflects the need for monitoring the calibration characteristics during testing. The calibration tests also aided in identifying faulty gauges which developed during the testing programme.

The series of calibration tests performed on the test pile to monitor the influence of confinement on the calibration characteristics of the load cell brought a number of interesting questions to light. These tests showed the need for further investigation into this phenomenon and the dangers of calibrating a test pile in one state and testing it in another.

9. The sand displacement monitoring system incorporating the Terra Plates, 'piano' wire, and displacement transducers proved efficient in the measurement of the vertical sand displacements. The Terra Plates moved with the soil, the 'piano' wire was relatively inextensible over the range of applied load, and the transducers were found to give a linear response over the range of

displacements encountered during testing.

10. The method of sand compaction by surface vibration was used in this investigation because it was felt that this method would cause less disturbance to the instrumentation buried in the sand and would create a more uniform sand mass rather than by using a poker vibrator. However, the degree of compaction using this method was only moderate as shown by the sand density results of Figure 7.19 and 7.20. The average relative densities were 0.22 and 0.10 for the vibrated and not vibrated sand layers respectively.

11. The load/penetration curves shown in Figure 7.2 were approximated by an initial linear portion extending to a pile penetration of 0.625mm and a final exponential portion of the form $P = A\delta^B$.

The initial linear portion of the load/penetration curves were found to be independent of the embedded length of pile and the sand density. This agrees with the statement by Vesic (1963) where he confirmed the belief that the mobilization of shear strength along a rupture surface is governed by the absolute displacement along that surface.

12. The average skin friction versus pile penetration curves shown in Figures 7.36 and 7.37, as well as the average skin friction versus embedded length of pile graphs shown in Figure 7.38 show a linear increase in skin friction at shallow depths but becoming constant at greater depths. This agrees with the observations of Vesic (1963); Tomlinson (1977) and others.

The values of the average ultimate skin friction determined from the load penetration curves, for embedded lengths of the pile ranging from 0.25-1.75m, were found to be between 4.0 and 6.6kN/m^2 for the vibrated sand and from 2.0 to 4.4 kN/m^2 for the not vibrated sand for pile penetration of 12mm. Tejchman (1969) found the average ultimate skin friction in compression for a 50mm diameter pile embedded 0.30m in a dry sand (mean particle size = 0.24mm, coefficient of uniformity = 1.7), at a porosity of 41%, to reach a value of 2.2 kN/m^2 after a pile settlement of 5.97mm had occurred.

Vesic (1964) recorded a mean value for the average ultimate skin friction for a 0.102m diameter pile, whose length of embeddment ranged from 0.5m to 3.0m, in a dry loose sand (mean particle size = 0.37mm, coefficient of uniformity = 2.5), with a relative density of between 20% - 40%, to be 7.0 kN/m^2 after an average pile penetration of 8.3m.

It should be noted that in the investigations of the two previously mentioned authors, the piles were subjected to both skin friction and end bearing.

13. The stress transfer curves are shown in Figure 7.8. These curves were approximated by a trigonometric curve of the form $Y=A\cos^2 nx$. The normalization of the stress transfer curves is discussed in section 7.4.3 and shown in Figure 7.43. These curves are similar to the curve proposed by Vesic (1963) and those obtained by Meyerhof and Sastry (1978) if the value for end bearing is eliminated. The curves of this figure show that no appreciable skin friction was developed along the upper portion

of the pile shaft. The average depth below the sand surface at which the skin friction began to develop was 1.5 pile diameters for the vibrated sand and 3.4 pile diameters for the notvibrated sand. The average depths at which the stress transfer curves reached peak values were approximately 5.1 and 7.4 pile diameters for the vibrated and not vibrated sand layers respectively.

As shown in Figure 7.43 the skin friction development increased along the length of the pile shaft, reached a peak value and decreased at greater depths. This decrease in skin friction in opposition to the increase in overburden pressure with depth illustrates the phenomenon of 'arching' as discussed in detail in Chapter 2. This 'arching' of lateral pressure around the pile at the lower portion of the pile causes the reduction of skin friction in this region.

14. The data presented in section 7.3.3 on the vertical displacement of the sand due to pile driving showed that the magnitude of the vertical soil displacement decreased with depth and radial distance. The magnitude of the vertical soil displacement was also found to be greater for the pile driving tests which were carried out in the notvibrated sand medium. The maximum recorded value of average vertical sand displacement was 0.16mm at a distance of one pile diameter from the piles central axis at a depth of 0.25m in the notvibrated sand mass.

15. The results of the five loading tests carried out on the final 1.75m depth of sand, presented in section 7.3.5 agree with the current theories that the sequence and direction of loading influence the carrying capacity of a pile. The ultimate loads obtained from the tensile test (pull-out) were less than those

which were measured for the compression tests (CRP and MLT). The sequence of testing appeared to affect the ultimate carrying capacity of the pile in compression though the average values for the tensile tests remained the same. This agreed with Tejchman's (1969) results who found the values of the ultimate carrying capacity for primary and secondary pulling tests to be approximately equal.

16. In section 7.4.4, an expression for the coefficient of earth pressure at the pile shaft is proposed which is based on the present experimental results as well as on the data from others; this is given in terms of pile depth D.

The relationship between Ks and D for the vibrated sand layers (Dr = 0.22) was

$$Ksv = \frac{5.53D^{(0.25)}}{[0.46\tan(28.9+2.85D)][15.30D+0.38D^2]} \qquad (7.14)$$

and for the notvibrated sand layers (Dr=0.10),

$$Ksn = \frac{3.16D^{(0.75)}}{[0.46\tan(28.0+1.65D)][15.17D+0.22D^2]} \qquad (7.15)$$

These relationships between Ks and D are shown graphically on Figure 7.45. The values of Ks were found to decrease as :

1. the density decreased and

2. the embedded length of the pile increased.

The values of Ks approached asymptotically the final values in the range suggested by Meyerhof (1951) (0.5 for loose and 1.0 for dense sand).

The values of Ks were found to be greater than one at shallow depths which supports the finding of Coyle and Sulaiman (1967).

8.2 Proposed Future Work

The work described in this Thesis was the design and manufacture of equipment for, and the monitoring of, vertical sand displacements, and the development of skin friction along a pile passing through a granular medium into an underlying clay stratum. The logical progression from the present research would be :

1. to monitor the horizontal as well as vertical sand displacements, possibly by using the Terra Plates,

2. the implementation of the set of five 'Core' load cells of varying sensitivities designed and manufactured during this research work of which only one has been used to date,

3. a further investigation into the influence of confinement of the test pile in the sand medium on the load cell calibration,

4. the measurement of the variation of the coefficient of lateral earth pressure K along the length of the pile. This could be accomplished by incorporating the contact stress transducers, developed at Cambridge University (Arthur and Roscoe 1961) into the outer sleeve of the 'Core' load cells.

5. As discussed in section 3.7 the frictionless cylinder could be modified to simulate the movement of an underlying clay stratum, as suggested by Tomlinson (1977).

6. The testing apparatus could also be readily adapted for studying group action.

7. As well as measuring skin friction an interesting exercise would be to fix a base plate to the toe of the pile and then to drive the pile into the sand measuring both skin friction and end bearing. The pile could be driven through a sand stratum and into an underlying clay layer. The load cells would enable the investigator to separate the two resistances.

8. Also, field investigations on instrumented piles would be of great importance to verify the practical application of the model scale studies to actual piling performance in the field.

REFERENCES

Alpan,I. (1964).'Estimating settlement of foundations on sands', *Civil Eng'g and Public Works Rev.*, vol.59, 1415-1418.

Arthur,J.R.F., and Roscoe,K.H. (1961). 'An earth pressure cell for the measurement of normal and shear stresses', *Civil Eng'g and Public Works Rev.*, vol.56, no.659, 765-770.

Banerjee,P.K., and Davies,T.G. (1977). 'Analysis of pile groups embedded in Gibson Soil,' *Proc. 9th Int.Conf. on Soil Mech. and Found. Eng., Japan*, vol.1, 381-386.

Berezantzev,V.G., Khristoforov,V.S., and Golubkov,V.N.(1961). 'Load bearing capacity and deformation of piled foundations', *Proc. 5th Int. Conf. on Soil Mech. and Found. Eng.*, vol.2, 11-15.

Brinch Hansen,J. (1968). 'A theory for skin friction on piles', *Geoteknisk Institut (The Danish Geotechnical Institute)*, Bulletin no.25, Copenhagen, 5-12.

Broms,B.B. and Silberman,J.O. (1964). 'Skin friction resistance for piles in cohesionless soils', *Sols Soils*, no.10, 33-43.

Budhu,M. (1979). 'Simple Shear Deformations of Sands' *PhD. Thesis*, Cambridge University, U.K..

Buisman,A.S.K. (1935). 'De weerstand van paalpunten in Zand', *De Ingenieur*, no.50, 25-28,31-35.

Burland,J.B. (1973). 'Shaft friction of piles in clay - a simple fundamental approach', *Ground Eng.*,vol.6, no.3, 30,32,37-42.

Caquot,A.(1934). 'Equilibre des massifs a frottement Interne', *Gauthier-Villars*, Paris.

Caquot,A. and Kerisel,J. (1948). 'General theory of the bearing capacity of piles', *Proc. 2nd Int.Conf. on Soil Mech. and Found. Eng.*, vol.5, 22-23.

Casagrande,A. (1932). 'The structure of clay and its importance in foundation engineering', *Jour. Boston Society of Civil Engineers*, vol.14, 168-208.

Chandler,R.J. (1968). 'The shaft friction of piles in cohesive soils in terms of effective stress', *Civil Engineering*, vol.3, no.3, 30-42.

Chan,S.F. and Hanna,T.H. (1979). 'The loading behaviour of initially bent large scale laboratory piles in sand'. *Canadian Geotechnical Journal*, vol.16, 43-58.

Chellis,R.D. (1961) *Pile Foundations*, McGraw-Hill, Tokyo.

Chin,F.K., and Chan,S.F. (1977). 'Experimental study of eccentric loading on single piles', *Proc. 9th Int. Conf. on Soil Mech. and Found. Eng., Japan*, vol.1, 459-462.

Cooke,R.W. (1974). 'Piled foundations: a survey of research at the Building Research Station', *BRE*, CP24/74.

Cooke,R.W. (1975). 'The settlement of friction pile foundations', *Proc. Conf. on Tall Buildings, Kuala Lumpar,* no.3, 7-19.

Cooke,R.W. and Price,G. (1973). 'Strains and displacements around friction piles', *Proc. 8th Int. Conf. on Soil Mech. and Found.Eng., Moscow,* vol.2, no.1, 53-60.

Cooke,R.W., Price,G. and Tarr,K. (1979). 'Jacked piles in London Clay: a study of load transfer and settlement under working conditions', *Geotechnique,* vol.29, no.2, 113-147.

Coyle,H.M. and Reese,L.C. (1966). 'Load transfer for axially loaded piles in clay'. *Jour. of Soil Mech. and Found. Div., ASCE,* vol.92, no.SM2, 1-26.

Coyle,H.M. and Sulaiman,I.H. (1967). 'Skin friction for steel piles in sand', *Jour. of Soil Mech. and Found. Div., ASCE,* vol.93, no.SM6, 261-278.

D'Appolonia,E. and Romualdi, J.P. (1963). 'Load transfer in end-bearing steel H-Piles', *Jour. Soil Mech. and Found.Eng. Div.ASCE,* vol.89, no.SM2, 1-25.

DeBeer,E.E. (1963). 'The scale effects in the transposition of the results of deep sounding tests on the ultimate bearing capacity of piles and caisson foundations', *Geotechnique,* vol.13, 39-75.

Denman,K.I.,Nicholls,R.A. and Symons,M.V. (1977). 'Model Studies of negative skin friction on pile groups',*Proc.Conf. on Large Ground Movements and Structures, U.W.I.S.T., Cardiff,* July 1977, Pentech Press, 252-271.

Dörr,H. (1922). *'Die Tragfähigkeit der Pfähle',* Verlag W. Ernst and Sohn, Berlin.

Dunham,C.W., (1950). *Foundations of Structures,* McGraw-Hill, New York.

Eastwood,W. and Anagnostov,V. (1962). 'Effects of base shape on the end bearing capacity of piles in granular soils'. *Civil Eng. and Public Works Review,* 1543-1544.

Franke,E. and Garbrecht,D. (1977). 'Test loading on 8 large bored piles in sand', *Proc. 9th Int. Conf. on Soil Mech. and Found.Eng.,* Japan, vol.1, 529-532.

Geddes,J.D. (1969). 'Boussinesq-based approximations to the vertical stresses caused by pile-type subsurface loadings', *Geotechnique,*vol.19, no.4, 509-514.

Girijavallabhan,C.V. and Reese, L.C. (1968). 'Finite Element Method for problems in soil mechanics', *Jour. of the Soil Mech. and Found. Div., ASCE,* March 1968, 473-496.

Gregerson,O.S., DiBiagio,E. and Aas,A. (1973). 'Load tests on friction piles in loose sand', *Norg. Geotek.Inst., Publ.*, no.99, 19-27.

Hanna,T.H. (1963). 'Model studies of foundation groups in sand', *Geotechnique*, vol.13, 334-351.

Hanna,T.H. (1973). *Foundation Instrumentation*, Trans Tech S.A., Switzerland.

Hanna,T.H. and Tan,R.H.S. (1971). 'The load movement behaviour of long piles', *Jour. of Materials, JMLSA*, vol.6, no.3, 532-554.

Hunter,A.H. and Davisson,M.T. (1969). 'Measurement of pile load transfer', *ASTM, special Technical Publ. 444*, 106-117.

Isaacs,D.V. (1931). 'Reinforced concrete pile formulae', *Inst. Aust. Engrs*, J.3, 305-323.

Ismael,N.F. and Klym,T.W. (1979). 'Uplift and bearing capacity of short piers in sand', *Jour. of the Geotech.Eng. Div., ASCE*, vol.105, no.GT5, 579-594.

Jaky,J. (1944). 'The Coefficient of Earth Pressure at Rest', *(Hungarian) Magyar Mernok es Epitesz Egylet Kozlonye.*

Jorden,E.E. (1977). 'Settlement in sand-methods of calculating and factor affecting', *Ground Engineering*, vol.10, no.1, 30-37.

Jumikis,A.R. (1967). *'Introduction to Soil Mechanics'* D.Van Nostrand Co. Inc., Canada.

Kezdi,A. (1972). 'Stability of Rigid Structures,' *Proc.5th European Conf.on Soil Mech. and Found.Eng. Madrid*, 105-130.

Khafagy,A.A.W. (1967). 'The Distribution of Pile Load in a Granular Medium', *Ph.D. Thesis*, Leeds, U.K.

Kim,J.B.,Singh,L.P. and Brungraber,R.J. (1979). 'Pile cap soil interaction from full-scale lateral load tests', *Jour. of the Geotech. Eng. Div., ASCE*, vol.105, no.GT5, 643-653.

Kishida,H. (1963). 'Stress distribution by model piles in sand', *Soil and Found.*, vol.4, no.1, 1-23.

Kishida,H. (1967). 'Ultimate bearing capacity of piles driven into loose sand', *Soil and Found.*, vol.7, no.3, 20-29.

Kishida,H. and Meyerhof,G.G. (1965). 'Bearing capacity of pile groups under eccentric loads in sand', *Proc. 6th Int.Conf. on Soil Mech., and Found. Eng., Montreal*, vol.2, 270-274.

Kolbuszewski,J.J. (1948). 'An experimental study of the maximum and minimum porosities of sands', *Proc. 2nd Int.Conf. on Soil Mech. and Found. Eng., Rotterdam*, vol.1, 158-165.

Little,A.L. (1961). *Foundations,* Edward Arnold (Publishers) Ltd,London.

Mansur,G.I. and Kaufman,J.M. (1956). 'Pile tests low-sill structure Old River, Louisiana', *Journ. of the Soil Mech. and Found. Div., ASCE,* vol.123, 1958, 715.

Massarsch,K.R. and Broms,B.B. (1977), 'Fracturing of soil caused by pile driving in clay', *Proc. 9th Int. Conf. on Soil Mech. and Found. Eng., Japan,* vol.1, 197-200.

Mattes,N.S. and Poulos,H.G. (1969). 'Settlement of a single compressible pile', *Jour. of the Soil Mech. and Found.Eng. Div.,ASCE,* vol.95, no.SM1, 189-207.

Meyerhof,G.G. (1951). 'The ultimate bearing capacity of foundations', *Geotechnique,* vol.2, 301-332.

Meyerhof,G.G. (1953). 'Bearing capacity of foundations under eccentric and inclined loads', *Proc. 3rd Int.Conf. on Soil Mech., Zurich,* vol.1, 440.

Meyerhof,G.G. (1956). 'Penetration tests and bearing capacity of cohesionless soils', *Jour. of the Soil Mech. and Found.Eng. Div., ASCE,* vol.866, 1-12.

Meyerhof,G.G. (1959). 'Compaction of sand and bearing capacity of piles', *Jour. of the Soil Mech. and Found.Eng.Div., ASCE,* vol.85, no.SM6, 1.

Meyerhof,G.G. (1960). 'The design of Franki Piles with special reference to groups in sand', *Symp. on the Design of Pile Foundations, Stockholm,* 105-123.

Meyerhof,G.G. (1963). 'Recent research on the bearing capacity of foundations', *Canadian Geotechnical Jour.,*vol.1, no.1, 16-26.

Meyerhof,G.G. (1974). 'State-of-the-art of penetration testing in countries outside Europe', *Proc. European Symp. on Penetration Testing, Stockholm,* vol.2, 1.

Meyerhof,G.G. (1976). 'Bearing capacity and settlement of piled foundations', *Jour. of the Geotechnical Eng,Div., ASCE,*vol.102, no.GT3, Proc. Paper 1 1962, March, 195-228.

Meyerhof,G.G., and Sastry,V.V.R.N. (1978). 'Bearing capacity of piles in layered soils: Part 1 Clay Overlying sand, Part 2 sand overlying clay', *Canadian Geotechnical Journal,* vol.15, no.2, 171-189.

Meyerhof,G.G. and Valsangkar,A.J. (1977). 'Bearing capacity of piles in layered soil', *Proc. 9th Int.Conf. on Soil Mech. and Found. Eng., Japan,* vol.1, 645-650.

Mindlin,R.D. (1936). 'Forces at a point at the interior of a semi-infinite solid', *Physics,* vol.8, 195-202.

Muller,R. (1939). 'Modellersuche über das Zusammenwirken von Pfählen', *Veröff. des Inst.der Deutschen Forschengsges. f.Bodenmech. (Degebo) an der Techn. Hochsch. Berlin,* vol.7, 9-27.

Orrje,O. and Broms,B.B. (1967). 'Effects of pile driving on soil properties, *Jour. of the Soil Mech. and Found.Div., ASCE,* Sept.1967, 59-73.

Parry,R.H.G. (1971). 'A direct method of estimating settlements in sand from SPT values', *Proc. of the Conf. of the Midlands Soil Mech. and Found. Eng. Society, Birmingham, England,* 29-37.

Parry,R.H.G. (1978). 'Estimating foundation settlements in sand from plate bearing tests', *Geotechnique,* no.1, 107-118.

Parry,R.H.G. and Swain,C.W. (1977). 'Effective stress methods of calculating skin friction on driven piles in soft clay', *Ground Engineering,* April 1977, vol.10, no.3, 24-26.

Paton,W.R. (1895). 'Treatise on Civil Engineering',

Peck,R.B. (1958). 'Study of the comparative behaviour of friction piles', *Special Report No.36, Highway Research Bd., Natl.Research Council, Washington, D.C.*.

Peck,R.B. and Bazarra,A.R.S.S. (1969). 'Discussion on settlement of spread footings on sand', *Jour. of the Soil Mech. and Found. Div., ASCE,* vol.95, no.SM3, 905-909.

Perren,F.J. (1978). 'A Case History of Piling in the Glacial Material of South Wales', *M.Phil.Thesis,* CNAA, London, U.K.

Potyondy,J.G. (1961). 'Skin friction between various soil and construction materials', *Geotechnique,* vol.11, 339-365.

Poulos,H.G. (1972). 'Load settlement prediction of piles and piers', *Jour. of the Soil Mech. and Found.Div.,ASCE,* vol.98, no.SM9,379-397.

Poulos,H.G. (1974). 'Some recent developments in the theoretical analysis of pile behaviour', *New Horizons in Soil Mechanics,* edited by Lee,I.K., Newnes-Butterworths, 237-279.

Poulos,H.G. (1979). 'Settlement of single piles in nonhomogeneous soil', *Jour. of the Geotechnical Eng. Div., ASCE,* vol.105, no.5, 627-641.

Poulos,H.G.and Davis,E.H. (1968). 'The settlement behaviour of single axially loaded incompressible piles and piers', *Geotechnique,* vol.18, no.3, 351-371.

Poulos,H.G. and Mattes,N.S. (1969). 'The behaviour of axially loaded end-bearing piles', *Geotechnique,* vol.19, no.2, 285-300.

Prandtl,L. (1920). 'Uber die Harte plastisher Korper'. *Nachrichten Kon. Gessel.der Wissenschaffer, Math.Phys.Klasse, Gottingen,* 74-75

Prandtl,L. (1921). 'Uber die Eindringungsfestingkeit plastisher Baustoffe und die Festigkeit von Schneiden', *Zeitschrift fur Angewandte Mathematik und Mechanik,* vol.1, no.1, 15-20.

Ramey,G.E. and Hudgins,A.P. (1977). 'Sensitivity and accuracy of the pile wave equation', *Ground Engineering,* vol.10, no.7, 45-47.

Reissner,H. (1934). 'Zum Erddruckproblem' *Proc. 1st Int. Conf. on Applied Mechanics, Delft,* 295-311.

Robinsky,E.I. and Morrison,C.F. (1964). 'Sand displacement and compaction around model friction piles', *Canadian Geotechnical Jour,* vol.1, no.2, 81-93.

Salas,J.A.J. and Belzunce,J.A. (1965). 'Resolution theorique de la distribution des forces dan les pieux', *Proc. 6th Int.Conf. on Soil Mech. and Found. Eng., Montreal,* vol.2, 309-313.

Schmertman,J.H. (1970). 'Static cone to compute static settlement over sand', *Jour. of the Soil Mech. and Found Div., ASCE,*vol.96, no.SM3, Proc.Paper 7302, 1011-1043.

Seed,H.B. and Reese,L.C. (1957). 'The action of soft clay along friction piles', *ASCE, Trans,* vol.122, 731.

Skempton,A.W. (1951). 'The bearing capacity of clays', *Proc. Building Research Congress, London,* vol.1, 180-189.

Skempton,A.W. (1959). 'Cast In-situ Bored Piles in London Clay,' *Geotechnique,* V.9, 153-173.

Skempton,A.W. Yassin,A.A. and Gibson,R.E. (1953). 'Theorie de la force portante des pieux dans le sable',*Annales de l'Inst. Techn. du Bâtiment et des Travaux Publics,* Mars-Avril 1953, 285-290.

Steenfelt,J.S. (1977). 'Scale effects on bearing capacity factor N_γ', *Proc. 9th Int.Conf. on Soil Mech. and Found. Eng., Japan,*vol.1,749-752.

Tavenas,F.A. and Audibert,J.M.E. (1977). 'Application of the wave equation to friction piles in sand',*Canadian Geotechnical Jour.,* vol.14, no.34, 34-51.

Tejchman,A. (1969). 'Skin friction of a model pile driven in sand', *Proc. of 3rd Budapest Conf. on Soil Mech. and Found. Eng.,* 666.

Terzaghi,K. (1936). 'Arching in sands', *Engineering News-Record,* May 14, 1936, 690-693.

Terzaghi,K. (1943). *Theoretical Soil Mechanics,* John Wiley and Sons, Inc. New York.

Terzaghi,K. and Peck,R.B. (1967). *Soil Mechanics in Engineering Practice,* John Wiley and Sons, Inc., New York, 2nd edition.

Thurman,A.G. and D'Appolonia E. (1965). 'Computed movement of friction and end-bearing piles embedded in uniform and stratified soils',*Proc. 6th Int.Conf. on Soil Mech. and Found. Eng., Montreal,* vol.2, 323-327.

Tomlinson,M.J. (1957). 'The adhesion of piles driven in clay soils', *Proc. 4th Int. Conf. on Soil Mech. and Found Eng., London,* vol.2,66-71.

Tomlinson,M.J. (1969). *Foundation Design and Construction,* Sir Isaac Pitman and Sons, Ltd., London, 2nd edition.

Tomlinson,M.J. (1977). *Pile Design and Construction Practice,* Viewpoint, Publications, London.

Tsytovich,N., Berezantsev,V. Dalmatov,B., and Abelev,M. (1974) *'Foundation Soils and Substructures',* Mir Publications.

Vaughn,J. (1975). *Application of B & K Equipment to Strain Measurements,* K.Larsen and Son, Denmark.

Vesic,A.B. (1963). 'Bearing capacity of deep foundations in sand', *National Acadamy of Science, National Research Council, Highway Research Record 39,* 112-153.

Vesic,A.B. (1964). 'Investigation of bearing capacity of piles in sand', *Publication No.3, Duke University (USA).*

Whitaker,T. (1970). *The Design of Piled Foundations,* Pergamon Press, London.

ERRATA

Page	Description